THE UNIVERSITY OF QUEENSLAND

AUSTRALIA

Synthesis of timed-release polymer nanoparticles

Nguyen Tran Thi Dat

BSc

A thesis submitted for the degree of Doctor of Philosophy at

The University of Queensland in 2014

Australian Institute for Bioengineering and Nanotechnology

Abstract

Polymeric carriers for drug and gene delivery have been successfully used in clinical applications, and developing to achieve greater efficacy. A successful polymeric carrier must not only protect the therapeutics from degradation but also increase the pharmacokinetic and biopharmaceutical properties of the therapeutic agents. Furthermore, releasing the therapeutic agents from nanocarriers at the desired target sites and with the correct dosage is important to enhance patient outcomes. Numerous polymeric systems for drug and gene delivery that can release bioactive agents through response to external (e.g., light, electric or magnetic source, and ultrasound) or internal triggers (e.g., pH, enzyme, and redox) have been designed. However, release mechanism using these triggers is restrictive in terms of in vivo applications as there is limited accessibility of external stimuli to tissues or organs; and the efficiency of internal triggers are variable between cell lines and even within the same tissue or organ. Some carriers are not degradable, raising the important issue of toxicity due to accumulation in the body and healthy cells. In addition, the time of release is mostly uncontrollable. The main aim of this thesis is to synthesize and study of novel non-triggered and timed-release polymeric carriers, such as micelles and hydrogel, based on thermoresponsive PNIPAM and self-degradable PDMAEA. In particular, we developed the understanding of the self-assembly and disassembly properties of thermoresponsive PNIPAM copolymerized with the self-degradable PDMAEA and hydrophobic components. This is one of the first examples where the disassembly time can be controlled on-demand in a wide range of experimental conditions.

Initially, the self-catalysed hydrolysis of PDMAEA together with hydrophobic polymers were employed to finely tune the LCST and disassembly time of thermoresponsive PNIPAM and thus control the release time of oligo DNA (i.e., mimic of siRNA) from the polymer complex. The diblock thermoresponsive copolymers were synthesized by Reversible addition-fragmentation chain transfer (RAFT) polymerization, which consisted of a hydrophilic block (e.g., PDMA) for stabilization and a second thermoresponsive block with three components (e.g., NIPAM, DMAEA, and BA or Styrene) for self-assembly and disassembly. The copolymers were fully water-soluble below LCST and self-assembled into core-shell spherical particles with an average diameter of approximately 25 nm above LCST (e.g., 37 ^{o}C) and with a narrow particle size distribution. When the amount of acid groups from degradation of cationic DMAEA units was sufficiently high to increase LCST of the copolymer above 37 °C, the polymer nanoparticles sharply disassembled to unimers (i.e., the core of the copolymer became water soluble). These nanoparticles showed excellent binding to oligo DNA without any leakage until full disassembly to unimers. Interestingly, the disassembly time of the nanoparticles and consequently the release time of oligo DNA could be precisely controlled. These particles could be easily modified with folic acid to enhance cellular uptake by osteosarcoma cells.

In the next step, we studied the influence in the change in the number of self-degradable DMAEA and hydrophobic BA units in the copolymer composition on the disassembly time (t_{start}) and time from the start of disassembly to full unimer formation ($t_{degrade}$). The results showed a dependence of the t_{start} and $t_{degrade}$ on the BA and DMAEA units. The mechanism of degradation was postulated to result from the degradation of the PDMAEA side groups to acrylic acid groups, which by increasing the LCST of the polymer to over 37 ^{o}C over time. Additionally, the polymer nanoparticles could be designed to self-assemble over a wide range of pHs and disassemble below a pH of 7.3. The polymer nanoparticles have potential for application in drug and gene delivery where timed controlled release is required.

The stabilization and self-disassembly of nanoparticles self-assembled from random thermoresponsive copolymers was further investigated in the presence of Sodium dodecyl sulphate (SDS) surfactant. Random copolymers of P(NIPAM-co-DMAEA-co-BA) and P(NIPAM-co-DMAEA-co-STY) were synthesized by RAFT polymerization. The polymers could self-assemble into nanoparticles stabilized by SDS with very narrow size distribution. The polymer particle size increased with the increase in SDS concentration, and these nanoparticles were stable under dilution. Increasing the amount of SDS, the LCST of copolymers were also increased due to more SDS molecules bound to PNIPAM molecules. In addition, the presence of SDS exhibited no influence on the self-degradation of DMAEA as well as self-disassembly characteristic of the polymer nanoparticles.

Based on the understanding of controllably timed-release polymer nanoparticle, non-triggerred degradable polymeric hydrogel was further designed. Random copolymers of thermoresponsive PNIPAM, self-catalysed hydrolysis PDMAEA, hydrophilic PEGMEA, and hydrophobic PBA were synthesized via RAFT polymerization. The thermoresponsive copolymers could form stable gel at temperature higher than the gelation point (e.g., 37 ^{o}C) and then self-degraded into sol state after different times without the need of any trigger. Moreover, the gelation temperature and degradation time were dependent on the number of DMAEA units. Gold nanoparticles coated with PDMA were encapsulated in the hydrogel and subsequently released at different rates through the degradation of the hydrogels. This novel non-triggered release hydrogel may find potential in applications where controlled-release is beneficial.

Declaration by author

This thesis is composed of my original work, and contains no material previously published or written by another person except where due reference has been made in the text. I have clearly stated the contribution by others to jointly-authored works that I have included in my thesis.

I have clearly stated the contribution of others to my thesis as a whole, including statistical assistance, survey design, data analysis, significant technical procedures, professional editorial advice, and any other original research work used or reported in my thesis. The content of my thesis is the result of work I have carried out since the commencement of my research higher degree candidature and does not include a substantial part of work that has been submitted to qualify for the award of any other degree or diploma in any university or other tertiary institution. I have clearly stated which parts of my thesis, if any, have been submitted to qualify for another award.

I acknowledge that an electronic copy of my thesis must be lodged with the University Library and, subject to the policy and procedures of The University of Queensland, the thesis be made available for research and study in accordance with the Copyright Act 1968 unless a period of embargo has been approved by the Dean of the Graduate School.

I acknowledge that copyright of all material contained in my thesis resides with the copyright holder(s) of that material. Where appropriate I have obtained copyright permission from the copyright holder to reproduce material in this thesis.

Publications during candidature

1. Thomson, D. A. C.; Tee, E. H. L.; Tran, N. T. D.; Monteiro, M. J.; Cooper, M. A., Oligonucleotide and Polymer Functionalized Nanoparticles for Amplification-Free Detection of DNA. *Biomacromolecules* **2012,** 13, (6), 1981-1989.
2. Tran, N. T. D.; Truong, N. P.; Gu, W.; Jia, Z.; Cooper, M. A.; Monteiro, M. J., Timed-Release Polymer Nanoparticles. *Biomacromolecules* **2013,** 14, (2), 495-502.
3. Tran, N. T. D.; Jia, Z.; Truong, N. P.; Cooper, M. A.; Monteiro, M. J., Fine Tuning the Disassembly Time of Thermoresponsive Polymer Nanoparticles. *Biomacromolecules* **2013,** 14, (10), 3463-3471.

Publications included in this thesis

1. Tran, N. T. D.; Truong, N. P.; Gu, W.; Jia, Z.; Cooper, M. A.; Monteiro, M. J., Timed-Release Polymer Nanoparticles. *Biomacromolecules* **2013,** 14, (2), 495-502. – Incorporated as Chapter 2.

   Tran, N. T. D. was responsible for 35% of conception and design, 35 % of analysis and interpretation of data, 35 % of drafting and writing. Nghia Truong Phuoc was responsible for 10 % of conception and design, 10 % of analysis and interpretation of data, 10 % of drafting and writing. Zhongfan Jia was responsible for 10 % conception and design, 10% of analysis and interpretation of data, 10 % of drafting and writing. Wenyi Gu was responsible for 5 % of analysis and interpretation of data. Matthew Cooper was responsible for 5 % conception and design, 5 % of drafting and writing. Michael Monteiro was responsible for 40 % of conception and design, 40 % of analysis and interpretation of data, 40 % of drafting and writing.

2. Tran, N. T. D.; Jia, Z.; Truong, N. P.; Cooper, M. A.; Monteiro, M. J., Fine Tuning the Disassembly Time of Thermoresponsive Polymer Nanoparticles. *Biomacromolecules* **2013,** 14, (10), 3463-3471. – Incorporated as Chapter 3.

   Tran, N. T. D. was responsible for 40% of conception and design, 40 % of analysis and interpretation of data, 40 % of drafting and writing. Zhongfan Jia was responsible for 5 % conception and design, 15% of analysis and interpretation of data, 10 % of drafting and writing. Nghia Truong Phuoc was responsible for 10 % of conception and design, 5 % of analysis and interpretation of data, 5 % of drafting and writing. Matthew Cooper was responsible for 5 % conception and design, 5 % of drafting and writing. Michael Monteiro was responsible for 40 % of conception and design, 40 % of analysis and interpretation of data, 40 % of drafting and writing.

Contributions by others to the thesis

The author acknowledges the following individuals who have contributed to this thesis:

Prof. Michael J. Monteiro, Dr. Zhongfan Jia, and Prof. Matthew Cooper for contributing to the conception, design, analysis and interpretation of the research detailed in this thesis.

Dr. Nghia Truong Phuoc and Dr. Wenyi Gu for contributing to the analysis of the research detailed in this thesis.

Statement of parts of the thesis submitted to qualify for the award of another degree

None.

Acknowledgements

First and foremost, I would like to express my gratitude and special thanks to my principle supervisor, Prof. Michael Monteiro. He patiently guided me step by step through out all the years, supported and encouraged me in pursuing my research project, tutored me the knowledge about polymer, corrected my English, or even instructed me how to give a good presentation for my confirmation which was one of the big milestones in my PhD. I also would like to specially thank my co-supervior, Prof. Matthew Cooper. His encouragement, support, and advice during my PhD meant so much to me. I would like to express my sincere thanks to my co-supervisor, Dr. Zhongfan Jia for his guidance, training, and help to get through my PhD.

I would like to thank the past and present group members who have contributed in one way or another to the success of my PhD. I really enjoyed the stimulating and fun environment that you provided. I also express my thanks to Nghia Truong, David Thomson, Wenyi Gu, Matt Trau, Tri Le, and Marianne Gillard for their help during my PhD and thesis preparation.

I would like to acknowledge receipt of the scholarship from UQ international, UQ graduate school and the Australian Institute for Bioengineering and Nanotechnology (AIBN). I also express my gratitude to AIBN, Institute for Molecular Bioscience (IMB), School of Chemistry & Molecular Biosciences (SCMB) for their state-of-the-art facilities and support from the staff members.

I am grateful to all my friends for their help, encouragement and care through difficult times. I also sincerely thank Vietnamese friends in Australia, particularly UQ funny group (Vietnamese) for their help, funny time, and entertainment through the journey of my PhD.

I am forever indebted to my parents, Vuong Quang Tran and Truc Thi Nguyen, and my siblings for everything they have provided me. Without them, I would have never made it this far. Lastly, I would like to convey my special thanks to my boyfriend Nghia for his love, care, patience, and support.

Keywords

Timed-release, polymer nanoparticles, micelles, hydrogel, Reversible addition-fragmentation chain transfer (RAFT).

Australian and New Zealand Standard Research Classifications (ANZSRC)

030306, Synthesis of Materials, 70 %

030301, Chemical Characterisation of Materials, 15 %

100703, Nanobiotechnology, 15 %

Fields of Research (FoR) Classification

0303, Macromolecular and Materials Chemistry, 90%

1007, Nanobiotechnology, 10%

TABLE OF CONTENTS

Chapter 2

Timed-Release Polymer Nanoparticles

Chapter 3

Fine Tuning the Disassembly Time of Thermoresponsive Polymer Nanoparticles

Chapter 4

Large timed-release polymer nanoparticles stabilized by SDS

Chapter 5

Non-triggered degradable thermoresponsive hydrogel for controlled release of gold nanoparticles

LIST OF FIGURES

LIST OF SCHEMES

LIST OF TABLES

LIST OF ABBREVIATIONS

siRNA – small interfering RNA

EPR – enhanced permeability and retention effect

LRP – ‘Living’ radical polymerizations

RAFT – Reversible addition-fragmentation chain transfer

PNIPAM – poly(N-isopropylacrylamide)

PDMA – poly(dimethylacrylamide)

PSTY – polystyrene

PBA – poly butyl acrylate

Poly(ethylene glycol) methyl ether acrylate (PEGMEA

PDMAEA – poly(2-dimethylaminoethyl acrylate)

ImPAA – N-(3-(1H-imidazol-1-yl)propyl)acrylamide

PAA – poly(acrylic acid)

SDS – Sodium Dodecyl Sulphate

MCEBTTC – methyl 2-(butylthiocarbonothioylthio) propanoate

AIBN – Azobisisobutyronitrile

CTA – Chain Transfer Agent

Macro CTA – Macro Chain Transfer Agent

NMR – Nuclear Magnetic Resonance

SEC – Size Exclusion Chromatography

MWD – Molecular Weight Distributions

PDI – Polydispersity Index

N/P – Nitrogen/phosphorus

M_n – number average molecular weight

DLS – Dynamic Light Scattering

SOP – Standard Operating Procedures

RI – refractive index

DMAc – N,N-Dimethylacetamide

PLK – polo-like kinase

OA – Osteoarthritis

TEM – Transmission Electron Microscopy

DMSO – Dimethylsulfoxide

$CHCl_3$ – Chloroform

THF – Tetrahydrofuran

Dichloromethane – DCM

Chapter 1-Introduction

1.1 Drug and gene delivery

Development of pharmaceuticals over the past two decades has found that the fundamental issue of drug development is in the method of delivery. Proper distribution of the drug and other therapeutic agents within the patient's body is one of the most important issues in the medicine.[1-5] Therapeutic agents such as drugs, proteins, DNA, and siRNA can be degraded in the low pH medium of stomach as well as by enzymes in the gastrointestinal (GI) tract.[6] Furthermore, some drugs are cytotoxic. Therefore, it is necessary to design and develop a suitable drug delivery system that can deliver bioactive therapeutic compounds to the human body effectively and safely.

1.1.1 The importance of delivery

Application of nanotechnology in the field of medicine is called nanomedicine and has been developed over the past few years. It has highlighted the importance of disease diagnostic and treatment that has high precision and remarkable efficacy. Recent advancements in nanomedicine have shown that many nanostructures and nanodevices have been employed to diagnose, treat, and prevent diseases.[1, 5, 7-14] Including the development of carriers for drug and gene delivery systems which has received significant attention over the past few decades.[3, 5, 7, 15-23]

An optimal drug delivery carrier should ensure that the bioactive agents are well protected against degradation by enzymes.[7, 24-27] Moreover, circulation, absorption, and solubility of the therapeutics need to be enhanced. Furthermore, drug delivery systems have to make sure that the bioactive agents are available at the sites of interest and at the required concentration for the precise time and required duration. The combination of these factors could result in the reduction in the frequency of drug administration decreasing drug toxicity as well as improving patient compliance.

1.1.2 Polymeric systems for drugs and genes delivery

Studies in the past two decades have shown that polymers are becoming the most promising class of biomaterials and are widely used in various medical applications.[28-30] Since the concept of polymer-drug conjugates in drug delivery pioneered by Ringsdorf in 1975, research in this field has been remarkable.[31] Along with the advancement of nanotechnology, polymeric materials have made significant progress in biomedical applications; for example drug and gene delivery, tissue engineering, biosensors, contact lens, vascular grafts, dental materials, and sophisticated artificial

organs. The vast number of developments in polymeric materials for biomedical application has been documented in some excellent books and journal reviews.[32-36]

Synthetic polymers are the most common platforms to create novel systems and methods for medical applications especially in the field of gene and drug delivery.[37-51] The structure of the synthetic polymers can be modified, thus it can be used to design systems for various applications in drug and gene delivery. Different approaches such as encapsulation, conjugation and complexion have been used to combine synthetic polymers with small molecular drugs or bio-macromolecules for use in drug delivery systems. The polymer provides an enhancement in the pharmacokinetic of the therapeutics as it not only protects the drug and gene from fast clearance in the blood circulation but also preserves the drug for a programmable time interval before going to targeted sites. The carriers can be designed to release the therapeutics at specific locations so that the concentration of these compounds can be increased to the threshold to enhance the treatment efficacy.[38]

A variety of different polymeric delivery systems such as polymersomes,[52-55] dendrimers,[56-58] micelles/particles,[59-72] and hydrogels,[73-83] film,[84, 85] etc. have been designed to be used in drug/gene delivery systems. However the micelles/particles and hydrogels are the most popular carriers utilized in the area of drug and gene delivery.

1.1.2.1 Polymeric micelles/particles

Polymeric micelles can be formed by self-assembly of amphiphilic copolymers in aqueous solution.[63, 67, 68, 86-89] These micelles have a core–shell structure, where the inner core is formed by the segregation of hydrophobic segment from the aqueous exterior and the outer shell is composed from the extension of the hydrophilic segments building a palisade around the inner core.[68, 71] Many different kinds of drugs and genes with varying characteristics can be incorporated into the micelles via different approaches such as encapsulation, conjugation, and complexion.[68, 70, 90-117] Therefore, the strength of interaction of polymeric micelles and therapeutics is able to be designed. In addition, as a soluble drug carrier with the size range of several tens of nanometer, polymeric micelles can preferentially accumulate in the target location due to the enhanced permeability and retention (EPR) effect (see Figure 1.1).

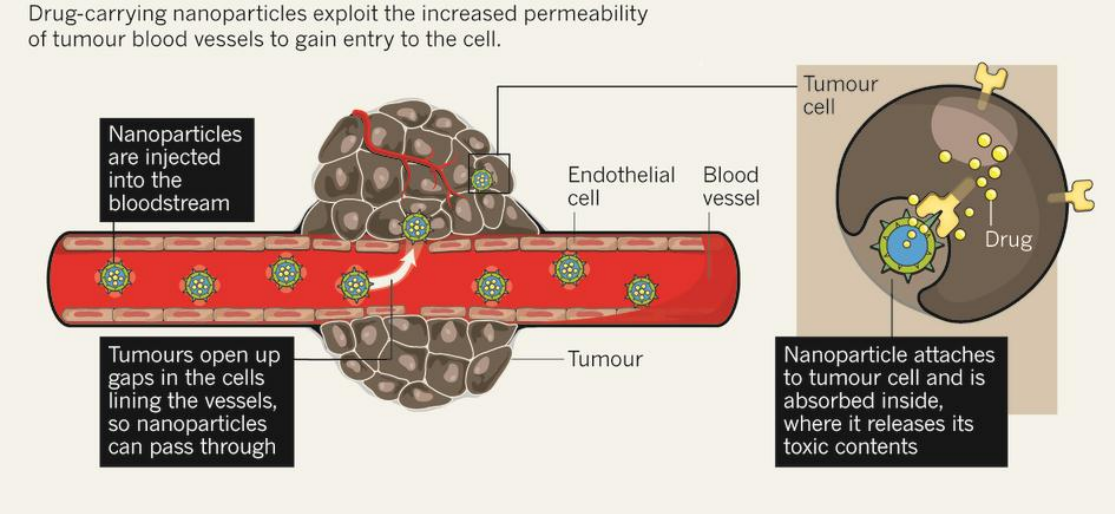

Figure 1.1 Polymer nanoparticles in drug delivery.[118]

Moreover, hydrophobic drug can be embedded in the inner core, thus the plasma degradation of therapeutics is significantly avoided.[13, 68, 71, 119, 120] These water soluble polymeric carriers also increase the solubility of the hydrophobic drugs. Furthermore, the stealth properties of the corona can prevent the micelles from recognition by reticuloendothelial system (RES) which may result in a longer blood circulation time leading to a better chance of targeting to a specific site.

1.1.2.2 Polymeric hydrogels

A hydrogel is a three-dimensional polymeric network with good permeability, high water content, biocompatibility, and tissue-like mechanical properties. There are two main types of hydrogels: physical and covalent cross-linked hydrogels.[74, 75, 79, 121, 122] In physical cross-linked hydrogels, the formation of hydrogel can be controlled by hydrogen bond, crystallized domains, aggregation, hydrophobic interaction, host-guest interaction, self-assembly, and temperature-induced sol-gel transition.[123-155] These hydrogels can undergo a reversible volume phase transition or sol-gel transitions in response to external (physical) stimuli, and thus have great potential in biomedical applications such as drug delivery, gene delivery, and tissue engineering. In drug and gene delivery, the therapeutics can be loaded into the gel matrix and protected from hydrolysis and enzyme degradation.[74, 75, 77, 78, 80, 121, 154] Through the application of proper stimuli on hydrogels, the physically cross-linked hydrogels are able to reverse to the corresponding solution state or change to degradation products that support the release of the therapeutic compounds.

With the emerging development in drug delivery the physiological environment needs to be considered in order to produce an effective polymeric drug delivery system. Therefore, smart polymers that are able to respond to the change of the physiological conditions within the human body have been persistently studied in the field of drug delivery over many decades.

Thermoresponsive polymers, a representative of smart polymers, are the most extensively exploited polymers in the designing of polymeric carriers for drug and gene delivery.[156]

1.1.3 Thermoresponsive polymers (TP) for drug and gene delivery

1.1.3.1 Thermoresponsive polymers

Thermoresponsive polymers are classified as one of the smart materials which can respond to changes in temperature. [37, 121, 156] Thermoresponsive polymers include two main types: Lower critical solution temperature (LCST) and Upper critical solution temperature (UCST). Polymers that become insoluble upon heating have a LCST. In contrast, polymers which become soluble upon heating have an UCST (Figure 1.2). The phase transition of the polymers reflects the competition between the hydrogen bonding interaction of the polymer molecules with surrounding water molecules and the intra-/intermolecules hydrogen bonding between the polymer molecules. When the intra/intermolecular hydrogen bonding interactions between polymer molecules predominate upon heating, the solubility of the polymer decreases. LCST and UCST can be explained by the free energy system in the Gibbs equation $\Delta G = \Delta H - T\Delta S$ (G: Gibbs free energy, H: enthalpy, and S: entropy). It is noted that the LCST is affected by entropy while the UCST is driven by enthalpy. Polymers that exhibited a LCST such as Poly(N-isopropylacrylamide) (PNIPAM) are the most heavily studied.

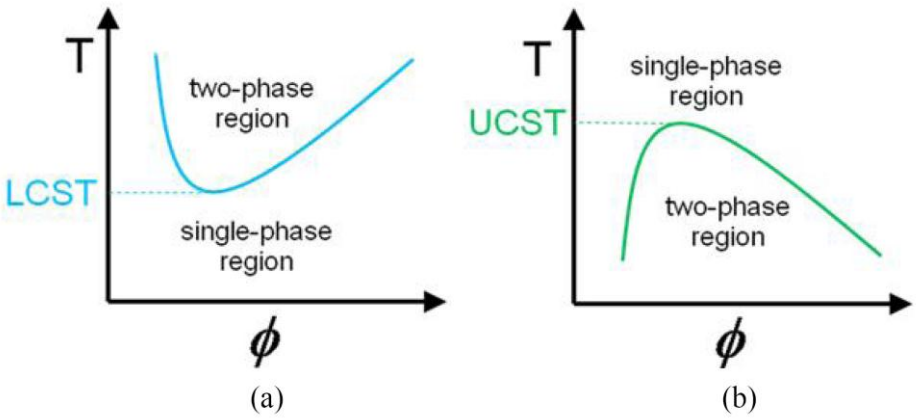

Figure 1.2 Temperature *vs.* polymer volume fraction, ϕ. Schematic illustration of phase diagrams for polymer solution (**a**) lower critical solution temperature (LCST) behavior and (**b**) upper critical solution temperature (UCST) behavior.[121]

1.1.3.2 Poly(N-isopropylacrylamide) (PNIPAM)

PNIPAM was reported as early as 1967 by Scarpa to possess a LCST near physiological temperature at 32-33 ^{o}C.[156] Many properties of PNIPAM (e.g., tuneable LCST, interactions with surfactants, etc.) and mechanism of its phase separation have been well-characterised and

understood over the last two decades. Moreover, PNIPAM have been using for many applications including biomedical materials.[72, 80, 81, 121, 156] Therefore, in this thesis, PNIPAM is chosen as a thermoresponsive polymer to investigate the novel self-disassembly strategy although it is slightly toxic.[157] This polymer is water soluble below its LCST through predominant hydrogen bonding interactions with the surrounding water molecules. When heating to above the LCST, the hydrogen bonding with water is disrupted leading to aggregation and collapse of the polymer chains (Figure 1.3).[156, 158-160] The LCST of PNIPAM can be manipulated by incorporating hydrophilic/hydrophobic components to shift the hydrophilic/hydrophobic balance. For example, incorporation of PNIPAM with a hydrophilic monomer increases the LCST, whereas with a hydrophobic monomer decreases the LCST. Based on this concept, several thermoresponsive micellar drug carriers prepared from PNIPAM containing copolymers have been reported.[161-166]

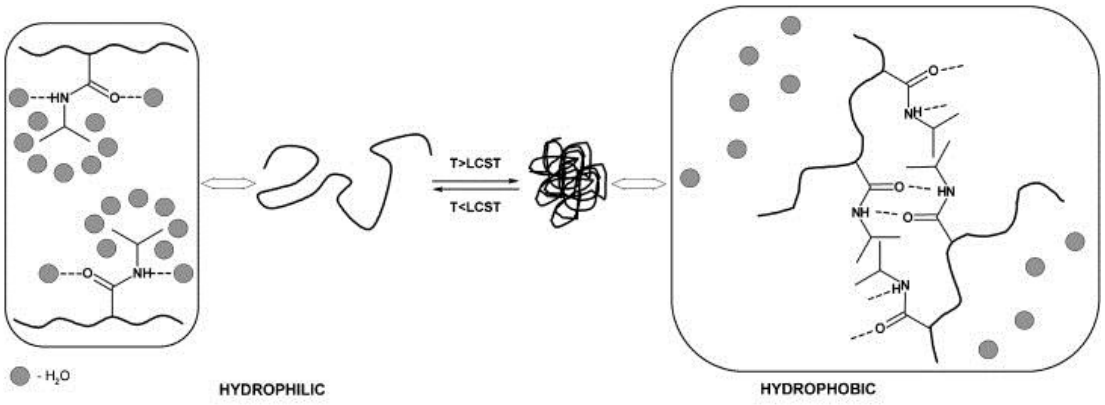

Figure 1.3 Illustration of temperature induced PNIPAM phase transition.[167]

1.1.3.3 Application of thermoresponsive property or polymer in drug and gene delivery and challenges

Thermoresponsive micelles in drug and gene delivery and challenges

Drug carriers prepared from block copolymers, where one of the blocks is able to undergo a lower critical solution temperature (LCST) phase transition, like PNIPAM, have drawn a lot of attention.[89, 168-174] Over the last couple of decades, many PNIPAM based micelles have been studied such as the thermoresponsive micelle poly(*N*-isopropylacryamide-*co*-methacrylic acid-*co*-octadecyl acrylate (P(NIPAM-co-MAA-co-ODA)). The polymer micelles can be formed at 20 ^{o}C, and are able to encapsulate 50-60% of aluminum chloride phthalocyanin.[86] Furthermore, micelles prepared from block copolymers poly(*N*-isopropylacryamide-*b*-styrene) (P(NIPAM-b-STY)) and poly(*N*-isopropylacryamide-*b*-butyl methacrylate) (P(NIPAM-b-BMA)), which have a hydrophobic core originating from the PSTY or PBMA and a hydrophilic shell formed by PNIPAM, have been employed to test the release of Adriamycin (ADR) in vitro.[175] However, the polymers were not degradable, which may cause toxicity problems, as the polymers may not be able to be eliminated

from the body. Degradable poly(D,L-lactide) (PLA) was employed to synthesize poly(N-isopropylacrylamide-co-N, N-dimethylacrylamide)-b-poly(DL-lactide) (P((NIPAM-co-DMA)-b-LA)) to address the degradation issues. The LCST of the polymer was adjustable to meet the requirement for a specific delivery system. The resulting micelles were used to investigate the loading and release of ADR. Nevertheless, the drug release rate was too slow (only 15 % release in 6 days) accompanying a high cytotoxic.[172] Another biodegradable polymer, poly(ε-caprolactone) (PCL), was utilized as a hydrophobic block in the copolymer P((NIPAM-co-DMA)-b-CL). In 10 h, 80% of Doxorubicin was released, which demonstrated a quick drug release behaviour.[176] Another micelle system of a triblock copolymer biotin-poly(ethylene glycol)-block-poly(N-isopropylacrylamide-co-N-hydroxymethylacrylamide) (Biotin-PEG-b-P(NIPAAm-co-HMAAm)-b-PMMA) exhibited 10% entrapment efficiency of Methotrexate (MTX) drug with pre-targeting property and was able to release 92% of the drug in 96 h, exhibiting a high potential as a drug delivery system.[177] However, the release of these cargos should only fall between 37 and 42 ^{o}C because denaturation and disruption of fine anatomical structure of some bioactive agents can happen at temperatures above this range.[178] Moreover, these micelles were prepared in the presence of an organic solvent which may cause toxicity. In addition, the encapsulated drugs release uncontrollably above copolymers LCST rather than below since the micelles were deformed above the LCST. Furthermore, the deformation of the micelles can be controlled by the temperature such as hyperthermia that may cause limitations on the application of these systems in vivo.[89, 176]

Micelle systems from diblock copolymers of PNIPAM and hydrophilic polymers can self-assemble without involving an organic solvent. The diblock copolymer can self-assemble in aqueous solution to form micelles in which the PNIPAM is the inner core andother hydrophilic block as outer hydrophilic shell, for example poly(N-isopropylacrylamide)-block- poly(ethylene glycol) (P(NIPAM-b-PEG)),[174] poly(*N*-isopropylacryamide-*b*- N,N-dimethylacrylamide) (P(NIPAM-b-DMA)),[179, 180] poly(N-isopropylacrylamide)-block- poly(acrylic acid) (P(NIPAM-b-AA)).[181] The micelles formed from self-assembly of diblock P(NIPAM-b-AA) in water were able to encapsulate doxorubicin (DOX). The release of DOX was investigated in different pH media. The drug released faster at pH 4 (90 % of in 10h) and slower in pH 7.2 (40 % in 40 h). However, in order to release the encapsulated drug in vivo, higher temperature was also required to deform the micelles as well as to enhance the drug release.[181] In addition, the release rate and release time of compounds from these micelles were not controllable. This may cause a negative effect to the efficacy of in-vivo applications.

Thermoresponsive hydrogels in drug and gene delivery and challenges

Thermoreponsive polymers are also widely used as hydrogels.[80-82, 161] The entanglement of the polymer chains or bridging of the self-assembled amphiphilic micelles at high concentration in solutions and above the LCST of thermoresponsive polymers results in the reversible in-situ formation of the physical hydrogel without the need of toxic cross-linkers (Figure 1.4). Furthermore, without cross-linkers, the micelle solutions are injectable before gelation at temperatures below its LCST. While heating to a temperature higher than its LCST results in the polymer solution transitioning to a gel state.[80-82, 161]

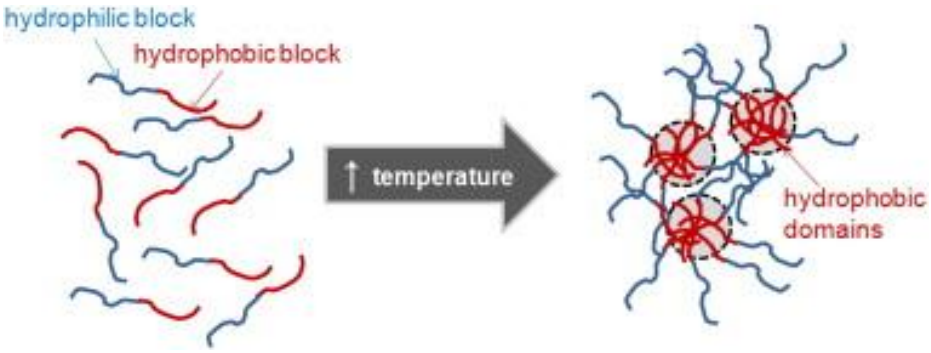

Figure 1.4 Mechanism of *in situ* physical gelation driven by hydrophobic interactions.[75]

Based on this concept, thermoresponsive hydrogels have been widely applied in drug and gene delivery systems where the active compounds can be mixed with polymer solution at below the polymer's LCST and firmly held inside carriers at above the LCST. For example, hydrogel achieved from random copolymer of PNIPAM and Oligolatide-(2-hydroxylmethyl methacrylate) (PNIPAM-co-oligoLA-HEMA) showed high encapsulation efficiency and sustained release of insulin to the retina over a 7 day period.[182, 183] PNIPAM also blended with poly(dimethyl siloxane) (PDMS) for protein delivery.[184] Nevertheless, these hydrogel systems were not able to degrade, which is the biggest issue for PNIPAM based hydrogels. Degradable polymers such as biodegradable poly(l-glutamic acid) was successfully introduced to PNIPAM based copolymers to form a degradable hydrogel.[185] However, the side product of degradation is toxic, limiting the application of these hydrogels in vivo. The Guan and Vernon groups built a novel hydrogel system from biodegradable PNIPAM copolymers which are poly(N-isopropylacrylamide)-co-poly(acrylic acid)-co-poly(dimethyl-γ-butyrolactone)-co-poly(hydroxylethyl methacrylate-co-poly(trimethylene carbonate)) (P(NIPAM-co-AA-co-DBA-co-HEMAPTMC)) and poly(N-isopropylacrylamide)-co-poly(acrylic acid)-co-poly(2-hydroxylethyl methacrylactate) (P(NIPAM-co-AA-co-HEMA-lactate)), respectively. The polymer solutions were able to form gel in-situ and then degrade. [80, 161, 186] In these systems, the hydrogels were formed at body temperature, 37 ^{o}C, yet became soluble at this temperature after degradation, allowing the by-product to be dissolved and excreted from body.

The hydrogel can be applied for both the delivery of genes and drugs.[186] Nevertheless, the degradation time of the hydrogel was not well-controlled which may affect the encapsulated agents (e.g, reduction in the bioactivity) as well as the efficacy of administration (e.g., insufficient dose at the required times).

1.2 Controlled release in drug and gene delivery

One of the most important features of delivery carriers is the ability to release the therapeutic agents in a controlled manner.[178, 187, 188] This raises the need of a facile approach to release the therapeutics in response to change of stimuli or in the surrounding environment. However, most of the traditional carriers are not able to respond to stimuli. Recently, stimuli-responsive polymers as delivery carriers have been extensively developed to produce carriers that can respond to the extracellular environment to release the cargo. The stimuli-responsive carriers can sharply response to the applied stimuli by undergoing physical and chemical changes. In other words, the release of the encapsulated bioactive agents can be triggered by the alteration in the structure of the carriers. The stimuli can be mainly divided into three categories, which are physical (e.g., light, temperature, ultrasound, magnetic, mechanical, electrical), chemical (e.g., solvent, ionic strength, electrochemical, pH), and biological (e.g., enzymes, receptors).

1.2.1 Physical (external) stimuli induced release

Physical stimuli that can alter the properties and supramolecular structure of the polymers such as light, temperature, electric field, magnetic field and ultrasound have been studied over the past decades.

1.2.1.1 Light

Light responsive polymers are a kind of smart polymer that are able to respond to either UV or visible light, to release encapsulated bioactive agents in a triggered manner (Figure 1.5). This allows for spatial and temporal control over the triggering period. The encapsulated compound can be released after the body is irradiated with a light source.[188-194] For example, sensitive light molecules such as leuco derivative and chromophore were introduced to the polymer to prepare a UV-light or visible light responsive carrier.[194-197] Photo cleavable linkers such as 2-nitrobenzyl ester linker was also employed to design light sensitive polymersomes for release of encapsulated fluorescin.[198] These carriers are able to respond according to the activation or deactivation of the irradiation resulting in the release of the encapsulated guests. However, the guest molecules can only be released when the tissue is able to absorb the light. In addition, this delivery system has

some common problems such as high initial release, low penetration depth of irradiation light, slow response of carriers towards the stimuli, and long application periods.[188] Moreover, there are some requirements for this delivery system that can cause adverse effects to patients during treatment. For example the patients have to stay in a dark place for a certain period of time to avoid early release and activation of the drug. However, the dark condition is also harmful for the patient.[178]

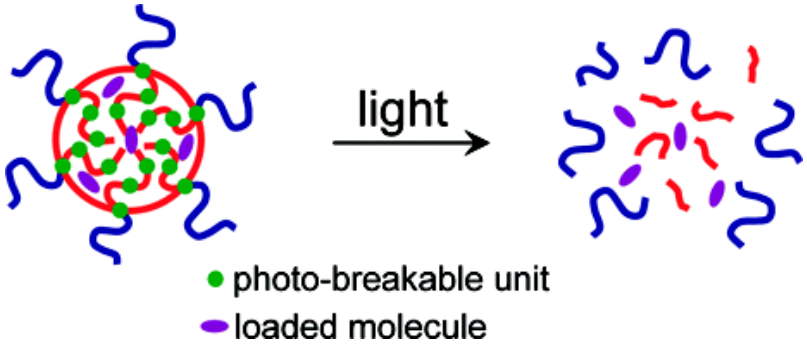

Figure 1.5 Schematic illustration of the difference between placing a photobreakable unit at only the block junction and repeatedly on the hydrophobic block.[199]

1.2.1.2 Ultrasound

Applying ultrasound as an external trigger to activate the release of active molecules from the polymeric matrix has been widely used and attracted much attention in the drug delivery field during the last decades.[192, 200-203] Some bioerodible polymers such as polyglycolide, polylactide, poly(bis(p-carboxyphenoxy)) alkane-anhydrides, etc, can be introduced to prepare ultrasound sensitive carriers for drug and gene delivery (Figure 1.6).[200, 204-206] The general mechanism of ultrasound regulated drug/gene delivery is that the ultrasound creates the thermal energy though micro–convection and inertia cavitation, causing cell membrane perturbation as well as increases the permeability of blood capillaries.[207] Although a number of ultrasound sensitive carriers including polymeric ultrasound contrast agents have been explored there are still several major issues with this method.[204, 208, 209] These include that the release controlled by ultrasound requires specialized equipment and should only be applied once the amount of carrier containing the encapsulated drugs is sufficiently accumulated at the target site, which depends on the pharmacokinetics of the delivery system.[178, 188, 192] In addition, high efficiency of induced release depends on the suitability of the ultrasound power, and the depth of the ultrasound impulse to the target site. Surgical implantation is sometimes required for non-biodegradable delivery systems.[188]

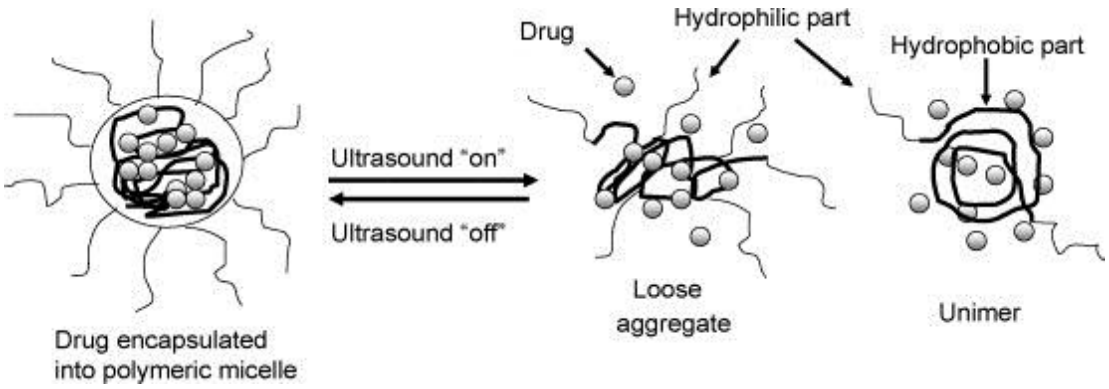

Figure 1.6 Ultrasound-responsive drug delivery from triblock copolymer micelles of poly(ethylene oxide)-b-poly(propylene oxide)-b-poly(ethylene oxide) (PEO-b-PPO-b- PEO).[210]

1.2.1.3 Magnetic

Several magnetic stimuli carriers have been developed for drug and gene delivery.[211-214] Magnetic release involves the utilization of a magnetic field to trigger the release of contents embedded into the polymeric scaffold.[215-217] For example, magnetite nanocrystals were embedded in Pluronic/poly(ethylene imine) shell crosslinked nanocapsules to trigger the delivery of siRNA.[218] To release the model guests from the carriers, a certain high frequency magnetic field is always required. However, the intensity of the magnetic field may be different among specific sites of action.[219] Moreover, there is a problem in scaling up the application from small animals with near surface targets to larger animals or humans because the depth of the magnetic field may have to be varied. In addition, the accumulation of the magnetic particles can block blood flow resulting in embolization. High concentration of the magnetic particles in the liver may also occur.[219]

1.2.1.4 Electrical field

The release of bioactive agents entrapped in the carrier triggered by electrical field application is also an attractive method in drug delivery.[220-222] This external stimulus provides control over the current magnitude, the electrical pulses duration, and the interval between pulses. Polyelectrolytes, which are ionisable, are common platforms for preparation of this delivery system. The delivery systems are able to shrink or swell under the influence of electric field due to anisotropic, thereby releasing the encapsulated agents.[223, 224] For example, fluorescein (or daunorubicin) was encapsulated in a nanoparticle prepared from conducting polymer (e.g., polypyrrole). These particles was suspended in a thermoresponsive hydrogel of poly((d,l-lactic acid)-co-(glycolic acid))-b-poly(ethylene oxide)-b-poly((d,l-lactic acid)-co-(glycolic acid)) (PLGA-PEG-PLGA).[225] The release of the drug from the nanoparticles was regulated by electric field application, which allowed the drug to diffuse through the hydrogel to the surroundings (Figure 1.7). However, one issue is

that it is necessary to maintain the level of the remote trigger to the specific location over the triggering period. Furthermore, the selection of electric current for triggering the drug release without stimulating the nerve endings in the surrounding tissue is also a major issue that needs to be considered.[188]

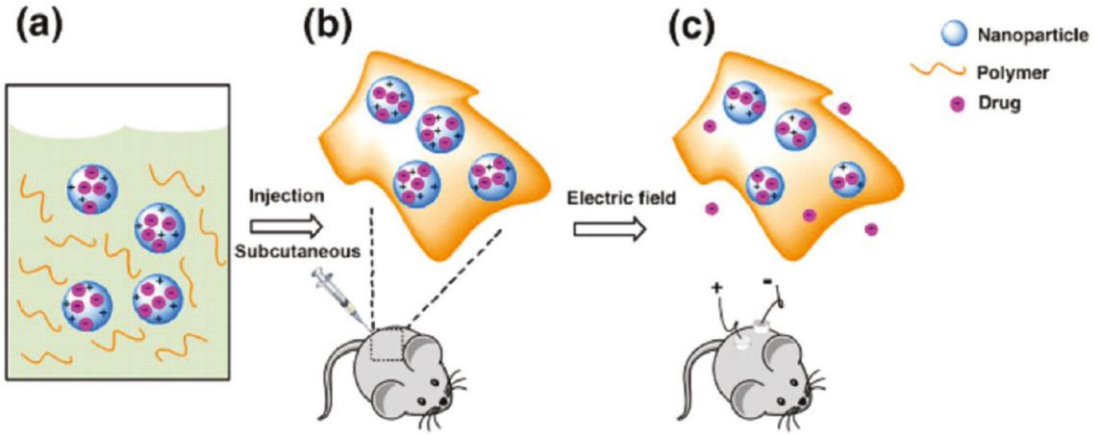

Figure 1.7 General schemes for the application of this system. (a) The nanoparticle polymer solution is (b) subcutaneously injected into a mouse, followed by (c) application of a DC electric field to induce release of the drug cargo inside the nanoparticles.[225]

1.2.2 Chemical and biological induced release

Chemical stimuli can trigger the release through molecular interactions between the polymers and these stimuli. Generally, this kind of carrier is classified into three types: pH responsive, ion responsive, and redox responsive carriers. The most studied chemical sensitive carriers for drug delivery are the pH responsive and redox responsive polymers.

1.2.2.1 pH

A sharp gradient change in the pH of the biological systems in cellular compartment and physiological environment motivated the design and development of pH sensitive carriers in drug and gene delivery systems.[38, 178, 188, 226] All pH sensitive polymers are polyelectrolytes that contain pendant acidic or basic groups that are ionisable in response to changes in environmental pH. Therapeutics can be loaded into the polymeric carriers via encapsulation, conjugation (e.g., conjugation of therapeutics to polymer via pH-dependent cleavable linkage), and complexation. In the proper pH environment, the protonation/deprotonation of the polymer can induce disassembly of micelles or the cleavage of labile linkage between polymer and the therapeutic agents result in the triggered release of the transported drugs (Figure 1.8).[116] There are two strategies used to control and trigger the release of loaded compounds. Each depends on the alteration of the pH of the environment. The strategy is either extracellular or intracellular release methods.[38, 178, 187] The pH of

physiological environment is 7.4 while the intracellular pH of cancer tissue can be 6.5-7.2 or even lower for some certain cancers. The pH of the intracellular compartments can also vary. For example, the pH value in the early endosome is 5-6, while for the late lysosome it drops to about 4-5. Taking advantage of pH gradient of extra- and intracellular environments, numerous polymer based pH responsive systems have been designed to selectively release therapeutics at target sites.[227-244] For example, Kataoka and colleagues designed polymeric micelles that self-assembled from poly(ethylene glycol)-poly-(aspartate hydrazone adriamycin), in which the anticancer drug, adriamycin, was conjugated to the hydrophobic segments through acid-sensitive hydrazone linkers.[245, 246] The micelles were stable and able to preserve the drugs under physiological conditions (pH 7.4) and selectively released them through the cleavage of the hydrazone linkers in response to the decrease in the intracellular pH of the endosomes and lysosomes (pH 5-6). However, differences in extracellular pH between normal and tumor tissues are not significant enough to obtain effective release of therapeutics. The non-specific and early release of the payload is not avoidable.[178]

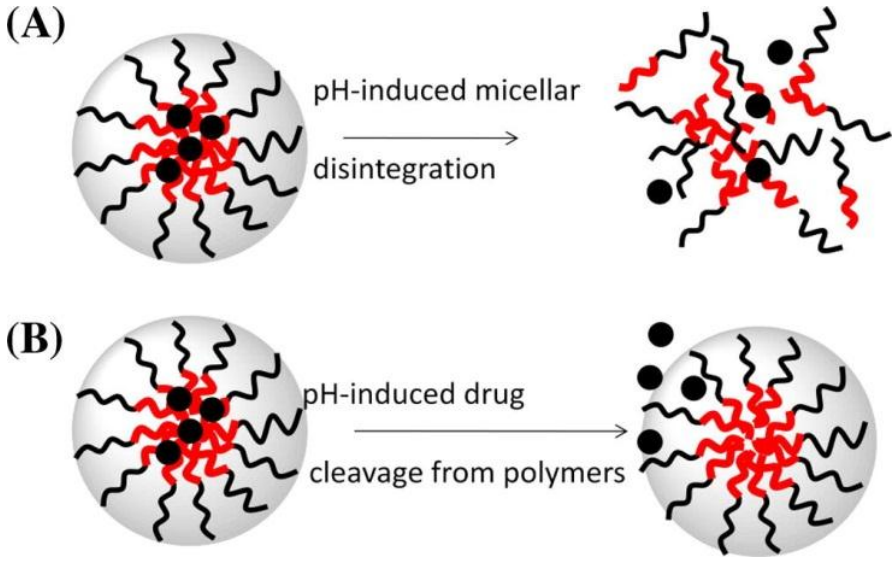

Figure 1.8 Two types of pH-sensitive micelles. (A) pH-induced disintegration of polymeric micelles; (B) pH-induced drug cleavage from polymers.[116]

1.2.2.2 Redox

It is well-established that the redox potential between extracellular and intracellular compartments is different.[247] The concentration of glutathione in the intracellular space is higher than in the extracellular space revealing a promising approach for the development of redox-sensitive carriers for intracellular delivery.[247] Therefore, in drug and gene delivery applications, the bioactive agents have to be protected by the carriers as they cross the cell membrane and become internalised by the cell before being disintegrated in the intracellular environment.[38, 178, 248] Polymers containing labile groups such as disulfide, which can be cleaved in reducing environments, have been employed in

designing many redox-sensitive carriers for drug and gene delivery systems (Figure 1.9).[249-259] For example, the Amiji group prepared thiolated gelatin by covalent modification of the primary amino groups of type B gelatin using 2-iminothiolane (Traut's reagent) for delivery of plasmid DNA in response to glutathione.[260, 261] Nevertheless, early breakdown of the carrier may occur because glutathione is also present in the extracellular environment.[178] Furthermore, the efficacy of delivery depends on the concentration of the intracellular redox potential which should be sufficient to trigger the degradation of the carriers. Additionally, differences in the trigger level in various cell lines is the challenge for this delivery system.[262]

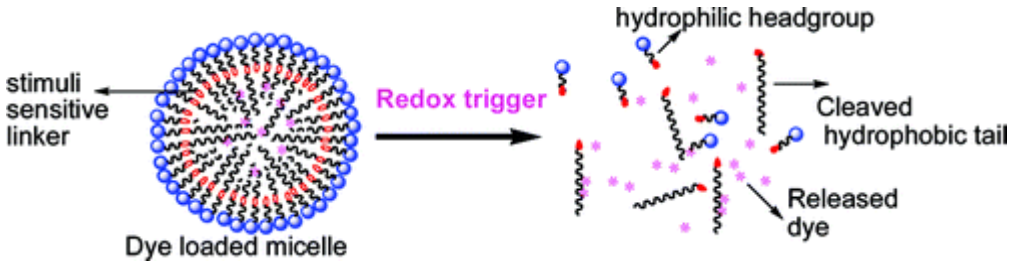

Figure 1.9 Schematic representation of stimuli-responsive micellar disassembly and guest release.[263]

1.2.3 Biologically induced release

The two representatives of biologically induced release are enzyme responsive and glucose responsive carriers.

1.2.3.1 Enzyme

Enzymes are potentially specific triggers that can be provided with large quantity while maintaining its high selectivity in triggering the delivery of drug and gene. The mechanism of this delivery system depends on the degradation carrier via the cleavage of ester or short peptide sequences by esterase or proteases triggered by enzymes in the living system.[178] In this kind of drug delivery system, enzymes are used to disrupt the polymer structure via polymer degradation, leading to dissociation or change in the morphology of the carriers. Enzyme degradable polymers or enzyme degradable linkages with different purposes have been used to design delivery platforms such as micelles and hydrogels (Figure 1.10).[51, 178, 264-267] Hennink and co-workers reported the preparation of micelles from triblock poly(oligo(ethylene glycol) monomethyl ether methacrylate)-b-peptide-b-poly(N-isopropylacryl) (POEGMA-b-peptide-b-PNIPAM).[268] The peptide can be selectively cleaved in the presence of matrix metalloproteinase (MMP) owing to the presence of an MMP-specific amino acid sequence in the middle peptide block of the triblock copolymer resulting in destabilization of the micellar nanoparticles. This makes these systems potentially suitable for

enzyme-triggered drug delivery. Although the degradation can work under mild conditions, the existence of enzyme is always required. Furthermore, the initial response time of this system is not precisely controlled.[226]

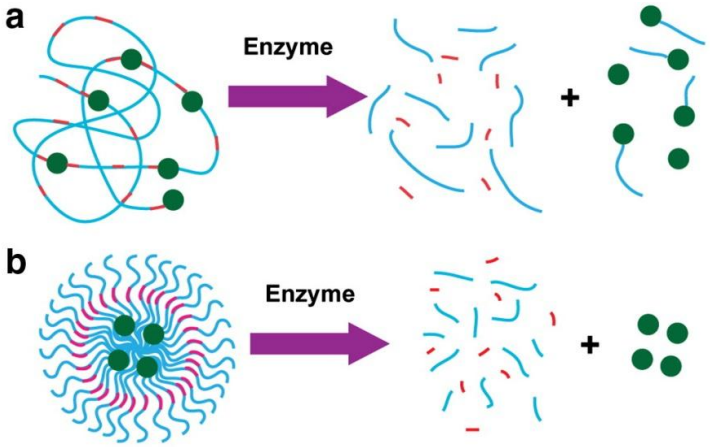

Figure 1.10 Enzyme-responsive nanomaterials for drug delivery.[267]

1.2.3.2 Glucose

Glucose responsive carriers for drug delivery such as insulin delivery has attracted remarkable attention over the past decades.[269] In this system, glucose oxidase (GOC) and glucose catalase (CAT) have been incorporated into the carrier loaded with insulin.[178] Glucose responsive polymer can combine with other responsive polymers such pH sensitive polymer, or enzyme sensitive polymer to engineer dual responsive carriers that have potential in insulin delivery (Figure 1.11).[270-272] In glucose environments, glucose oxidase (GOC) oxidizes glucose to gluconic acid which triggers the cleavage of the linkage of polymer and insulin or changes the conformation of the dual responsive carriers (e.g., pH and glucose responsive carrier) leading to release of the loaded insulin. However, the cleavage of the linkages or the change in the conformation is mainly regulated by the level of glucose in the body which may not be controllable. This drawback, therefore, may limit the application of this kind of carrier in designing systems for drug delivery.

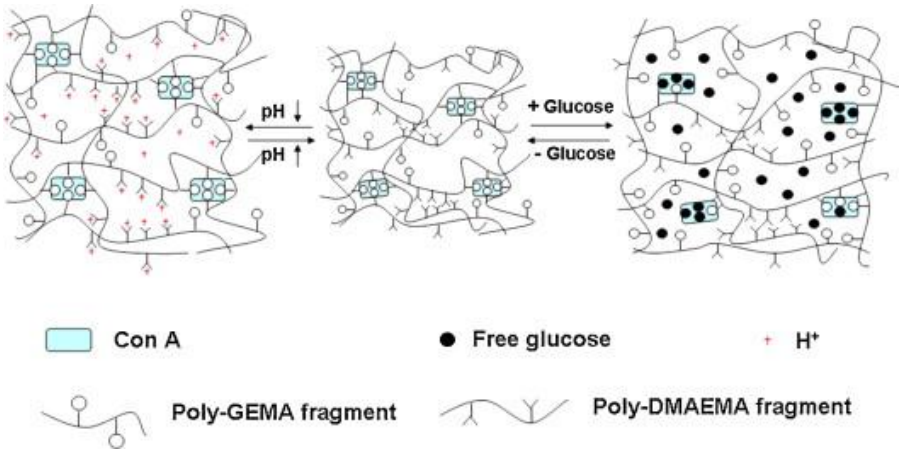

Figure 1.11 Schematic illustration of the structural changes in response to glucose and pH.[270]

1.2.4 The importance of timed-release and challenges

Generally, the release mechanism of the drug delivery systems mostly depends on either external (remote) or internal (environmental) stimuli. Nevertheless, accessibility of remote stimuli to tissues or organs is limited, and the level of environmental triggers can be different between cell lines and even within the same tissue or organ. Some smart polymer based delivery systems are thus limited in application, in complicated in vivo environments, although these systems may work very well in vitro.[273] Therefore, it is necessary to build up delivery system which is able to load and release bioactive agents independent of any external or internal stimuli in a controlled approach.

Recently, the Monteiro group has reported a novel polymeric carrier based on Poly(2-dimethylaminoethyl acrylate) (PDMAEA) that is able to release genetic material without any external or internal trigger. PDMAEA is a cationic polymer that can degrade through a self-catalyzed hydrolysis process independent of both the polymer molecular weight and solution pH.[274, 275] This self-catalyzed hydrolysis process of PDMAEA creates poly(acrylic acid) and 2-(dimethylamino) ethanol, both of which cause little or no toxicity to cells. The polymer can strongly bind, protect, and then release oligo DNA (a mimic for siRNA) in a time dependent manner. This polymer was also incorporated in the block copolymer poly(2-di methylaminoethyl acrylate)-b-P(N-(3-(1H-imidazol-1-yl)propyl) acrylamide-co-poly(butyl acrylate) (P(DMAEA-b-(ImPAA-co-BA))) to build up the carrier for the delivery of siRNA.[276] The polymer carrier is able to mimic the influenza virus escape mechanism from endosome and can timely release the siRNA to the cytosol through the degradation of PDMAEA. The polymer can degrade to benign products that showed no toxicity even at N/P of 300 exhibiting the potential for repeatable doses and long-term treatment of diseases.[277] This work suggested that siRNA delivery can specifically kill cells without the need of a dual delivery system that delivers both siRNA and a chemo-therapeutics. Furthermore, this block copolymer P(DMAEA-b-(ImPAA-co-BA)) was used to bind/complex, protect ,and release of plasmid DNA (pDNA). [278] Both entry pathways of the plasmid DNA/polymer complexes into the cell and the nucleus were investigated. The polyplex was taken up by HEK293 cells via clathrin-mediated endocytosis (CME) pathway and then rapidly escaped the endosome at a specific time, and facilitated the transport of the pDNA for the occurrence gene expression. pDNA was delivered to nucleus 7 times higher than commercial PEI Max after 24h. Although the release manner is time-dependent, the release time of these polymeric carriers is not able to control. Therefore, developing novel timed-release delivery systems that can release therapeutics in a controllable manner is the utmost priority in the field of timed-release materials.

1.3 RAFT polymerization

The Reversible addition−fragmentation chain-transfer polymerization (RAFT) is considered a powerful synthetic tool in polymer synthesis. In the RAFT technique, chain transfer agent (CTA) including dithioester, xanthate, dithiocarbamates, and trithiocarbonates compounds can be used to polymerize a wide range of monomers as well as reaction condition.[279, 280] The trithiocarbonates compound which is non-toxic can be applied in biomedical fields. The nature of the Z and R groups (Figure 1.12) which are the key to the structural features of this agent determines the effectiveness and its versatility. Based on these advantages, numerous polymer architectures such as functional polymer, gradient polymer, star polymers, cyclopolymers and block copolymers with controlled molecular weight and polydispersity have been synthesized by the RAFT technique.[281, 282] Therefore, RAFT is the technique utilized for polymer synthesis in this project.

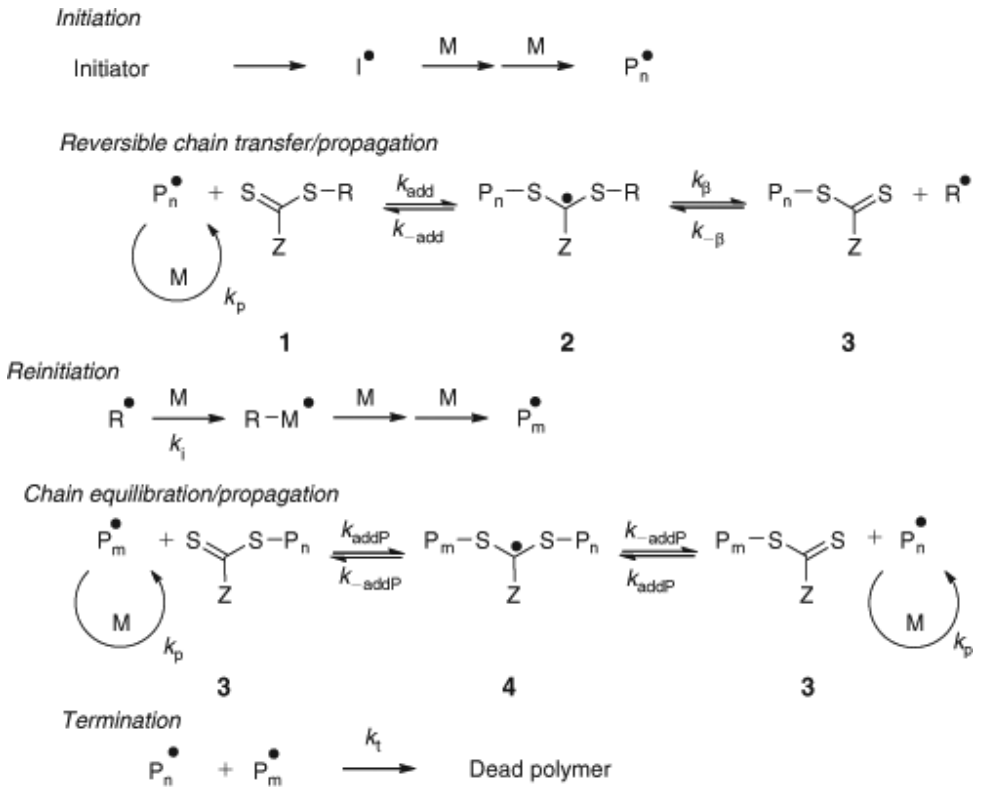

Figure 1.12 Mechanism of RAFT polymerization.[281]

1.4 Objectives and outlines of thesis

The main objective of the work described in this thesis was to synthesize and study novel timed-release polymeric nanoparticles and hydrogels based on thermoresponsive PNIPAM and self-degradable PDMAEA. In particular, efforts were made towards understanding the self-assembly and self-disassembly characteristics of thermoresponsive PNIPAM in the presence of self-degradable components and other factors such as hydrophilic and hydrophobic contents as well as surfactants. Such understanding established some general design principles to serve as guidelines for developing the next generation of nanocarriers with controllable timed-release characteristics.

Chapter 2 demonstrates the use of self-degradable PDMAEA together with hydrophobic components to finely tune the LCST and disassembly time of thermoresponsive PNIPAM as well as to control the release time of oligo DNA or siRNA from the polymer complex. The polymers consists of a hydrophilic block (e.g., PDMA) for stabilization and a second thermoresponsive block with three components (e.g., NIPAM, DMAEA and Styrene or BA) for self-assembly and disassembly. The diblock copolymer is fully water-soluble at temperatures below the second block's LCST, and when heated to 37 °C. The polymer self-assembles into a narrow size distribution of nanoparticles with an average diameter of approximately 25 nm. The nanoparticles are able to disassemble to unimers when the amount of acids groups from degradation of cationic DMAEA units is sufficiently high to increase the LCST of the second block above 37 °C. The nanoparticles show excellent binding to oligo DNA without any leakage until full disassembly to unimers and can only be taken up by osteosarcoma cells when coated with a transfection agent, folic acid.

Chapter 3 details the effect of the number of self-catalyzed degradable DMAEA and hydrophobic units (e.g., butyl acrylate and styrene) on both micelle disassembly time (t_{start}) and time from the start of disassembly to full unimer formation ($t_{degrade}$) of the novel timed-release nanoparticles. The t_{start} increases linearly with an increase in the number of hydrophobic BA units in the second block due to the decrease in LCST. By controlling the second block's composition, t_{start} therefore could be predicted. Additionally, the $t_{degrade}$ decreases when increasing the amount of DMAEA units in the second block. The ability to tune both t_{start} and $t_{degrade}$ allows the use of such timed-release nanoparticles for a wide range of applications.

Chapter 4 investigates the influence of surfactant on the formation of the polymeric micelles as well as LCST and the disassembly profile of the random polymers of thermoresponsive PNIPAM with self-degradable and hydrophobic components. At temperatures above the copolymer LCST,

SDS can stabilize the nanoparticles. The nanoparticle sizes have a very narrow distribution and can be controlled by manipulating SDS concentration. Moreover, the LCST of copolymers increases when the amount of SDS increases. The nanoparticles are stable when diluted. Furthermore, the addition of SDS does not affect the self-degradation of DMAEA as well as self-disassembly characteristic of the copolymer.

Chapter 5 describes the synthesis of a novel non-trigger release hydrogel system based on a series of self-degradable random copolymers synthesized from thermoresponsive NIPAM, self-catalysed hydrolysis DMAEA, hydrophilic PEGMEA, and hydrophobic BA. The thermoresponsive copolymers can form a stable gel at temperatures higher than the gelation point and then self-degrade into sol state after different times without the need of triggers. Moreover, the gelation temperature and degradation time can be controlled by manipulating the DMAEA units. Gold nanoparticles coated with PDMA can be encapsulated in the hydrogel and subsequently are able to be released at different rates. This novel non-trigger release hydrogel may find potential for applications where controlled-release is beneficial.

1.5 References

1. Jain, K., Nanodiagnostics: application of nanotechnology in molecular diagnostics. *Expert Rev. Mol. Diagn.* **2003,** 3, (2), 153-161.
2. Freitas Jr, R. A., What is nanomedicine? *Nanomedicine: Nanotechnology, Biology and Medicine* **2005,** 1, (1), 2-9.
3. Shaffer, C., Nanomedicine transforms drug delivery. *Drug Discov. Today* **2005,** 10, (23–24), 1581-1582.
4. Labhasetwar, V., Nanotechnology for drug and gene therapy: the importance of understanding molecular mechanisms of delivery. *Curr. Opin. Biotechnol.* **2005,** 16, (6), 674-680.
5. Sahoo, S. K.; Parveen, S.; Panda, J. J., The present and future of nanotechnology in human health care. *Nanomedicine: Nanotechnology, Biology and Medicine* **2007,** 3, (1), 20-31.
6. Lee, V. H. L.; Yamamoto, A., Penetration and enzymatic barriers to peptide and protein absorption. *Adv. Drug Delivery Rev.* **1989,** 4, (2), 171-207.
7. Sahoo, S. K.; Labhasetwar, V., Nanotech approaches to drug delivery and imaging. *Drug Discov. Today* **2003,** 8, (24), 1112-1120.
8. Cheng, M. M.-C.; Cuda, G.; Bunimovich, Y. L.; Gaspari, M.; Heath, J. R.; Hill, H. D.; Mirkin, C. A.; Nijdam, A. J.; Terracciano, R.; Thundat, T.; Ferrari, M., Nanotechnologies for biomolecular detection and medical diagnostics. *Curr. Opin. Chem. Biol.* **2006,** 10, (1), 11-19.
9. Emerich, D. F., Nanomedicine – prospective therapeutic and diagnostic applications. *Expert Opin. Biol. Ther.* **2005,** 5, (1), 1-5.
10. Li, K. C. P.; Pandit, S. D.; Guccione, S.; Bednarski, M. D., Molecular imaging applications in nanomedicine. *Biomedical Microdevices* **2004,** 6, (2), 113-116.
11. Safari, J.; Zarnegar, Z., Advanced drug delivery systems: Nanotechnology of health design A review. *Journal of Saudi Chemical Society* **2014,** 18, (2), 85-99.
12. Farokhzad, O. C.; Langer, R., Nanomedicine: Developing smarter therapeutic and diagnostic modalities. *Adv. Drug Delivery Rev.* **2006,** 58, (14), 1456-1459.
13. Kamaly, N.; Xiao, Z.; Valencia, P. M.; Radovic-Moreno, A. F.; Farokhzad, O. C., Targeted polymeric therapeutic nanoparticles: design, development and clinical translation. *Chem. Soc. Rev.* **2012,** 41, (7), 2971-3010.
14. Koo, H.; Huh, M. S.; Sun, I.-C.; Yuk, S. H.; Choi, K.; Kim, K.; Kwon, I. C., In Vivo Targeted Delivery of Nanoparticles for Theranosis. *Acc. Chem. Res.* **2011,** 44, (10), 1018-1028.
15. Moghimi, S. M.; Hunter, A. C.; Murray, J. C., Nanomedicine: current status and future prospects. *The FASEB Journal* **2005,** 19, (3), 311-330.
16. Wilkinson, J. M., Nanotechnology applications in medicine. *Med. Device Technol.* **2003,** 14, (5), 29-31.
17. Peer, D.; Karp, J. M.; Hong, S.; Farokhzad, O. C.; Margalit, R.; Langer, R., Nanocarriers as an emerging platform for cancer therapy. *Nat Nano* **2007,** 2, (12), 751-760.
18. Bae, Y.; Fukushima, S.; Harada, A.; Kataoka, K., Design of Environment-Sensitive Supramolecular Assemblies for Intracellular Drug Delivery: Polymeric Micelles that are Responsive to Intracellular pH Change. *Angew. Chem. Int. Ed.* **2003,** 42, (38), 4640-4643.
19. Hubbell, J. A.; Chilkoti, A., Nanomaterials for Drug Delivery. *Science* **2012,** 337, (6092), 303-305.
20. Farokhzad, O. C.; Langer, R., Impact of Nanotechnology on Drug Delivery. *ACS Nano* **2009,** 3, (1), 16-20.
21. Petros, R. A.; DeSimone, J. M., Strategies in the design of nanoparticles for therapeutic applications. *Nat. Rev. Drug Discov.* **2010,** 9, (8), 615-627.
22. Barreto, J. A.; O'Malley, W.; Kubeil, M.; Graham, B.; Stephan, H.; Spiccia, L., Nanomaterials: Applications in Cancer Imaging and Therapy. *Adv. Mater.* **2011,** 23, (12), H18-H40.
23. Shi, J.; Votruba, A. R.; Farokhzad, O. C.; Langer, R., Nanotechnology in Drug Delivery and Tissue Engineering: From Discovery to Applications. *Nano Lett.* **2010,** 10, (9), 3223-3230.

24. Kubik, T.; Bogunia-Kubik, K.; Sugisaka, M., Nanotechnology on duty in medical applications. *Curr. Pharm. Biotechnol.* **2005,** 6, (1), 17-33.
25. Kayser, O.; Lemke, A.; Hernández-Trejo, N., The impact of nanobiotechnology on the development of new drug delivery systems. *Curr. Pharm. Biotechnol.* **2005,** 6, (1), 3-5.
26. Orive, G.; Hernández, R. M.; Gascón, A. R. g.; Domínguez-Gil, A.; Pedraz, J. L., Drug delivery in biotechnology: present and future. *Curr. Opin. Biotechnol.* **2003,** 14, (6), 659-664.
27. Vasir, J. K.; Labhasetwar, V., Targeted drug delivery in cancer therapy. *Technol. Cancer Res. Treat.* **2005,** 4, (4), 363-374.
28. Griffith, L. G., Polymeric biomaterials. *Acta Mater.* **2000,** 48, (1), 263-277.
29. Langer, R.; Tirrell, D. A., Designing materials for biology and medicine. *Nature* **2004,** 428, (6982), 487-492.
30. Metzke, M.; O'Connor, N.; Maiti, S.; Nelson, E.; Guan, Z. B., Saccharide-peptide hybrid copolymers as biomaterials. *Angew Chem Int Edit* **2005,** 44, (40), 6529-6533.
31. Ringsdorf, H., Structure and Properties of Pharmacologically Active Polymers. *J Polym Sci Pol Sym* **1975**, (51), 135-153.
32. Angelova, N. H., D., Tibtech: 1999; Vol. 17.
33. Guelcher, S. H., J., *An introduction to Biomaterials*. CRC Press: 2006.
34. Park, J. B. B., J.D.; , *Biomaterials: Principles and Applications* CRC Press: 2002.
35. Ratner, B. D. H., A.S; Schoen, F.J; Lemon, J.E. Eds, *Biomaterials Science*. Academic Press: Orlando, 1996.
36. Shalaby, S. W., *Biommedical Polymers, Designes to Degrade Systems*. Hanser Gardner Publications, Inc.: Cincinnati, 1994.
37. Schmaljohann, D., Thermo- and pH-responsive polymers in drug delivery. *Adv. Drug Delivery Rev.* **2006,** 58, (15), 1655-1670.
38. Ganta, S.; Devalapally, H.; Shahiwala, A.; Amiji, M., A review of stimuli-responsive nanocarriers for drug and gene delivery. *J. Controlled Release* **2008,** 126, (3), 187-204.
39. Liu, S.; Maheshwari, R.; Kiick, K. L., Polymer-Based Therapeutics. *Macromolecules* **2009,** 42, (1), 3-13.
40. Dhal, P.; Holmes-Farley, S. R.; Huval, C.; Jozefiak, T., Polymers as Drugs. In *Polymer Therapeutics I*, Satchi-Fainaro, R.; Duncan, R., Eds. Springer Berlin Heidelberg: 2006; Vol. 192, pp 9-58.
41. Kiick, K. L., Polymer Therapeutics. *Science* **2007,** 317, (5842), 1182-1183.
42. Duncan, R., Polymer conjugates as anticancer nanomedicines. *Nat. Rev. Cancer* **2006,** 6, (9), 688-701.
43. Watson, K. J.; Anderson, D. R.; Nguyen, S. T., Toward Polymeric Anticancer Drug Cocktails from Ring-Opening Metathesis Polymerization. *Macromolecules* **2001,** 34, (11), 3507-3509.
44. Kim, Y. S.; Gil, E. S.; Lowe, T. L., Synthesis and Characterization of Thermoresponsive-co-Biodegradable Linear−Dendritic Copolymers. *Macromolecules* **2006,** 39, (23), 7805-7811.
45. York, A. W.; Kirkland, S. E.; McCormick, C. L., Advances in the synthesis of amphiphilic block copolymers via RAFT polymerization: Stimuli-responsive drug and gene delivery. *Adv. Drug Delivery Rev.* **2008,** 60, (9), 1018-1036.
46. Ulery, B. D.; Nair, L. S.; Laurencin, C. T., Biomedical applications of biodegradable polymers. *Journal of Polymer Science Part B: Polymer Physics* **2011,** 49, (12), 832-864.
47. Hoste, K.; De Winne, K.; Schacht, E., Polymeric prodrugs. *Int. J. Pharm.* **2004,** 277, (1–2), 119-131.
48. Khandare, J.; Minko, T., Polymer–drug conjugates: Progress in polymeric prodrugs. *Prog. Polym. Sci.* **2006,** 31, (4), 359-397.
49. Anil, M.; Ankur, S. K., *Polymers for Biomedical Applications*. American Chemical Society: 2008; Vol. 977, p 438.
50. Bajpai, A. K.; Shukla, S. K.; Bhanu, S.; Kankane, S., Responsive polymers in controlled drug delivery. *Prog. Polym. Sci.* **2008,** 33, (11), 1088-1118.

51. Esser-Kahn, A. P.; Odom, S. A.; Sottos, N. R.; White, S. R.; Moore, J. S., Triggered Release from Polymer Capsules. *Macromolecules* **2011,** 44, (14), 5539-5553.
52. Onaca, O.; Enea, R.; Hughes, D. W.; Meier, W., Stimuli-Responsive Polymersomes as Nanocarriers for Drug and Gene Delivery. *Macromol. Biosci.* **2009,** 9, (2), 129-139.
53. Discher, B. M.; Won, Y.-Y.; Ege, D. S.; Lee, J. C.-M.; Bates, F. S.; Discher, D. E.; Hammer, D. A., Polymersomes: Tough Vesicles Made from Diblock Copolymers. *Science* **1999,** 284, (5417), 1143-1146.
54. Ahmed, F.; Discher, D. E., Self-porating polymersomes of PEG–PLA and PEG–PCL: hydrolysis-triggered controlled release vesicles. *J. Controlled Release* **2004,** 96, (1), 37-53.
55. Brinkhuis, R. P.; Rutjes, F. P. J. T.; van Hest, J. C. M., Polymeric vesicles in biomedical applications. *Polym Chem-Uk* **2011,** 2, (7), 1449-1462.
56. Shcharbin, D.; Shakhbazau, A.; Bryszewska, M., Poly(amidoamine) dendrimer complexes as a platform for gene delivery. *Expert Opin. Drug Deliv.* **2013,** 10, (12), 1687-1698.
57. Yavuz, B.; #xe7; in; Bozda; #x11f; Pehlivan, S.; #xdc; nl; #xfc; , N.; #x15f; en, Dendrimeric Systems and Their Applications in Ocular Drug Delivery. *The Scientific World Journal* **2013,** 2013, 13.
58. Madaan, K.; Kumar, S.; Poonia, N.; Lather, V.; Pandita, D., *Dendrimers in drug delivery and targeting: Drug-dendrimer interactions and toxicity issues*. 2014; Vol. 6, p 139-150.
59. Hubbell, J. A., Enhancing Drug Function. *Science* **2003,** 300, (5619), 595-596.
60. Rapoport, N., Physical stimuli-responsive polymeric micelles for anti-cancer drug delivery. *Progress in Polymer Science (Oxford)* **2007,** 32, (8-9), 962-990.
61. Nasongkla, N.; Shuai, X.; Ai, H.; Weinberg, B. D.; Pink, J.; Boothman, D. A.; Gao, J., cRGD-Functionalized Polymer Micelles for Targeted Doxorubicin Delivery. *Angew. Chem.* **2004,** 116, (46), 6483-6487.
62. Jones, M.-C.; Leroux, J.-C., Polymeric micelles – a new generation of colloidal drug carriers. *Eur. J. Pharm. Biopharm.* **1999,** 48, (2), 101-111.
63. Kwon, G. S.; Okano, T., Polymeric micelles as new drug carriers. *Adv. Drug Delivery Rev.* **1996,** 21, (2), 107-116.
64. Xiong, X.-B.; Falamarzian, A.; Garg, S. M.; Lavasanifar, A., Engineering of amphiphilic block copolymers for polymeric micellar drug and gene delivery. *J. Controlled Release* **2011,** 155, (2), 248-261.
65. Husseini, G. A.; Pitt, W. G., Micelles and nanoparticles for ultrasonic drug and gene delivery. *Adv. Drug Delivery Rev.* **2008,** 60, (10), 1137-1152.
66. Zhao, Y., Light-Responsive Block Copolymer Micelles. *Macromolecules* **2012,** 45, (9), 3647-3657.
67. Kwon, G. S.; Kataoka, K., Block copolymer micelles as long-circulating drug vehicles. *Adv. Drug Delivery Rev.* **1995,** 16, (2–3), 295-309.
68. Kataoka, K.; Harada, A.; Nagasaki, Y., Block copolymer micelles for drug delivery: design, characterization and biological significance. *Adv. Drug Delivery Rev.* **2001,** 47, (1), 113-131.
69. Gaucher, G.; Dufresne, M.-H.; Sant, V. P.; Kang, N.; Maysinger, D.; Leroux, J.-C., Block copolymer micelles: preparation, characterization and application in drug delivery. *J. Controlled Release* **2005,** 109, (1–3), 169-188.
70. Kedar, U.; Phutane, P.; Shidhaye, S.; Kadam, V., Advances in polymeric micelles for drug delivery and tumor targeting. *Nanomedicine: Nanotechnology, Biology and Medicine* **2010,** 6, (6), 714-729.
71. Rösler, A.; Vandermeulen, G. W. M.; Klok, H.-A., Advanced drug delivery devices via self-assembly of amphiphilic block copolymers. *Adv. Drug Delivery Rev.* **2001,** 53, (1), 95-108.
72. Cammas, S.; Suzuki, K.; Sone, C.; Sakurai, Y.; Kataoka, K.; Okano, T., Thermo-responsive polymer nanoparticles with a core-shell micelle structure as site-specific drug carriers. *J. Controlled Release* **1997,** 48, (2–3), 157-164.
73. Lee, S. C.; Kwon, I. K.; Park, K., Hydrogels for delivery of bioactive agents: A historical perspective. *Adv. Drug Delivery Rev.* **2013,** 65, (1), 17-20.

74. Vermonden, T.; Censi, R.; Hennink, W. E., Hydrogels for Protein Delivery. *Chem. Rev.* **2012,** 112, (5), 2853-2888.
75. Hoare, T. R.; Kohane, D. S., Hydrogels in drug delivery: Progress and challenges. *Polymer* **2008,** 49, (8), 1993-2007.
76. Kretlow, J. D.; Klouda, L.; Mikos, A. G., Injectable matrices and scaffolds for drug delivery in tissue engineering. *Adv. Drug Delivery Rev.* **2007,** 59, (4–5), 263-273.
77. Hoffman, A. S., Hydrogels for biomedical applications. *Adv. Drug Delivery Rev.* **2002,** 54, (1), 3-12.
78. Gupta, P.; Vermani, K.; Garg, S., Hydrogels: from controlled release to pH-responsive drug delivery. *Drug Discov. Today* **2002,** 7, (10), 569-579.
79. Hennink, W. E.; van Nostrum, C. F., Novel crosslinking methods to design hydrogels. *Adv. Drug Delivery Rev.* **2002,** 54, (1), 13-36.
80. Li, Z.; Guan, J., Thermosensitive hydrogels for drug delivery. *Expert Opin. Drug Deliv.* **2011,** 8, (8), 991-1007.
81. Gong, C.; Qi, T.; Wei, X.; Qu, Y.; Wu, Q.; Luo, F.; Qian, Z., Thermosensitive Polymeric Hydrogels As Drug Delivery Systems. *Curr. Med. Chem.* **2013,** 20, (1), 79-94.
82. Jeong, B.; Kim, S. W.; Bae, Y. H., Thermosensitive sol–gel reversible hydrogels. *Adv. Drug Delivery Rev.* **2012,** 64, Supplement, (0), 154-162.
83. Hatefi, A.; Amsden, B., Biodegradable injectable in situ forming drug delivery systems. *J. Controlled Release* **2002,** 80, (1–3), 9-28.
84. Zelikin, A. N., Drug Releasing Polymer Thin Films: New Era of Surface-Mediated Drug Delivery. *ACS Nano* **2010,** 4, (5), 2494-2509.
85. Yan, W.; Hsiao, V. K. S.; Zheng, Y. B.; Shariff, Y. M.; Gao, T.; Huang, T. J., Towards nanoporous polymer thin film-based drug delivery systems. *Thin Solid Films* **2009,** 517, (5), 1794-1798.
86. Taillefer, J.; Jones, M. C.; Brasseur, N.; van Lier, J. E.; Leroux, J. C., Preparation and characterization of ph-responsive polymeric micelles for the delivery of photosensitizing anticancer drugs. *J. Pharm. Sci.* **2000,** 89, (1), 52-62.
87. Liu, X.-M.; Yang, Y.-Y.; Leong, K. W., Thermally responsive polymeric micellar nanoparticles self-assembled from cholesteryl end-capped random poly(N-isopropylacrylamide-co-N,N-dimethylacrylamide): synthesis, temperature-sensitivity, and morphologies. *J. Colloid Interface Sci.* **2003,** 266, (2), 295-303.
88. Kwon, G. S., Diblock Copolymer Nanoparticles for Drug Delivery. **1998,** 15, (5), 32.
89. Wei, H.; Cheng, S.-X.; Zhang, X.-Z.; Zhuo, R.-X., Thermo-sensitive polymeric micelles based on poly(N-isopropylacrylamide) as drug carriers. *Prog. Polym. Sci.* **2009,** 34, (9), 893-910.
90. Masayuki, Y.; Mizue, M.; Noriko, Y.; Teruo, O.; Yasuhisa, S.; Kazunori, K.; Shohei, I., Polymer micelles as novel drug carrier: Adriamycin-conjugated poly(ethylene glycol)-poly(aspartic acid) block copolymer. *J. Controlled Release* **1990,** 11, (1–3), 269-278.
91. Jung, B.; Jeong, Y.-C.; Min, J.-H.; Kim, J.-E.; Song, Y.-J.; Park, J.-K.; Park, J.-H.; Kim, J.-D., Tumor-binding prodrug micelles of polymer-drug conjugates for anticancer therapy in HeLa cells. *J. Mater. Chem.* **2012,** 22, (18), 9385-9394.
92. Yokoyama, M.; Inoue, S.; Kataoka, K.; Yui, N.; Sakurai, Y., Preparation of adriamycin-conjugated poly(ethylene glycol)-poly(aspartic acid) block copolymer. A new type of polymeric anticancer agent. *Die Makromolekulare Chemie, Rapid Communications* **1987,** 8, (9), 431-435.
93. Cammas, S.; Matsumoto, T.; Okano, T.; Sakurai, Y.; Kataoka, K., Design of functional polymeric micelles as site-specific drug vehicles based on poly(α-hydroxy ethylene oxide-co-β-benzyl L-aspartate) block copolymers. *Materials Science and Engineering C* **1997,** 4, (4), 241-247.
94. Kataoka, K.; Matsumoto, T.; Yokoyama, M.; Okano, T.; Sakurai, Y.; Fukushima, S.; Okamoto, K.; Kwon, G. S., Doxorubicin-loaded poly(ethylene glycol)-poly(β-benzyl-L-

aspartate) copolymer micelles: Their pharmaceutical characteristics and biological significance. *J. Controlled Release* **2000,** 64, (1-3), 143-153.
95. Kwon, G.; Naito, M.; Yokoyama, M.; Okano, T.; Sakurai, Y.; Kataoka, K., Block copolymer micelles for drug delivery: Loading and release of doxorubicin. *J. Controlled Release* **1997,** 48, (2-3), 195-201.
96. Harada, A.; Kataoka, K., Novel Polyion Complex Micelles Entrapping Enzyme Molecules in the Core. 2. Characterization of the Micelles Prepared at Nonstoichiometric Mixing Ratios. *Langmuir* **1999,** 15, (12), 4208-4212.
97. Katayose, S.; Kataoka, K., Water-Soluble Polyion Complex Associates of DNA and Poly(ethylene glycol)−Poly(l-lysine) Block Copolymer. *Bioconjugate Chem.* **1997,** 8, (5), 702-707.
98. Katayose, S.; Kataoka, K., Remarkable increase in nuclease resistance of plasmid DNA through supramolecular assembly with poly(ethylene glycol)—poly(L-lysine) block copolymer. *J. Pharm. Sci.* **1998,** 87, (2), 160-163.
99. Boussif, O.; Zanta, M. A.; Behr, J. P., Optimized galenics improve in vitro gene transfer with cationic molecules up to 1000-fold. *Gene Ther.* **1996,** 3, (12), 1074-1080.
100. Vinogradov, S. V.; Bronich, T. K.; Kabanov, A. V., Self-Assembly of Polyamine−Poly(ethylene glycol) Copolymers with Phosphorothioate Oligonucleotides. *Bioconjugate Chem.* **1998,** 9, (6), 805-812.
101. Vinogradov, S.; Batrakova, E.; Li, S.; Kabanov, A., Polyion Complex Micelles with Protein-Modified Corona for Receptor-Mediated Delivery of Oligonucleotides into Cells. *Bioconjugate Chem.* **1999,** 10, (5), 851-860.
102. Yokoyama, M.; Okano, T.; Sakurai, Y.; Suwa, S.; Kataoka, K., Introduction of cisplatin into polymeric micelle. *J. Controlled Release* **1996,** 39, (2-3), 351-356.
103. Yokoyama, M.; Miyauchi, M.; Yamada, N.; Okano, T.; Sakurai, Y.; Kataoka, K.; Inoue, S., Characterization and anticancer activity of the micelle-forming polymeric anticancer drug adriamycin-conjugated poly(ethylene glycol)-poly(aspartic acid) block copolymer. *Cancer Res.* **1990,** 50, (6), 1693-1700.
104. Kataoka, K.; Togawa, H.; Harada, A.; Yasugi, K.; Matsumoto, T.; Katayose, S., Spontaneous Formation of Polyion Complex Micelles with Narrow Distribution from Antisense Oligonucleotide and Cationic Block Copolymer in Physiological Saline. *Macromolecules* **1996,** 29, (26), 8556-8557.
105. Shen, Y.; Li, Q.; Tu, J.; Zhu, J., Synthesis and characterization of low molecular weight hyaluronic acid-based cationic micelles for efficient siRNA delivery. *Carbohydr. Polym.* **2009,** 77, (1), 95-104.
106. Hrubý, M.; Koňák, C.; Ulbrich, K., Polymeric micellar pH-sensitive drug delivery system for doxorubicin. *J. Controlled Release* **2005,** 103, (1), 137-148.
107. La, S. B.; Okano, T.; Kataoka, K., Preparation and characterization of the micelle-forming polymeric drug indomethacin-incorporated poly(ethylene oxide)–poly(β-benzyl L-aspartate) block copolymer micelles. *J. Pharm. Sci.* **1996,** 85, (1), 85-90.
108. Yokoyama, M.; Okano, T.; Sakurai, Y.; Kataoka, K., Improved synthesis of adriamycin-conjugated poly (ethylene oxide)-poly (aspartic acid) block copolymer and formation of unimodal micellar structure with controlled amount of physically entrapped adriamycin. *J. Controlled Release* **1994,** 32, (3), 269-277.
109. Chan, J. M.; Zhang, L.; Yuet, K. P.; Liao, G.; Rhee, J. W.; Langer, R.; Farokhzad, O. C., PLGA-lecithin-PEG core-shell nanoparticles for controlled drug delivery. *Biomaterials* **2009,** 30, (8), 1627-1634.
110. Wang, Y.; Yu, L.; Han, L.; Sha, X.; Fang, X., Difunctional Pluronic copolymer micelles for paclitaxel delivery: Synergistic effect of folate-mediated targeting and Pluronic-mediated overcoming multidrug resistance in tumor cell lines. *Int. J. Pharm.* **2007,** 337, (1–2), 63-73.
111. Hamaguchi, T.; Matsumura, Y.; Suzuki, M.; Shimizu, K.; Goda, R.; Nakamura, I.; Nakatomi, I.; Yokoyama, M.; Kataoka, K.; Kakizoe, T., NK105, a paclitaxel-incorporating micellar

nanoparticle formulation, can extend in vivo antitumour activity and reduce the neurotoxicity of paclitaxel. *Br. J. Cancer* **2005,** 92, (7), 1240-1246.
112. Nakanishi, T.; Fukushima, S.; Okamoto, K.; Suzuki, M.; Matsumura, Y.; Yokoyama, M.; Okano, T.; Sakurai, Y.; Kataoka, K., Development of the polymer micelle carrier system for doxorubicin. *J. Controlled Release* **2001,** 74, (1-3), 295-302.
113. Nishiyama, N.; Okazaki, S.; Cabral, H.; Miyamoto, M.; Kato, Y.; Sugiyama, Y.; Nishio, K.; Matsumura, Y.; Kataoka, K., Novel Cisplatin-Incorporated Polymeric Micelles Can Eradicate Solid Tumors in Mice. *Cancer Res.* **2003,** 63, (24), 8977-8983.
114. Wakebayashi, D.; Nishiyama, N.; Itaka, K.; Miyata, K.; Yamasaki, Y.; Harada, A.; Koyama, H.; Nagasaki, Y.; Kataoka, K., Polyion Complex Micelles of pDNA with Acetal-poly(ethylene glycol)-poly(2-(dimethylamino)ethyl methacrylate) Block Copolymer as the Gene Carrier System: Physicochemical Properties of Micelles Relevant to Gene Transfection Efficacy. *Biomacromolecules* **2004,** 5, (6), 2128-2136.
115. Wakebayashi, D.; Nishiyama, N.; Yamasaki, Y.; Itaka, K.; Kanayama, N.; Harada, A.; Nagasaki, Y.; Kataoka, K., Lactose-conjugated polyion complex micelles incorporating plasmid DNA as a targetable gene vector system: Their preparation and gene transfecting efficiency against cultured HepG2 cells. *J. Controlled Release* **2004,** 95, (3), 653-664.
116. Xiong, X.-B.; Binkhathlan, Z.; Molavi, O.; Lavasanifar, A., Amphiphilic block co-polymers: Preparation and application in nanodrug and gene delivery. *Acta Biomater.* **2012,** 8, (6), 2017-2033.
117. Yokoyama, M.; Kwon, G. S.; Okano, T.; Sakurai, Y.; Seto, T.; Kataoka, K., Preparation of micelle-forming polymer-drug conjugates. *Bioconjugate Chem.* **1992,** 3, (4), 295-301.
118. Wright, J., Nanotechnology: Deliver on a promise. *Nature* **2014,** 509, (7502), S58-S59.
119. Brannon-Peppas, L.; Blanchette, J. O., Nanoparticle and targeted systems for cancer therapy. *Adv. Drug Delivery Rev.* **2004,** 56, (11), 1649-1659.
120. Brigger, I.; Dubernet, C.; Couvreur, P., Nanoparticles in cancer therapy and diagnosis. *Adv. Drug Delivery Rev.* **2012,** 64, Supplement, (0), 24-36.
121. Ward, M. A.; Georgiou, T. K., Thermoresponsive Polymers for Biomedical Applications. *Polymers* **2011,** 3, (3), 1215-1242.
122. Qiu, Y.; Park, K., Environment-sensitive hydrogels for drug delivery. *Adv. Drug Delivery Rev.* **2001,** 53, (3), 321-339.
123. Mi, L.; Fischer, S.; Chung, B.; Sundelacruz, S.; Harden, J. L., Self-assembling protein hydrogels with modular integrin binding domains. *Biomacromolecules* **2006,** 7, (1), 38-47.
124. Reddy, T. T.; Lavenant, L.; Lefebvre, J.; Renard, D., Swelling behavior and controlled release of theopylline and sulfamethoxazole drugs in β-lactoglobulin protein gels obtained by phase separation in water/ethanol mixture. *Biomacromolecules* **2006,** 7, (1), 323-330.
125. Wood, K. C.; Boedicker, J. Q.; Lynn, D. M.; Hammond, P. T., Tunable drug release from hydrolytically degradable layer-by-layer thin films. *Langmuir* **2005,** 21, (4), 1603-1609.
126. Kozlovskaya, V.; Kharlampieva, E.; Mansfield, M. L.; Sukhishvili, S. A., Poly(methacrylie acid) hydrogel films and capsules: Response to pH and ionic strength, and encapsulation of macromolecules. *Chem. Mater.* **2006,** 18, (2), 328-336.
127. Berg, M. C.; Zhai, L.; Cohen, R. E.; Rubner, M. F., Controlled drug release from porous polyelectrolyte multilayers. *Biomacromolecules* **2006,** 7, (1), 357-364.
128. Guvendiren, M.; Messersmith, P. B.; Shull, K. R., Self-assembly and adhesion of DOPA-modified methacrylic triblock hydrogels. *Biomacromolecules* **2008,** 9, (1), 122-128.
129. Li, C.; Tang, Y.; Armes, S. P.; Morris, C. J.; Rose, S. F.; Lloyd, A. W.; Lewis, A. L., Synthesis and characterization of biocompatible thermo-responsive gelators based on ABA triblock copolymers. *Biomacromolecules* **2005,** 6, (2), 994-999.
130. Madsen, J.; Armes, S. P.; Lewis, A. L., Preparation and aqueous solution properties of new thermoresponsive biocompatible ABA triblock copolymer gelators. *Macromolecules* **2006,** 39, (22), 7455-7457.

131. Li, S.; El Ghzaoui, A.; Dewinck, E., Rheology and drug release properties of bioresorbable hydrogels prepared from polylactide/poly(ethylene glycol) block copolymers. *Macromol. Symp.* **2005,** 222, 23-35.
132. Lee, J.; Bae, Y. H.; Sohn, Y. S.; Jeong, B., Thermogelling aqueous solutions of alternating multiblock copolymers of poly(L-lactic acid) and poly(ethylene glycol). *Biomacromolecules* **2006,** 7, (6), 1729-1734.
133. Shim, W. S.; Kim, S. W.; Lee, D. S., Sulfonamide-based pH- and temperature-sensitive biodegradable block copolymer hydrogels. *Biomacromolecules* **2006,** 7, (6), 1935-1941.
134. Park, S. Y.; Lee, Y.; Bae, K. H.; Ahn, C. H.; Park, T. G., Temperature/pH-sensitive hydrogels prepared from pluronic copolymers end-capped with carboxylic acid groups via an oligolactide spacer. *Macromol. Rapid Commun.* **2007,** 28, (10), 1172-1176.
135. Mequanint, K.; Patel, A.; Bezuidenhout, D., Synthesis, swelling behavior, and biocompatibility of novel physically cross-linked polyurethane-block-poly(glycerol methacylate) hydrogels. *Biomacromolecules* **2006,** 7, (3), 883-891.
136. Dai, H.; Chen, Q.; Qin, H.; Guan, Y.; Shen, D.; Hua, Y.; Tang, Y.; Xu, J., A Temperature-Responsive Copolymer Hydrogel in Controlled Drug Delivery. *Macromolecules* **2006,** 39, (19), 6584-6589.
137. Miquelard-Garnier, G.; Demeures, S.; Creton, C.; Hourdet, D., Synthesis and rheological behavior of new hydrophobically modified hydrogels with tunable properties. *Macromolecules* **2006,** 39, (23), 8128-8139.
138. Kretschmann, O.; Schmitz, S.; Ritter, H., Microwave-assisted synthesis of associative hydrogels. *Macromol. Rapid Commun.* **2007,** 28, (11), 1265-1269.
139. Ajayaghosh, A.; Varghese, R.; Praveen, V. K.; Mahesh, S., Evolution of nano- to microsized spherical assemblies of a short oligo(p-phenylene-ethynylene) into superstructured organogels. *Angewandte Chemie - International Edition* **2006,** 45, (20), 3261-3264.
140. Wang, C.; Zhang, D.; Xiang, J.; Zhu, D., New organogels based on an anthracene derivative with one urea group and its photodimer: Fluorescence enhancement after gelation. *Langmuir* **2007,** 23, (18), 9195-9200.
141. Miyauchi, M.; Takashima, Y.; Yamaguchi, H.; Harada, A., Chiral supramolecular polymers formed by host-guest interactions. *J. Am. Chem. Soc.* **2005,** 127, (9), 2984-2989.
142. Miyauchi, M.; Hoshino, T.; Yamaguchi, H.; Kamitori, S.; Harada, A., A [2]rotaxane capped by a cyclodextrin and a guest: Formation of supramolecular [2]rotaxane polymer. *J. Am. Chem. Soc.* **2005,** 127, (7), 2034-2035.
143. Weng, W.; Benjamin Beck, J.; Jamieson, A. M.; Rowan, S. J., Understanding the mechanism of gelation and stimuli-responsive nature of a class of metallo-supramolecular gels. *J. Am. Chem. Soc.* **2006,** 128, (35), 11663-11672.
144. Deng, W.; Yamaguchi, H.; Takashima, Y.; Harada, A., A chemical-responsive supramolecular hydrogel from modified cyclodextrins. *Angewandte Chemie - International Edition* **2007,** 46, (27), 5144-5147.
145. Loh, X. J.; Peh, P.; Liao, S.; Sng, C.; Li, J., Controlled drug release from biodegradable thermoresponsive physical hydrogel nanofibers. *J. Controlled Release* **2010,** 143, (2), 175-182.
146. Gong, C.; Shi, S.; Dong, P.; Kan, B.; Gou, M.; Wang, X.; Li, X.; Luo, F.; Zhao, X.; Wei, Y.; Qian, Z., Synthesis and characterization of PEG-PCL-PEG thermosensitive hydrogel. *Int. J. Pharm.* **2009,** 365, (1–2), 89-99.
147. Cui, Z.; Lee, B. H.; Pauken, C.; Vernon, B. L., Degradation, cytotoxicity, and biocompatibility of NIPAAm-based thermosensitive, injectable, and bioresorbable polymer hydrogels. *Journal of Biomedical Materials Research Part A* **2011,** 98A, (2), 159-166.
148. Vermonden, T.; Jena, S. S.; Barriet, D.; Censi, R.; van der Gucht, J.; Hennink, W. E.; Siegel, R. A., Macromolecular Diffusion in Self-Assembling Biodegradable Thermosensitive Hydrogels. *Macromolecules* **2009,** 43, (2), 782-789.

149. Guan, J.; Hong, Y.; Ma, Z.; Wagner, W. R., Protein-Reactive, Thermoresponsive Copolymers with High Flexibility and Biodegradability. *Biomacromolecules* **2008,** 9, (4), 1283-1292.
150. Makino, K.; Hiyoshi, J.; Ohshima, H., Kinetics of swelling and shrinking of poly (N-isopropylacrylamide) hydrogels at different temperatures. *Colloids and Surfaces B: Biointerfaces* **2000,** 19, (2), 197-204.
151. Henderson, E.; Lee, B. H.; Cui, Z.; McLemore, R.; Brandon, T. A.; Vernon, B. L., In vivo evaluation of injectable thermo-sensitive polymer with time-dependent LCST. *J. Biomed. Mater. Res. A* **2009,** 90, (4), 1186-1197.
152. Han, C. K.; Bae, Y. H., Inverse thermally-reversible gelation of aqueous N-isopropylacrylamide copolymer solutions. *Polymer* **1998,** 39, (13), 2809-2814.
154. Oh, J. K.; Drumright, R.; Siegwart, D. J.; Matyjaszewski, K., The development of microgels/nanogels for drug delivery applications. *Prog. Polym. Sci.* **2008,** 33, (4), 448-477.
155. Ruel-Gariépy, E.; Leroux, J.-C., In situ-forming hydrogels—review of temperature-sensitive systems. *Eur. J. Pharm. Biopharm.* **2004,** 58, (2), 409-426.
156. Roy, D.; Brooks, W. L. A.; Sumerlin, B. S., New directions in thermoresponsive polymers. *Chem. Soc. Rev.* **2013,** 42, (17), 7214-7243.
157. Vihola, H.; Laukkanen, A.; Valtola, L.; Tenhu, H.; Hirvonen, J., Cytotoxicity of thermosensitive polymers poly(N-isopropylacrylamide), poly(N-vinylcaprolactam) and amphiphilically modified poly(N-vinylcaprolactam). *Biomaterials* **2005,** 26, (16), 3055-3064.
158. Scarpa, J. S.; Mueller, D. D.; Klotz, I. M., Slow hydrogen-deuterium exchange in a non-.alpha.-helical polyamide. *J. Am. Chem. Soc.* **1967,** 89, (24), 6024-6030.
159. Schild, H. G., Poly (N-Isopropylacrylamide) - Experiment, Theory and Application. *Prog. Polym. Sci.* **1992,** 17, (2), 163-249.
160. Fujishige, S.; Kubota, K.; Ando, I., Phase transition of aqueous solutions of poly(N-isopropylacrylamide) and poly(N-isopropylmethacrylamide). *The Journal of Physical Chemistry* **1989,** 93, (8), 3311-3313.
161. Lee, B. H.; Vernon, B., In Situ-Gelling, Erodible N-Isopropylacrylamide Copolymers. *Macromol. Biosci.* **2005,** 5, (7), 629-635.
162. Stile, R. A.; Burghardt, W. R.; Healy, K. E., Synthesis and Characterization of Injectable Poly(N-isopropylacrylamide)-Based Hydrogels That Support Tissue Formation in Vitro. *Macromolecules* **1999,** 32, (22), 7370-7379.
163. Vernon, B.; Kim, S. W.; Bae, Y. H., Thermoreversible copolymer gels for extracellular matrix4. *J. Biomed. Mater. Res.* **2000,** 51, (1), 69-79.
164. Neradovic, D.; Hinrichs, W. L. J.; Kettenes-van den Bosch, J. J.; Hennink, W. E., Poly(N-isopropylacrylamide) with hydrolyzable lactic acid ester side groups: a new type of thermosensitive polymer. *Macromol. Rapid Commun.* **1999,** 20, (11), 577-581.
165. Neradovic, D.; van Steenbergen, M. J.; Vansteelant, L.; Meijer, Y. J.; van Nostrum, C. F.; Hennink, W. E., Degradation Mechanism and Kinetics of Thermosensitive Polyacrylamides Containing Lactic Acid Side Chains. *Macromolecules* **2003,** 36, (20), 7491-7498.
166. Neradovic, D.; van Nostrum, C. F.; Hennink, W. E., Thermoresponsive Polymeric Micelles with Controlled Instability Based on Hydrolytically Sensitive N-Isopropylacrylamide Copolymers. *Macromolecules* **2001,** 34, (22), 7589-7591.
167. Dimitrov, I.; Trzebicka, B.; Müller, A. H. E.; Dworak, A.; Tsvetanov, C. B., Thermosensitive water-soluble copolymers with doubly responsive reversibly interacting entities. *Prog. Polym. Sci.* **2007,** 32, (11), 1275-1343.
168. De, P.; Gondi, S. R.; Sumerlin, B. S., Folate-Conjugated Thermoresponsive Block Copolymers: Highly Efficient Conjugation and Solution Self-Assembly. *Biomacromolecules* **2008,** 9, (3), 1064-1070.
169. Chung, J. E.; Yokoyama, M.; Okano, T., Inner core segment design for drug delivery control of thermo-responsive polymeric micelles. *J. Controlled Release* **2000,** 65, (1-2), 93-103.

170. Kohori, F.; Sakai, K.; Aoyagi, T.; Yokoyama, M.; Sakurai, Y.; Okano, T., Preparation and characterization of thermally responsive block copolymer micelles comprising poly(N-isopropylacrylamide-b-DL-lactide). *J. Controlled Release* **1998,** 55, (1), 87-98.
171. Nakayama, M.; Okano, T., Polymer terminal group effects on properties of thermoresponsive polymeric micelles with controlled outer-shell chain lengths. *Biomacromolecules* **2005,** 6, (4), 2320-2327.
172. Kohori, F.; Sakai, K.; Aoyagi, T.; Yokoyama, M.; Yamato, M.; Sakurai, Y.; Okano, T., Control of adriamycin cytotoxic activity using thermally responsive polymeric micelles composed of poly(N-isopropylacrylamide-co-N,N- dimethylacrylamide)-b-poly(D,L-lactide). *Colloids and Surfaces B: Biointerfaces* **1999,** 16, (1-4), 195-205.
173. Cammas-Marion, S.; Okano, T.; Kataoka, K., Functional and site-specific macromolecular micelles as high potential drug carriers. *Colloids and Surfaces B: Biointerfaces* **1999,** 16, (1-4), 207-215.
174. Topp, M. D. C.; Dijkstra, P. J.; Talsma, H.; Feijen, J., Thermosensitive Micelle-Forming Block Copolymers of Poly(ethylene glycol) and Poly(N-isopropylacrylamide). *Macromolecules* **1997,** 30, (26), 8518-8520.
175. Chung, J. E.; Yokoyama, M.; Yamato, M.; Aoyagi, T.; Sakurai, Y.; Okano, T., Thermo-responsive drug delivery from polymeric micelles constructed using block copolymers of poly(N-isopropylacrylamide) and poly(butylmethacrylate). *J. Controlled Release* **1999,** 62, (1-2), 115-127.
176. Nakayama, M.; Okano, T.; Miyazaki, T.; Kohori, F.; Sakai, K.; Yokoyama, M., Molecular design of biodegradable polymeric micelles for temperature-responsive drug release. *J. Controlled Release* **2006,** 115, (1), 46-56.
177. Cheng, C.; Wei, H.; Shi, B. X.; Cheng, H.; Li, C.; Gu, Z. W.; Cheng, S. X.; Zhang, X. Z.; Zhuo, R. X., Biotinylated thermoresponsive micelle self-assembled from double-hydrophilic block copolymer for drug delivery and tumor target. *Biomaterials* **2008,** 29, (4), 497-505.
178. Fleige, E.; Quadir, M. A.; Haag, R., Stimuli-responsive polymeric nanocarriers for the controlled transport of active compounds: Concepts and applications. *Adv. Drug Delivery Rev.* **2012,** 64, (9), 866-884.
179. Convertine, A. J.; Lokitz, B. S.; Vasileva, Y.; Myrick, L. J.; Scales, C. W.; Lowe, A. B.; McCormick, C. L., Direct Synthesis of Thermally Responsive DMA/NIPAM Diblock and DMA/NIPAM/DMA Triblock Copolymers via Aqueous, Room Temperature RAFT Polymerization†. *Macromolecules* **2006,** 39, (5), 1724-1730.
180. Li, K.; Cao, Y., Thermo-Responsive Behavior of Block and Random Copolymers of N-Isopropylamide/N,N-Dimethylacrylamide Synthesized via Reversible Addition—Fragmentation Chain Transfer Polymerization. *Soft Materials* **2010,** 8, (3), 226-238.
181. Li, G.; Song, S.; Guo, L.; Ma, S., Self-assembly of thermo- and pH-responsive poly(acrylic acid)-b-poly(N-isopropylacrylamide) micelles for drug delivery. *J Polym Sci Pol Chem* **2008,** 46, (15), 5028-5035.
182. Misra, G. P.; Singh, R. S. J.; Aleman, T. S.; Jacobson, S. G.; Gardner, T. W.; Lowe, T. L., Subconjunctivally implantable hydrogels with degradable and thermoresponsive properties for sustained release of insulin to the retina. *Biomaterials* **2009,** 30, (33), 6541-6547.
183. Zhang, J.-T.; Keller, T. F.; Bhat, R.; Garipcan, B.; Jandt, K. D., A novel two-level microstructured poly(N-isopropylacrylamide) hydrogel for controlled release. *Acta Biomater.* **2010,** 6, (10), 3890-3898.
184. Zhang, J. T.; Petersen, S.; Thunga, M.; Leipold, E.; Weidisch, R.; Liu, X. L.; Fahr, A.; Jandt, K. D., Micro-structured smart hydrogels with enhanced protein loading and release efficiency. *Acta Biomater.* **2010,** 6, (4), 1297-1306.
185. Zhao, C.; Zhuang, X.; He, P.; Xiao, C.; He, C.; Sun, J.; Chen, X.; Jing, X., Synthesis of biodegradable thermo- and pH-responsive hydrogels for controlled drug release. *Polymer* **2009,** 50, (18), 4308-4316.

186. Li, Z.; Wang, F.; Roy, S.; Sen, C. K.; Guan, J., Injectable, Highly Flexible, and Thermosensitive Hydrogels Capable of Delivering Superoxide Dismutase. *Biomacromolecules* **2009,** 10, (12), 3306-3316.
187. Kinam, P.; Randall, J. M., *Controlled Drug Delivery*. American Chemical Society: 2000; Vol. 752, p 478.
188. Priya James, H.; John, R.; Alex, A.; Anoop, K. R., Smart polymers for the controlled delivery of drugs – a concise overview. *Acta Pharmaceutica Sinica B* **2014,** 4, (2), 120-127.
189. You, J.; Shao, R.; Wei, X.; Gupta, S.; Li, C., Near-infrared light triggers release of paclitaxel from biodegradable microspheres: Photothermal effect and enhanced antitumor activity. *Small* **2010,** 6, (9), 1022-1031.
190. Goodwin, A. P.; Mynar, J. L.; Ma, Y.; Fleming, G. R.; Fréchet, J. M. J., Synthetic Micelle Sensitive to IR Light via a Two-Photon Process. *J. Am. Chem. Soc.* **2005,** 127, (28), 9952-9953.
191. Yui, N.; Okano, T.; Sakurai, Y., Photo-responsive degradation of heterogeneous hydrogels comprising crosslinked hyaluronic acid and lipid microspheres for temporal drug delivery. *J. Controlled Release* **1993,** 26, (2), 141-145.
192. Bawa, P.; Pillay, V.; Choonara, Y. E.; du Toit, L. C., Stimuli-responsive polymers and their applications in drug delivery. *Biomedical Materials* **2009,** 4, (2).
193. Jiang, J.; Tong, X.; Zhao, Y., A new design for light-breakable polymer micelles. *J. Am. Chem. Soc.* **2005,** 127, (23), 8290-8291.
194. Jin, Q.; Mitschang, F.; Agarwal, S., Biocompatible drug delivery system for photo-triggered controlled release of 5-fluorouracil. *Biomacromolecules* **2011,** 12, (10), 3684-3691.
195. Mamada, A.; Tanaka, T.; Kungwatchakun, D.; Irie, M., Photoinduced phase transition of gels. *Macromolecules* **1990,** 23, (5), 1517-1519.
196. Suzuki, A.; Tanaka, T., Phase transition in polymer gels induced by visible light. *Nature* **1990,** 346, (6282), 345-347.
197. Ichimura, K.; Oh, S. K.; Nakagawa, M., Light-driven motion of liquids on a photoresponsive surface. *Science* **2000,** 288, (5471), 1624-1626.
198. Cabane, E.; Malinova, V.; Menon, S.; Palivan, C. G.; Meier, W., Photoresponsive polymersomes as smart, triggerable nanocarriers. *Soft Matter* **2011,** 7, (19), 9167-9176.
199. Han, D.; Tong, X.; Zhao, Y., Fast Photodegradable Block Copolymer Micelles for Burst Release. *Macromolecules* **2011,** 44, (3), 437-439.
200. Rapoport, N. Y.; Christensen, D. A.; Fain, H. D.; Barrows, L.; Gao, Z., Ultrasound-triggered drug targeting of tumors in vitro and in vivo. *Ultrasonics* **2004,** 42, (1–9), 943-950.
201. Lavon, I.; Kost, J., Mass transport enhancement by ultrasound in non-degradable polymeric controlled release systems. *J. Controlled Release* **1998,** 54, (1), 1-7.
202. Kost, J.; Leong, K.; Langer, R., Ultrasonically controlled polymeric drug delivery. *Makromolekulare Chemie. Macromolecular Symposia* **1988,** 19, (1), 275-285.
203. Pitt, W. G.; Husseini, G. A.; Staples, B. J., Ultrasonic Drug Delivery – A General Review. *Expert Opin. Drug Deliv.* **2004,** 1, (1), 37-56.
204. El-Sherif, D. M.; Wheatley, M. A., Development of a novel method for synthesis of a polymeric ultrasound contrast agent. *Journal of Biomedical Materials Research Part A* **2003,** 66A, (2), 347-355.
205. Lathia, J. D.; Leodore, L.; Wheatley, M. A., Polymeric contrast agent with targeting potential. *Ultrasonics* **2004,** 42, (1–9), 763-768.
206. Du, L.; Jin, Y.; Zhou, W.; Zhao, J., Ultrasound-Triggered Drug Release and Enhanced Anticancer Effect of Doxorubicin-Loaded Poly(D,L-Lactide-Co-Glycolide)-Methoxy-Poly(Ethylene Glycol) Nanodroplets. *Ultrasound Med. Biol.* **2011,** 37, (8), 1252-1258.
207. Gao, Z.-G.; Fain, H. D.; Rapoport, N., Controlled and targeted tumor chemotherapy by micellar-encapsulated drug and ultrasound. *J. Controlled Release* **2005,** 102, (1), 203-222.

208. El-Sherif, D. M.; Lathia, J. D.; Le, N. T.; Wheatley, M. A., Ultrasound degradation of novel polymer contrast agents. *Journal of Biomedical Materials Research Part A* **2004,** 68A, (1), 71-78.
209. Basude, R.; Wheatley, M. A., Generation of ultraharmonics in surfactant based ultrasound contrast agents: use and advantages. *Ultrasonics* **2001,** 39, (6), 437-444.
210. Roy, D.; Cambre, J. N.; Sumerlin, B. S., Future perspectives and recent advances in stimuli-responsive materials. *Prog. Polym. Sci.* **2010,** 35, (1–2), 278-301.
211. McBain, S. C.; Yiu, H. H. P.; Dobson, J., Magnetic nanoparticles for gene and drug delivery. *Int. J. Nanomedicine* **2008,** 3, (2), 169-180.
212. Mosbach, K.; Schröder, U., Preparation and application of magnetic polymers for targeting of drugs. *FEBS Lett.* **1979,** 102, (1), 112-116.
213. Alexiou, C.; Arnold, W.; Klein, R. J.; Parak, F. G.; Hulin, P.; Bergemann, C.; Erhardt, W.; Wagenpfeil, S.; Lübbe, A. S., Locoregional Cancer Treatment with Magnetic Drug Targeting. *Cancer Res.* **2000,** 60, (23), 6641-6648.
214. Podaru, G.; Ogden, S.; Baxter, A.; Shrestha, T.; Ren, S.; Thapa, P.; Dani, R. K.; Wang, H.; Basel, M. T.; Prakash, P.; Bossmann, S. H.; Chikan, V., Pulsed Magnetic Field Induced Fast Drug Release from Magneto Liposomes via Ultrasound Generation. *The Journal of Physical Chemistry B* **2014,** 118, (40), 11715-11722.
215. Pankhurst, Q. A.; Connolly, J.; Jones, S. K.; Dobson, J., Applications of magnetic nanoparticles in biomedicine. *Journal of Physics D-Applied Physics* **2003,** 36, (13), R167-R181.
216. Harris, L. A.; Goff, J. D.; Carmichael, A. Y.; Riffle, J. S.; Harburn, J. J.; St. Pierre, T. G.; Saunders, M., Magnetite Nanoparticle Dispersions Stabilized with Triblock Copolymers. *Chem. Mater.* **2003,** 15, (6), 1367-1377.
217. Kondo, A.; Fukuda, H., Preparation of thermo-sensitive magnetic hydrogel microspheres and application to enzyme immobilization. *J. Ferment. Bioeng.* **1997,** 84, (4), 337-341.
218. Lee, K.; Bae, K. H.; Lee, Y.; Lee, S. H.; Ahn, C. H.; Park, T. G., Pluronic/polyethylenimine shell crosslinked nanocapsules with embedded magnetite nanocrystals for magnetically triggered delivery of siRNA. *Macromol. Biosci.* **2010,** 10, (3), 239-245.
219. Dobson, J., Magnetic nanoparticles for drug delivery. *Drug Dev. Res.* **2006,** 67, (1), 55-60.
220. Miller, L. L.; Smith, G. A.; An-Cheng, C.; Qin-Xin, Z., Electrochemically controlled release. *J. Controlled Release* **1987,** 6, (1), 293-296.
221. Schmidt, D. J.; Moskowitz, J. S.; Hammond, P. T., Electrically triggered release of a small molecule drug from a polyelectrolyte multilayer coating. *Chem. Mater.* **2010,** 22, (23), 6416-6425.
222. Leprince, L.; Dogimont, A.; Magnin, D.; Demoustier-Champagne, S., Dexamethasone electrically controlled release from polypyrrole-coated nanostructured electrodes. *J. Mater. Sci.: Mater. Med.* **2010,** 21, (3), 925-930.
223. Murdan, S., Electro-responsive drug delivery from hydrogels. *J. Controlled Release* **2003,** 92, (1-2), 1-17.
224. TANAKA, T.; NISHIO, I.; SUN, S.-T.; UENO-NISHIO, S., Collapse of Gels in an Electric Field. *Science* **1982,** 218, (4571), 467-469.
225. Ge, J.; Neofytou, E.; Cahill, T. J.; Beygui, R. E.; Zare, R. N., Drug Release from Electric-Field-Responsive Nanoparticles. *ACS Nano* **2011,** 6, (1), 227-233.
226. Cabane, E.; Zhang, X.; Langowska, K.; Palivan, C. G.; Meier, W., Stimuli-Responsive Polymers and Their Applications in Nanomedicine. *Biointerphases* **2012,** 7, (1), -.
227. Shim, W. S.; Kim, J. H.; Kim, K.; Kim, Y. S.; Park, R. W.; Kim, I. S.; Kwon, I. C.; Lee, D. S., pH- and temperature-sensitive, injectable, biodegradable block copolymer hydrogels as carriers for paclitaxel. *Int. J. Pharm.* **2007,** 331, (1), 11-18.
228. Lee, E. S.; Na, K.; Bae, Y. H., Polymeric micelle for tumor pH and folate-mediated targeting. *J. Controlled Release* **2003,** 91, (1-2), 103-113.

229. Ishida, T.; Kirchmeier, M. J.; Moase, E. H.; Zalipsky, S.; Allen, T. M., Targeted delivery and triggered release of liposomal doxorubicin enhances cytotoxicity against human B lymphoma cells. *Biochimica et Biophysica Acta - Biomembranes* **2001,** 1515, (2), 144-158.
230. Shigeta, K.; Kawakami, S.; Higuchi, Y.; Okuda, T.; Yagi, H.; Yamashita, F.; Hashida, M., Novel histidine-conjugated galactosylated cationic liposomes for efficient hepatocyte-selective gene transfer in human hepatoma HepG2 cells. *J. Controlled Release* **2007,** 118, (2), 262-270.
231. Yamada, Y.; Shinohara, Y.; Kakudo, T.; Chaki, S.; Futaki, S.; Kamiya, H.; Harashima, H., Mitochondrial delivery of mastoparan with transferrin liposomes equipped with a pH-sensitive fusogenic peptide for selective cancer therapy. *Int. J. Pharm.* **2005,** 303, (1-2), 1-7.
232. Fattal, E.; Couvreur, P.; Dubernet, C., "Smart" delivery of antisense oligonucleotides by anionic pH-sensitive liposomes. *Adv. Drug Delivery Rev.* **2004,** 56, (7), 931-946.
233. Hui, H.; Xiao-Dong, F.; Zhong-Lin, C., Thermo- and pH-sensitive dendrimer derivatives with a shell of poly(N,N-dimethylaminoethyl methacrylate) and study of their controlled drug release behavior. *Polymer* **2005,** 46, (22), 9514-9522.
234. Dufresne, M. H.; Le Garrec, D.; Sant, V.; Leroux, J. C.; Ranger, M., Preparation and characterization of water-soluble pH-sensitive nanocarriers for drug delivery. *Int. J. Pharm.* **2004,** 277, (1-2), 81-90.
235. Benns, J. M.; Choi, J. S.; Mahato, R. I.; Park, J. S.; Sung Wan, K., pH-Sensitive cationic polymer gene delivery vehicle: N-Ac-poly(L-histidine)-graft-poly(L-lysine) comb shaped polymer. *Bioconjugate Chem.* **2000,** 11, (5), 637-645.
236. Lee, Y.; Fukushima, S.; Bae, Y.; Hiki, S.; Ishii, T.; Kataoka, K., A Protein Nanocarrier from Charge-Conversion Polymer in Response to Endosomal pH. *J. Am. Chem. Soc.* **2007,** 129, (17), 5362-5363.
237. Aryal, S.; Hu, C.-M. J.; Zhang, L., Polymer−Cisplatin Conjugate Nanoparticles for Acid-Responsive Drug Delivery. *ACS Nano* **2009,** 4, (1), 251-258.
238. Na, K.; Lee, E. S.; Bae, Y. H., Adriamycin loaded pullulan acetate/sulfonamide conjugate nanoparticles responding to tumor pH: pH-dependent cell interaction, internalization and cytotoxicity in vitro. *J. Controlled Release* **2003,** 87, (1-3), 3-13.
239. Murthy, N.; Campbell, J.; Fausto, N.; Hoffman, A. S.; Stayton, P. S., Design and synthesis of pH-responsive polymeric carriers that target uptake and enhance the intracellular delivery of oligonucleotides. *J. Controlled Release* **2003,** 89, (3), 365-374.
240. Kamada, H.; Tsutsumi, Y.; Yoshioka, Y.; Yamamoto, Y.; Kodaira, H.; Tsunoda, S. I.; Okamoto, T.; Mukai, Y.; Shibata, H.; Nakagawa, S.; Mayumi, T., Design of a pH-Sensitive Polymeric Carrier for Drug Release and Its Application in Cancer Therapy. *Clin. Cancer Res.* **2004,** 10, (7), 2545-2550.
241. Ulbrich, K.; Etrych, T.; Chytil, P.; Jelínková, M.; Říhová, B., Antibody-targeted polymer-doxorubicin conjugates with pH-controlled activation. *J. Drug Targeting* **2004,** 12, (8), 477-489.
242. Drevs, J.; Hofmann, I.; Marmé, D.; Unger, C.; Kratz, F., In vivo and in vitro efficacy of an acid-sensitive albumin conjugate of adriamycin compared to the parent compound in murine renal-cell carcinoma. *Drug Delivery: Journal of Delivery and Targeting of Therapeutic Agents* **1999,** 6, (2), 89-95.
243. Leroux, J. C.; Roux, E.; Le Garrec, D.; Hong, K.; Drummond, D. C., N-isopropylacrylamide copolymers for the preparation of pH-sensitive liposomes and polymeric micelles. *J. Controlled Release* **2001,** 72, (1-3), 71-84.
244. Shim, W. S.; Kim, S. W.; Choi, E. K.; Park, H. J.; Kim, J. S.; Lee, D. S., Novel pH sensitive block copolymer micelles for solvent free drug loading. *Macromol. Biosci.* **2006,** 6, (2), 179-186.
245. Bae, Y.; Nishiyama, N.; Fukushima, S.; Koyama, H.; Yasuhiro, M.; Kataoka, K., Preparation and biological characterization of polymeric micelle drug carriers with intracellular pH-

triggered drug release property: Tumor permeability, controlled subcellular drug distribution, and enhanced in vivo antitumor efficacy. *Bioconjugate Chem.* **2005,** 16, (1), 122-130.
246. Bae, Y.; Jang, W. D.; Nishiyama, N.; Fukushima, S.; Kataoka, K., Multifunctional polymeric micelles with folate-mediated cancer cell targeting and pH-triggered drug releasing properties for active intracellular drug delivery. *Mol. BioSyst.* **2005,** 1, (3), 242-250.
247. Schafer, F. Q.; Buettner, G. R., Redox environment of the cell as viewed through the redox state of the glutathione disulfide/glutathione couple. *Free Radic. Biol. Med.* **2001,** 30, (11), 1191-1212.
248. Mintzer, M. A.; Simanek, E. E., Nonviral Vectors for Gene Delivery. *Chem. Rev.* **2008,** 109, (2), 259-302.
249. Neu, M.; Germershaus, O.; Mao, S.; Voigt, K. H.; Behe, M.; Kissel, T., Crosslinked nanocarriers based upon poly(ethylene imine) for systemic plasmid delivery: In vitro characterization and in vivo studies in mice. *J. Controlled Release* **2007,** 118, (3), 370-380.
250. Cerritelli, S.; Velluto, D.; Hubbell, J. A., PEG-SS-PPS: Reduction-sensitive disulfide block copolymer vesicles for intracellular drug delivery. *Biomacromolecules* **2007,** 8, (6), 1966-1972.
251. Li, Y.; Xiao, K.; Luo, J.; Xiao, W.; Lee, J. S.; Gonik, A. M.; Kato, J.; Dong, T. A.; Lam, K. S., Well-defined, reversible disulfide cross-linked micelles for on-demand paclitaxel delivery. *Biomaterials* **2011,** 32, (27), 6633-6645.
252. Ryu, J. H.; Roy, R.; Ventura, J.; Thayumanavan, S., Redox-sensitive disassembly of amphiphilic copolymer based micelles. *Langmuir* **2010,** 26, (10), 7086-7092.
253. Carlisle, R. C.; Etrych, T.; Briggs, S. S.; Preece, J. A.; Ulbrich, K.; Seymour, L. W., Polymer-coated polyethylenimine/DNA complexes designed for triggered activation by intracellular reduction. *The Journal of Gene Medicine* **2004,** 6, (3), 337-344.
254. Matsumoto, S.; Christie, R. J.; Nishiyama, N.; Miyata, K.; Ishii, A.; Oba, M.; Koyama, H.; Yamasaki, Y.; Kataoka, K., Environment-responsive block copolymer micelles with a disulfide cross-linked core for enhanced siRNA delivery. *Biomacromolecules* **2009,** 10, (1), 119-127.
255. Takae, S.; Miyata, K.; Oba, M.; Ishii, T.; Nishiyama, N.; Itaka, K.; Yamasaki, Y.; Koyama, H.; Kataoka, K., PEG-detachable polyplex micelles based on disulfide-linked block catiomers as bioresponsive nonviral gene vectors. *J. Am. Chem. Soc.* **2008,** 130, (18), 6001-6009.
256. Wang, Y. C.; Wang, F.; Sun, T. M.; Wang, J., Redox-responsive nanoparticles from the single disulfide bond-bridged block copolymer as drug carriers for overcoming multidrug resistance in cancer cells. *Bioconjugate Chem.* **2011,** 22, (10), 1939-1945.
257. Sun, P.; Zhou, D.; Gan, Z., Novel reduction-sensitive micelles for triggered intracellular drug release. *J. Controlled Release* **2011,** 155, (1), 96-103.
258. Yan, Y.; Johnston, A. P. R.; Dodds, S. J.; Kamphuis, M. M. J.; Ferguson, C.; Parton, R. G.; Nice, E. C.; Heath, J. K.; Caruso, F., Uptake and intracellular fate of disulfide-bonded polymer hydrogel capsules for doxorubicin delivery to colorectal cancer cells. *ACS Nano* **2010,** 4, (5), 2928-2936.
259. Ng, S. L.; Such, G. K.; Johnston, A. P. R.; Antequera-García, G.; Caruso, F., Controlled release of DNA from poly(vinylpyrrolidone) capsules using cleavable linkers. *Biomaterials* **2011,** 32, (26), 6277-6284.
260. Kommareddy, S.; Amiji, M., Preparation and evaluation of thiol-modified gelatin nanoparticles for intracellular DNA delivery in response to glutathione. *Bioconjugate Chem.* **2005,** 16, (6), 1423-1432.
261. Kommareddy, S.; Amiji, M., Poly(ethylene glycol)-modified thiolated gelatin nanoparticles for glutathione-responsive intracellular DNA delivery. *Nanomedicine: Nanotechnology, Biology, and Medicine* **2007,** 3, (1), 32-42.
262. Saito, G.; Swanson, J. A.; Lee, K.-D., Drug delivery strategy utilizing conjugation via reversible disulfide linkages: role and site of cellular reducing activities. *Adv. Drug Delivery Rev.* **2003,** 55, (2), 199-215.

263. Ghosh, S.; Irvin, K.; Thayumanavan, S., Tunable Disassembly of Micelles Using a Redox Trigger. *Langmuir* **2007,** 23, (15), 7916-7919.
264. Ulijn, R. V., Enzyme-responsive materials: a new class of smart biomaterials. *J. Mater. Chem.* **2006,** 16, (23), 2217-2225.
265. Ghadiali, J. E.; Stevens, M. M., Enzyme-Responsive Nanoparticle Systems. *Adv. Mater.* **2008,** 20, (22), 4359-4363.
266. Hu, J.; Zhang, G.; Liu, S., Enzyme-responsive polymeric assemblies, nanoparticles and hydrogels. *Chem. Soc. Rev.* **2012,** 41, (18), 5933-5949.
267. de la Rica, R.; Aili, D.; Stevens, M. M., Enzyme-responsive nanoparticles for drug release and diagnostics. *Adv. Drug Delivery Rev.* **2012,** 64, (11), 967-978.
268. de Graaf, A. J.; Mastrobattista, E.; Vermonden, T.; van Nostrum, C. F.; Rijkers, D. T. S.; Liskamp, R. M. J.; Hennink, W. E., Thermosensitive Peptide-Hybrid ABC Block Copolymers Obtained by ATRP: Synthesis, Self-Assembly, and Enzymatic Degradation. *Macromolecules* **2012,** 45, (2), 842-851.
269. Napoli, A.; Boerakker, M. J.; Tirelli, N.; Nolte, R. J. M.; Sommerdijk, N. A. J. M.; Hubbell, J. A., Glucose-oxidase based self-destructing polymeric vesicles. *Langmuir* **2004,** 20, (9), 3487-3491.
270. Yin, R.; Tong, Z.; Yang, D.; Nie, J., Glucose and pH dual-responsive concanavalin A based microhydrogels for insulin delivery. *Int. J. Biol. Macromol.* **2011,** 49, (5), 1137-1142.
271. Ravaine, V.; Ancla, C.; Catargi, B., Chemically controlled closed-loop insulin delivery. *J. Controlled Release* **2008,** 132, (1), 2-11.
272. Kang, S. I.; Bae, Y. H., A sulfonamide based glucose-responsive hydrogel with covalently immobilized glucose oxidase and catalase. *J. Controlled Release* **2003,** 86, (1), 115-121.
273. Zhang, Y.; Chan, H. F.; Leong, K. W., Advanced materials and processing for drug delivery: The past and the future. *Adv. Drug Delivery Rev.* **2013,** 65, (1), 104-120.
274. Truong, N. P.; Jia, Z.; Burges, M.; McMillan, N. A. J.; Monteiro, M. J., Self-Catalyzed Degradation of Linear Cationic Poly(2-dimethylaminoethyl acrylate) in Water. *Biomacromolecules* **2011,** 12, (5), 1876-1882.
275. Truong, N. P.; Jia, Z.; Burgess, M.; Payne, L.; McMillan, N. A. J.; Monteiro, M. J., Self-Catalyzed Degradable Cationic Polymer for Release of DNA. *Biomacromolecules* **2011,** 12, (10), 3540-3548.
276. Truong, N. P.; Gu, W.; Prasadam, I.; Jia, Z.; Crawford, R.; Xiao, Y.; Monteiro, M. J., An influenza virus-inspired polymer system for the timed release of siRNA. *Nat. Commun.* **2013,** 4, 1902.
277. Gu, W.; Jia, Z.; Truong, N. P.; Prasadam, I.; Xiao, Y.; Monteiro, M. J., Polymer Nanocarrier System for Endosome Escape and Timed Release of siRNA with Complete Gene Silencing and Cell Death in Cancer Cells. *Biomacromolecules* **2013,** 14, (10), 3386-3389.
278. Gillard, M.; Jia, Z.; Hou, J. J. C.; Song, M.; Gray, P. P.; Munro, T. P.; Monteiro, M. J., Intracellular Trafficking Pathways for Nuclear Delivery of Plasmid DNA Complexed with Highly Efficient Endosome Escape Polymers. *Biomacromolecules* **2014,** 15, (10), 3569-3576.
279. Lowe, A. B.; McCormick, C. L., Reversible addition–fragmentation chain transfer (RAFT) radical polymerization and the synthesis of water-soluble (co)polymers under homogeneous conditions in organic and aqueous media. *Prog. Polym. Sci.* **2007,** 32, (3), 283-351.
280. Boyer, C.; Bulmus, V.; Davis, T. P.; Ladmiral, V.; Liu, J.; Perrier, S., Bioapplications of RAFT Polymerization. *Chem. Rev.* **2009,** 109, (11), 5402-5436.
281. Moad, G.; Rizzardo, E.; Thang, S. H., Radical addition–fragmentation chemistry in polymer synthesis. *Polymer* **2008,** 49, (5), 1079-1131.
282. Gody, G.; Maschmeyer, T.; Zetterlund, P. B.; Perrier, S., Rapid and quantitative one-pot synthesis of sequence-controlled polymers by radical polymerization. *Nat. Commun.* **2013,** 4.

Chapter 2

Timed-Release Polymer Nanoparticles

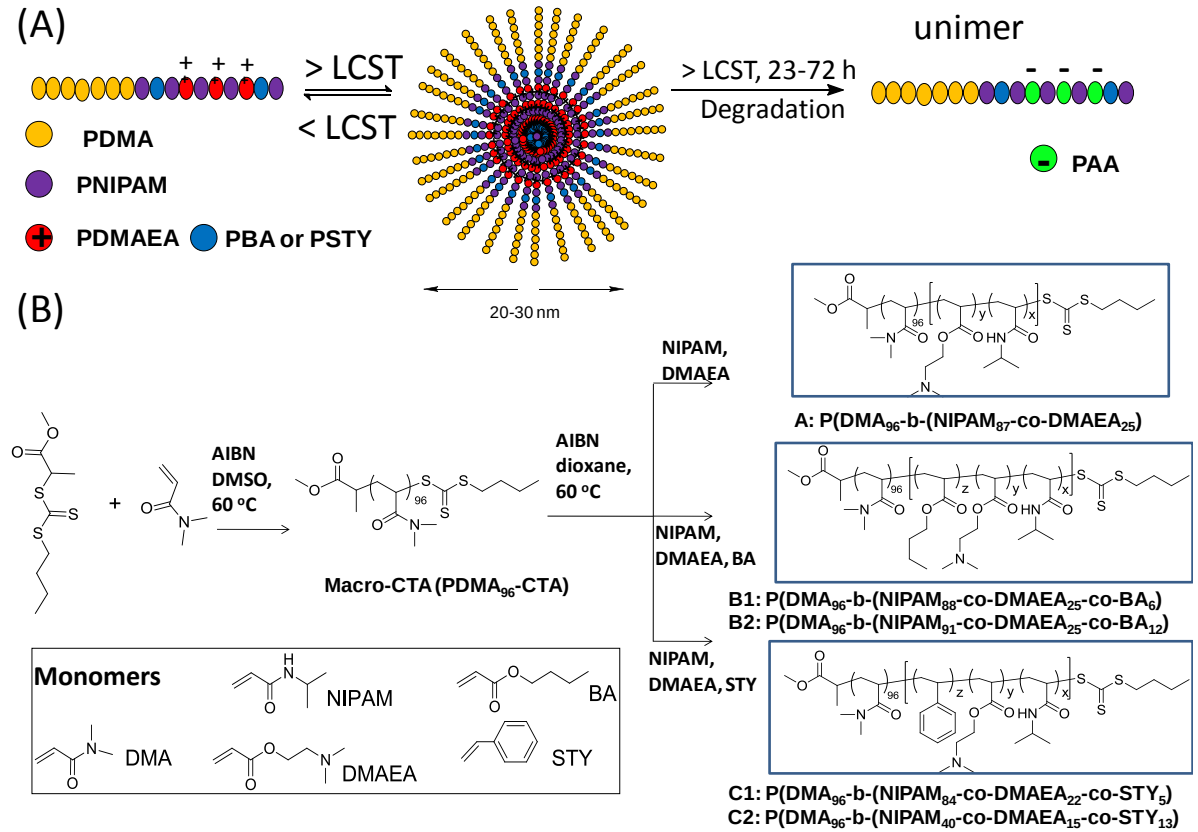

Triggered-release of encapsulated therapeutics from nanoparticles without remote or environmental triggers was demonstrated in this work. Disassembly of the polymer nanoparticles to unimers at precise times allowed the controlled release of oligo DNA. The polymers used in this study consisted of a hydrophilic block for stabilization and second thermoresponsive block for self-assembly and disassembly. At temperatures below the second block's LCST (i.e., below 37 °C for in vitro assays), the diblock copolymer was fully water-soluble, and when heated to 37 °C, the polymer self-assembled into a narrow size distribution of nanoparticles with an average diameter of approximately 25 nm. The thermoresponsive nature of the second block could be manipulated in situ by the self-catalyzed degradation of cationic 2-(dimethylamino) ethyl acrylate (DMAEA) units to negatively charged acrylic acid groups and when the amount of acid groups was sufficiently high to increase the LCST of the second block above 37 °C. The disassembly of the nanoparticles could be controlled from 10 to 70 h. The use of these nanoparticles as a combined therapy, in which one or more agents can be released in a predetermined way, has the potential to improve the personal point of care treatment of patients.

2.1 Introduction

Triggered-release of encapsulated materials from nanoparticles has attracted considerable attention for the on-demand release of compounds.[1-4] The potential applications range from drug delivery, to fragrance release, to self-healing materials.[5-7] Degradation or disassembly of nanoparticles can be activated either remotely through external light,[8-10] electric or magnetic sources,[11-13] or through environmental triggers such as in vivo biological changes (e.g., pH changes[14-16] or localized enzyme activity.[17-19] While these triggers represent elegant methods for selective release, there are still many applications where remotely activated triggers cannot be used. Environmental triggers (such as pH, enzymatic degradation, temperature) have other issues due to their variability within cell lines and within the same tissue.[20, 21] In such cases, new nontriggered release delivery materials are required that would act in an environment independent manner. We believe that nanoparticles, which release their payload at specific times in the absence of an external trigger, would be of great interest for the controlled release of small molecules and biological therapeutic agents. Therefore, nanoparticles must be designed to encapsulate and release the therapeutic agent on-demand to impart a rapid effect. These nanoparticles after release should be nontoxic, allowing the application of multiple doses for high effective therapeutic effects. Thermoresponsive polymer (e.g., poly(N-isopropylacrylamide); PNIPAM) nanoparticles have been used for such a purpose,[22] in which polymeric micelles degrade to unimers through an acid or base hydrolysis process. However, even a small change in pH (from 7.5 to 7.2) could slow the degradation rate by a factor of 2.[23] If such polymer nanoparticles were used in vivo, the variability of pH within cells and at, for example, tumors will cause the noncontrolled release of the therapeutic. To overcome this significant hurdle, we will incorporate a self-catalyzed polymer (poly (2 (dimethylamino)-ethyl acrylate); PDMAEA) into the second hydrophobic block with PNIPAM. The degradation rate in water of PDMAEA to poly(acrylic acid) is independent of the physiological pH ranging from 5.5 to 10.1,[24] making such timed-release micelles ideal for many biological applications where precise release of the payload is required within any physiological environment.

2.1.1 Aim of the Chapter

The aim of this chapter was to design polymer nanoparticles to disassemble and thus release their payload at a desired time independent of the local microenvironment. We synthesized diblock thermoresponsive copolymers PDMA-b-P(NIPAM-co-DMAEA-co-BA) and PDMA-b-P(NIPAM-co-DMAEA-co-STY) by Reversible addition-fragmentation chain transfer (RAFT) polymerization. The polymers are water soluble below their lower critical solution temperature (LCST, < 37 °C), and when heated to 37 °C (i.e., above the polymers' LCST), self-assemble to form small nanoparticles of approximately 20 nm with narrow size distribution. Through the self-catalyzed

hydrolysis of PDMAEA, the polymer nanoparticles rapidly disassemble after desired times to biologically nontoxic negatively charged diblock unimers (see Scheme 2.1). The self-assembly of the polymers in water above the polymers' LCST was investigated by Dynamic Light Scattering (DLS). Furthermore, the disassembly of the polymer nanoparticles was monitored over time. In addition, the binding and release of oligo DNA (a mimic of siRNA) and cell uptake of the polymer nanoparticle into osteosarcoma cells were studied.

2.2 Experimental

2.2.1 Materials

Dioxane (Alrich, 99%), carbondisulfide (Alrich, 99%), 1-butanethiol (Alrich, 99%), methyl bromopropionate (Alrich, 98%), and dimethyl sulfoxide (DMSO, Alrich >99.9%), N, N-dimethylformamide (DMF: Labscan, AR grade), dichloromethane (DCM: Labscan, AR grade), *N*-(*t*-BOC-aminopropyl)methacrylamide (Polysciences, 100%), trifluoroacetic acid (TFA: Merck, AR grade), triethylamine (TEA: Fluka, 98%), tri(2-carboxyethyl) phosphine hydrochloride solution (TCEP: Aldrich, 98 %), *N*-Ethyl-*N*′-(3-dimethylaminopropyl)carbodiimide hydrochloride (EDC.HCl: Alrich, premium), *N*-hydroxysuccinimide (NHS: Alrich, 98 %), Hexylamine (Alrich, 99 %), Folic acid (Alrich, ≥ 97 %) were used as received. Styrene (STY, Aldrich, 99 %), dimethylacrylamide (DMA, Aldrich, 99 %), 2-(dimethylamino) ethyl acrylate (DMAEA, Sigma-Aldrich, 98%), and butyl acrylate (BA, Aldrich, 99%) were passed through a column of basic alumina (activity I) to remove inhibitor. *N*-isopropylacrylamide (NIPAM, Aldrich, 97 %) was recrystallized from hexane. Azobisisobutyronitrile (AIBN) was also recrystallized twice from methanol prior to use. 9-27 Oligo DNA was synthesized by Invitrogen, 9-27F+R–MW=14998 (23bp), Sense: 5'-GTCAGAAATAGAAACTGGTCATC-3' Antisense: 5'-GATGACCAGTTTCTATTTCTGAC3'. Milli-Q Water (18.2 MΩcm^{-1}) was generated using a Millipore Milli-Q academic water purification system. All other chemicals and solvents used were of at least analytical grade and used as received.

2.2.2 Synthetic procedures

*2.2.2.1 Synthesis of the Chain Transfer Agent (CTA), Methyl 2-(butylthiocarbonothioylthio) propanoate (MCEBTTC).*The synthesized MCEBTTC was carried out according to the literature procedure.[25] Carbondisulfide (3.1 mL, 0.051 mol) in dichloromethane (50 mL) was added dropwise to a stirred solution of 1-butanethiol (5 mL, 0.047 mol) and triethylamine (7.2 mL, 0.051 mol) in dichloromethane (25 mL) over 30 min at 0 ^{o}C under an argon atmosphere. The solution gradually turned yellow during the addition. After complete addition, the solution was stirred at room

temperature for 30 min. Methyl bromopropionate (5.7 mL, 0.051 mol) in dichloromethane (25 mL) was then added dropwise over 30 min and the solution stirred for 2 h. The dichloromethane was removed under nitrogen and the residue dissolved in diethylether. The solution was then washed with cold 10% HCl solution (3 x 50 mL) and Milli-Q water (3 x 50 mL) and dried over anhydrous $MgSO_4$. The ether was removed under vacuum, and the residual yellow oil was purified by column chromatography (19:1 petroleum ether/ethyl acetate on silica, second band) (yield = 76 %). ^{1}H NMR ($CDCl_3$) δ 0.90 (t, *J* = 7.5 Hz, 3H, CH_3), 1.40 (m, *J* = 7.5 Hz, 2H, CH_2), 1.57 (d, *J* = 7.5 Hz, 3H, CH_3), 1.66 (q, *J* = 7.5 Hz, 2H, CH_2), 3.34 (t, *J* = 7.5 Hz, 2H, CH_2), 3.73 (s, 3H, CH_3), 4.80 (q, *J* = 7.5 Hz, 1H, CH).

2.2.2.2 Synthesis of poly (N, N-diethylacrylamide) macro chain transfer agent (PDMA macro-CTA). DMA (10.40 mL, 0.10 mol), MCEBTTC (25.42 mg, 1.01 x 10^{-3} mol), and AIBN (14.10 mg, 8.57 x 10^{-5} mol) were dissolved in DMSO in a 50 mL dry Schlenk flask equipped with a magnetic stirrer bar. The mixture was deoxygenated by purging with Argon for 30 min and then heated to 60 ^{o}C for 2 h. The reaction was stopped by cooling to 0 ^{o}C in an ice bath and exposed to the air. The solution was then diluted with dichloromethane (500 mL) and washed with brine (3x100 mL). The DCM was then dried over anhydrous $MgSO_4$, filtered and reduced in volume by rotary evaporation. The polymer was recovered by precipitation into large excess of diethyl ether (1 L), and isolated by filtration. The polymer was re-dissolved in acetone and precipitated in diethyl ether. The re-dissolving and precipitation process was repeated 2 times. The polymer was filtered and then dried under high vacuum for 24 h at room temperature to give a yellow powder product (yield = 71%). M_n = 8200, PDI = 1.14 (SEC-RI calibrated using PSTY Standards in DMAc solution containing 0.03 wt% of LiCl), M_n = 10000 (SEC-Triple Detection, dn/dc = 0.081); M_n = 9769 (^{1}H NMR). ^{1}H NMR (500 MHz, $CDCl_3$): δ 0.87 (C*H*$_3$CH$_2$CH$_2$-), 1.09 (C*H*$_3$-(CH-COO)-), 2.84-3.05 ((C*H*$_3$)$_2$-N-), 3.29 (-C*H*$_2$-S-(C=S)-S-), 3.60 (C*H*$_3$O-(C=O)-), 5.14 (-(C=S)-S-C*H*-).

2.2.2.3 Synthesis of block copolymers of NIPAM and DMAEA from PDMA macro-CTA (A). NIPAM (1.00 g, 8.85 x 10^{-3} mol), DMAEA (0.34 mL, 2.21 x 10^{-3} mol), PDMA macro-CTA (725.66 mg, 8.85 x 10^{-5} mol) and AIBN (1.45 mg, 8.85 x 10^{-6} mol) were dissolved in 20 mL of dioxane in a 50 mL dry Schlenk flask equipped with a magnetic stirrer bar. The mixture was deoxygenated by purging with Argon for 30 min and then heated to 60 ^{o}C for 7 h under Argon. The reaction was stopped by cooling to 0 ^{o}C in an ice bath and exposed to air. The solution was precipitated in diethyl ether (500 mL) and filtered. The polymer was re-dissolved in acetone and precipitated in diethyl ether. The re-dissolving and precipitating process were repeated twice. The yellow powder product was dried under high vacuum at room temperature for 48 h (yield = 78 %).

2.2.2.4 Synthesis of block copolymers of NIPAM, DMAEA, and BA from PDMA macro-CTA (B1, B2). For a polymerization with 5.04 % of BA in the second block, NIPAM (1.00 g, 8.85 x 10^{-3} mol), DMAEA (0.34 mL, 2.21 x 10^{-3} mol), BA (0.083 mL, 5.75 x 10^{-4} mol), PDMA macro-CTA (725.66 mg, 8.85 x 10^{-5} mol) and AIBN (1.45 mg, 8.85 x 10^{-6} mol) were dissolved in 20 mL of dioxane in a 50 mL dry Schlenk flask equipped with a magnetic stirrer bar. The mixture was deoxygenated by purging with Argon for 30 min and then heated to 60 ^{o}C for 8 h under Argon. The reaction was stopped by cooling to 0 ^{o}C in an ice bath and exposed to air. The solution was precipitated in diethyl ether (500 mL) and filtered. The polymer was re-dissolved in acetone and precipitated in diethyl ether. Re-dissolving and precipitating were repeated twice. The yellow powder product was dried under high vacuum at room temperature for 48 h (yield = 75 %). For a polymerization with 9.38 % of BA in the second block, the same procedure was performed as above but with double the amount of BA (0.18 mL, 1.24 x 10^{-3} mol) (yield = 72 %).

2.2.2.5 Synthesis of block copolymers of NIPAM, DMAEA, and STY from PDMA macro-CTA (C1, C2). For a polymerization with 4.50 % of STY in the second block, NIPAM (1.00 g, 8.85 x 10^{-3} mol), DMAEA (0.34 mL, 2.21 x 10^{-3} mol), STY (0.067 mL, 5.75 x 10^{-4} mol), PDMA macro-CTA (725.66 mg, 8.85 x 10^{-5} mol) and AIBN (1.45 mg, 8.85 x 10^{-6} mol) were dissolved in 20 mL of dioxane in a 50 mL dry Schlenk flask equipped with a magnetic stirrer bar. The mixture was deoxygenated by purging with Argon for 30 min and then heated to 60 ^{o}C for 45 h under Argon. The reaction was stopped by cooling to 0 ^{o}C in an ice bath and exposed to air. The solution was precipitated in diethyl ether (500 mL) and filtered. The polymer was re-dissolved in acetone and precipitated in diethyl ether. Re-dissolving and precipitating were repeated twice. The yellow powder product was dried under high vacuum at room temperature for 48 h (yield = 76 %). For a polymerization with 19.11 % of STY in the second block, the same procedure was performed as above, but with double the amount of STY (0.14 mL, 1.24 x 10^{-3} mol) and for reaction time of 60 h (yield = 78 %).

2.2.2.6 Lower Critical Solution Temperature (LCST) of the Block Copolymer as determined by DLS. Polymer samples were weighed in vials and dissolved in cold Milli-Q water at the concentration 10 mg/mL. These solutions were immediately kept in an ice bath, and then filtered directly into DLS curvets using 0.45 μm cellulose syringe filter. For measurement of the LCST, the polymer solutions were cooled to 5 ^{o}C by DLS machine, and the measurements were carried out by slowly increasing the temperature of DLS machine from 5 ^{o}C to 60 ^{o}C using Standard operating procedures (SOP) software.

2.2.2.7 Disassembly Kinetics of Block Copolymer Nanoparticles at 37 ^{o}C by DLS. The number-average particle diameter was measured for each sample to determine the disassembly time of the nanoparticles. Polymer samples were weighed in vials and dissolved in cold Milli-Q water at the concentration 5 mg/mL. These solutions were immediately kept in ice bath, and then filtered directly into DLS curvets using 0.45 μm cellulose syringe filter. The samples were kept at 37 ^{o}C water bath and the particle size at different time intervals was measured. The particles size and polydispersity index (PDI_{DLS}) were calculated based on five measurements. With polymer sample coded A, the sample was heated and kept at 45 ^{o}C for measurement.

2.2.2.8 Lower Critical Solution Temperature (LCST) of the Block Copolymer after the polymers particles fully degraded by DLS. Polymer B1, B2, C1, and C2 were weighed in vials and dissolved in cold Milli-Q water at the concentration 10 mg/mL. These solutions were then cooled in an ice bath, and filtered directly into DLS curvets using 0.45 μm cellulose syringe filter. These polymer solutions B1, B2, C1, and C2 were then kept in water bath at 37 ^{o}C for 27 h, 73 h, 26 h, and 53 h, respectively before being measured polymer particle sizes by DLS. The measurements of LCST were carried out by slowly increasing the temperature of DLS machine from 5 ^{o}C to 70 ^{o}C using SOP software.

2.2.2.9 Studying of binding ability of Oligo DNA 9-27 and thermoresponsive block copolymers at different nitrogen-to-phosphorus (N/P) ratios. 1.0 μg of Oligo DNA 9-27 (0.5 μg/μL) was complexed with each block copolymers at different nitrogen-to-phosphorus (N/P) ratios 0.5, 1, 2, 5 and 10 in a total amount volume of 100 μL of Milli-Q water. After shaking with a vortexer, the mixtures were allowed to complex without stirring for 30 min in an ice bath. The polymers/oligo DNA complexes were then kept at 37 ^{o}C in a water bath for another 15 min and run at the same time on one gel. In preparation for the gel, the complexes (20 μL) were quickly mixed with 5 μL of DNA loading dye, and immediately loaded into a 2 % agarose gel containing TAE buffer and ethidium bromide. The gels were immersed in 1x TAE buffer (heated to 50 ^{o}C). Oligo DNA 9-27 (1.0 μg) without polymer as a control. The gels were set to run in this preheat buffer for 12 min at 80 V before being visualized using a UV transilluminator. The other complexes at different nitrogen-to-phosphorus (N/P) ratios 0.5, 1, 2, 5 and 10 in a total amount volume of 100 μL of Milli-Q water were prepared with the same protocol and polymer particle sizes measured by DLS.

2.2.2.10 Studying of binding and release of Oligo DNA 9-27 / thermoresponsive block copolymers complexes. 1.0 μg of Oligo DNA 9-27 (0.5 μg/μL) was complexed with polymer at a nitrogen-to-phosphorus (N/P) ratio of 10 in a total amount volume of 100 μL of Milli-Q water. After shaking

with a vorterxer, the mixtures were allowed to complex without stirring for 30 min in an ice bath. The polymers/oligo DNA complexes were kept at 37 ^{o}C in a water bath for different times and run at the same time on one gel. The complexes (20 μL) were quickly mixed with 5 μL of DNA loading dye, and immediately loaded into a 2% agarose gel containing TAE buffer and ethidium bromide (Bio-rad). The gels were immersed in 1x TAE buffer (preheated to 50 ^{o}C). Oligo DNA 9-27 (1.0 μg) without polymer as a control. The gels were run in 1x TAE buffer (heated to 50 ^{o}C) for 12 min at 80 V before being visualized using a UV transilluminator.

2.2.2.12 Synthesis of Folic acid conjugated to a thermoresponsive polymer (H).

Synthesis of random copolymer P(NIPAM-co-BA) (D) by RAFT polymerization. NIPAM (2.00 g, 1.77 x 10^{-2} mol), BA (0.38 mL, 2.65 x 10^{-3} mol), MCEBTTC (44.68 mg, 1.77 x 10^{-4} mol), and AIBN (2.90 mg, 1.77 x 10^{-5} mol) were dissolved in 12 mL of dioxane in a 50 mL dry Schlenk flask equipped with a magnetic stirrer bar. The mixture was deoxygenated by purging with Argon for 30 min and then heated to 60 ^{o}C for 17.5 h under Argon. The reaction was stopped by cooling to 0 ^{o}C in an ice bath and exposed to air. The solution was precipitated in diethyl ether (500 mL) and filtered. The polymer was re-dissolved in acetone and precipitated in diethyl ether. The re-dissolving and precipitating process were repeated twice. The yellow powder product was dried under high vacuum at room temperature for 24 h (yield = 72 %).

Synthesis of block copolymer RAFT-PDMA-b-P(NIPAM-co-BA) (E) from P(NIPAM-co-BA) macro-CTA. DMA (0.63 mL, 6.09 x 10^{-3} mol), P(NIPAM-co-BA) macro-CTA (D) (0.80 g, 6.09 x 10^{-5} mol), and AIBN (1.00 mg, 6.09 x 10^{-6} mol) were dissolved in 8 mL of DMSO in a dry Schlenk tube equipped with a magnetic stirrer bar. The mixture was deoxygenated by purging with Argon for 30 min and then heated to 60 ^{o}C for 16.5 h under Argon. The reaction was stopped by cooling to 0 ^{o}C in an ice bath and exposed to air. The solution was then diluted with dichloromethane (500 mL) and washed with brine (3x100 mL). The dichloromethane was then dried over anhydrous $MgSO_4$, filtered and reduced in volume by rotary evaporation. The polymer was recovered by precipitation in diethyl ether (500 mL) and filtered. The polymer was re-dissolved in acetone and precipitated in diethyl ether. The re-dissolving and precipitating process were repeated twice. The yellow powder product was dried under high vacuum at room temperature for 48 h. (yield = 72 %).

Synthesis of Boc-protected amine functional copolymer (F) by Michael addition of copolymer (E) with N-(t-BOC-aminopropyl) methacrylamide. Copolymer E (0.5 g, 2.20 x 10^{-5} mol), TCEP (63.15 mg, 2.20 x 10^{-4} mol) were dissolved in 1.5 mL of DMF in a dry Schlenk tube equipped with a magnetic stirrer bar. The mixture was deoxygenated by purging with Argon for 30 min. At the same

time, TEA (31.3 μL, 2.20 x 10^{-4} mol), hexamine (31.4 μL, 2.20 x 10^{-4} mol) and 1.5 mL of DMF were added in another dry Schlenk tube and purged by Argon for 30 min. The mixture of TEA, hexamine, and DMF in the second tube was then transferred to the first tube by a deoxygenated syringe needle. The combined mixture was then kept stirring at room temperature under Argon flow for overnight and then dialysed against acetone for 1 day. The dialysed solution was concentrated to 1mL and precipitated three times in Diethyl ether. The white powder product was then dried under high vacuum at room temperature for 24 hours (yield = 85 %).

Synthesis of amine functional copolymer (G) by deprotection of copolymer (F) with TFA. Copolymer F (0.35 g, 1.54 x 10^{-5} mol), TFA (0.82 mL, 1.08 x 10^{-2} mol) were dissolved in 2 mL of DCM in a dry Schlenk tube equipped with a magnetic stirrer bar. The mixture was then stirred at room temperature for overnight. The DCM in the solution was then removed blown by under Nitrogen flow for 1 hour. The viscous solution was redissolved in 1.5 mL of DCM. The residue TFA in the solution was neutralized by 1 mL of TEA. The solution was then passed through a 0.45 μm PTFE syringe filter, concentrated to 1mL by Nitrogen flow. The concentrated solution was then precipitated in Diethyl ether three times. The white powder product was then dried under high vacuum at room temperature for 24 hours (yield = 80 %).

Synthesis of folic acid functional copolymer H. Copolymer G (0.20 g, 8.81 x 10^{-6} mol), Folate (11.66 mg, 2.64 x 10^{-5} mol), EDC.HCl (10.13 mg, 5.29 x 10^{-5} mol), and NHS (3.04 mg, 2.64 x 10^{-5} mol) were dissolved in 3.3 mL of DMSO/H_2O (10/1 V/V) in a dry Schlenk tube equipped with a magnetic stirrer bar. The mixture was then stirred at room temperature for 24 h and dialysed against cold Milli Q water for 24 h. The yellow solid, folate, was removed by filtration. The filtrate was frozen and freeze-dried for 2.5 days to give the pale yellow fluffy powder (yield = 60 %).

2.2.2.12 Cell uptaken assay. The osteosarcoma U-2OS cells were cultured in 24-well plate (1x10^5/well) in completed DMEM medium. Folic acid functionalized copolymer H was mixed with copolymer B1, B2, C1 and C2, respectively, and dissolved in cold (ice-bath) nuclease-free water to give a copolymer solution with 15 mol % of folic acid (Scheme S3). A model siRNA, a 21nt oligo DNA conjugated with Cy3 (DNA-Cy3), was diluted and added to the polymers. The N/P ratio of polymer to siRNA was 50/1. The mixtures were incubated in ice-bath for 30 minutes to allow the complexation between positive charged polymer and negative charged siRNA, followed by incubation at 37^{o}C (above the LCST for all the copolymers) for 10 minutes to allow the formation of polymer/siRNA nanoparticles. They were then added to the cells to reach the final concentration of the siRNA 50 nM for cell uptake. The cells were then incubated for 10 hours before washing

with PBS buffer and fixation with 4% paraffinformaldehyde. The cell nuclei were stained with Hoechst 33341 and cell uptake was viewed under fluorescent microscope.

2.2.3 Analytic methodologies

^{1}H, ^{1}D DOSY, and ^{2}D DOSY Nuclear Magnetic Resonance (^{1}H NMR). All NMR spectra were recorded on Bruker DRX 500 MHz using external locks ($CDCl_3$ or D_2O or DMSO-d6) and referenced to the residual non-deuterated solvent ($CHCl_3$ or H_2O or DMSO). After samples were well dissolved in $CDCl_3$ or D_2O or DMSO-d6, samples solutions were then transferred to NMR tubes. With samples in $CDCl_3$, the spectrometer was set at 25 ^{o}C for determination of polymer structure. With samples in D_2O, the spectrometer was set at different temperatures for determination of the polymer structure before and after degradation. With samples in DMSO-d6, a DOSY experiment was run at 25 ^{o}C to acquire spectra to suppress any small molecule or solvent signals by increasing the pulse gradient and increasing d (*p30*) from 1 ms to 3 ms.

Size Exclusion Chromatography (SEC) and Triple Detection_ Size Exclusion Chromatography (TD-SEC). Analysis of the molecular weight distributions of the polymers were determined using a Polymer Laboratories GPC50 Plus equipped with differential refractive index detector. Absolute molecular weights of polymers were determined using a Polymer Laboratories GPC50 Plus equipped with dual angle laser light scattering detector, viscometer, and differential refractive index detector. HPLC grade N,N-dimethylacetamide (DMAc, containing 0.03 wt % LiCl) was used as the eluent at a flow rate of 1.0 mL/min. Separations were achieved using two PLGel Mixed B (7.8 x 300 mm) SEC columns connected in series and held at a constant temperature of 50 ^{o}C. The triple detection system was calibrated using a 2 mg/mL PSTY standard (Polymer Laboratories: M_wt = 110K, d*n*/d*c* = 0.16 mL/g and IV = 0.5809). Samples of known concentration were freshly prepared in DMAc + 0.03 wt % LiCl and passed through a 0.45 μm PTFE syringe filter prior to injection. The absolute molecular weights and d*n*/d*c* values were determined using Polymer Laboratories Multi Cirrus software based on the quantitative mass recovery technique.

Dynamic Light Scattering (DLS). Dynamic light scattering measurements were performed using a Malvern Zetasizer Nano Series running DTS software and operating a 4 mW He-Ne laser at 633 nm. Analysis was performed at an angle of 173° and a constant temperature of 25 °C. The sample refractive index (RI) was set at 1.59 for polystyrene. The dispersant viscosity and RI were set to 0.89 $Ns.m^{-2}$ and 1.33, respectively. The number-average hydrodynamic particle size and polydispersity index are reported. The polydispersity index (PDI) was used to describe the width of the particle size distribution. It was calculated from a Cumulants analysis of the DLS measured

intensity autocorrelation function and is related to the standard deviation of the hypothetical Gaussian distribution (i.e., $PDI_{PSD} = \sigma^2/Z_D^2$, where σ is the standard deviation and Z_D is the Z average mean size).

2.3 Result and Discussion

The diblock copolymer was designed (Scheme 2.1B) to have a first block that provides steric stabilization to the nanoparticles in water and a second block to be both thermoresponsive and able to undergo a self-catalyzed hydrolysis reaction in water. First, the stabilizing hydrophilic poly(dimethyl acrylamide),[26] PDMA, was prepared using the Reversible addition−fragmentation chain transfer (RAFT) polymerization technique with a number-average molecular weight (M_n) of 8200 and polydispersity index (PDI) of 1.14. This polymer was then blocked with PNIPAM and PDMAEA to form the random second block. PNIPAM has an LCST close to 32 °C;[27, 28] at temperatures below its LCST, the PNIPAM is fully water-soluble, but when heated above its LCST, it becomes water insoluble.[29, 30] We have studied the self-catalytic degradation behavior of the cationic PDMAEA, which transforms into the negatively charged poly(acrylic acid) (PAA) in water over time (see Scheme A2.1 in Appendix A).[24] This polymer was shown to degrade at the same rate regardless of its molecular weight or pH (ranging from pH 5.5 to 10.1) and could bind and release negatively charged oligo DNA (a mimic of siRNA).[24, 31]The significant advantages of this polymer include its high binding to negative biomolecules, high transfection (or uptake) into cells, and full release of negatively charged biomolecules through ionic repulsion after degradation.[31] The resulting nontoxic PAA eliminates the accumulation of highly toxic cationic polymers, especially when repeat doses are required. The polymer, P(DMA_{96}-b ($NIPAM_{87}$-co- $DMAEA_{25}$)), with an M_n of 34500 and PDI of 1.23, was shown to have an LCST starting at 39 °C (see Table 2.1 and Figure A2.19), and when heated to 45 °C in water, it formed nanoparticles of 25 nm in diameter with a very narrow size distribution (0.095, where values <0.1 represents distributions that are narrow). These polymer particles changed from 25 to 19 nm in water over the first 5 h due to the intrabinding of negatively charged side groups with the positively charged ones (see Figure A2.20 in Appendix A). After 5 h, there was a sharp decrease in size over 1 h due to the disassembly to diblock unimers. Unfortunately, this polymer had an LCST well above 37 °C and would not be suitable as a drug delivery device for in vivo systems. We therefore modified the polymer to reduce the LCST well below 37 °C.

Table 2.1 Lower critical solution temperature (LCST), hydrodynamic diameter (D_h), Polydispersities (PDI) and degradation times for thermoresponsive block copolymers determined by dynamic light scattering (DLS).

Polymer	LCST (^oC)[a]	D_h (nm) (PDI)[b]	t_{start} ($t_{degrade}$)[d]
A: P(DMA_{96}-b-($NIPAM_{87}$-co-$DMAEA_{25}$))	39.0 - 41.0	25.12 (0.095)[c]	5.5 (1)[c]
B1: P(DMA_{96}-b-($NIPAM_{88}$-co-$DMAEA_{25}$-co-BA_6))	25.0 - 29.0	27.02 (0.028)	21 (5.5)
B2: P(DMA_{96}-b-($NIPAM_{91}$-co-$DMAEA_{25}$-co-BA_{12}))	17.0 - 21.0	25.31 (0.047)	66 (5.75)
C1: P(DMA_{96}-b-($NIPAM_{84}$-co-$DMAEA_{22}$-co-STY_5))	26.0 - 30.0	27.46 (0.024)	17 (5.44)
C2: P(DMA_{96}-b-($NIPAM_{40}$-co-$DMAEA_{15}$-co-STY_{13}))	15.0 - 19.0	19.99 (0.063)	47 (6.8)

[a]LCST determined by DLS (10 mg/mL). [b]Hydrodynamic diameter (D_h) determined by DLS (5 mg/mL) at 37 ^oC, [c]D_h determined by DLS (5 mg/mL) at 45 ^oC. [d]Disassembly time at 37 ^oC: t_{start} = time when the size starts to decrease; $t_{degrade}$ = time from t_{start} to formation of unimers.

One method for decreasing the LCST of polymers involves incorporating a hydrophobic monomer. The greater the weight fraction of a hydrophobic monomer in the copolymer the lower the LCST,[32, 33] conversely, the greater the amount of a hydrophilic monomer in the copolymer the higher the LCST.[34-36] In this work, we incorporated either styrene (STY) or butyl acrylate (BA) with increasing mol % into the diblock copolymer (see Table A2.1 for M_n and PDI values) to lower the LCST to below 37 °C. Polymer B1 (5% mol fraction of BA in the second block, P(DMA_{96}-b-($NIPAM_{88}$-co-$DMAEA_{25}$-co-BA_6))) gave an LCST between 25 and 29 °C, and when the soluble polymer in water was heated to 37 °C, nanoparticles of approximately 27 nm formed with a narrow size distribution (Table 2.1). Increasing the weight fraction of BA in the second block to 9.4 mol % (B2; P(DMA_{96}-b-($NIPAM_{91}$-co-$DMAEA_{25}$-co-BA_{12}))) resulted in a marked decrease in the LCST, ranging from 17 to 21 °C. When this polymer was heated in water to 37 °C, we observed a narrow particle size distribution with an average size close to 25 nm. The incorporation of 4.5 mol % STY (C1; P(DMA_{96}-b-($NIPAM_{84}$-co-$DMAEA_{22}$-co-STY_5))) resulted in the lowering of the LCST similar to that of 5 mol % BA (B1), in which the LCST ranged between 26 and 30 °C. This polymer produced a narrow size distribution of nanoparticles with an average size close to 27 nm when heated to 37 °C, which was again similar to the size produced from polymer B1. Increasing the amount of STY to 19 mol % (C2, P(DMA_{96}-b-($NIPAM_{40}$-co-$DMAEA_{15}$- co-BA_{13}))) decreased the LCST down to a range between 15 and 19 °C, which was only 2 °C lower than for B2. The size of these polymer nanoparticles at 37 °C was 20 nm. The difference between B2 and C2 was due to the difference in the molecular weights and, in particular, the differences between the number of the comonomer units (see Table A2.1). The Appendix A provides all the LCST data for the five polymers synthesized in this work. The four polymers, B1 to C2, were then solubilized in water and

heated to 37 °C. The resulting polymer nanoparticles were stored at this temperature and the change in size measured over time by dynamic light scattering (DLS). Figure 2.1 showed the change in size for the four polymers over 100 h. Nanoparticles from polymer B1 decreased in size from 27 to 18 nm after 8 h levelling off at this size until 21 h, after which time there was a rapid decrease in size to that consistent of diblock unimers (~5 nm) after 26.5 h. The pH of the polymer solution was measured to be 7.6 before and after full degradation of the PDMAEA side groups. This pH is below the pK_a for PDMAEA (8.3 for the monomer) [37] and above the pK_a of PAA (4.3), suggesting that both cationic and anionic species will be ionized in water. These data are consistent with a three stage degradation process leading to disassembly: first, the small number of initially degraded side chains (now negatively charged) will bind with the positively charged side groups to decrease the size of the nanoparticles; second, a plateau region where no change in size is observed; and third, the nanoparticles disassemble to unimers over ~5.5 h. A similar three stage size change was also observed for the other three polymers. Polymer B2 showed that the plateau time could be extended until 66 h, after which disassembly to unimers occurred over a 5.8 h period. When 4.5% mol fraction of STY was incorporated in the copolymer (i.e., C1), a similar three stage behavior similar to that of B1 was observed. Disassembly started after 17 h, and the polymer fully disassembled into unimers after a further 5.4 h. With a similar trend, polymer C2 (19 mol % STY in the second block) started to disassemble after 47 h, and was fully disassembled to unimers after a further 6.8 h. The data in Figure 2.1 clearly showed that the disassembly process for all polymers could be controlled, suggesting that we could control the time at which disassembly occurs by simply manipulating the hydrophobic monomer content in the second block. In addition, the time for disassembly for all polymers was approximately 6 h, suggesting the same release profile of the payload from the nanoparticles regardless of the time at the start of disassembly.

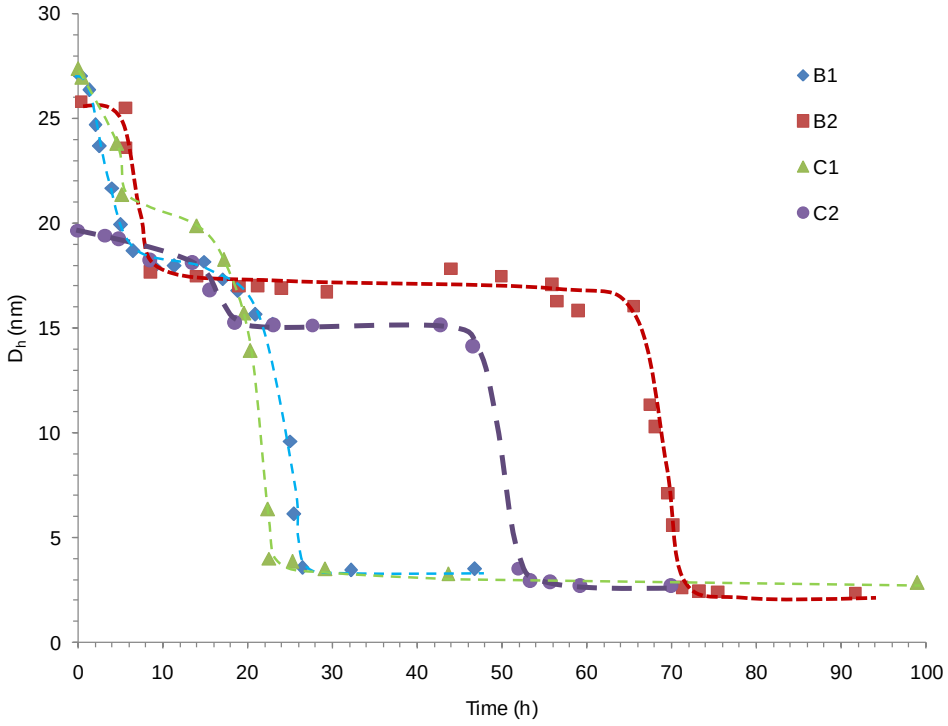

Figure 2.1 Degradation kinetics profiles for B1, B2, C1, and C2. The data were averaged from five measurements by DLS at polymer solution concentration of 5 mg/mL at 37 °C.

The sharp disassembly profile observed in Figure 2.1 supports a change in the thermoresponsive nature of the polymers as the DMAEA side groups undergo a self-catalyzed hydrolysis. The LCST of the four polymers (B1 to C2) measured approximately 30 min after full disassembly to unimers (see Table 2.2 and Appendix A) showed that the LCST of polymers B1 to C2 were above 37 °C (ranging between 39 and 41 °C for B1 and C1, and 37−39 °C for B2 and C2). The data demonstrated that with the increase in the degradation of DMAEA side groups to carboxylic acids, the diblock copolymer's LCST increased, and when the LCST became greater than 37 °C, disassembly to water-soluble unimers occurred. This mechanism resulted in a sharp disassembly transition from spherical nanoparticles to water-soluble diblock copolymer unimers. When the polymers were allowed to be stored for one month at 37 °C, no LCST was observed even at temperatures as high as 70 °C.

Table 2.2 Lower critical solution temperature (LCST), hydrodynamic diameter (D_h), Polydispersities (PDI) for the block copolymers after being fully degraded (i.e., full conversion of DMAEA to acrylic acid (AA)).

Polymer	Time (h)[a]	LCST (^oC)[b]	D_h (nm)[c]
B1	27	39.0 - 41.0	16.67 ± 1.32
B2	73	37.0 - 39.0	15.66 ± 1.42
C1	26	39.0 - 41.0	15.39 ± 1.08
C2	53	37.0 - 39.0	12.56 ± 0.15

[a]Time after which the LCST of the polymer was determined. [b] LCST determined by DLS (10 mg/mL).

[c]Hydrodynamic diameter (D_h) determined by DLS (5 mg/mL) at a temperature just above the LCST.

Polymer/DNA Binding, Release, and Cell Uptake. The efficient delivery of siRNA holds great promise in the cure for cancers and infectious diseases.[38-41] For siRNA-based delivery carriers to reach their full potential, they must be protected from enzymatic degradation, efficiently be taken up by cells, and the siRNA released with controlled and reproducible pharmacokinetics.[42-44] The main problems with positively charged polymers for siRNA delivery are (i) the difficulty to fully release the siRNA[45-47] and (ii) their high toxicity, which becomes problematic after repeat doses due to accumulation in tissues.[27, 48] We previously showed that PDMAEA can readily bind to oligo DNA (a 9−27 oligo DNA that is a close analog to siRNA) and once the side groups have degraded to negatively charged carboxylic acid groups release all the negatively charged oligo DNA.[24, 31] However, the homopolymer PDMAEA gave no control over the release profile. In this current work, we will use the well-proven model compound oligo DNA to determine whether the release profiles of the oligo DNA from four polymers (B1 to C2) were the same as the disassembly profiles, as shown in Figure 2.1.

The oligo DNA and polymer were mixed in an ice bath at an N/P ratio of 10 (i.e., the ratio of nitrogen on the polymer to phosphorus on the oligo DNA) and allowed to stand for 30 min without stirring and then heated to 37 °C. This N/P ratio was chosen as it showed complete binding with the oligo DNA (see Figure A2.25 in Appendix A). It was found that there was no change in the size of the nanoparticles (between 20 to 30 nm in diameter) when measured at 37 °C (i.e., above the LCST of the polymers) in the absence or presence of oligo DNA, as shown in Table A2.2. To determine the ability of the oligo DNA to bind with the polymer nanoparticles, we performed agarose gel retardation assays. The oligo DNA cannot enter the gel when bound or complexed to the polymer nanoparticles. All four polymer nanoparticles strongly bound with oligo DNA at an N/P (nitrogen to phosphorus) ratio of 10 after incubation for 1 h (Figure 2.2). This assay also provided insight into the leakage of oligo DNA over time and the release of oligo DNA over time. There was no evidence

of leakage of any oligo DNA from polymer B after 20 h, and release of all oligo DNA was observed after 26 h. This release profile was consistent with the disassembly profile shown in Figure 2.1. Disassembly occurred after 21 h and full disassembly after a further 5.5 h, supporting the release of all oligo DNA after 26 h. Polymers B2, C1, and C2 also showed the same trends, with the release time of all oligo DNA consistent with the full disassembly time of the polymer nanoparticles (see Table 2.1). Importantly, there was no leakage of oligo DNA until disassembly commenced. These findings support the timed and controlled release of the oligo DNA by manipulating the LCST of the polymer above 37 °C as a function of the DMAEA degradation to PAA.

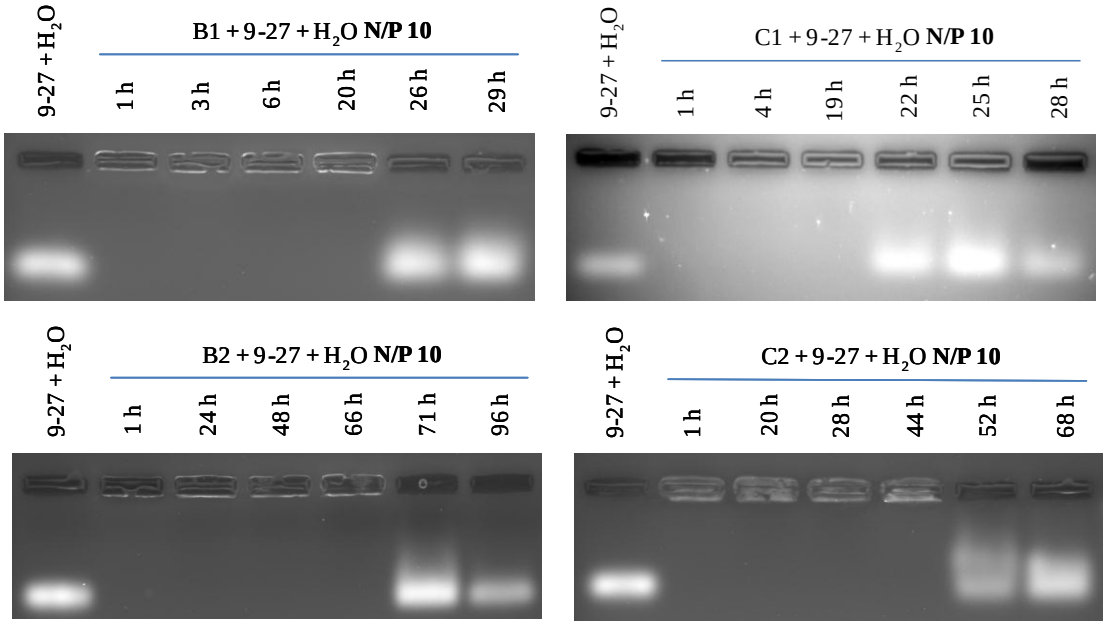

Figure 2.2 Agarose gel assay for binding and release of Oigo DNA 9-27 from the polymer/DNA complex nanoparticles at different times in Milli-Q water at N/P Ratio 10. Soluble copolymers in Milli-Q water were incubated with DNA (N/P ratio 10) at below their LCST for 30 min and then heated and kept at 37 ^{o}C for agarose gel retardation assay over different times.

To test whether these timed-release nanoparticles could be taken up by cells prior to degradation to unimers, we mixed Cy3 oligo DNA with our polymers and added these complexes to osteosarcoma U2OS cells at 37 °C and were then incubated for 10 h. All polymers showed little or no uptake. Folic acid was then coupled to the end of a thermoresponsive polymer G ($PDMA_{99}$-b-P($NIPAM_{97}$-co-BA_{13})) to form polymer H (Figure 2.3A, and see Appendix A) as a binding agent to cancer cells. Polymer H (15 mol %) was coassembled with each of the polymers B1−C2 and complexed with Cy3-DNA in one pot. This represents a simple but effective method to surface functionalization such nanoparticles without changing the disassociation properties of polymer B1 to C2. The uptake (Figure 2.3B) of Cy3 oligo DNA with a representative polymers C2 and H was high (Figure 2.3B

(i)), while C2 and H polymers only (Figure 2.3B (ii)) and Cy3 oligo DNA (Figure 2.3B (iii)) showed no uptake.

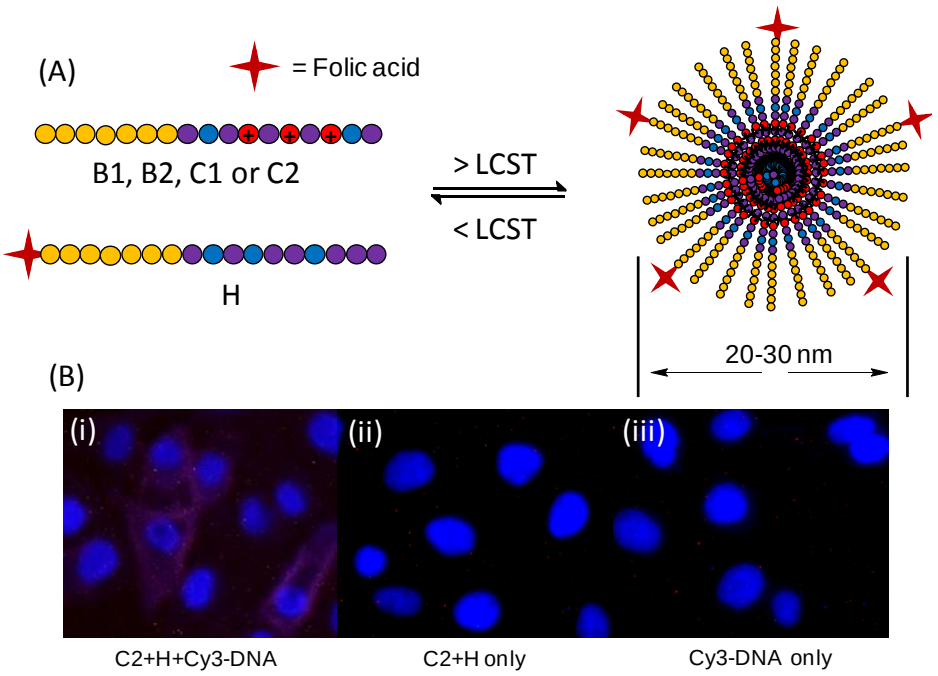

Figure 2.3 (A) Synthesis of folic acid functionalized timed-release nanoparticles. (B) Fluorescent microscopy photos of the osteosarcoma U2OS cells dosed with 50 nM Cy3 oligo DNA and copolymer polyplexes in completed DMEM medium. N/P ratio (i.e polymer to siRNA) was 50:1 in water at 37 ^{o}C. They were then added to the cells and were incubated for 10 hours before washing with PBS buffer and fixation with 4% paraffin formaldehyde. The cell nuclei were stained with Hoechst 33341 and cell uptake viewed under fluorescent microscope. Photos (i) copolymers C2+H+Cy3-DNA, (ii) C2+H and (iii) Cy3-DNA.

2.4 Conclusion

In conclusion, we have demonstrated the use of designer diblock copolymer nanoparticles to release, as a proof of concept, oligo DNA (a proven model compound for biological therapeutics) on-demand using a timed disassembly process. The release mechanism does not require activation from remote sources or biological or pH triggers. The polymers used in this study consisted of a hydrophilic block for stabilization and a second thermoresponsive block for self-assembly and disassembly. At temperatures below the second block's LCST (i.e., below 37 °C for in vitro assays), the diblock copolymer was fully water-soluble, and when heated to 37 °C, the polymer self-assembled into a narrow size distribution of nanoparticles with an average diameter of approximately 25 nm. The thermoresponsive nature of the second block could be manipulated in situ by the self-catalyzed degradation of cationic DMAEA units to negatively charged acrylic acid

groups, and when the amount of acids groups was sufficiently high to increase the LCST of the second block above 37 °C, the nanoparticles disassembled to unimers over approximately 5−6 h. The disassembly time of 5−6 h was similar regardless of the time when the nanoparticles started to disassemble, and the polymers showed excellent binding to oligo DNA without any leakage until full disassembly to unimers. These naked nanoparticles could only be taken up by osteosarcoma cells when coated with a transfection agent, folic acid. We used a coassembly method using the polymers B1−C2 and a folic acid functionalized thermoresponsive polymer to produce nanoparticles with folic acid on the surface and without changing the disassembly profiles of the B1−C2 polymers. The well-defined and controlled release profiles observed in this work represent a significant step toward controlled release in the absence of an external trigger and, with our coassembly method, allows for other functional molecules to be decorated on the nanoparticle surface. This new nanoparticle technology could enable sophisticated combination therapies. For example, one or more therapeutic agents encapsulated in different timed-release nanoparticles, in which this particle mixture could be used in a one dosing regimen for tailored release of the agents when required. They could be programmed to release certain therapeutics at the time after administration when optimal biodistribution of the particles has occurred and when the agents will have maximal pharmacodynamic effect, and then slowly and consistently over time. One key application we are exploring is in improved methods for delivery of antitumor agents, leading to an optimized therapeutic index for cancer therapy.

2.5 References

1. Esser-Kahn, A. P.; Odom, S. A.; Sottos, N. R.; White, S. R.; Moore, J. S., Triggered Release from Polymer Capsules. *Macromolecules* **2011,** 44, (14), 5539-5553.
2. Johnston, A. P. R.; Such, G. K.; Caruso, F., Triggering Release of Encapsulated Cargo. *Angew. Chem. Int. Ed.* **2010,** 49, (15), 2664-2666.
3. Motornov, M.; Roiter, Y.; Tokarev, I.; Minko, S., Stimuli-responsive nanoparticles, nanogels and capsules for integrated multifunctional intelligent systems. *Prog. Polym. Sci.* **2010,** 35, (1–2), 174-211.
4. De Geest, B. G.; Sukhorukov, G. B.; Möhwald, H., The pros and cons of polyelectrolyte capsules in drug delivery. *Expert Opin. Drug Deliv.* **2009,** 6, (6), 613-624.
5. Brun-Graeppi, A. K. A. S.; Richard, C.; Bessodes, M.; Scherman, D.; Merten, O.-W., Cell microcarriers and microcapsules of stimuli-responsive polymers. *J. Controlled Release* **2011,** 149, (3), 209-224.
6. Shchukin, D. G.; Grigoriev, D. O.; Mohwald, H., Application of smart organic nanocontainers in feedback active coatings. *Soft Matter* **2010,** 6, (4), 720-725.
7. Soliman, M.; Allen, S.; Davies, M. C.; Alexander, C., Responsive polyelectrolyte complexes for triggered release of nucleic acid therapeutics. *Chem. Commun. (Camb.)* **2010,** 46, (30), 5421-5433.
8. Pastine, S. J.; Okawa, D.; Zettl, A.; Fréchet, J. M. J., Chemicals On Demand with Phototriggerable Microcapsules. *J. Am. Chem. Soc.* **2009,** 131, (38), 13586-13587.
9. Li, Y.; Tang, Y.; Yang, K.; Chen, X.; Lu, L.; Cai, Y., Facile Synthesis and Photo-Tunable Properties of a Photosensitive Polymer Whose Chromophores Bound with pH-Labile Cyclic Acetal Linkages. *Macromolecules* **2008,** 41, (13), 4597-4606.
10. Bohlender, C.; Wolfram, M.; Goerls, H.; Imhof, W.; Menzel, R.; Baumgaertel, A.; Schubert, U. S.; Mueller, U.; Frigge, M.; Schnabelrauch, M.; Wyrwa, R.; Schiller, A., Light-triggered NO release from a nanofibrous non-woven. *J. Mater. Chem.* **2012,** 22, (18), 8785-8792.
11. Lu, Z.; Prouty, M. D.; Guo, Z.; Golub, V. O.; Kumar, C. S. S. R.; Lvov, Y. M., Magnetic Switch of Permeability for Polyelectrolyte Microcapsules Embedded with Co@Au Nanoparticles. *Langmuir* **2005,** 21, (5), 2042-2050.
12. Hu, S.-H.; Tsai, C.-H.; Liao, C.-F.; Liu, D.-M.; Chen, S.-Y., Controlled Rupture of Magnetic Polyelectrolyte Microcapsules for Drug Delivery. *Langmuir* **2008,** 24, (20), 11811-11818.
13. Caruso, M. M.; Schelkopf, S. R.; Jackson, A. C.; Landry, A. M.; Braun, P. V.; Moore, J. S., Microcapsules containing suspensions of carbon nanotubes. *J. Mater. Chem.* **2009,** 19, (34), 6093-6096.
14. MacKinnon, N.; Guérin, G. r.; Liu, B.; Gradinaru, C. C.; Rubinstein, J. L.; Macdonald, P. M., Triggered Instability of Liposomes Bound to Hydrophobically Modified Core−Shell PNIPAM Hydrogel Beads. *Langmuir* **2009,** 26, (2), 1081-1089.
15. Chan, Y.; Wong, T.; Byrne, F.; Kavallaris, M.; Bulmus, V., Acid-Labile Core Cross-Linked Micelles for pH-Triggered Release of Antitumor Drugs. *Biomacromolecules* **2008,** 9, (7), 1826-1836.
16. Zhang, L.; Bernard, J.; Davis, T. P.; Barner-Kowollik, C.; Stenzel, M. H., Acid-Degradable Core-Crosslinked Micelles Prepared from Thermosensitive Glycopolymers Synthesized via RAFT Polymerization. *Macromol. Rapid Commun.* **2008,** 29, (2), 123-129.
17. Johnston, A. P. R.; Lee, L.; Wang, Y.; Caruso, F., Controlled Degradation of DNA Capsules with Engineered Restriction-Enzyme Cut Sites. *Small* **2009,** 5, (12), 1418-1421.
18. Cavalieri, F.; Postma, A.; Lee, L.; Caruso, F., Assembly and Functionalization of DNA−Polymer Microcapsules. *ACS Nano* **2009,** 3, (1), 234-240.
19. Glangchai, L. C.; Caldorera-Moore, M.; Shi, L.; Roy, K., Nanoimprint lithography based fabrication of shape-specific, enzymatically-triggered smart nanoparticles. *J. Controlled Release* **2008,** 125, (3), 263-272.

20. Jain, R. K.; Stylianopoulos, T., Delivering nanomedicine to solid tumors. *Nat. Rev. Clin. Oncol.* **2010,** 7, (11), 653-664.
21. Wong, C.; Stylianopoulos, T.; Cui, J.; Martin, J.; Chauhan, V. P.; Jiang, W.; Popović, Z.; Jain, R. K.; Bawendi, M. G.; Fukumura, D., Multistage nanoparticle delivery system for deep penetration into tumor tissue. *Proceedings of the National Academy of Sciences* **2011,** 108, (6), 2426-2431.
22. de Jong, S. J.; Arias, E. R.; Rijkers, D. T. S.; van Nostrum, C. F.; Kettenes-van den Bosch, J. J.; Hennink, W. E., New insights into the hydrolytic degradation of poly(lactic acid): participation of the alcohol terminus. *Polymer* **2001,** 42, (7), 2795-2802.
23. van Nostrum, C. F.; Veldhuis, T. F. J.; Bos, G. W.; Hennink, W. E., Hydrolytic degradation of oligo(lactic acid): a kinetic and mechanistic study. *Polymer* **2004,** 45, (20), 6779-6787.
24. Truong, N. P.; Jia, Z.; Burges, M.; McMillan, N. A. J.; Monteiro, M. J., Self-Catalyzed Degradation of Linear Cationic Poly(2-dimethylaminoethyl acrylate) in Water. *Biomacromolecules* **2011,** 12, (5), 1876-1882.
25. Urbani, C. N.; Monteiro, M. J., Nanoreactors for Aqueous RAFT-Mediated Polymerizations. *Macromolecules* **2009,** 42, (12), 3884-3886.
26. Sebakhy, K. O.; Kessel, S.; Monteiro, M. J., Nanoreactors to Synthesize Well-defined Polymer Nanoparticles: Decoupling Particle Size from Molecular Weight. *Macromolecules* **2010,** 43, (23), 9598-9600.
27. You, Y. Z.; Hong, C. Y.; Pan, C. Y.; Wang, P. H., Synthesis of a Dendritic Core–Shell Nanostructure with a Temperature-Sensitive Shell. *Adv. Mater.* **2004,** 16, (21), 1953-1957.
28. Wang, X.; Qiu, X.; Wu, C., Comparison of the Coil-to-Globule and the Globule-to-Coil Transitions of a Single Poly(N-isopropylacrylamide) Homopolymer Chain in Water. *Macromolecules* **1998,** 31, (9), 2972-2976.
29. Schild, H. G., Poly(N-isopropylacrylamide): experiment, theory and application. *Prog. Polym. Sci.* **1992,** 17, (2), 163-249.
30. Zhang, X.-Z.; Zhuo, R.-X., Dynamic Properties of Temperature-Sensitive Poly(N-isopropylacrylamide) Gel Cross-Linked through Siloxane Linkage. *Langmuir* **2000,** 17, (1), 12-16.
31. Truong, N. P.; Jia, Z.; Burgess, M.; Payne, L.; McMillan, N. A. J.; Monteiro, M. J., Self-Catalyzed Degradable Cationic Polymer for Release of DNA. *Biomacromolecules* **2011,** 12, (10), 3540-3548.
32. Chee, C. K.; Rimmer, S.; Shaw, D. A.; Soutar, I.; Swanson, L., Manipulating the Thermoresponsive Behavior of Poly(N-isopropylacrylamide). 1. On the Conformational Behavior of a Series of N-Isopropylacrylamide−Styrene Statistical Copolymers. *Macromolecules* **2001,** 34, (21), 7544-7549.
33. Yin, X.; Hoffman, A. S.; Stayton, P. S., Poly(N-isopropylacrylamide-co-propylacrylic acid) Copolymers That Respond Sharply to Temperature and pH. *Biomacromolecules* **2006,** 7, (5), 1381-1385.
34. Feil, H.; Bae, Y. H.; Feijen, J.; Kim, S. W., Effect of comonomer hydrophilicity and ionization on the lower critical solution temperature of N-isopropylacrylamide copolymers. *Macromolecules* **1993,** 26, (10), 2496-2500.
35. Taylor, L. D.; Cerankowski, L. D., Preparation of films exhibiting a balanced temperature dependence to permeation by aqueous solutions—a study of lower consolute behavior. *Journal of Polymer Science: Polymer Chemistry Edition* **1975,** 13, (11), 2551-2570.
36. Chiklis, C. K.; Grasshoff, J. M., Swelling of thin films. I. Acrylamide–N-isopropylacrylamide copolymers in water. *Journal of Polymer Science Part A-2: Polymer Physics* **1970,** 8, (9), 1617-1626.
37. van de Wetering, P.; Zuidam, N. J.; van Steenbergen, M. J.; van der Houwen, O. A. G. J.; Underberg, W. J. M.; Hennink, W. E., A Mechanistic Study of the Hydrolytic Stability of Poly(2-(dimethylamino)ethyl methacrylate). *Macromolecules* **1998,** 31, (23), 8063-8068.

38. Pecot, C. V.; Calin, G. A.; Coleman, R. L.; Lopez-Berestein, G.; Sood, A. K., RNA interference in the clinic: challenges and future directions. *Nat. Rev. Cancer* **2011,** 11, (1), 59-67.
39. Davis, M. E.; Zuckerman, J. E.; Choi, C. H. J.; Seligson, D.; Tolcher, A.; Alabi, C. A.; Yen, Y.; Heidel, J. D.; Ribas, A., Evidence of RNAi in humans from systemically administered siRNA via targeted nanoparticles. *Nature* **2010,** 464, (7291), 1067-1070.
40. Kole, R.; Krainer, A. R.; Altman, S., RNA therapeutics: beyond RNA interference and antisense oligonucleotides. *Nat. Rev. Drug Discov.* **2012,** 11, (2), 125-140.
41. Crunkhorn, S., RNA interference: Clinical gene-silencing success. *Nat. Rev. Drug Discov.* **2010,** 9, (5), 359-359.
42. Zhang, Y.; Satterlee, A.; Huang, L., In Vivo Gene Delivery by Nonviral Vectors: Overcoming Hurdles[quest]. *Mol. Ther.* **2012,** 20, (7), 1298-1304.
43. Juliano, R.; Bauman, J.; Kang, H.; Ming, X., Biological Barriers to Therapy with Antisense and siRNA Oligonucleotides. *Mol. Pharm.* **2009,** 6, (3), 686-695.
44. Morrissey, D. V.; Lockridge, J. A.; Shaw, L.; Blanchard, K.; Jensen, K.; Breen, W.; Hartsough, K.; Machemer, L.; Radka, S.; Jadhav, V.; Vaish, N.; Zinnen, S.; Vargeese, C.; Bowman, K.; Shaffer, C. S.; Jeffs, L. B.; Judge, A.; MacLachlan, I.; Polisky, B., Potent and persistent in vivo anti-HBV activity of chemically modified siRNAs. *Nat Biotech* **2005,** 23, (8), 1002-1007.
45. Miyata, K.; Kakizawa, Y.; Nishiyama, N.; Harada, A.; Yamasaki, Y.; Koyama, H.; Kataoka, K., Block Catiomer Polyplexes with Regulated Densities of Charge and Disulfide Cross-Linking Directed To Enhance Gene Expression. *J. Am. Chem. Soc.* **2004,** 126, (8), 2355-2361.
46. Schaffer, D. V.; Fidelman, N. A.; Dan, N.; Lauffenburger, D. A., Vector unpacking as a potential barrier for receptor-mediated polyplex gene delivery. *Biotechnol. Bioeng.* **2000,** 67, (5), 598-606.
47. Plank, C.; Tang, M. X.; Wolfe, A. R.; Szoka, F. C., Jr., Branched cationic peptides for gene delivery: role of type and number of cationic residues in formation and in vitro activity of DNA polyplexes. *Hum. Gene. Ther.* **1999,** 10, (2), 319-32.
48. Piest, M.; Lin, C.; Mateos-Timoneda, M. A.; Lok, M. C.; Hennink, W. E.; Feijen, J.; Engbersen, J. F. J., Novel poly(amido amine)s with bioreducible disulfide linkages in their diamino-units: Structure effects and in vitro gene transfer properties. *J. Controlled Release* **2008,** 130, (1), 38-45.

Chapter 3

Fine Tuning the Disassembly Time of Thermoresponsive Polymer Nanoparticles

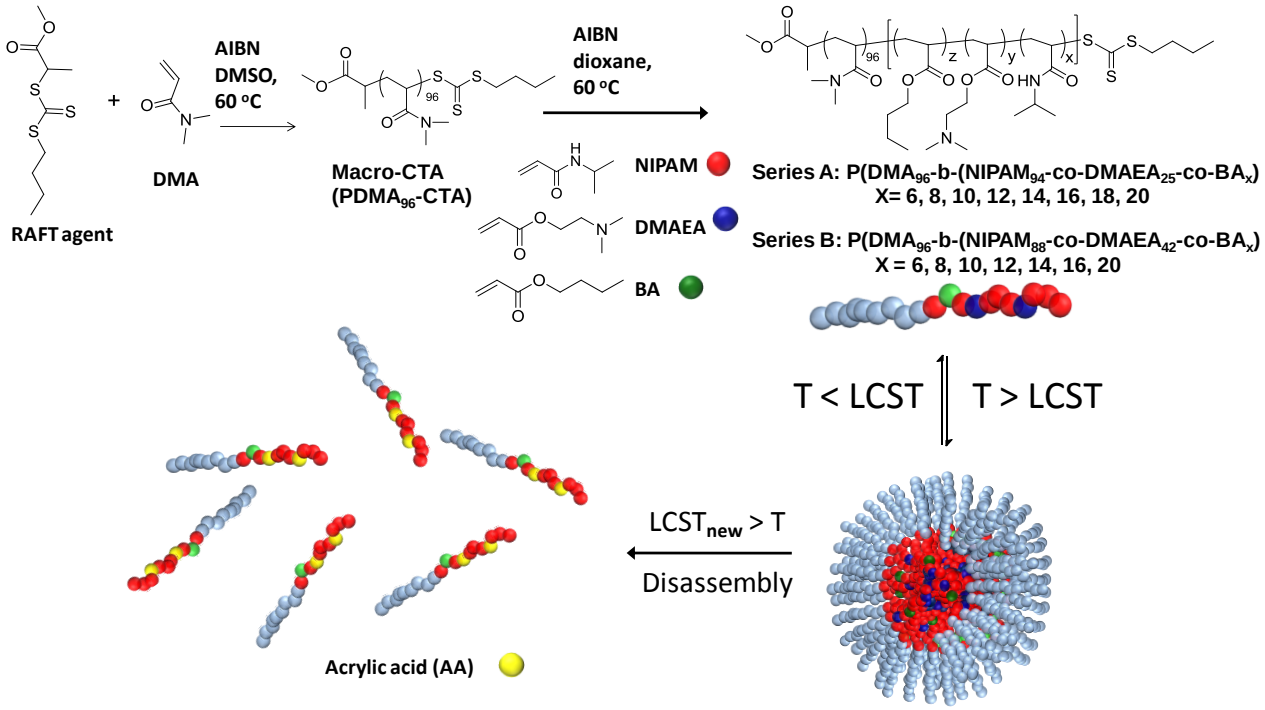

Timed-released disassembly of nanoparticles without a remote trigger or environmental cues is demonstrated in this work. The Reversible addition−fragmentation chain transfer (RAFT) polymerization allowed the fine-tuning of the chemical composition in the diblock copolymers, in which the first block consisted of a hydrophilic monomer (DMA) and the second random block consisted of three different monomers: (a) the thermoresponsive NIPAM, (b) the self-catalyzed hydrolyzable DMAEA, and (c) the hydrophobic BA. These diblock copolymers were solubilized in water below the lower critical solution temperature (LCST) of the thermoresponsive second block, and heated to 37 °C (i.e., >LCST) to form small micelle nanoparticles with a narrow particle size distribution. As DMAEA hydrolyzed to acrylic acid groups, the LCST of the diblock increased, and the time at the start of micelle disassembly (t_{start}) corresponded to the point where the LCST was equal to the solution temperature (i.e., 37 °C). The high water content in the PNIPAM core allowed an even degradation of the core over time. The copolymer composition allowed fine control over t_{start}, as this time was linearly dependent upon the BA units in the second block. These nanoparticles could also be designed to be stable (i.e., not disassemble) over a wide pH range or disassemble below a pH of 7.3. Additionally, the time from the start of disassembly to full unimer formation ($t_{degrade}$) could be controlled by the amount of DMAEA units in the second block. A longer $t_{degrade}$

(~5.5 h) was found when the number of DMAEA units was 42 compared to $t_{degrade}$ of 1.1 h for 25 units. The nanoparticles designed in this work, through fine control of the polymer chemical composition, have the potential for drug delivery purposes for timed-release of drugs and prodrugs and other wide-ranging applications where timed-release would be beneficial.

3.1 Introduction

The "on-demand" triggered disassembly of polymer nanoparticles has attracted attention for use in many applications, ranging from drug delivery, to fragrance release, to nanoreactors. [1-8] The most utilized methods for disassembly are via pH change,[9-11] acid or base degradation of polymer side groups,[12] light,[13-16] enzymatic cleavage of chemical linkers,[17-19] and electrical or magnetic stimulation.[20-22] Diblock copolymers, consisting of a permanent hydrophilic first block and a thermoresponsive polymer (e.g., poly(N-isopropylacrylamide), PNIPAM) and other trigger-susceptible monomer units in a second random block, self-assemble into micelles above the LCST (lower critical solution temperature) of the thermoresponsive polymer.[5, 6, 23]These micelles can disassemble using one of the external triggers described above.[24, 25] Environmental triggers (such as pH, enzymatic activity, temperature) may be difficult to control in practice and will have significant variability depending upon the application; an aspect that becomes important in biological and other applications. Developing new self-triggered disassembly methods would represent an advance in "smart" materials overcoming the variability and enabling applications, where external sources are not viable. Recently, we found that the cationic poly(2- (dimethylamino)ethyl acrylate (PDMAEA) could self-catalyze into the negatively charged poly(acrylic acid) (PAA).[26] The rate of PDMAEA degradation in water was found to be independent of the studied pH range (i.e., 5.5 to 10.1) and independent of the molecular weight. The cationic nature of PDMAEA allowed strong binding of an oligo DNA (a model compound for siRNA) and its release after 24 h due to the DMAEAs hydrolysis to the nontoxic PAA.[27] The degradation to the nontoxic PAA has the potential for multidose applications, especially important in drug delivery. The PDMAEA/oligo DNA complex was rapidly taken up by 80% of cells in less than 4 h, providing sufficient time for release of the oligo DNA in the cytosol. We utilized the self-degradation mechanism of PDMAEA in polymer nanoparticles to deliver and release siRNA to knockdown biochemical pathways in cells.[3] The diblock copolymer consisted of a first PDMAEA block joined to a random second block of P(N-(3-(1Himidazol-1-yl)propyl)acrylamide (PImPAA) and poly(butylacrylate) (PBA).[3] The first PDMAEA block bound to siRNA transfected the cells and released siRNA after 17 h, while the second block (P(ImPAA-co-BA)) was designed to induce fusion with the endosome membrane and allowed the siRNA/polymer complex to escape into the cytosol. The in vitro results showed selective and potent knockdown of two very different cell lines at approximately 80% at an N/P

(nitrogen on the polymer to phosphorus on the oligonucleotide) ratio of only 10,[3] and at N/P ratios greater than 10 we observed near complete knocked down of cells.[2] Controlling the release time of oligo DNA or siRNA from the polymer complex could be achieved using a thermoresponsive diblock copolymer that formed micelles (~25 nm) above the LCST of the thermoresponsive block.[28] The first block consisted of the permanent hydrophilic poly(dimethyl acrylamide) (PDMA), and the second block consisted of a random block of the thermoresponsive NIPAM, DMAEA, BA, and styrene (STY) units. Using various ratios of monomer units in the second block, we could control the micelle disassembly time from 20 to 70 h (denoted as t_{start}) with four polymer variants. By increasing the hydrophobic units of either BA or STY, the disassembly time could be increased, representing the first nontriggered disassembly method independent of pH. Interestingly, the time from the start of disassembly to full unimer formation for all polymers was ~5 h (denoted as $t_{degrade}$), and allowed release of oligo DNA after time t (=t_{start} + $t_{degrade}$).

3.1.1 Aim of the Chapter

The goal of this chapter is not only to control the disassembly time (t_{start}), with great precision but also control time from the start of disassembly to full unimer formation ($t_{degrade}$) by systematically dialing in the number of DMAEA and BA units in the second block. We synthesized two series of diblock thermoresponsive copolymers PDMA-b-P(NIPAM-co-DMAEA-co-BA) by Reversible addition− fragmentation chain transfer (RAFT) polymerization (see Scheme 3.1). In this work, we varied the number of self-degradable DMAEA unit and hydrophobic BA unit in order to investigate the influence of these change in polymer composition on the t_{start} and $t_{degrade}$ of the self-assembled polymer nanoparticles. Moreover, the mechanism of the disassembly was also studied. The effect of the pH medium on the self-assembly of the polymer nanoparticles was also evaluated.

3.2 Experimental

3.2.2 Materials

Dioxane (Aldrich, 99%), carbondisulfide (Aldrich, 99%), 1-butanethiol (Aldrich, 99%), methyl bromopropionate (Aldrich, 98%), dimethyl sulfoxide (DMSO, Aldrich >99.9%), dichloromethane (DCM: Labscan, AR grade), buffer concentrate at pH = 7 (Fluka –Sigma Aldrich), and 10X Phosphate buffered Saline (Gibco-Life Technology) were used as received. The following monomers were purified by passing through a basic alumina (activity I) column to remove inhibitor: styrene (STY, Aldrich, 99 %), dimethylacrylamide (DMA, Aldrich, 99 %), N,N-(dimethylamino) ethyl acrylate (DMAEA, Sigma-Aldrich, 98%), and butyl acrylate (BA, Aldrich, 99%). N-Isopropylacrylamide (NIPAM, Aldrich, 97 %) was purified by recrystallization from hexane.

Azobisisobutyronitrile (AIBN) was also recrystallized twice from methanol prior to use. Milli-Q Water (18.2 MΩcm-1) was generated using a Millipore Milli-Q academic water purification system. All other chemicals and solvents used were of at least analytical grade and used as received. The chain transfer agent (CTA), methyl 2-(butylthiocarbonothioylthio)propanoate (MCEBTTC) was synthesized according to the literature procedure,[5] and found to have a low toxicity.[4]

3.2.2 Synthetic procedures

*3.2.2.1 Synthesis of Poly(N, N-diethylacrylamide) Macro Chain Transfer Agent (PDMA96 Macro-CTA).*DMA (25.99 mL, 0.25mol), MCEBTTC (636.6 mg, 2.50 x 10^{-3} mol), and AIBN (33.10 mg, 2.02 x 10^{-4} mol) were dissolved in 50 mL DMSO in a 100 mL dry Schlenk flask equipped with a magnetic stirrer bar. The mixture was deoxygenated by purging with argon for 1 h and then heated to 60 ^{o}C for 3 h. The reaction was stopped by cooling to 0 ^{o}C in an ice bath and exposed to the air. The solution was then diluted with dichloromethane (500 mL) and washed with brine (3x100 mL). The DCM fraction was then dried over anhydrous $MgSO_4$, filtered and reduced in volume by rotary evaporation. The polymer was recovered by precipitation into large excess of diethyl ether (1 L), and isolated by filtration. The polymer was re-dissolved in acetone and precipitated in diethyl ether. The re-dissolving and precipitation process was repeated two times. The polymer was filtered and then dried under high vacuum for 24 h at room temperature to give a yellow powder product (yield = 81%): M_n = 9700, PDI =1.03 (SEC-Triple Detection using PSTY Standards in DMAc solution containing 0.03 wt% of LiCl, dn/dc = 0.081); M_n = 9770 (^{1}H NMR). ^{1}H NMR (500 MHz, $CDCl_3$): δ 0.87 (C*H*$_3$CH$_2$CH$_2$-), 1.09 (C*H*$_3$-(CH-COO)-), 2.84-3.05 ((C*H*$_3$)$_2$-N-), 3.29 (-C*H*$_2$-S-(C=S)-S-), 3.60 (C*H*$_3$O-(C=O)-), 5.14 (-(C=S)-S-C*H*-).

3.2.2.2 Synthesis of block copolymers of NIPAM, DMAEA, and BA from PDMA96 Macro-CTA (A1 to A8). In a typical reaction, NIPAM (1.00 g, 8.85 x 10^{-3} mol), DMAEA (0.34 mL, 2.21 x 10^{-3} mol), BA in different amounts (see Table A3.1), $PDMA_{96}$ macro-CTA (725.66 mg, 7.43 x 10^{-5} mol) and AIBN (1.45 mg, 8.85 x 10^{-6} mol) were dissolved in 6 mL of dioxane in a 20 mL dry Schlenk flask equipped with a magnetic stirring bar. The mixture was deoxygenated by purging with argon for 30 min and then heated to 60 ^{o}C under argon. The reaction time of the reactions (A1 to A8) is listed in Table 3.1. The reaction was stopped by cooling to 0 ^{o}C in an ice bath and exposed to air. The solution was precipitated in diethyl ether (500 mL) and filtered. The polymer was re-dissolved in acetone and precipitated in diethyl ether. The re-dissolving and precipitating steps were repeated twice. The yellow powder product was dried under high vacuum at room temperature for 48 h.

3.2.2.3 Synthesis of block copolymers of NIPAM, DMAEA, and BA from PDMA96 Macro-CTA (B1to B7). In a typical reaction, NIPAM (1.00 g, 8.85 x 10^{-3} mol), DMAEA (0.62 mL, 3.98 x 10^{-3} mol), BA with different amounts (see Table A3.2), PDMA macro-CTA (725.66 mg, 7.43 x 10^{-5} mol) and AIBN (1.45 mg, 8.85 x 10^{-6} mol) were dissolved in 6 mL of dioxane in a 20 mL dry Schlenk flask equipped with a magnetic stirring bar. The mixture was deoxygenated by purging with argon for 30 min and then heated to 60 ^{o}C under argon. The reaction time of the reactions (B1to B7) is listed in Table 3.2. The reaction was stopped by cooling to 0 ^{o}C in an ice bath and exposed to air. The solution was precipitated in diethyl ether (500 mL) and filtered. The polymer was re-dissolved in acetone and precipitated in diethyl ether. The re-dissolving and precipitating steps were repeated twice. The yellow powder product was dried under high vacuum at room temperature for 48 h.

3.2.2.4 Preparation of buffer solution

(i) pH 5.5. Sodium acetate (540.0 mg, 6.6 mmol), and acetic acid (54.0 mg, 0.9 mmol) were dissolved in 50 mL of Milli-Q water. The pH was checked by a pH meter. *(ii) pH 6.5.* Sodium dihydrogen phosphate (68.5 mL, 0.2 M) was mixed with disodium hydrogen phosphate (31.5 mL, 0.2 M). The total solution was made up to 200 mL with Milli-Q water. The pH was checked by a pH meter. *(iii) pH 8.* Potassium dihydrogen phosphate (50 mL, 0.2M) was mixed with sodium hydroxide (46.8 mL, 0.2M). The total solution was made up to 200 mL with Milli-Q water. The pH was checked by a pH meter. *(iv) pH pH 7.0 and 7.4.* The buffer solutions with pH at 7.0 and 7.4 were directly diluted from the 10X stock solution (pH 7.0, Fluka–Sigma Alrich; pH 7.4, Gibco-Life Technology)

3.2.2.5 Lower Critical Solution Temperature (LCST) of the block copolymer as determined by DLS. Polymer samples were weighed in vials and dissolved in cold Milli-Q water or buffer solution at different pH values and at a concentration of 10 mg/mL. These solutions were immediately placed in an ice bath, and then filtered directly into DLS cuvettes using 0.45 μm cellulose syringe filter. For measurement of the LCST, the polymer solutions were cooled to 5 or 10 ^{o}C in a DLS machine, and the measurements were carried out by slowly increasing the temperature in the DLS machine from 5 or 10 ^{o}C to 60 ^{o}C using the Standard operating procedures (SOP) software.

3.2.2.6 Lower Critical Solution Temperature (LCST) of the block copolymer after hydrolysis at different times as determined by DLS. Polymer samples were weighed in vials and dissolved in cold Milli-Q water at a concentration 10 mg/mL. These solutions were immediately placed in an ice bath, and then filtered directly into DLS cuvettes using 0.45 μm cellulose syringe filter. These

cuvettes were then kept in a water bath at 37 ^{o}C. The LCST of the hydrolysed samples at different times were then measured by the DLS. The measurements were carried out by slowly increasing the DLS temperature from 10 to 60 ^{o}C using SOP software over 3 h.

3.2.2.7 Disassembly kinetics of block copolymer nanoparticles at 37 ^{o}C by DLS. The number-average particle diameter was measured for each sample to determine the disassembly time of the nanoparticles. Polymer samples were weighed in vials and dissolved in cold Milli-Q water at the concentration of 5 mg/mL. These solutions were immediately placed in an ice bath, and then directly filtered into DLS cuvettes using 0.45 μm cellulose syringe filter. The samples were kept at 37 ^{o}C water bath and the particle size at different time intervals was measured in DLS machine set at 37 ^{o}C. The particles size and polydispersity index (PDI_{DLS}) were averaged from five measurements.

3.2.2.8 Disassembly Kinetics of block copolymer nanoparticles in different buffer solutions at 37 ^{o}C by DLS. The number-average particle diameter was measured for each sample to determine the disassembly time of the nanoparticles. Polymer samples were weighed in vials and dissolved in cold Milli-Q water at the concentration 5.55 mg/mL. These solutions were immediately placed in an ice bath, and 1 mL of the solution was filtered directly into DLS cuvettes using 0.45 μm cellulose syringe filter. The particle size was measured in DLS set at 37 ^{o}C. At the same time, 45 mL of the polymer solution (5.55 mg/mL) was transferred in a 50 mL centrifuge tube, and then placed in a 37 ^{o}C water bath for 5 min. 5 mL of a 10X or 1M buffer solution of a known pH value was mixed with the polymer solution in the tube to obtain the final solution concentration of 5 mg/mL. The pH value of the final solution was checked by a pH meter. This solution was then directly filtered into DLS cuvettes using a 0.45 μm cellulose syringe filter and measured the particle size at different time intervals in DLS set at 37 ^{o}C

3.2.3 Analytic methodologies

^{1}H Nuclear Magnetic Resonance (NMR). All NMR spectra were recorded on Bruker DRX 500 MHz using external locks ($CDCl_3$) and referenced to the residual non-deuterated solvent ($CHCl_3$).

Size Exclusion Chromatography (SEC) and Triple Detection Size Exclusion Chromatography (TD-SEC). The molecular weight distributions (MWDs) of the polymers were determined using a Polymer Laboratories GPC50 Plus equipped with differential refractive index detector and the absolute MWDs of polymers were determined using a Polymer Laboratories GPC50 Plus equipped with dual angle laser light scattering detector, viscometer, and differential refractive index detector.

HPLC grade *N*,*N*-dimethylacetamide (DMAc, containing 0.03 wt % LiCl) was used as the eluent at a flow rate of 1.0 mL/min. Separations were achieved using two PLGel Mixed B (7.8 x 300 mm) SEC columns connected in series and held at a constant temperature of 50 ^{o}C. The triple detection system was calibrated using a 2 mg/mL PSTY standard (Polymer Laboratories: M_{wt} = 110K, d*n*/d*c* = 0.16 mL/g and IV = 0.5809). Samples of known concentration were freshly prepared in DMAc + 0.03 wt % LiCl and passed through a 0.45 μm PTFE syringe filter prior to injection. The absolute molecular weights and d*n*/d*c* values were determined using Polymer Laboratories Multi Cirrus software based on the quantitative mass recovery technique.

Dynamic Light Scattering (DLS). Dynamic light scattering measurements were performed using a Malvern Zetasizer Nano Series running DTS software and operating a 4 mW He-Ne laser at 633 nm. Analysis was performed at an angle of 173°. The sample refractive index (RI) was set at 1.59 for polystyrene. The dispersant viscosity and RI were set to 0.89 $Ns.m^{-2}$ and 1.33, respectively. The number-average hydrodynamic particle size and polydispersity index are reported. The polydispersity index (PDI) was used to describe the width of the particle size distribution. It was calculated from a Cumulants analysis of the DLS measured intensity autocorrelation function and is related to the standard deviation of the hypothetical Gaussian distribution (i.e., $PDI_{PSD} = \sigma^2/Z_D^2$, where σ is the standard deviation and Z_D is the Z average mean size).

pH meter. pH of the buffer solution was checked by using a HORIBA pH meter calibrated by standard buffer solution pH 7.0, pH 4.0, and pH 10.0.

3.3 Result and Discussion

Preparation of the thermoresponsive diblock copolymers with near precise control over the number of units of each monomer (i.e., DMA, NIPAM, DMAEA, and BA) can be achieved using "living" radical polymerization. Reversible addition−fragmentation chain transfer (RAFT) polymerization allows the incorporation of various monomers to build the desired homo or block copolymers with narrow molecular weight distributions and thus with fine control over the copolymer chemical composition.[29-34] In this work, we first used RAFT to form the permanent hydrophilic polymer (PDMA) Macro-CTA with a number-average molecular weight (M_n) of 9700 (which is close to that found by ^{1}H NMR of 9770 giving 96 units of DMA by accounting for the molecular weight of the RAFT agent) and polydispersity index (PDI_{SEC}) of 1.03, as measured by triple detection SEC. This low PDI_{SEC} value should be regarded as a slight underestimation of the true value due to the lower scattering at very low molecular weights. This Macro-CTA was then combined with blocks of NIPAM, DMAEA, and BA in various molar ratios to produce two series of diblock copolymers (see

Tables A3.1 and A3.2 in Appendix B). The SEC traces in Figure A3.1 showed that most of Macro CTA was converted to diblock copolymer, suggesting excellent block efficiency. The $M_n$values for all polymers determined by triple detection SEC were close to those found by ^{1}H NMR (see Tables 3.1 and 3.2), and the polydispersity index by triple detection SEC for both series of polymers was less than 1.07, which was found to be a slight underestimation when compared to the PDI_{SEC} of approximately 1.22 determined by RI-SEC (data not shown).

The conversion of all monomers determined by ^{1}H NMR for Series A was restricted to between 76 and 80% to minimize the variation in the number of units for NIPAM (∼94) and DMAEA (∼25) in Series A (i.e., A1−8), as shown in Tables 3.1 and A3.1. Series B polymerizations gave conversions close to 74% with even less variation between the NIPAM (∼87) and DMAEA (∼ 42) units from B1 to B7 (Tables 3.2 and A3.2). The number of BA units was systematically increased from 6 to 20 for both Series A and B, allowing the fine-tuning not only of the polymer chemical composition but of the disassembly time as will be described below.

Table 3.1 Reaction time, conversion, Molecular weights, Polydispersities (PDI_{SEC}), ^{1}H NMR, Lower Critical Solution Temperature (LCST), Hydrodynamic Diameter (D_h), Polydispersities (PDI_{DLS}) describing the width of the particle size distribution, and degradation times for thermoresponsive block copolymers (A1−8).

	Polymer	Polym. time (h)	Total conv. (%)[a]	SEC-Triple detection[b]		^{1}H NMR[c]	LCST (^{o}C)[d]	D_h (nm) (PDI)[e]	t_{start} ($t_{degrade}$)[f]
				M_n	PDI	M_n			
A1	P(DMA_{96}-b-($NIPAM_{88}$-co-$DMAEA_{24}$-co-BA_6))	8	76	27800	1.05	23900	25-29	27.02 (0.028)	21 (5.5)
A2	P(DMA_{96}-b-($NIPAM_{94}$-co-$DMAEA_{25}$-co-BA_8))	8	78	28300	1.04	25000	23-29	29.93 (0.053)	35.5 (5.4)
A3	P(DMA_{96}-b-($NIPAM_{94}$-co-$DMAEA_{25}$-co-BA_{10}))	8.5	78	28100	1.05	25200	21-29	29.55 (0.018)	47.5 (5.6)
A4	P(DMA_{96}-b-($NIPAM_{91}$-co-$DMAEA_{25}$-co-BA_{12}))	9	77	24100	1.04	25100	17-21	25.31 (0.047)	66 (5.75)
A5	P(DMA_{96}-b-($NIPAM_{93}$-co-$DMAEA_{25}$-co-BA_{14}))	11	78	28700	1.05	25600	15-19	25.85 (0.056)	73.5 (5.8)
A6	P(DMA_{96}-b-($NIPAM_{93}$-co-$DMAEA_{25}$-co-BA_{16}))	11	78	28100	1.05	25800	13-17	25.19 (0.040)	79.9 (5.7)
A7	P(DMA_{96}-b-($NIPAM_{93}$-co-$DMAEA_{25}$-co-BA_{18}))	15.5	78	28400	1.06	26100	11-15	25.07 (0.024)	85.9 (5.5)
A8	P(DMA_{96}-b-($NIPAM_{97}$-co-$DMAEA_{25}$-co-BA_{20}))	15.5	80	30700	1.04	26800	10-15	24.93 (0.045)	93.5 (5.6)

[a]Total conversion of the polymer (Total conv.) was calculated by: Total conv. =[[(conv. $_{NIPAM}$ x 119) + (conv. $_{DMAEA}$ x 30) + (conv.$_{BA}$ x [BA])] / (119+30+ [BA])] x 100, where the monomer feeding ratios and conversions of each monomers were given in Table A3.1.

[b]Triple detection SEC in DMAc (with 0.03 wt % LiCl)with PSTY as standards. Calculations were based on the d*n*/d*c* and polymer concentration.

[c]Molecular weight determined by ^{1}H NMR were calculated based on the repeating units of NIPAM (N_{NIPAM}), BA (N_{BA}), DMAEA (N_{DMAEA}), $PDMA_{96}$-Macro CTA, and molecular weight of MCEBTTC (252.42): M_n = (N_{NIPAM} x 113) + (N_{BA} x 128.2) + (N_{DMAEA} x 143) + [(96 x 99.131) + 252.42)].

[d]LCST determined by DLS (10 mg/mL).

[e]Hydrodynamic diameter (D_h) and PDI determined by DLS (5 mg/mL) at 37 ^{o}C.

[f]Disassembly time at 37 ^{o}C measured by DLS: t_{start} = time when the size starts to decrease; $t_{degrade}$ = time from t_{start} to formation of unimers.

Table 3.2 Reaction time, conversion, Molecular weights, Polydispersities (PDI_{SEC}), ^1H NMR, Lower Critical Solution Temperature (LCST), Hydrodynamic Diameter (D_h), Polydispersities (PDI_{DLS}) describing the width of the particle size distribution, and degradation times for thermoresponsive block copolymers (B1−7).

	Polymer	Polym. time (h)	Total conv. (%)[a]	SEC-Triple detection[b]		^1H NMR[c]	LCST (^oC)[d]	D_h (nm) (PDI)[e]	t_{start} ($t_{degrade}$)[f]
				M_n	PDI	M_n			
B1	$P(DMA_{96}$-b-$(NIPAM_{87}$-co-$DMAEA_{42}$-co-$BA_6))$	14	73	28400	1.05	26300	27-37	30.02 (0.032)	10.3 (1.1)
B2	$P(DMA_{96}$-b-$(NIPAM_{88}$-co-$DMAEA_{41}$-co-$BA_8))$	14	74	29200	1.04	26600	25-35	29.21 (0.025)	12.9 (1.1)
B3	$P(DMA_{96}$-b-$(NIPAM_{87}$-co-$DMAEA_{43}$-co-$BA_{10}))$	14	74	29000	1.05	27000	23-33	27.98 (0.028)	14.9 (1.1)
B4	$P(DMA_{96}$-b-$(NIPAM_{85}$-co-$DMAEA_{42}$-co-$BA_{12}))$	15	73	29400	1.07	26900	21-31	26.81 (0.041)	17.4 (1.1)
B5	$P(DMA_{96}$-b-$(NIPAM_{85}$-co-$DMAEA_{42}$-co-$BA_{14}))$	15	73	29200	1.05	27100	19-29	26.49 (0.046)	22.4 (1.1)
B6	$P(DMA_{96}$-b-$(NIPAM_{88}$-co-$DMAEA_{42}$-co-$BA_{16}))$	15	74	30200	1.04	27700	17-25	26.48 (0.020)	25.7 (0.9)
B7	$P(DMA_{96}$-b-$(NIPAM_{87}$-co-$DMAEA_{43}$-co-$BA_{20}))$	15.5	74	30500	1.05	28300	13-25	25.58 (0.013)	34.3 (1.0)

[a] Total conversion of the polymer (Total conv.) was calculated by: Total conv. =[[(conv. $_{NIPAM}$ x 119) + (conv. $_{DMAEA}$ x 30) + (conv.$_{BA}$ x [BA])] / (119+30+ [BA])] x 100, where the monomer feeding ratios and conversions of each monomers were given in Table A3.2.

[b] Triple detection SEC in DMAc (with 0.03 wt % LiCl)with PSTY as standards. Calculations were based on the d*n*/d*c* and polymer concentration.

[c] Molecular weight determined by ^1H NMR were calculated based on the repeating units of NIPAM (N_{NIPAM}), BA (N_{BA}), DMAEA (N_{DMAEA}), $PDMA_{96}$-Macro CTA, and molecular weight of MCEBTTC (252.42): $M_n = (N_{NIPAM} \times 113) + (N_{BA} \times 128.2) + (N_{DMAEA} \times 143) + [(96 \times 99.131) + 252.42)]$.

[d] LCST determined by DLS (10 mg/mL).

[e] Hydrodynamic diameter (D_h) and PDI determined by DLS (5 mg/mL) at 37 ^oC.

[f] Disassembly time at 37 ^oC measured by DLS: t_{start} = time when the size starts to decrease; $t_{degrade}$ = time from t_{start} to formation of unimers.

The potential use of timed-release polymer nanoparticles in drug delivery applications requires that the LCST of the thermoresponsive hydrophobic block must be below 37 °C (i.e., below body temperature) in order to form nanoparticles.The diblock copolymer, P(DMA_{96}-b-($NIPAM_{87}$-co-$DMAEA_{25}$), did not form nanoparticles at 37 °C due to its higher LCST (39 to 41 °C).[28] However, the LCST of PNIPAM can be modulated through its chain-end functionality[35] and through manipulating the amount of hydrophilic or hydrophobic monomer units incorporated within the thermoresponsive block.[36, 37] Incorporation of hydrophilic monomer units will increase the LCST and hydrophobic monomer units will decrease the LCST. In our system, the incorporation of hydrophilic DMAEA units in the second random block should increase the LCST, while incorporating hydrophobic BA units will counterbalance this effect, allowing us to produce a polymer with an LCST below 37 °C. Tables 3.1 and 3.2 showed that the LCST can be finely tuned by varying the BA content for Series A and B, respectively. In this work, the LCST is defined as a temperature range observed from the initial increase in hydrodynamic diameter (D_h) to where D_h initially reaches its upper value. We define the LCST as this small temperature range due to slight variations in the D_h temperature profiles between samples, and in many cases the micelle formation transition is not sharp and well-defined. For example, A1 showed an initial increase in D_h at 25 °C and reached its initial upper D_h at 29 °C (i.e., the start of the plateau region), a temperature range of 4 °C (see Figure A3.5 in Appendix B); in which the LCST was denoted in Table 3.1 ranging between 25 and 29 °C. With an increase in the number of BA units from 6 to 20, the initial change in D_h (i.e., lower value of the LCST range in Tables 3.1 and 3.2) decreased from 25 to 10 °C for Series A and from 27 to 13 °C for Series B; a trend also observed for the upper LCST value.

For these nanoparticles to have great efficacy in cancer therapy applications, they must be small to diffuse and penetrate deep into the center of the tumor where the most aggressive tumor cells reside.[38] Recent work has demonstrated that the size of the nanoparticles plays an important role in this respect: small particles close to 10 nm can diffuse and penetrate into the tumor two or three times further than particles of 60 and 120 nm.[39] The micelle sizes for the two series of polymers was small, ranging from 25 to 30 nm, and importantly with a very narrow particle size distributions (PSD) determined from their low PDI_{DLS} values of below 0.06 from DLS (see Tables 3.1 and 3.2). It should be noted that PDI_{DLS} value of less than 0.1 represents a narrow PSD. The slight decrease in D_h from approximately 30 to 25 nm with an increase in the number of BA units for both polymer series was presumably due to the greater hydrophobic content. Series A polymer when mixed with water and incubated (i.e., heated to and maintained) at 37 °C formed micelles with a solution pH of 7.6. The disassembly properties as monitored by DLS were shown in Figure 3.1A. There was a small decrease in size after the first few hours of incubation due to the ionic binding between the

newly formed negatively charged acrylic acid side groups (from self-catalysis of DMAEA) and non-degraded cationic DMAEA units. The D_h remained relatively constant until a sharp transition due to the micelle disassembly. The time to disassemble was dependent upon the BA (Table 3.1), and with greater BA content the time to disassemble (denoted t_{start}) increased. There was a linear relationship between the number of the BA units in the copolymer and t_{start}, providing a predictive means to select t_{start} for the desired application. The time (i.e., $t_{degrade}$) from t_{start} to full micelle disassembly to unimers, observed when D_h was approximately 5−7 nm, for Series A was consistently ∼5.5 h. Series B polymers were nearly identical to Series A but the number of DMAEA units was increased from 25 to 42. This change in DMAEA units as shown in Figure 3.1B gave much shorter t_{start} values. For example, for 20 units of BA in the copolymer, t_{start} reduced from 93.5 h (A8) to 34.3 h (B7).There was also a linear relationship for Series B between t_{start} and the number of BA units. Interestingly, the time to full micelle disassembly ($t_{degrade}$) was also much shorter and consistent at ∼1.1 h for the B series. Taken together, Series A and B polymers showed that both t_{start} and $t_{degrade}$ could be controlled independently.

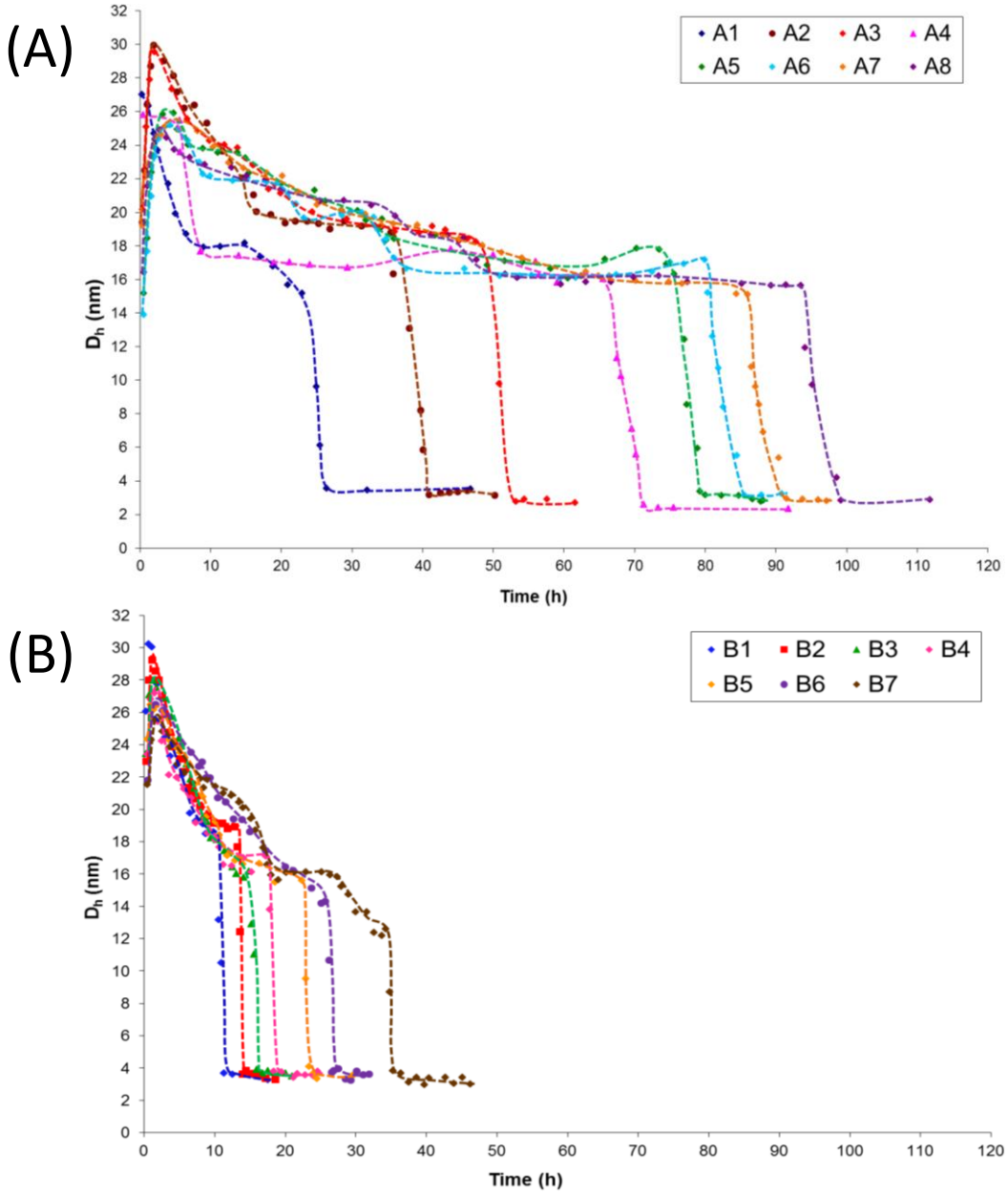

Figure 3.1 Degradation kinetics profiles for polymers A1 to A8 (A) and polymers B1 to B7 (B) in Milli-Q water at 37 °C. The data were averaged from five measurements by DLS at polymer solution concentration of 5 mg/mL.

The sharp disassembly time of either 5.5 or 1.1 h was directly related to the self-catalyzed hydrolysis of the DMAEA units changing the LCST behavior of the thermoresponsive second block. We measured the LCST of A1, A8, B1, and B7 as a function of time at 37 °C with the clear observation that the LCST of all four polymers increased over time (Figure A3.6 in Appendix B). The data demonstrated that with the increase in the degradation of DMAEA side groups to carboxylic acids, the diblock copolymer's LCST increased, and when the LCST became greater than 37 °C, disassembly to water-soluble unimers occurred. Figure 3.2 showed the rate of change of the LCST changed with time for these four polymers. Both A1 and B1 (i.e., with 6 BA units) had an

initial LCST of 27 °C that reached 38 °C in 21 and 10 h, respectively, corresponding to t_{start} (in Tables 3.1 and 3.2). The rate of LCST change over time was similar for A1, B1, and B7, while A8 showed a two-step LCST profile. When the polymers were allowed to be stored in water for one month at 37 °C, no LCST was observed even at temperatures as high as 70 °C.

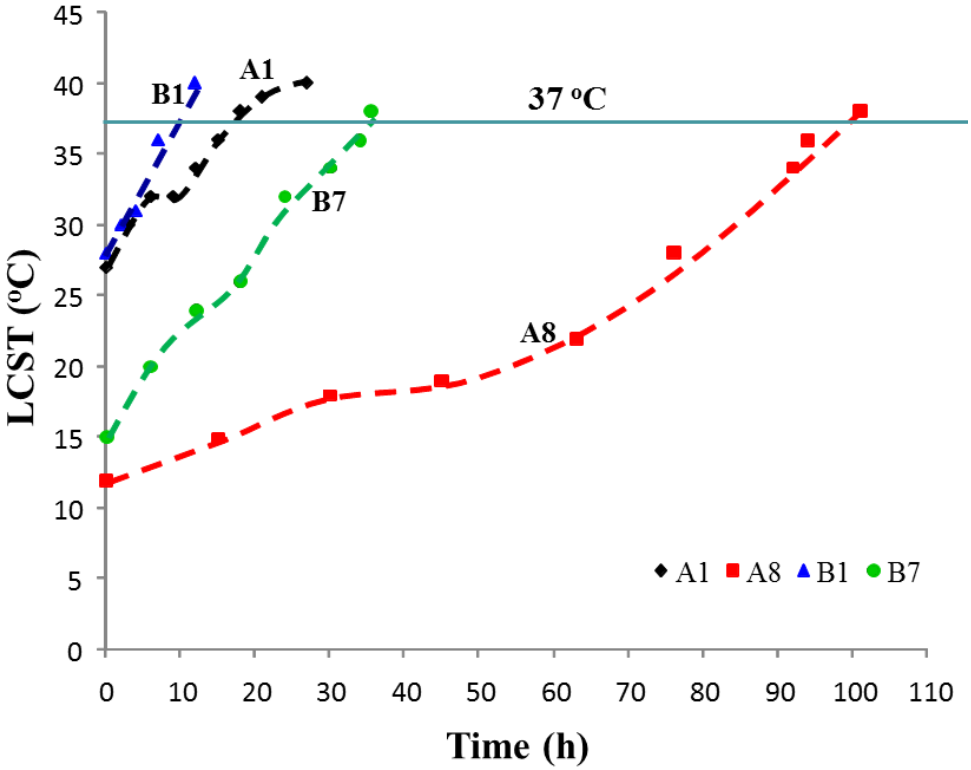

Figure 3.2 The rate of change in the LCST of polymer **A1**: P(DMA$_{96}$-b-(NIPAM$_{88}$-co-DMAEA$_{24}$-co-BA$_{6}$)); **A8**: P(DMA$_{96}$-b-(NIPAM$_{97}$-co-DMAEA$_{25}$-co-BA$_{20}$)); **B1**: P(DMA$_{96}$-b-(NIPAM$_{87}$-co-DMAEA$_{42}$-co-BA$_{6}$)); **B7**: P(DMA$_{96}$-b-(NIPAM$_{87}$-co-DMAEA$_{43}$-co-BA$_{20}$)) in Milli-Q water after incubation in water bath at 37 °C at different time points. The data were averaged from five measurements by DLS at polymer solution concentration 10 mg/mL.

The coil to globule transition (i.e., > LCST) for PNIPAM results in precipitation of PNIPAM out of water. Dehydration of PNIPAM chains at temperatures above the LCST drives the coils to collapse due to hydrophobic interactions between the isopropyl groups and intra hydrogen bonding between the amide groups.[40] This has been interpreted as resulting in a hydrophobic PNIPAM environment above the LCST. The level of dehydration from the coil required for collapse is actually rather small, suggesting that the percentage of bound water within the globule is still high, ranging from 50 to 80%.[41-43] This data suggests that although there are hydrophobic pockets within our polymer micelles, there remains high water content for the self-catalyzed hydrolysis of the DMAEA units, allowing a linear rate of LCST change for A1, B1, and B7. The high BA to DMAEA content in A8 suggests some restriction of water to the hydrophobic pockets within the micelle, thus retarding

hydrolysis of the DMAEA units in these regions. If water was fully restricted from a hydrophobic micelle core, one would expect a slow surface degradation process, resulting in shorter (t_{start}) and significantly longer ($t_{degrade}$) disassembly times.

In the treatment of tumors, the nanoparticle delivery device should accumulate at the tumor site by utilizing the EPR effect.[44] It is now well established that the extracellular environment around the tumor cells is acidic between 6.5 to 6.9 due to cell secretion of lactate and H^+ to the extracellular space.[45, 46] The question we wanted to answer was how our nanoparticles behaved in different pH environments since the DMAEA units would be protonated at lower pH values (pK_a of PDMAEA = 7.1). Selected polymers from Series A and B (i.e., A1, A3, B5, and B7) were self-assembled in solutions with pH ranging from 6.5 to 8 at 37 °C. The size of the nanoparticles at a pH of 8 was small (~26 nm) with a narrow PSD for all polymers (see Table 3.3). Decreasing the pH showed little or no change in the size for A3 and B7 over the pH range studied (Figure 3.3). However, for A1 and B5, there was a sharp and rapid disassembly to form unimers below a pH of 7.3. It was found that the LCST of the four polymers increased with a decrease in pH (Table 3.3 and Figures A3.7A to A3.10A in Appendix B). This trend was due to the greater ionization of the DMAEA units in the second block. For A1 and B5, the LCST at a pH below 7.3 was well above the mixture temperature of 37 °C. In the case of A3 and B7, the additional BA units maintained the LCST below the mixture temperature, resulting in little change in particle size. It was found that at a pH of 5.5, all four polymers had an LCST greater than 83 °C (as determined from the change in turbidity), and thus did not form nanoparticles at 37 °C. The disassembly time (t_{start}) also decreased linearly with a decrease in pH as shown in Table 3.3 (and Figures A3.7B to A3.10B). For example, t_{start} for A3 decreased from 53.8 to 38.3 h with a decrease in pH from 8 to 6.5. Interestingly, $t_{degrade}$ did not alter remaining relatively constant at 5.5 h for the A polymers and 1.1 h for the B polymers. The data demonstrated that our nanoparticles (e.g., A1 and B5) can be designed to disassemble in a low pH environment, similar to that of the extracellular environment of a tumor,[46] or be designed to be stable in a low pH environment and disassemble after a designated time (e.g., A3 and B7).

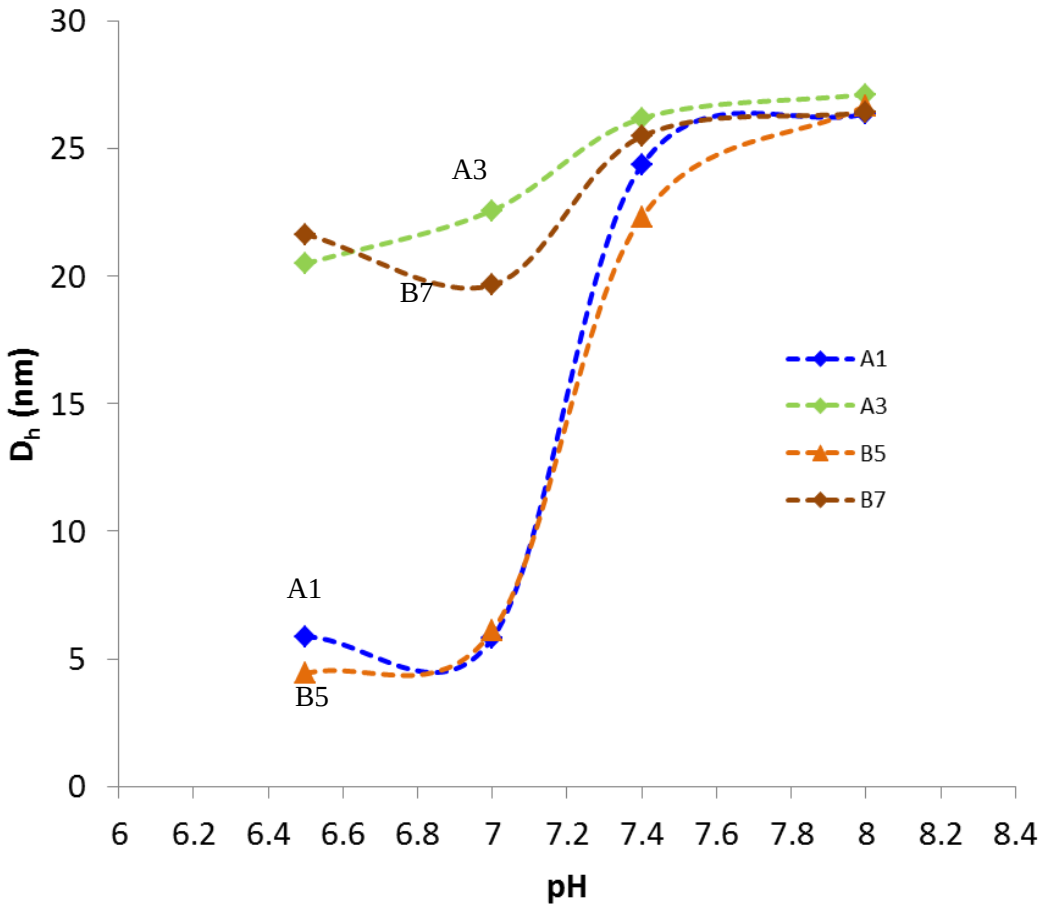

Figure 3.3 Hydrodynamic diameter (D_h) for the polymer particles from polymer **A1**: P(DMA_{96}-b-($NIPAM_{88}$-co-$DMAEA_{24}$-co-BA_6)), **A3**: P(DMA_{96}-b-($NIPAM_{94}$-co-$DMAEA_{25}$-co-BA_{10})), **B5**:P(DMA_{96}-b-($NIPAM_{85}$-co-$DMAEA_{42}$-co-BA_{14})) and **B7**: P(DMA_{96}-b-($NIPAM_{87}$-co-$DMAEA_{43}$-co-BA_{20})) in different buffer solutions at 37 ^{o}C. The data were averaged from five measurements by DLS at polymer solution concentration 5 mg/mL.

Table 3.3 Lower Critical Solution Temperature (LCST), Hydrodynamic Diameter (D_h), Polydispersities (PDI_{DLS}), and degradation times for thermoresponsive block copolymers.

Polymer	LCST (^oC)[a] in buffer solutions					D_h (nm) (PDI)[c] at 37 ^oC				t_{start} ($t_{degrade}$)[d] at 37 ^oC			
	pH 5.5	pH 6.5	pH 7	pH 7.4	pH 8	pH 6.5	pH 7	pH 7.4	pH 8	pH 6.5	pH 7	pH 7.4	pH 8
A1	87[b]	39-55	37-55	27-41	23-41	5.87 (0.216)	5.80 (0.277)	24.35 (0.031)	26.36 (0.025)	DNM [e]	DNM [e]	17.9 (5.29)	25.3 (5.41)
A3	85[b]	35-50	33-45	21-33	19-31	20.49 (0.126)	22.57 (0.128)	26.18 (0.076)	27.12 (0.048)	38.3 (5.3)	40.1 (5.6)	43.7 (5.8)	53.8 (5.7)
B5	90[b]	41-57	39-55	23-37	21-35	4.44 (0.234)	6.09 (0.231)	22.31 (0.050)	26.68 (0.029)	DNM [e]	DNM [e]	19.06 (1.15)	25.82 (1.56)
B7	83[b]	33-50	31-45	15-27	17-29	21.64 (0.042)	19.65 (0.102)	25.48 (0.037)	26.41 (0.046)	26.5 (1.10)	29.3 (1.33)	33.5 (1.10)	37.2 (1.08)

[a] LCST measured by DLS (10 mg/mL).

[b] LCST was determined by measuring the turbid point of the polymer solution.

[c] Hydrodynamic diameter (D_h) determined by DLS (5 mg/mL) at 37 ^oC.

[d] Disassembly time at 37 ^oC: t_{start} = time when the size starts to decrease, $t_{degrade}$ = time from t_{start} to formation of unimers.

[e] DNM: 'did not micellize'.

3.4 Conclusion

In conclusion, we have demonstrated the utilization of RAFT mediated polymerization to fine-tune the number and types of monomer units in a diblock copolymer. This fine control over polymer chemical composition allowed a study of the micelle disassembly times for two series of thermoresponsive diblock copolymers. The self-hydrolysis of the DMAEA units in water to acrylic acid side groups resulted in an increase in the LCST, and once the LCST increased above the polymer/water solution temperature (in our case, 37 °C) the micelles disassembled to unimers. The time to disassembly (t_{start}) increased linearly with an increase in the number of BA units in the second block. By controlling the second block's composition, t_{start} could be predicted, allowing the use of such timed-release nanoparticles for a wide range of applications. Additionally, the time from the start of disassembly to full unimer formation ($t_{degrade}$) could be controlled by the amount of DMAEA units in the second block. A shorter $t_{degrade}$ (~1.1 h) was found when the number of DMAEA units was 42 compared to $t_{degrade}$ of 5.5 h for 25 units. The mechanism of degradation of the DMAEA units within the core of the micelle results from the high water content bound to PNIPAM. This allows DMAEA to hydrolyze evenly throughout the core, resulting in sharp disassembly transitions. The polymer micelles with a low number of BA units disassembled at a pH less than 7.3, while incorporating a higher number of BA units increased stability (i.e., no disassembly observed until a pH of 5.5). It could be envisaged that combinations of nanoparticles (e.g., A1 and A3) could release their payload at the site of the tumor (where the extracellular pH is less than 7.3) and further penetrate to inside the tumor for an effective therapeutic effect. The formation of small and uniform polymer nanoparticles has great potential in drug delivery where drugs or prodrugs could be released after desired times, or delivery to tumors where due to their small size they could penetrate deep into the tumor. These nanoparticles could also be designed to be pH sensitive and act to release at both the extracellular environment of the tumor and also deep inside. These nanoparticles will also have potential for applications where timed-release is beneficial.

3.5 References

1. Brun-Graeppi, A. K. A. S.; Richard, C.; Bessodes, M.; Scherman, D.; Merten, O.-W., Cell microcarriers and microcapsules of stimuli-responsive polymers. *J. Controlled Release* **2011,** 149, (3), 209-224.
2. Gu, W.; Jia, Z.; Truong, N. P.; Prasadam, I.; Xiao, Y.; Monteiro, M. J., Polymer Nanocarrier System for Endosome Escape and Timed Release of siRNA with Complete Gene Silencing and Cell Death in Cancer Cells. *Biomacromolecules* **2013,** 14, (10), 3386-3389.
3. Truong, N. P.; Gu, W.; Prasadam, I.; Jia, Z.; Crawford, R.; Xiao, Y.; Monteiro, M. J., An influenza virus-inspired polymer system for the timed release of siRNA. *Nat. Commun.* **2013,** 4, 1902.
4. Chang, C.-W.; Bays, E.; Tao, L.; Alconcel, S. N. S.; Maynard, H. D., Differences in cytotoxicity of poly(PEGA)s synthesized by reversible addition-fragmentation chain transfer polymerization. *Chem. Commun. (Camb.)* **2009**, (24), 3580-3582.
5. Urbani, C. N.; Monteiro, M. J., Nanoreactors for Aqueous RAFT-Mediated Polymerizations. *Macromolecules* **2009,** 42, (12), 3884-3886.
6. Zayas, H. A.; Truong, N. P.; Valade, D.; Jia, Z.; Monteiro, M. J., Narrow molecular weight and particle size distributions of polystyrene 4-arm stars synthesized by RAFT-mediated miniemulsions. *Polym Chem-Uk* **2013,** 4, (3), 592-599.
7. Soliman, M.; Allen, S.; Davies, M. C.; Alexander, C., Responsive polyelectrolyte complexes for triggered release of nucleic acid therapeutics. *Chem. Commun. (Camb.)* **2010,** 46, (30), 5421-5433.
8. Shchukin, D. G.; Grigoriev, D. O.; Mohwald, H., Application of smart organic nanocontainers in feedback active coatings. *Soft Matter* **2010,** 6, (4), 720-725.
9. MacKinnon, N.; Guérin, G. r.; Liu, B.; Gradinaru, C. C.; Rubinstein, J. L.; Macdonald, P. M., Triggered Instability of Liposomes Bound to Hydrophobically Modified Core−Shell PNIPAM Hydrogel Beads. *Langmuir* **2009,** 26, (2), 1081-1089.
10. Chan, Y.; Wong, T.; Byrne, F.; Kavallaris, M.; Bulmus, V., Acid-Labile Core Cross-Linked Micelles for pH-Triggered Release of Antitumor Drugs. *Biomacromolecules* **2008,** 9, (7), 1826-1836.
11. Zhang, L.; Bernard, J.; Davis, T. P.; Barner-Kowollik, C.; Stenzel, M. H., Acid-Degradable Core-Crosslinked Micelles Prepared from Thermosensitive Glycopolymers Synthesized via RAFT Polymerization. *Macromol. Rapid Commun.* **2008,** 29, (2), 123-129.
12. Soga, O.; van Nostrum, C. F.; Hennink, W. E., Poly(N-(2-hydroxypropyl) Methacrylamide Mono/Di Lactate): A New Class of Biodegradable Polymers with Tuneable Thermosensitivity. *Biomacromolecules* **2004,** 5, (3), 818-821.
13. Pastine, S. J.; Okawa, D.; Zettl, A.; Fréchet, J. M. J., Chemicals On Demand with Phototriggerable Microcapsules. *J. Am. Chem. Soc.* **2009,** 131, (38), 13586-13587.
14. Li, Y.; Tang, Y.; Yang, K.; Chen, X.; Lu, L.; Cai, Y., Facile Synthesis and Photo-Tunable Properties of a Photosensitive Polymer Whose Chromophores Bound with pH-Labile Cyclic Acetal Linkages. *Macromolecules* **2008,** 41, (13), 4597-4606.
15. Bohlender, C.; Wolfram, M.; Goerls, H.; Imhof, W.; Menzel, R.; Baumgaertel, A.; Schubert, U. S.; Mueller, U.; Frigge, M.; Schnabelrauch, M.; Wyrwa, R.; Schiller, A., Light-triggered NO release from a nanofibrous non-woven. *J. Mater. Chem.* **2012,** 22, (18), 8785-8792.
16. Karaki, F.; Kabasawa, Y.; Yanagimoto, T.; Umeda, N.; Firman; Urano, Y.; Nagano, T.; Otani, Y.; Ohwada, T., Visible-Light-Triggered Release of Nitric Oxide from N-Pyramidal Nitrosamines. *Chemistry – A European Journal* **2012,** 18, (4), 1127-1141.
17. Johnston, A. P. R.; Lee, L.; Wang, Y.; Caruso, F., Controlled Degradation of DNA Capsules with Engineered Restriction-Enzyme Cut Sites. *Small* **2009,** 5, (12), 1418-1421.
18. Cavalieri, F.; Postma, A.; Lee, L.; Caruso, F., Assembly and Functionalization of DNA−Polymer Microcapsules. *ACS Nano* **2009,** 3, (1), 234-240.

19. Glangchai, L. C.; Caldorera-Moore, M.; Shi, L.; Roy, K., Nanoimprint lithography based fabrication of shape-specific, enzymatically-triggered smart nanoparticles. *J. Controlled Release* **2008,** 125, (3), 263-272.
20. Lu, Z.; Prouty, M. D.; Guo, Z.; Golub, V. O.; Kumar, C. S. S. R.; Lvov, Y. M., Magnetic Switch of Permeability for Polyelectrolyte Microcapsules Embedded with Co@Au Nanoparticles. *Langmuir* **2005,** 21, (5), 2042-2050.
21. Hu, S.-H.; Tsai, C.-H.; Liao, C.-F.; Liu, D.-M.; Chen, S.-Y., Controlled Rupture of Magnetic Polyelectrolyte Microcapsules for Drug Delivery. *Langmuir* **2008,** 24, (20), 11811-11818.
22. Caruso, M. M.; Schelkopf, S. R.; Jackson, A. C.; Landry, A. M.; Braun, P. V.; Moore, J. S., Microcapsules containing suspensions of carbon nanotubes. *J. Mater. Chem.* **2009,** 19, (34), 6093-6096.
23. Neradovic, D.; van Nostrum, C. F.; Hennink, W. E., Thermoresponsive Polymeric Micelles with Controlled Instability Based on Hydrolytically Sensitive N-Isopropylacrylamide Copolymers. *Macromolecules* **2001,** 34, (22), 7589-7591.
24. Shi, Y.; van den Dungen, E. T. A.; Klumperman, B.; van Nostrum, C. F.; Hennink, W. E., Reversible Addition–Fragmentation Chain Transfer Synthesis of a Micelle-Forming, Structure Reversible Thermosensitive Diblock Copolymer Based on the N-(2-Hydroxy propyl) Methacrylamide Backbone. *ACS Macro Letters* **2013,** 2, (5), 403-408.
25. de Jong, S. J.; Arias, E. R.; Rijkers, D. T. S.; van Nostrum, C. F.; Kettenes-van den Bosch, J. J.; Hennink, W. E., New insights into the hydrolytic degradation of poly(lactic acid): participation of the alcohol terminus. *Polymer* **2001,** 42, (7), 2795-2802.
26. Truong, N. P.; Jia, Z.; Burges, M.; McMillan, N. A. J.; Monteiro, M. J., Self-Catalyzed Degradation of Linear Cationic Poly(2-dimethylaminoethyl acrylate) in Water. *Biomacromolecules* **2011,** 12, (5), 1876-1882.
27. Truong, N. P.; Jia, Z.; Burgess, M.; Payne, L.; McMillan, N. A. J.; Monteiro, M. J., Self-Catalyzed Degradable Cationic Polymer for Release of DNA. *Biomacromolecules* **2011,** 12, (10), 3540-3548.
28. Tran, N. T. D.; Truong, N. P.; Gu, W.; Jia, Z.; Cooper, M. A.; Monteiro, M. J., Timed-Release Polymer Nanoparticles. *Biomacromolecules* **2013,** 14, (2), 495-502.
29. Monteiro, M. J., Modeling the molecular weight distribution of block copolymer formation in a reversible addition–fragmentation chain transfer mediated living radical polymerization. *J Polym Sci Pol Chem* **2005,** 43, (22), 5643-5651.
30. Monteiro, M. J., Design strategies for controlling the molecular weight and rate using reversible addition–fragmentation chain transfer mediated living radical polymerization. *J Polym Sci Pol Chem* **2005,** 43, (15), 3189-3204.
31. Moad, G.; Rizzardo, E.; Thang, S. H., Living Radical Polymerization by the RAFT Process – A Third Update. *Aust. J. Chem.* **2012,** 65, (8), 985-1076.
32. York, A. W.; Kirkland, S. E.; McCormick, C. L., Advances in the synthesis of amphiphilic block copolymers via RAFT polymerization: Stimuli-responsive drug and gene delivery. *Adv. Drug Delivery Rev.* **2008,** 60, (9), 1018-1036.
33. Klumperman, B.; van den Dungen, E. T. A.; Heuts, J. P. A.; Monteiro, M. J., RAFT-Mediated Polymerization—A Story of Incompatible Data? *Macromol. Rapid Commun.* **2010,** 31, (21), 1846-1862.
34. Boyer, C.; Bulmus, V.; Davis, T. P.; Ladmiral, V.; Liu, J.; Perrier, S., Bioapplications of RAFT Polymerization. *Chem. Rev.* **2009,** 109, (11), 5402-5436.
35. Furyk, S.; Zhang, Y.; Ortiz-Acosta, D.; Cremer, P. S.; Bergbreiter, D. E., Effects of end group polarity and molecular weight on the lower critical solution temperature of poly(N-isopropylacrylamide). *J Polym Sci Pol Chem* **2006,** 44, (4), 1492-1501.
36. Feil, H.; Bae, Y. H.; Feijen, J.; Kim, S. W., Effect of comonomer hydrophilicity and ionization on the lower critical solution temperature of N-isopropylacrylamide copolymers. *Macromolecules* **1993,** 26, (10), 2496-2500.

37. Shibayama, M.; Mizutani, S.-y.; Nomura, S., Thermal Properties of Copolymer Gels Containing N-Isopropylacrylamide. *Macromolecules* **1996,** 29, (6), 2019-2024.
38. Wong, C.; Stylianopoulos, T.; Cui, J.; Martin, J.; Chauhan, V. P.; Jiang, W.; Popović, Z.; Jain, R. K.; Bawendi, M. G.; Fukumura, D., Multistage nanoparticle delivery system for deep penetration into tumor tissue. *Proceedings of the National Academy of Sciences* **2011,** 108, (6), 2426-2431.
39. Popović, Z.; Liu, W.; Chauhan, V. P.; Lee, J.; Wong, C.; Greytak, A. B.; Insin, N.; Nocera, D. G.; Fukumura, D.; Jain, R. K.; Bawendi, M. G., A Nanoparticle Size Series for In Vivo Fluorescence Imaging. *Angew. Chem. Int. Ed.* **2010,** 49, (46), 8649-8652.
40. Cho, E. C.; Lee, J.; Cho, K., Role of Bound Water and Hydrophobic Interaction in Phase Transition of Poly(N-isopropylacrylamide) Aqueous Solution. *Macromolecules* **2003,** 36, (26), 9929-9934.
41. Chu, B.; Wu, C., Coil-globule transition: Self-assembly of a single polymer chain. *Macromol. Symp.* **1996,** 106, (1), 421-423.
42. Heskins, M.; Guillet, J. E., Solution Properties of Poly(N-isopropylacrylamide). *Journal of Macromolecular Science: Part A - Chemistry* **1968,** 2, (8), 1441-1455.
43. Pelton, R., Poly(N-isopropylacrylamide) (PNIPAM) is never hydrophobic. *J. Colloid Interface Sci.* **2010,** 348, (2), 673-674.
44. Perrault, S. D.; Walkey, C.; Jennings, T.; Fischer, H. C.; Chan, W. C. W., Mediating Tumor Targeting Efficiency of Nanoparticles Through Design. *Nano Lett.* **2009,** 9, (5), 1909-1915.
45. Griffiths, J. R., Are cancer cells acidic? *Br. J. Cancer* **1991,** 64, (3), 425-427.
46. Wojtkowiak, J. W.; Verduzco, D.; Schramm, K. J.; Gillies, R. J., Drug Resistance and Cellular Adaptation to Tumor Acidic pH Microenvironment. *Mol. Pharm.* **2011,** 8, (6), 2032-2038.

Chapter 4

Large timed-release polymer nanoparticles stabilized by SDS

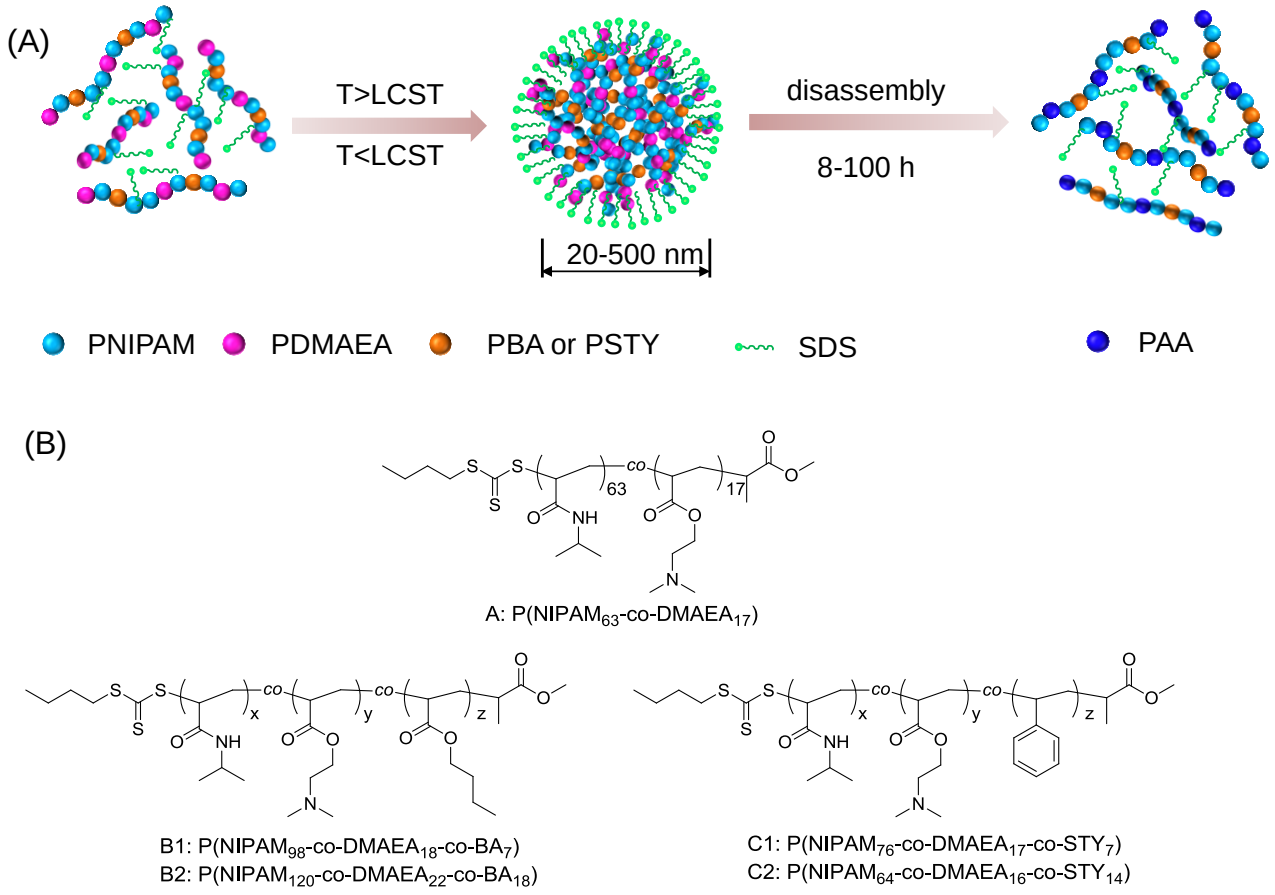

The self-assembly, stabilization and self-disassembly of thermoresponsive nanoparticles from the random copolymer of thermoresponsive PNIPAM, hydrophobic PBA or PSTY and self-catalyzed hydrolysis poly(N, N-dimethylaminoethyl acrylate) (PDMAEA) were investigated in the presence of sodium dodecyl sulphate (SDS) surfactant. The polymers could self-assemble into large SDS stabilized nanoparticles with a very narrow size distribution. The polymer particle size can be tuned by changing the SDS concentration, and these nanoparticles were stable upon dilution. Increasing the amount of SDS resulted in higher LCST of the copolymers due to a greater amount of bound SDS molecules to the PNIPAM backbone. Furthermore, the presence of SDS did not influence the self-degradation process of DMAEA. The polymer nanoparticles self-disassembled into unimers in a precisely time-controlled manner.

4.1 Introduction

Stimulus-responsive polymers that are able to change their physicochemical properties in response to stimuli such as temperature,[1, 2] pH,[3-5] light,[6-9] magnetic field,[10-13] ultrasonication,[14-16] oxidation-reduction,[17-21] and enzyme activity[22-24] have attracted significant attention in wide range of areas including those related to microfluidic,[25] textile,[26] and sensors.[27] Thermoresponsive polymers, e.g., Poly(N-isopropyl acrylamide) (PNIPAM), are the most extensively exploited stimuli in the field of responsive polymers.[28] PNIPAM exhibits a typical lower critical solution temperature (i.e., LCST) of about 32 ^{o}C. When the polymer chains are hydrated, they expanded to a hydrophilic water swollen state below the LCST while when they are dehydrated, they collapsed to a hydrophilic globular state above the LCST.[29-34] Amphiphilic copolymers of PNIPAM can self-assemble into various nanostructures including nanoparticles upon heating in polymer aqueous solution above the LCST.[28, 35-38]

In chapter 1 and 2, we have designed thermoresponsive copolymers with an adjustable LCST that can self-assemble into small polymer nanoparticles and then disassemble into unimers at a precise time.[39, 40] We have reported the synthesis of thermoresponsive block copolymers in which the first block consisted of the hydrophilic poly(dimethyl acrylamide) (PDMA), and the second blocks consisted of the random polymers of thermoresponsive PNIPAM, hydrophobic PBA or PSTY and self-catalyzed poly(N, N-dimethylaminoethyl acrylate) (PDMAEA). The block copolymers, PDMA-b-P(NIPAM-co-DMAEA-co-BA) and PDMA-b-P(NIPAM-co-DMAEA-co-STY), are able to form nanoparticles when the solution is heated above its LCST (i.e., > 37 ^{o}C) producing nanoparticles with a small hydrodynamic diameter (D_h) of 25 nm and a size distribution less than 0.063 (where values less than 0.1 represent a narrow distribution). The self-catalyzed hydrolysis of DMAEA side groups to carboxylic acid increases over time,[41] resulting in the increase in the LCST of the diblock copolymers, and when the LCST raises above 37 ^{o}C, a sharp disassembly of the polymer particles to unimers occurs.[39] By varying the composition (i.e., hydrophobic and hydrophilic units), we then are able to tune the LCST of the copolymers and therefore create a series of block copolymer nanoparticles which are stable in water from 10 to 95 h.[40] However, nanoparticle sizes of the diblock copolymer were unchanged when changing polymer composition.

Sodium dodecyl sulphate (SDS), a widely used anionic surfactant, has been found to increase the LCST of PNIPAM through hydrophobic interaction between the dodecyl tail of SDS and the isopropyl side groups of PNIPAM. [42-47] The interaction of PNIPAM and SDS has been studied for many decades to explore this binding process. For example, Binkert and coworkers conducted a series of work on SDS/PNIPAM systems by time-resolved fluorescence and dynamic light scattering (i.e., DLS) techniques.[42, 43] They suggested that at the temperature below the LCST of PNIPAM there are polymer-bound SDS micelles attached along the PNIPAM chain that results in

the increase of the LCST. Above the LCST, PNIPAM globules are stabilized from precipitation through the bound SDS.[43] This effect is called intermolecular solubilization.[42] However, in most of these SDS/PNIPAM interaction studies, the maximum SDS concentration used is about the critical micelle concentration (i.e., CMC) of SDS and the concentration of PNIPAM is below 0.1 wt%.[42, 44, 45, 47] The interaction on nanoparticle formation at much higher concentrations of both SDS and PNIPAM has not been investigated.

4.1.1 Aim of the Chapter

In this chapter, we investigated the self-assembly, stabilization and self-catalyzed disassembly of large thermoresponsive particles the random copolymers P(NIPAM-co-DMAEA-co-BA) and P(NIPAM-co-DMAEA-co-STY) stabilized by SDS (see Scheme 4.1). We demonstrated that even at a high weight fractions of polymer (2.5 wt%) and high SDS concentration (26.4 mM), large and stable polymer nanoparticles (e.g., up to 500 nm) could be formed above the LCST (e.g., 37 ^{o}C). Moreover, the particle size could be tuned by changing the SDS concentration. The particles could disassemble into unimers by decreasing the temperature to below the LCST, but when heated back above the LCST produce particles with the same size, representing a reversible assembly/disassembly process. The particles could also be diluted by approximately ten times without a change in size until the critical aggregation concentration was reached. It was also found that the self-catalysed hydrolysis property of PDMAEA was not affected by SDS, and as such the time required for disassembly of the polymer nanoparticles could be precisely controlled.

4.2 Experimental

4.2.1 Materials

Dioxane (99%) was used as received from Sigma-Aldrich. Styrene (STY, 99 %, Aldrich), 2-(dimethylamino) ethyl acrylate (DMAEA, 98%, Sigma-Aldrich), and butyl acrylate (BA, 99%, Aldrich) were passed through a column of basic alumina (activity I) to remove inhibitor. *N*-isopropylacrylamide (NIPAM, Aldrich, 97 %) was recrystallized from hexane. Azobisisobutyronitrile (AIBN) was also recrystallized twice from methanol prior to use. Sodium dodecyl sulphate (SDS: Aldrich, 99 %), Potassium chloride (KCl, Alrich). Milli-Q Water (18.2 MΩcm^{-1}) was generated using a Millipore Milli-Q academic water purification system. All other chemicals and solvents used were of at least analytical grade and used as received. The Chain Transfer Agent (CTA), Methyl 2-(butylthiocarbonothioylthio) propanoate (MCEBTTC) was synthesized according to the literature procedure.[48]

4.2.2 Synthetic procedures

4.2.2.1 Synthesis of random copolymers of P(NIPAM-co-DMAEA) (A). NIPAM (4.00 g, 3.54 x 10^{-2} mol), DMAEA (1.37 mL, 8.85 x 10^{-3} mol), MCEBTTC (44.6 mg, 1.77 x 10^{-4} mol) and AIBN (5.8 mg, 3.54 x 10^{-5} mol) were dissolved in 20 mL of dioxane in a 50 mL dry Schlenk flask equipped with magnetic stirrer bar. The mixture was deoxygenated by purging with argon for 30 min and then heated to 60 ^{o}C for 15 h under argon. The reaction was stopped by cooling to 0 ^{o}C by an ice bath and exposed to air. The solution was precipitated in diethyl ether (500 mL) and filtered. The polymer was redissolved in acetone and precipitated in diethyl ether. The re-dissolving and precipitating process were repeated twice. The yellow powder product was dried under high vacuum at room temperature for 48 h (yield = 92%).

4.2.2.2 Synthesis of random copolymers of P(NIPAM-co-DMAEA-co-BA) (B1, B2). Typically, NIPAM (4.00 g, 3.54 x 10^{-2} mol), DMAEA (1.37 mL, 8.85 x 10^{-3} mol), BA (0.33 mL, 2.30 x 10^{-3} mol for **B1** or 0.71 mL, 4.96 x 10^{-3} mol for **B2**), MCEBTTC (44.6 mg, 1.77 x 10^{-4} mol) and AIBN (5.8 mg, 3.54 x 10^{-5} mol) were dissolved in 20 mL of dioxane in a 50 mL dry Schlenk flask equipped with magnetic stirrer bar. The mixture was deoxygenated by purging with Argon for 30 min and then heated to 60 ^{o}C for 16 h under argon. The reaction was stopped by cooling to 0 ^{o}C by an ice bath and exposed to air. The solution was precipitated in diethyl ether (500 mL) and filtered. The polymer was re-dissolved in acetone and precipitated in diethyl ether. The re-dissolving and precipitating process were repeated twice. The yellow powder product was dried under high vacuum at room temperature for 48 h (yield = 87.6% for **B1** and 87.8% for **B2**).

4.2.2.3 Synthesis of random copolymers of P(NIPAM-co-DMAEA-co-STY) (C1, C2). Typically, NIPAM (4.00 g, 3.54 x 10^{-2} mol), DMAEA (1.37 mL, 8.85 x 10^{-3} mol), STY (0.27 mL, 2.30 x 10^{-3} mol for **C1** and 0.57 mL, 4.96 x 10^{-3} mol for **C2**), MCEBTTC (44.6 mg, 1.77 x 10^{-4} mol) and AIBN (5.8 mg, 3.54 x 10^{-5} mol) were dissolved in 20 mL of dioxane in a 50 mL dry Schlenk flask equipped with magnetic stirrer bar. The mixture was deoxygenated by purging with argon for 30 min and then heated to 60 ^{o}C for 48 h (**C1**) or 72 h (**C2**) under argon. The reaction was stopped by cooling to 0 ^{o}C by an ice bath and exposed to air. The solution was precipitated in diethyl ether (500 mL) and filtered. The polymer was re-dissolved in acetone and precipitated in diethyl ether. The re-dissolving and precipitating process were repeated twice. The yellow powder product was dried under high vacuum at room temperature for 48 h (yield = 89.2% for **C1** and 80.2% for **C2**).

4.2.2.4 Diameter of polymer nanoparticles of the random copolymers in differently concentrated SDS solutions determined by DLS. SDS was dissolved in Milli-Q water to obtain differently

concentrated SDS solutions (8.2, 12.3, 16.4, 20.5, and 24.6 mM) Polymer samples were weighed in vials. The prepared SDS solutions were then added to the polymers to give polymer solutions with concentration 2.5 wt%. These solutions were immediately placed in an ice bath to facilitate the dissolution. The polymer solutions were then filtered directly into DLS cuvettes using 0.45 μm cellulose syringe filter. In a typical measurement, the polymer nanoparticle diameter (D_h) and polydispersity index (PDI) was measured in DLS machine set at 37 ^oC. The present data were averaged from five measurements.

4.2.2.5 Lower Critical Solution Temperature (LCST) of the random copolymers in differently concentrated SDS solutions determined by DLS. SDS was dissolved in Milli-Q water to obtain differently concentrated SDS solutions (8.2, 12.3, 16.4, 20.5, and 24.6 mM). Polymer samples were weighed in vials. The prepared SDS solutions were then added to the polymers to give polymer solutions with concentration 2.5 wt%. These polymer solutions were immediately placed in an ice bath to facilitate the dissolution. The polymer solution was then filtered directly into DLS cuvettes using 0.45 μm cellulose syringe filter. In a typical measurement of the LCST, the polymer solution was cooled to 5 ^oC in a DLS machine, and the measurement of polymer nanoparticle diameter (D_h) was carried out by gradually increasing the temperature in the DLS machine from 5 ^oC to 60 ^oC at 2 ^oC intervals using the Standard operating procedures (SOP) software.

4.2.2.6 Diameter of polymer nanoparticles (D_h) of the random copolymers in 24.6 mM SDS solutions slowly diluted with pre-warmed 10 mM KCl solution determined by DLS. SDS was dissolved in Milli-Q water to obtain 24.6 mM solution. Polymer samples were weighed in vials. The prepared SDS solutions were then added to the polymers to give polymer solutions with concentration 2.5 wt%. These solutions were immediately placed in an ice bath to facilitate the dissolution. The polymer solutions were then filtered directly into DLS cuvettes using 0.45 μm cellulose syringe filter. Polymer solutions in the cuvettes were heated up to 37 ^oC in DLS afterwards. These solutions were then slowly diluted from 2.5 wt% to 0.1 wt% with 37 ^oC 10mM KCl solution. The polymer nanoparticle diameter and polydispersity index (PDI) were measured at 37 ^oC by DLS. The present data were averaged from five measurements.

4.2.2.7 Thermal history of random copolymers in 24.6 mM SDS solutions. SDS was dissolved in Milli-Q water to obtain 24.6 mM solution. Polymer samples were weighed in vials. The prepared SDS solutions were then added to the polymers to give polymer solutions with concentration 2.5 wt%. These polymer solutions were immediately placed in an ice bath to facilitate the dissolution. The polymer solution was then filtered directly into DLS cuvettes using 0.45 μm cellulose syringe

filter. The polymer nanoparticle diameter (D_h) was measured in DLS with a cycle of gradual decrease/increase temperature from 37 ^oC to 20 ^oC and then from 20 ^oC to 50 ^oC using the SOP software.

4.2.2.8 Disassembly kinetics of the random copolymers nanoparticles in differently concentrated SDS solutions determined by DLS. The nanoparticle diameter was measured over time to determine the disassembly time of the nanoparticles. SDS was dissolved in Milli-Q water to obtain differently concentrated SDS solutions (8.2, 12.3, 16.4, 20.5, and 24.6 mM). Polymer samples were weighed in vials. The prepared SDS solutions were then added to the polymers to give polymer solutions with concentration 2.5 wt%. These solutions were immediately placed in an ice bath to facilitate the dissolution. The polymer solution was then filtered directly into DLS cuvettes using 0.45 μm cellulose syringe filter. In a typical measurement, the polymer nanoparticle diameter (D_h) was measured in DLS machine set at 37 ^oC over time.

4.2.2.9 Lower Critical Solution Temperature (LCST) of the random copolymers in 12.3 mM SDS solution after hydrolysis at different times determined by DLS. SDS solution was prepared by dissolving SDS in Milli-Q water to concentration 12.3 mM. Polymer samples were weighed in vials. The prepared SDS solution was then added to the polymers to give polymer solutions with concentration 2.5 wt%. These polymer solutions were immediately placed in an ice bath to facilitate the dissolution. The polymer solution was then filtered directly into DLS cuvettes using 0.45 μm cellulose syringe filter. These cuvettes were then kept in a water bath at 37 ^oC to obtain hydrolysed samples. The LCST of the hydrolysed samples at different times were then measured by the DLS. The measurements were carried out by measuring nanoparticle diameter of the polymer (D_h) while gradually increasing the DLS temperature from 15 to 60 ^oC using SOP software over 3 h.

4.2.3 Analytic methodologies

^1H Nuclear Magnetic Resonance (^1H NMR). All ^1H NMR spectra were recorded on Bruker DRX 500 MHz using external locks ($CDCl_3$ or D_2O) and referenced to the residual non-deuterated solvent ($CHCl_3$ or H_2O). After samples were well dissolved in $CDCl_3$ or D_2O, samples solutions were then transferred to NMR tubes. With samples in $CDCl_3$, the spectrometer was set at 25 ^oC for determination of polymer structure. With samples in D_2O, the spectrometer was set at different temperatures for determination of the polymer structure before and after degradation.

Size Exclusion Chromatography (SEC). Analysis of the molecular weight (M_n) and molecular weight distribution (PDI) of the polymers was accomplished using a Waters 2695 separations

module, fitted with a Waters 410 refractive index detector maintained at 35 ^{o}C, a Waters 996 photodiode array detector, and two Ultrastyragel linear columns (7.8 x 300 mm) arranged in series. These columns were maintained at 40 ^{o}C for all analyses and are capable of separating polymers in the molecular weight range of 500-4 million g/mol with high resolution. The dried polymer was dissolved in tetrahydrofuran (THF) to a concentration of 1 mg/mL and then filtered through a 0.45 μm PTFE syringe filter. All samples were eluted at a flow rate of 1.0 mL/min. Calibration was performed using narrow molecular weight PSTY standards (PDI ≤ 1.1) ranging from 500 to 2 million g/mol. Data acquisition was performed using Empower software, and molecular weights were calculated relative to polystyrene standards.

Dynamic Light Scattering (DLS). Measurements were performed using a Malvern Zetasizer Nano Series running DTS software and operating a 4 mW He-Ne laser at 633 nm. Analysis was performed at an angle of 173^{o}. The sample refractive index (RI) was set at 1.59 for polystyrene. The dispersant viscosity and RI were set to 0.89 Ns.m^{-2} and 1.33, respectively. The number-average hydrodynamic particle size and polydispersity index are reported. The polydispersity index (PDI_{PDS}) was used to describe the width of the particle size distribution. It was calculated from a Cumulants analysis of the DLS measured intensity autocorrelation function and is related to the standard deviation of the hypothetical Gaussian distribution (i.e., $PDI_{PSD} = \sigma^2/Z_D^2$, where σ is the standard deviation and Z_D is the Z average mean size).

4.3 Result and Discussion

Polymer synthesis. Reversible addition-fragmentation chain transfer (RAFT) polymerization is a technique that allows control over the molecular weight of a wide range of monomers, including acrylates and acrylamides, to produce homo or block copolymers with narrow molecular weight distributions and controlled copolymer chemical composition.[49, 50] In this work, we synthesized a series of thermoresponsive random copolymers by RAFT polymerization in which MCEBTTC was employed as the chain transfer agent (CTA). Table 4.1 summarizes the polymerization conditions and resultant copolymer characterization by ^{1}H NMR and size exclusion chromatography (SEC). Addition of BA allowed the polymerization to reach a greater conversion. On the other hand, the addition of STY monomer (C1 and C2) required a longer polymerization time than those with only acrylate and acrylamide monomers (A, B1 and B2) to reach a similar conversion. This is due to the low propagation rate constant (k_p) of STY compared to the acrylates or acrylamides. We found that regardless of the polymerizatrion times, all polymers were obtained with narrow molecular weight distributions ranging with PDI_{SEC} values from 1.12 to 1.18 (Table 4.1, Figure A4.1 in Appendix C), indicating a well-controlled "living" radical polymerization. The ^{1}H NMR spectra (Figure A4.2)

showed the presence of protons at 3.63 ppm and 3.30 ppm assigned to R (**l**) and Z (**b**) of the RAFT agent, respectively. The ^{1}H NMR spectra was also used to calculate the repeating units of each monomer and the molecular weight of polymers (Table A4.1). The results showed that the molecular weight of polymers obtained from ^{1}H NMR were quite similar to those determined from SEC (Table 4.1, Table A4.1 and Figure A4.2).

Table 4.1 Reaction time, molecular weights, polydispersities (PDI), and ^{1}H NMR data of RAFT polymerization of thermoresponsive random copolymers at 60 ^{o}C in dioxane [a]

Polymer code	Reaction time (h)	SEC		^{1}H NMR						
				Monomer conversion (%)				Total conversion (%)	M_n	Percentage of BA or STY (%)
		M_n	PDI	NIPAM	DMAEA	BA	STY			
A	15	9600	1.14	31.5	34.0	-	-	32.0	9800	-
B1	16	12800	1.13	49.0	34.0	53.0	-	46.4	14800	5.70
B2	16	14900	1.12	60.0	44.0	64.0	-	57.6	19270	11.25
C1	48	9500	1.14	38.0	34.0	-	54.0	38.0	12000	7.00
C2	72	10200	1.18	32.0	32.0	-	50.0	33.8	11230	14.90

[a]All repeating units and detailed calculation were presented in Table A4.1.

Self-assembly and disassembly of nanoparticles. In Chapters 2 and 3, we used the hydrophilic PDMA as the first block of the copolymer PDMA-b-P(NIPAM-co-DMAEA-co-BA) and PDMA-b-P(NIPAM-co-DMAEA-co-STY) to act as the steric stabilizer for the polymer nanoparticles, producing particles with a narrow particle size distribution.[39, 40] The random copolymer made in this chapter will precipitate upon heating above the LCST. The addition of surfactant could provide such stabilization above the LCST. It has been reported that the SDS can bind to the backbone of PNIPAM and stabilize the resultant nanoparticles from precipitation above the LCST.[43] Therefore, we studied the influence of SDS on stabilizing the random copolymers particles at high polymer concentration (2.5 wt%) above the LCST.[44-47] This weight fraction of polymer was significantly higher than previous studies. Each polymer solution (2.5 wt%) was mixed with different SDS concentrations (8.2, 12.3, 16.4, 20.5, and 24.6 mM) and then directly heated to 37 ^{o}C. The temperature of 37 ^{o}C was chosen for this study in order to compare this system with nanoparticles reported from our previous work (i.e., Chapters 2 and 3).[39, 40] The results in Table 4.2 and Figure A4.5 showed that all polymer self-assembled into nanoparticles at 37 ^{o}C with the exception of polymer A, which remained as unimers (data not shown). The reason was due to polymer A having an LCST greater than 37 ^{o}C. Importantly, the size distribution of the polymer particles of B1, B2, C1 and C2 was very narrow (PDI_{DLS} < 0.1, in which a value less than 0.1 represents narrow distribution by DLS). This was confirmed by the similar D_h values (Number mean, Volume means,

Intensity means, and Z-average) of the polymer nanoparticles in each SDS concentration by DLS. Interestingly, this particle size distribution was in agreement with the results achieved from the polymer particles stabilized by PDMA in our previous works,[39, 40] demonstrating that the SDS provided adequate stability.

The particle size of all four polymers (B1-C2) could be tuned by changing the SDS concentration while maintaining a narrow particle size distribution. When the SDS concentration was increased, the particle size was also found to increase. For example, the number mean value of polymer B1 (5.7 mol% of BA) was 64.83 nm in 8.2 mM SDS solution, increased to 195.58 nm in a 16.4 mM SDS solution, and further increased to 502.56 nm in a 24.6 mM SDS solution. Similarly, the polymer C1 (7 mol% fraction of STY) formed a particle size of 78.76 nm in a 8.2 mM SDS solution and increased to 140.82 nm and 233.36 nm when the concentration of SDS increased to 16.4 mM and 24.6 mM, respectively. A similar trend of particle size as a function of SDS concentration was also observed for the polymer B2 and C2. In nearly all cases, the polydispersity of the distribution was below 0.1, demonstrating that the polymer particles could be increased to larger sizes while still maintaining anarrow distribution. The increase in the particle size with higher SDS concentration above the LCST of polymers was consistent with the work reported by Binkert,[42, 43] who found that through the strong hydrophobic interactions between the SDS tails and the isopropyl groups of PNIPAM the particle size increased due to ionic repulsion of the neighboring negatively charged SDS head groups. They proposed that the morphology would consist of an open internal morphology similar to that of a vesicle. Elucidation of the internal morphological of our polymer by TEM or Cryo-TEM was challenging because sample preparation was below the LCST (e.g., at 25 ^{o}C for TEM or < 0 ^{o}C for Cryo-TEM).

Table 4.2 D_h and Polydispersities (PDI_{DLS}) copolymers determined at 37 ^oC by Dynamic Light Scattering (DLS). The polymer concentration was 2.5 wt% in five different sodium dodecyl sulfate (SDS) solution concentrations at 8.2, 12.3, 16.4, 20.5, and 24.6 mM.

SDS concentration (mol/L)	D_h at 37 ^oC																			
	B1: P(NIPAM$_{98}$-co-DMAEA$_{18}$-co-BA$_7$)					B2: P(NIPAM$_{120}$-co-DMAEA$_{22}$-co-BA$_{18}$)					C1: P(NIPAM$_{76}$-co-DMAEA$_{17}$-co-STY$_7$)					C2: P(NIPAM$_{64}$-co-DMAEA$_{16}$-co-STY$_{14}$)				
	PDI (DLS)	Number mean	Intensity mean	Volume mean	Z-Average	PDI (DLS)	Number mean	Intensity mean	Volume mean	Z-Average	PDI (DLS)	Number mean	Intensity mean	Volume mean	Z-Average	PDI (DLS)	Number mean	Intensity mean	Volume mean	Z-Average
8.2	0.188	64.83	197.72	152.20	159.28	0.043	43.39	60.42	50.64	56.74	0.043	78.76	106.90	93.59	100.56	0.080	20.58	31.34	24.63	28.64
12.3	0.013	153.42	181.54	179.98	174.72	0.045	46.91	64.23	54.36	60.43	0.044	119.02	153.48	145.70	144.40	0.062	25.22	37.13	29.94	34.41
16.4	0.018	198.58	230.64	232.84	220.00	0.023	49.19	65.15	56.27	61.95	0.042	140.82	171.60	168.18	164.16	0.047	27.06	37.66	31.36	35.33
20.5	0.089	268.22	339.82	362.98	310.62	0.050	57.15	78.48	66.78	73.66	0.042	187.24	210.24	211.46	203.64	0.048	31.59	44.96	36.94	41.96
24.6	0.057	502.56	564.74	646.94	524.92	0.026	72.79	95.15	83.92	90.44	0.083	233.36	298.62	311.98	271.86	0.049	35.98	49.76	41.70	46.66

To determine the temperature that the polymer can form particles (i.e., LCST of the polymers), the five polymers (2.5 wt%) in 12.3 mM SDS solution were heated from 5 ^{o}C to 60 ^{o}C at 2 ^{o}C intervals until the formation of stable polymer particles. The results in Figure 4.1 and Table 4.3 showed that all polymer particles (B1, B2, C1 and C2) formed at 37 ^{o}C (i.e the polymer's LCSTs were below 37 ^{o}C); the only exception was polymer A whose LCST was 38 ^{o}C. At 37 ^{o}C polymer A remains as a unimer. The higher LCST of copolymer A compared to the other copolymers at the same SDS concentration (i.e., 12.3 mM) was a result of its higher hydrophilicity contributed from the hydrophilic DMAEA. It has been demonstrated that increasing the hydrophilicity of the thermoresponsive polymer, an increase in the PNIPAM's LCST will be observed and an increase in the hydrophobicity of the polymer will decrease the LCST.[51] Upon heating this polymer solution to 45 ^{o}C, polymer A self-assembled into polymer nanoparticle with 794.1 nm in diameter. When the hydrophobic component such as BA or STY was incorporated in the polymer, the LCST of the polymer decreased, consistent with our previously reported results.[39, 40] Polymer B1 (P($NIPAM_{98}$-co-$DMAEA_{18}$-co-BA_{7})) that contained 5.7 % mol fraction of BA gave an LCST of 30 ^{o}C in 12.3 mM SDS solution, and when polymer solution was heated to 37 ^{o}C, the polymer self-assembled into polymer nanoparticle with a diameter of 245.94 nm and PDI_{DLS} of 0.094 (Table 4.3). This particle size was slightly different with the value reported in Table 4.2 (153.42 nm) which may be due to the differences in the methods of heating the polymer solutions (directly heating versus slow gradual heating to 37 ^{o}C; the latter used to measure the LCST). Increasing the amount of BA to 11.25 % mol in polymer B2, the LCST of the polymer B2 (P ($NIPAM_{120}$-co-$DMAEA_{22}$-co-BA_{18})) lowered to 24 ^{o}C, resulting in a smaller size of 120.34 nm at 37 ^{o}C. Similarly, when adding 7% and 14.90 % mol fraction of STY to polymer C1 (P($NIPAM_{76}$-co-$DMAEA_{17}$-co-STY_{7})) and C2 (P($NIPAM_{64}$-co-$DMAEA_{16}$-co-STY_{14})), respectively, the LCST of the polymers dropped down to 28 ^{o}C for C1 and 19 ^{o}C for C2. Particle sizes of C1 and C2 were 141.26 nm and 32.63 nm at 37 ^{o}C, respectively.

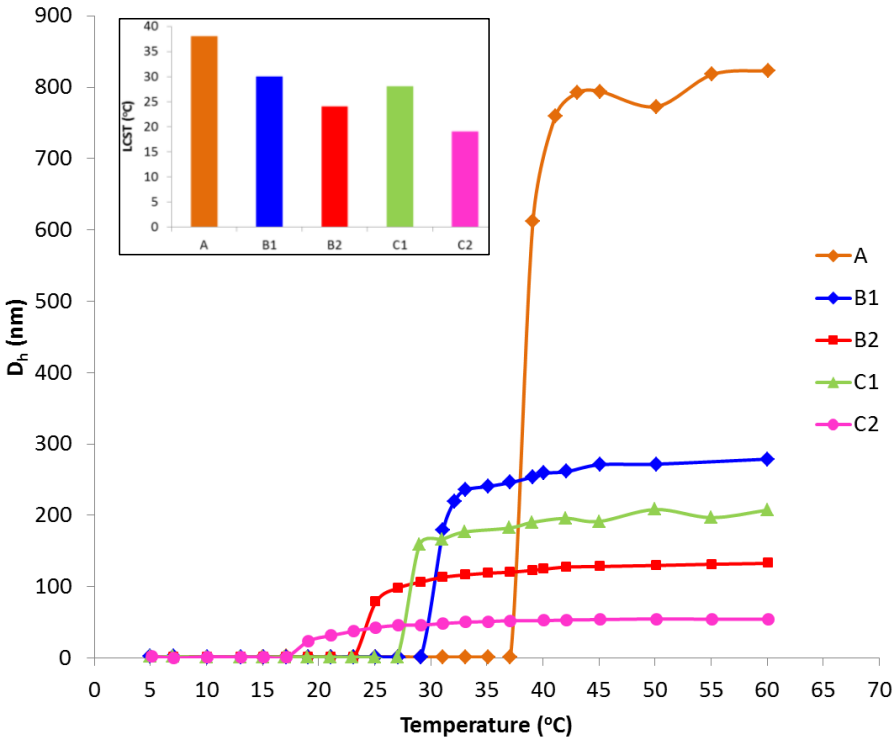

Figure 4.1 D_h vs temperature of polymer (A) P(NIPAM$_{63}$-co-DMAEA$_{17}$), (B1) P(NIPAM$_{98}$-co-DMAEA$_{18}$-co-BA$_7$), (B2) P(NIPAM$_{120}$-co-DMAEA$_{22}$-co-BA$_{18}$), (C1) P(NIPAM$_{76}$-co-DMAEA$_{17}$-co-STY$_7$), and (C2) P(NIPAM$_{64}$-co-DMAEA$_{16}$-co-STY$_{14}$) 12.3 mM SDS solution. The data were reported as average numbers from five measurements on DLS machine. Polymer concentration was 2.5 wt%. Inset: LCST vs polymer.

Table 4.3 Lower Critical Solution Temperature (LCST), Hydrodynamic Diameter (D_h), Polydispersities (PDI_{DLS}) and disassembly times for thermoresponsive random copolymers determined by Dynamic Light Scattering (DLS). The polymer concentration was 2.5 wt% in 12.3 mM SDS solution

	Polymer	LCST (^oC)	D_h (nm) (PDI_{DLS})[a]	Disassembly time t_{start} ($t_{degrade}$)[c] (h)
A	P(NIPAM$_{63}$-co-DMAEA$_{17}$)	38	794.10 (0.451)[b]	3.60 (4.1)[b]
B1	P(NIPAM$_{98}$-co-DMAEA$_{18}$-co-BA$_7$)	30	245.94 (0.094)	11.30 (6.0)
B2	P(NIPAM$_{120}$-co-DMAEA$_{22}$-co-BA$_{18}$)	24	120.34 (0.056)	40.00 (6.2)
C1	P(NIPAM$_{76}$-co-DMAEA$_{17}$-co-STY$_7$)	28	231.26 (0.044)	17.80 (6.2)
C2	P(NIPAM$_{64}$-co-DMAEA$_{16}$-co-STY$_{14}$)	19	52.42 (0.028)	95.00 (6.0)

[a] Data were measured by slowly heating polymer solutions from 5 ^oC to 60 ^oC (LCST determination) in DLS. The values were averaged from five measurements at 37 ^oC.[b] Reported value at 45 ^oC.[c] Disassembly time t_{start} = time when the size starts to decrease; $t_{degrade}$ = time from t_{start} to formation of unimers.

The LCST of the polymers (e.g., B1 and C1) were further investigated over a wide range of SDS concentrations. The data showed the LCST of polymer also increased linearly with an increase in SDS concentration (Figure 4.2, A4.6, A4.7 and Table A4.2). At higher SDS concentrations, more SDS molecules can bind to PNIPAM resulting in a greater hydrophilicity and thus higher LCST, which was consistent with the previous studies.[45, 46, 52]

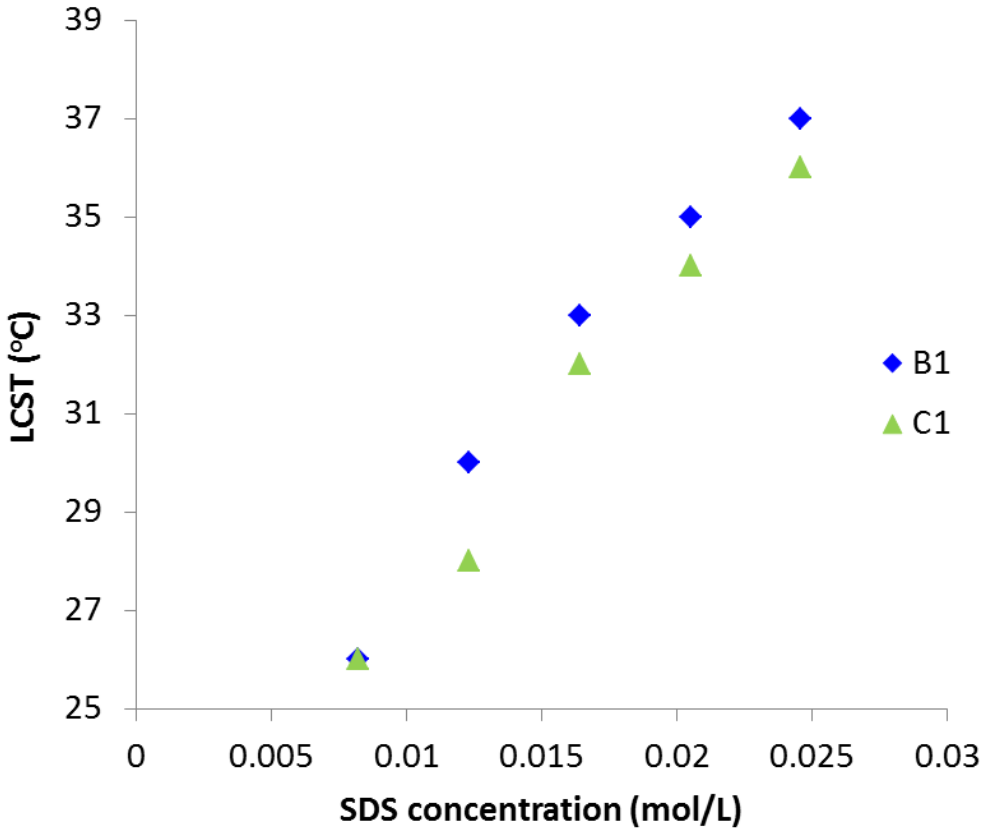

Figure 4.2 LCST vs SDS concentrations of polymer (B1) P(NIPAM$_{98}$-co-DMAEA$_{18}$-co-BA$_7$ and (C1) P(NIPAM$_{76}$-co-DMAEA$_{17}$-co-STY$_7$) when the polymers were dissolved in five different Sodium dodecyl sulfate (SDS) solution concentrations: 8.2, 12.3, 16.4, 20.5, and 24.6 mM. The data were reported as average numbers from five measurements on DLS machine. Polymer concentration was 2.5 wt%.

To test the stability of the polymer nanoparticles in SDS, the particles (e.g., B1, C1) underwent heating/cooling cycles and even a significant dilution. The polymers B1 and C1 were dissolved in a solution of 24.6 mM of SDS with a weight fraction of 2.5 wt %. The solution was heated to 37 ^{o}C to form stable particles with size of 550 nm for B1 and 264 nm for C1. The solution was gradually cooled to 20 ^{o}C in the DLS machine using the Standard operating procedures (SOP) program. A sharp decrease of the size was observed at 35 ^{o}C and the solution was then heated gradually to 55 ^{o}C. The size profile of heating cycle perfectly overlaid the cooling cycle, indicating reversibility and temperature stablity of the particles as shown in Figure 4.3A. Polymer C1 showed a similar result as

depicted in Figure 4.3B. Further experiments were carried out by diluting the polymer particles by adding 10 mM pre-heated KCl solution from 2.5 wt % down to 0.05 wt % and monitoring the size change at 37 ^{o}C. Figure 4.3C and 4.3D showed the size dependence on the weight fraction of polymer B1 and C1, respectively. Surprisingly, upon the dilution, the size of particles made from B1 and C1 was kept relatively constant with narrow distribution (PSD_{DLS}<0.1). A dramatic decrease of the particles size took place when the concentration of polymer dropped to below 0.3 wt% for B1 and 0.1 wt% for C1. When the polymer B1 solution reached approximately 10-fold dilution corresponding with a solution of 0.25 wt% polymer and 2.46 mM SDS (i.e., well below the CMC of the SDS, which is close to 8.2 mM), the polymer particles were no longer stabilized and rapidly changed in size from approximately 500 to 110 nm (Figure 4.3C). A similar process was also found for the polymer C1 solution, which underwent almost 25-folder dilution (Figure 4.3D). The sharp decrease in size can be considered as the weight fraction below which the particles disassemble and can be considered as the critical aggregation concentration (CAC).

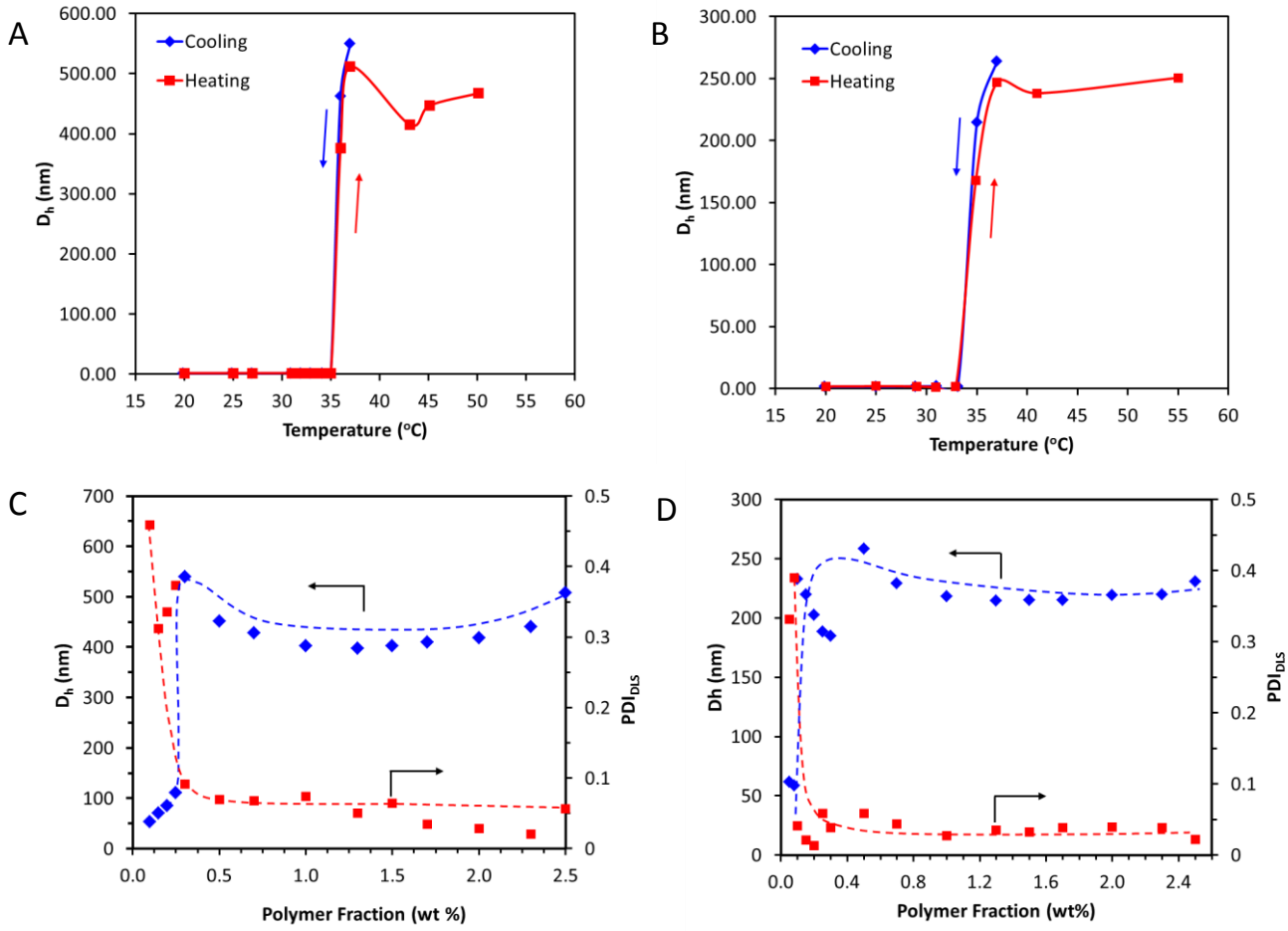

Figure 4.3 Polymer/SDS particles from polymer (A) B1 and (B) C1 over cooling and heating cycles, and D_h and PDI_{DLS} of the particles from polymer (C) B1 and (D) C1 upon dilution with 10 mM pre-warmed KCl solution at 37 ^{o}C (initial polymer concentration was 2.5 wt%, SDS 24.6 mM).

We then investigated the influence of SDS on disassembly profiles of the polymer nanoparticles by measuring the decrease in the particle size over time using dynamic light scattering (DLS). Due to the high LCST of the polymer A, well above 37 ^{o}C, the degradation kinetic of the polymer A was conducted at 45 ^{o}C. In 12.3 mM SDS solution, the polymer self-assembled into particles with diameter 276.23 nm. The size increase slowly over 3.6 h, and then fully dissociated to unimers after 7.7 h (Figure A4.8). For the other four polymers (B1 to C2), the degradation profiles were studied at 37 ^{o}C in order to compare with the degradation profile of the thermoresponsive block copolymers found in our previous work.[39, 40] The four polymers were solubilized in water at 2.5 wt% in a solution of SDS at a concentration of 12.3 mM, and directly heated to 37 ^{o}C. The polymer nanoparticles were then kept at 37 ^{o}C, and the nanoparticle size of the four polymers was measured over 120 h. The nanoparticle B1 (5.7 % mol BA) was produced with initial average size of about 191.62 nm, which was almost identical with the result presented in Table 4.2. This size then increased to about 220 nm after approximately 11 h and rapidly disassembled to unimers after 17.3 h (Figure 4.4A and Table 4.3). The increase in particle size may result from electrostatic repulsion between the negatively charged carboxylic acid groups formed through the hydrolysis of PDMAEA side groups and negatively charged SDS molecules. The additional negative charge on the polymer will result in an increase in size, similar to the observation by Walter et al.[42, 43] A similar observation was also found for the other polymers. Increasing BA to 11.25 % mol fraction, a smaller nanoparticle size was observed with diameter approximately 60.76 nm which then slowly increased to 100 nm at 40 h before dropping to 5 nm after a further 6.2 h. Similarly, the size of the polymer nanoparticle C1 which contained 7% mol fraction of STY started at around 141.26 nm in diameter and increased to about 180 nm in first 17.8 h and then quickly dissociated to unimers after 24 h. Incorporation of 14 mol % of STY in C2, produced an elevation in the size of C2 polymer nanoparticle from 32.63 nm to around 100 nm in 95 h before disassembling to unimers at approximately 101 h (Figure 4.4A in Appendix C). Furthermore, the time to disassemble (t_{start}) of the polymers with higher hydrophobic BA or STY (B2, C2) was longer, but the time (i.e., $t_{degrade}$), determined from t_{start} to full micelle disassembly to unimers (D_h ~5nm), was almost identical at ~6 h for the four polymers having similar units of DMAEA (~ 18 units) (see Table 4.3). This result exhibited that t_{start} was controlled by the LCST while $t_{degrade}$ was dependent on the DMAEA units, which is consistent with our previous work.[39, 40] The data suggested that the disassembly time ($t_{start,}$ $t_{degrade}$) of the polymer nanoparticles can be independently controlled by simply changing the composition of the copolymers.

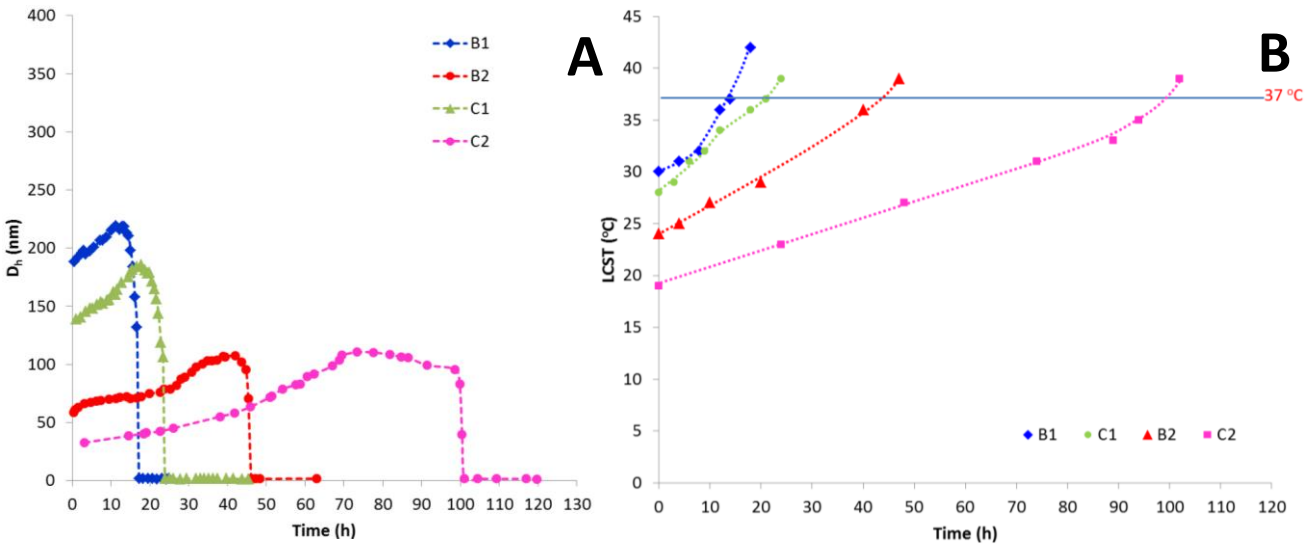

Figure 4.4 Degradation kinetic profile (A) and the rate of change in the LCST (B) of polymer (B1) P(NIPAM$_{98}$-co-DMAEA$_{18}$-co-BA$_7$) incubated at 37 ^{o}C, determined by dynamic light scattering (DLS). The polymer concentration was 2.5wt% in 12.3 mM SDS solution.

The polymer solutions were also kept at 37 ^{o}C for different times before measuring their LCST to investigate the rate of change in the LCST over time. Figure 4.4B showed that the LCST of the polymers shifted to a higher value over time. We observed that the change in the LCST of the polymers was quite consistent with the degradation profile of the polymers in Figure 4.4A. The LCST of the polymer B1 increased to 42 ^{o}C, after which time the polymer became unimers. An increase in LCST was also observed for polymer B2. After the polymer nanoparticle disassembled at 37 ^{o}C, the LCST of the polymer reached 39 ^{o}C. For both polymer C1 and C2, the LCST of the two polymers were 39 ^{o}C after the disassembly of the polymer nanoparticles to unimers occurred (Table A4.3, Figure A4.9-A4.12). The data demonstrated that the rate of LCST change corresponded with the increase in the degradation of PDMAEA to the more hydrophilic polyacrylic acid (PAA) resulting in the increase in LCST of the copolymers. When the formation of PAA was sufficient to shift LCST of the polymer to above 37 °C, rapid disassembly to water-soluble unimers occurred. The shift of LCST over 37 ^{o}C was the reason for the sharp disassembly of the polymer particles shown in Figure 4.4A. This result demonstrated that the degradation of PDMAEA was not affected by the addition of SDS, consistent with the self-catalysed hydrolysis characteristic of the PDMAEA. Furthermore, the disassembly of the polymer particle was mainly caused by the increase in LCST due to the degradation of PDMAEA. The disassembly profiles of the four polymers (B1-C2) were also studied in 24.6 mM SDS solution. Similar to 12.3 mM SDS solution, we found that the polymers possessing higher mol fraction of BA or STY provided longer degradation times (Figure A4.13 and Table A4.4). The disassembly time for the polymer nanoparticles increased from 8.17 h for B1 to 15.82 h for B2. Similarly, polymer nanoparticles C1 and C2 dissociated after 10.12

h and 37.77 h, respectively. The disassembly profiles of these four polymers suggested that the disassembly time can be precisely controlled by simply manipulating not only the polymer composition but also the SDS concentration.

To understand more about the influence of SDS concentration on the disassembly time of the polymer nanoparticles at 37 ^{o}C, the disassembly profiles of polymer B1 and C1 was investigated at four different SDS concentrations 12.3, 16.4, 20.5, and 24.6 mM (Figure A4.14 and Table A4.2). The summarized data in Figure 4.5 clearly showed that a greater SDS concentration led to a shorter disassembly time, consistent with the change in the LCST of the polymers as a function of the SDS concentrations reported in Figure 4.2. This data once again confirmed that higher SDS concentration results in greater LCST of the polymers contributing to the shorter disassembly time of the polymer particles.

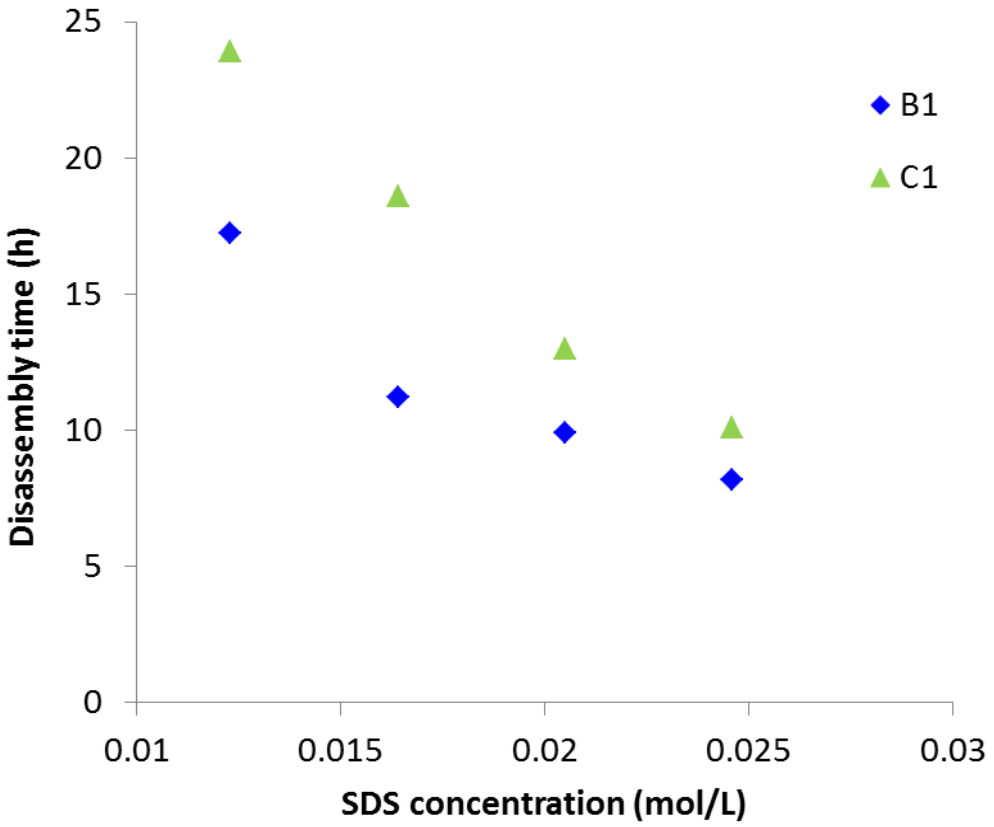

Figure 4.5 Disassembly time of B1: P(NIPAM$_{98}$-co-DMAEA$_{18}$-co-BA$_{7}$) and C1: P(NIPAM$_{76}$-co-DMAEA$_{17}$-co-STY$_{7}$) (B) as a function of SDS concentration determined at 37 ^{o}C by DLS. The polymer concentration was 2.5 wt% in different SDS solution concentrations: 12.3, 16.4, 20.5, and 24.6 mM.

4.4 Conclusion

In conclusion, we synthesized a series of well-defined random copolymers by one-pot Reversible addition-fragmentation chain transfer (RAFT) polymerization of monomers NIPAM, DMAEA and BA or STY. Above the LCST (i.e., 37 ^{o}C), these polymers could self-assemble into nanoparticles at high polymer weight fraction (2.5 wt%) and high SDS concentration (ranging from 8.2 mM up to 24.6 mM). Interestingly, the self-assembled polymer nanoparticles with large particle size (e.g., up to ~500nm) could be stabilized by SDS and demonstrated a very narrow size distribution. Furthermore, polymer particle size could be tuned, which was dependent on SDS concentration (e.g., higher SDS concentration resulted in larger particle size). Moreover, the particles size could be reversed through heating/cooling cycles, and dilution of the particles did not alter the size or change its narrow size distribution. The SDS concentration also influenced the LCST of the polymer as proved by higher polymer LCST in higher SDS concentration. Moreover, the hydrolysis of the side group of PDMAEA was not affected by SDS. The hydrolysis of PDMAEA side groups to carboxylic acid groups caused an increase in the LCST of the polymer over time, and when the LCST of the polymer increased above 37 ^{o}C, rapid disassembly of the polymer nanoparticles to unimers occurred. By controlling the SDS concentration (i.e., control in the LCST of the polymer) and the polymer composition, the disassembly time of the polymer nanoparticles can be precisely controlled.

4.5 References

1. Crespy, D.; Rossi, R. M., Temperature-responsive polymers with LCST in the physiological range and their applications in textiles. *Polymer International* **2007,** 56, (12), 1461-1468.
2. Nagase, K.; Kobayashi, J.; Okano, T., Temperature-responsive intelligent interfaces for biomolecular separation and cell sheet engineering. *J R Soc Interface* **2009,** 6 Suppl 3, S293-309.
3. Dai, S.; Ravi, P.; Tam, K. C., pH-Responsive polymers: synthesis, properties and applications. *Soft Matter* **2008,** 4, (3), 435-449.
4. Schmaljohann, D., Thermo- and pH-responsive polymers in drug delivery. *Advanced Drug Delivery Reviews* **2006,** 58, (15), 1655-1670.
5. Rodríguez-Hernández, J.; Lecommandoux, S., Reversible Inside−Out Micellization of pH-responsive and Water-Soluble Vesicles Based on Polypeptide Diblock Copolymers. *Journal of the American Chemical Society* **2005,** 127, (7), 2026-2027.
6. Vollmer, M. S.; Clark, T. D.; Steinem, C.; Ghadiri, M. R., Photoswitchable Hydrogen-Bonding in Self-Organized Cylindrical Peptide Systems. *Angewandte Chemie International Edition* **1999,** 38, (11), 1598-1601.
7. Jochum, F. D.; Theato, P., Temperature and light sensitive copolymers containing azobenzene moieties prepared via a polymer analogous reaction. *Polymer* **2009,** 50, (14), 3079-3085.
8. Jochum, F. D.; zur Borg, L.; Roth, P. J.; Theato, P., Thermo- and Light-Responsive Polymers Containing Photoswitchable Azobenzene End Groups. *Macromolecules* **2009,** 42, (20), 7854-7862.
9. Jiang, J.; Tong, X.; Zhao, Y., A New Design for Light-Breakable Polymer Micelles. *Journal of the American Chemical Society* **2005,** 127, (23), 8290-8291.
10. Szabó, D.; Szeghy, G.; Zrínyi, M., Shape Transition of Magnetic Field Sensitive Polymer Gels. *Macromolecules* **1998,** 31, (19), 6541-6548.
11. Keng, P. Y.; Shim, I.; Korth, B. D.; Douglas, J. F.; Pyun, J., Synthesis and Self-Assembly of Polymer-Coated Ferromagnetic Nanoparticles. *ACS Nano* **2007,** 1, (4), 279-292.
12. Czaun, M.; Hevesi, L.; Takafuji, M.; Ihara, H., A novel approach to magneto-responsive polymeric gels assisted by iron nanoparticles as nano cross-linkers. *Chemical Communications* **2008**, (18), 2124-2126.
13. Xulu, P. M.; Filipcsei, G.; Zrínyi, M., Preparation and Responsive Properties of Magnetically Soft Poly(N-isopropylacrylamide) Gels. *Macromolecules* **2000,** 33, (5), 1716-1719.
14. Rapoport, N. Y.; Christensen, D. A.; Fain, H. D.; Barrows, L.; Gao, Z., Ultrasound-triggered drug targeting of tumors in vitro and in vivo. *Ultrasonics* **2004,** 42, (1–9), 943-950.
15. Kost, J.; Leong, K.; Langer, R., Ultrasound-enhanced polymer degradation and release of incorporated substances. *Proceedings of the National Academy of Sciences* **1989,** 86, (20), 7663-7666.
16. Marin, A.; Muniruzzaman, M.; Rapoport, N., Mechanism of the ultrasonic activation of micellar drug delivery. *Journal of Controlled Release* **2001,** 75, (1–2), 69-81.
17. Cerritelli, S.; Velluto, D.; Hubbell, J. A., PEG-SS-PPS: Reduction-Sensitive Disulfide Block Copolymer Vesicles for Intracellular Drug Delivery. *Biomacromolecules* **2007,** 8, (6), 1966-1972.
18. Zhang, L.; Liu, W.; Lin, L.; Chen, D.; Stenzel, M. H., Degradable Disulfide Core-Cross-Linked Micelles as a Drug Delivery System Prepared from Vinyl Functionalized Nucleosides via the RAFT Process. *Biomacromolecules* **2008,** 9, (11), 3321-3331.
19. Vogt, A. P.; Sumerlin, B. S., Temperature and redox responsive hydrogels from ABA triblock copolymers prepared by RAFT polymerization. *Soft Matter* **2009,** 5, (12), 2347-2351.
20. Meng, F.; Hennink, W. E.; Zhong, Z., Reduction-sensitive polymers and bioconjugates for biomedical applications. *Biomaterials* **2009,** 30, (12), 2180-2198.
21. Dong, W.-F.; Kishimura, A.; Anraku, Y.; Chuanoi, S.; Kataoka, K., Monodispersed Polymeric Nanocapsules: Spontaneous Evolution and Morphology Transition from Reducible

Hetero-PEG PICmicelles by Controlled Degradation. *Journal of the American Chemical Society* **2009,** 131, (11), 3804-3805.
22. Ulijn, R. V., Enzyme-responsive materials: a new class of smart biomaterials. *Journal of Materials Chemistry* **2006,** 16, (23), 2217-2225.
23. Toledano, S.; Williams, R. J.; Jayawarna, V.; Ulijn, R. V., Enzyme-Triggered Self-Assembly of Peptide Hydrogels via Reversed Hydrolysis. *Journal of the American Chemical Society* **2006,** 128, (4), 1070-1071.
24. Thornton, P. D.; Mart, R. J.; Ulijn, R. V., Enzyme-Responsive Polymer Hydrogel Particles for Controlled Release. *Advanced Materials* **2007,** 19, (9), 1252-1256.
25. Harmon, M. E.; Tang, M.; Frank, C. W., A microfluidic actuator based on thermoresponsive hydrogels. *Polymer* **2003,** 44, (16), 4547-4556.
26. Hu, J. L.; Meng, H. P.; Li, G. Q.; Ibekwe, S. I., A review of stimuli-responsive polymers for smart textile applications. *Smart Materials and Structures* **2012,** 21, (5).
27. Richter, A.; Paschew, G.; Klatt, S.; Lienig, J.; Arndt, K. F.; Adler, H. J. P., Review on hydrogel-based pH sensors and microsensors. *Sensors* **2008,** 8, (1), 561-581.
28. Roy, D.; Brooks, W. L. A.; Sumerlin, B. S., New directions in thermoresponsive polymers. *Chemical Society Reviews* **2013,** 42, (17), 7214-7243.
29. Kujawa, P.; Aseyev, V.; Tenhu, H.; Winnik, F. M., Temperature-Sensitive Properties of Poly(N-isopropylacrylamide) Mesoglobules Formed in Dilute Aqueous Solutions Heated above Their Demixing Point. *Macromolecules* **2006,** 39, (22), 7686-7693.
30. Okada, Y.; Tanaka, F., Cooperative Hydration, Chain Collapse, and Flat LCST Behavior in Aqueous Poly(N-isopropylacrylamide) Solutions. *Macromolecules* **2005,** 38, (10), 4465-4471.
31. Kujawa, P.; Segui, F.; Shaban, S.; Diab, C.; Okada, Y.; Tanaka, F.; Winnik, F. M., Impact of End-Group Association and Main-Chain Hydration on the Thermosensitive Properties of Hydrophobically Modified Telechelic Poly(N-isopropylacrylamides) in Water. *Macromolecules* **2005,** 39, (1), 341-348.
32. Wu, C.; Zhou, S., Thermodynamically Stable Globule State of a Single Poly(N-isopropylacrylamide) Chain in Water. *Macromolecules* **1995,** 28, (15), 5388-5390.
33. Fujishige, S.; Kubota, K.; Ando, I., Phase transition of aqueous solutions of poly(N-isopropylacrylamide) and poly(N-isopropylmethacrylamide). *The Journal of Physical Chemistry* **1989,** 93, (8), 3311-3313.
34. Schild, H. G., Poly (N-Isopropylacrylamide) - Experiment, Theory and Application. *Prog Polym Sci* **1992,** 17, (2), 163-249.
35. Wei, H.; Cheng, S.-X.; Zhang, X.-Z.; Zhuo, R.-X., Thermo-sensitive polymeric micelles based on poly(N-isopropylacrylamide) as drug carriers. *Prog Polym Sci* **2009,** 34, (9), 893-910.
36. Chung, J. E.; Yokoyama, M.; Yamato, M.; Aoyagi, T.; Sakurai, Y.; Okano, T., Thermo-responsive drug delivery from polymeric micelles constructed using block copolymers of poly(N-isopropylacrylamide) and poly(butylmethacrylate). *Journal of Controlled Release* **1999,** 62, (1–2), 115-127.
37. Liu, X.-M.; Yang, Y.-Y.; Leong, K. W., Thermally responsive polymeric micellar nanoparticles self-assembled from cholesteryl end-capped random poly(N-isopropylacrylamide-co-N,N-dimethylacrylamide): synthesis, temperature-sensitivity, and morphologies. *Journal of Colloid and Interface Science* **2003,** 266, (2), 295-303.
38. Cammas, S.; Suzuki, K.; Sone, C.; Sakurai, Y.; Kataoka, K.; Okano, T., Thermo-responsive polymer nanoparticles with a core-shell micelle structure as site-specific drug carriers. *Journal of Controlled Release* **1997,** 48, (2–3), 157-164.
39. Tran, N. T. D.; Truong, N. P.; Gu, W.; Jia, Z.; Cooper, M. A.; Monteiro, M. J., Timed-Release Polymer Nanoparticles. *Biomacromolecules* **2013,** 14, (2), 495-502.
40. Tran, N. T. D.; Jia, Z.; Truong, N. P.; Cooper, M. A.; Monteiro, M. J., Fine Tuning the Disassembly Time of Thermoresponsive Polymer Nanoparticles. *Biomacromolecules* **2013,** 14, (10), 3463-3471.

41. Truong, N. P.; Jia, Z. F.; Burges, M.; McMillan, N. A. J.; Monteiro, M. J., Self-Catalyzed Degradation of Linear Cationic Poly(2-dimethylaminoethyl acrlyate) in Water. *Biomacromolecules* **2011,** 12, (5), 1876-1882.
42. Meewes, M.; Ricka, J.; Desilva, M.; Nyffenegger, R.; Binkert, T., Coil Globule Transition of Poly(N-Isopropylacrylamide) - a Study of Surfactant Effects by Light-Scattering. *Macromolecules* **1991,** 24, (21), 5811-5816.
43. Walter, R.; Rička, J.; Quellet, C.; Nyffenegger, R.; Binkert, T., Coil−Globule Transition of Poly(N-isopropylacrylamide): A Study of Polymer−Surfactant Association. *Macromolecules* **1996,** 29, (11), 4019-4028.
44. Uehara, N.; Ogawa, M., Interaction of Poly(N-isopropylacrylamide) with Sodium Dodecyl Sulfate below the Critical Aggregation Concentration. *Langmuir* **2014,** 30, (22), 6367-6372.
45. Chen, J.; Gong, X.; Yang, H.; Yao, Y.; Xu, M.; Chen, Q.; Cheng, R., NMR Study on the Effects of Sodium n-Dodecyl Sulfate on the Coil-to-Globule Transition of Poly(N-isopropylacrylamide) in Aqueous Solutions. *Macromolecules* **2011,** 44, (15), 6227-6231.
46. Chen, J.; Xue, H.; Yao, Y.; Yang, H.; Li, A.; Xu, M.; Chen, Q.; Cheng, R., Effect of Surfactant Concentration on the Complex Structure of Poly(N-isopropylacrylamide)/Sodium n-Dodecyl Sulfate in Aqueous Solutions. *Macromolecules* **2012,** 45, (13), 5524-5529.
47. Mylonas, Y.; Staikos, G.; Lianos, P., Investigation of the Poly(N-isopropylacrylamide)-Sodium Dodecyl Sulfate Complexation with Viscosity, Dialysis, and Time-resolved Fluorescence-Quenching Measurements. *Langmuir* **1999,** 15, (21), 7172-7175.
48. Urbani, C. N.; Monteiro, M. J., Nanoreactors for Aqueous RAFT-Mediated Polymerizations. *Macromolecules* **2009,** 42, (12), 3884-3886.
49. Moad, G.; Rizzardo, E.; Thang, S. H., Radical addition-fragmentation chemistry in polymer synthesis. *Polymer* **2008,** 49, (5), 1079-1131.
50. Smith, A. E.; Xu, X. W.; Mccormick, C. L., Stimuli-responsive amphiphilic (co)polymers via RAFT polymerization. *Prog Polym Sci* **2010,** 35, (1-2), 45-93.
51. Feil, H.; Bae, Y. H.; Feijen, J.; Kim, S. W., Effect of comonomer hydrophilicity and ionization on the lower critical solution temperature of N-isopropylacrylamide copolymers. *Macromolecules* **1993,** 26, (10), 2496-2500.
52. Mears, S. J.; Deng, Y.; Cosgrove, T.; Pelton, R., Structure of Sodium Dodecyl Sulfate Bound to a Poly(NIPAM) Microgel Particle. *Langmuir* **1997,** 13, (7), 1901-1906.

Chapter 5

Non-triggered degradable thermoresponsive hydrogel for controlled release of gold nanoparticles

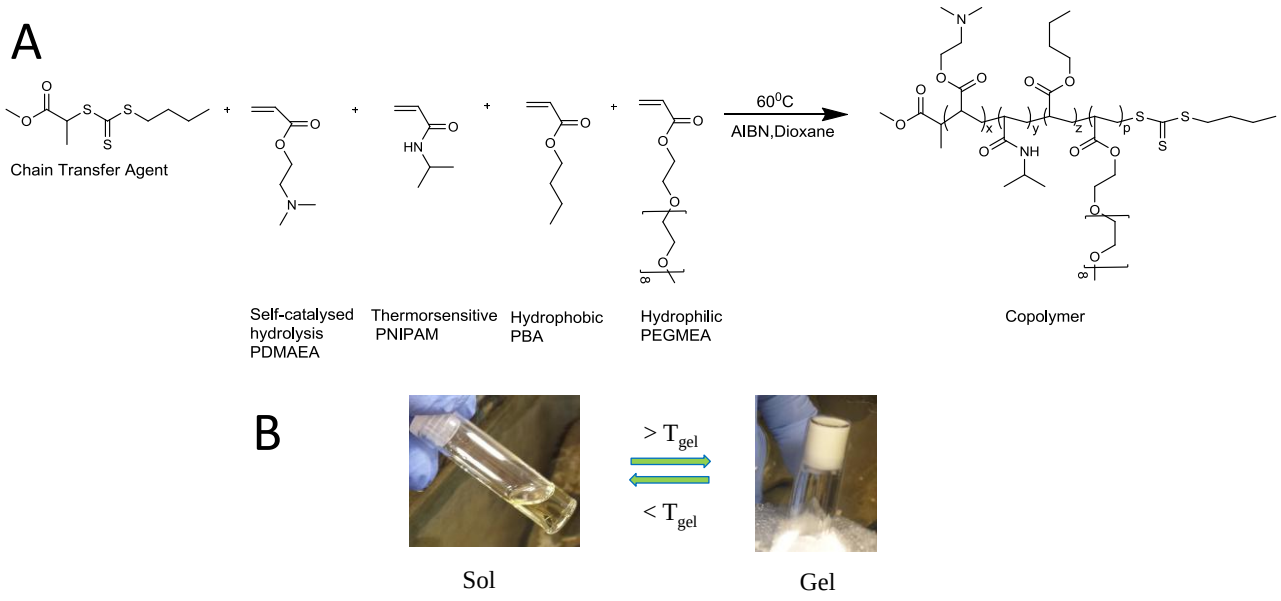

Polymeric hydrogels as carriers have attracted a lot of attention for applications in drug and gene delivery systems. In this chapter, a novel self-degradable release hydrogel system was designed. The hydrogels were prepared based on a series of random copolymers synthesized from NIPAM, self-catalysed hydrolysis DMAEA, hydrophilic PEGMEA, and hydrophobic BA (P(NIPAM-co-DMAEA-co-PEGMEA-co-BA)) via Reversible addition−fragmentation chain transfer (RAFT) polymerization. The thermoresponsive copolymers formed a stable gel at temperature higher than the gelation point and then self-degraded into sol state over time without the need of any triggers. Moreover, the gelation temperature and degradation time increased with increase in the DMAEA units. Gold nanoparticles coated with PDMA were encapsulated in the hydrogel and subsequently released at different rates through the degradation of the hydrogel.

5.1 Introduction

Thermoresponsive polymers and their copolymers have attracted significant attention for biomedical applications such as drug delivery, cell immobilization, in-situ gelling implantation and tissue engineering.[1-3] Based on the particular properties of the thermoresponsive PNIPAM,[4-13] it has been employed in the synthesis and development of injectable hydrogels because gelation can be obtained by simply altering the temperature above the LCST of the polymer without any chemical/photo cross-linking which may cause cytotoxicity issues.[7, 14-18] It has been reported that the sol-gel transition of the polymer solution is the result of chain entanglement as well as the physical junction, which forms from hydrophobic interaction between collapsed polymer globules and the expanding polymer coils.[19] However, these hydrogels are non-degradable which may cause chronic inflammatory response and thus limits the application of such hydrogels in vivo.[20]

Various efforts have been made to create thermoresponsive degradable hydrogels. For example, biodegradable PNIPAM-based hydrogels can be achieved by the incorporation of PNIPAM with degradable polymers or crosslinkers.[21-24] The presence of crosslinkers can limit the hydrogel's injectability, and the degradation of such hydrogel systems requires the existence of triggers (e.g., enzymes). Another limitation is that the variations in environmentally triggered stimuli between cell lines and even within the same tissue or organ may result in different rates of degradation and inconsistent data between in vitro and in vivo experiments. Therefore the application of thermoresponsive degradable hydrogels as delivery systems can sometimes be limited. [25, 26]

To address the issue of biodegradation, PNIPAM based copolymers that possess different gelation temperatures before and after degradation have been developed. In these degradable hydrogel systems, PNIPAM was copolymerized with hydrolysable side groups containing polymers. Polymer solutions exhibited sol state at below 37 ^{o}C, this allows the polymer solution to be injectable before gelation. Increase in temperature to 37 ^{o}C results in the polymer solution transitioning to a gel state. After degradation of the side groups, the hydrogel returns to sol state, which allows the degradation products to dissolve into the bodily fluids and to be eliminated from the body.[20, 27-30] However, the degradation rates of these hydrogels are not able to be controlled.[27, 29, 30]

In previous chapters, we have reported a type of polymer micelles with well-controlled disassembly time that was formed by self-assembly of thermoresponsive diblock copolymer PDMA-b-P(NIPAM-co-DMAEA-co-BA).[12, 13] PDMAEA can self-hydrolyse to poly acrylic acid (PAA) independent of molecular weight or pH environment.[31, 32] The degradation product, PAA, increased the LCST of the polymer resulting in the disassembly of the polymer nanoparticle at a precisely controlled time without the need of a trigger.[12, 13]

5.1.1 Aim of the Chapter

The goal of this chapter is to synthesize a novel non-triggered degradable hydrogel system based on a series of hydrolyzable random copolymers of thermoresponsive PNIPAM, self-catalyzed hydrolysis PDMAEA, hydrophilic PEGMEA, and hydrophobic PBA (P(NIPAM-co-DMAEA-co-PEGMEA-co-BA)). The Reversible addition-fragmentation chain transfer (RAFT) was employed to synthesize these random thermoresponsive copolymers. The gelation temperature of polymer solutions was investigated by both DSC and vial inverting method. Moreover, the water content and the degradation of the hydrogels were studied. In addition, PDMA functionalized gold nanoparticles (PDMA-AuNPs) were employed as a model drug to be encapsulated into the hydrogels. The releases of PDMA-AuNPs from the hydrogels were then monitored over time by UV-vis spectroscopy.

5.2 Experimental

5.2.1 Materials

Dioxane (Alrich, 99%), carbondisulfide (Alrich, 99%), 1-butanethiol (Alrich, 99%), methyl bromopropionate (Alrich, 98%), and dimethyl sulfoxide (DMSO, Alrich >99.9%), dichloromethane (DCM: Labscan, AR grade), Styrene (STY, Aldrich, 99 %), 2-(dimethylamino) ethyl acrylate (DMAEA, Sigma-Aldrich, 98%), Poly(ethylene glycol) methyl ether acrylate (PEGMEA, Sigma-Aldrich) and butyl acrylate (BA, Aldrich, 99%) were passed through a column of basic alumina (activity I) to remove inhibitor. N-isopropylacrylamide (NIPAM, Aldrich, 97 %) was recrystallized from hexane. Azobisisobutyronitrile (AIBN) was also recrystallized twice from methanol prior to use. Hydrogen tetrachloroaurate (III) hydrate ($HAuCl_4 \cdot 3H_2O$; Aldrich, 99.9%), trisodium citrate dehydrate (Na_3Ct; Aldrich, 99%). Milli-Q Water (18.2 MΩcm-1) was generated using a Millipore Milli-Q academic water purification system. All other chemicals and solvents used were of at least analytical grade and used as received.

5.2.2 Synthetic procedures

5.2.2.1 Synthesis of the Chain Transfer Agent (CTA), Methyl 2-(butylthiocarbonothioylthio) propanoate (MCEBTTC). The synthesized MCEBTTC was carried out according to the literature procedure[33]. Carbondisulfide (3.1 mL, 0.051 mol) in dichloromethane (50 mL) was added dropwise to a stirred solution of 1-butanethiol (5 mL, 0.047 mol) and triethylamine (7.2 mL, 0.051 mol) in dichloromethane (25 mL) over 30 min at 0 ^{o}C under an argon atmosphere. The solution gradually turned yellow during the addition. After complete addition, the solution was stirred at room temperature for 30 min. Methyl bromopropionate (5.7 mL, 0.051 mol) in dichloromethane (25 mL)

was then added dropwise over 30 min and the solution stirred for 2 h. The dichloromethane was removed under nitrogen and the residue dissolved in diethylether. The solution was then washed with cold 10% HCl solution (3 x 50 mL) and Milli-Q water (3 x 50 mL) and dried over anhydrous $MgSO_4$. The ether was removed under vacuum, and the residual yellow oil was purified by column chromatography (19:1 petroleum ether/ethyl acetate on silica, second band). ^{1}H NMR ($CDCl_3$) δ 0.90 (t, *J* = 7.5 Hz, 3H, CH_3), 1.40 (m, *J* = 7.5 Hz, 2H, CH_2), 1.57 (d, *J* = 7.5 Hz, 3H, CH_3), 1.66 (q, *J* = 7.5 Hz, 2H, CH_2), 3.34 (t, *J* = 7.5 Hz, 2H, CH_2), 3.73 (s, 3H, CH_3), 4.80 (q, *J* = 7.5 Hz, 1H, CH).

5.2.2.2 Synthesis of random copolymers. P($NIPAM_{198}$-co-$DMAEA_{12}$-co-BA_8-co-$PEGMEA_{14}$) *(A).* NIPAM (2.00 g, 1.77 x 10^{-2} mol), DMAEA (0.205 mL, 1.33 x 10^{-3} mol), PEGMEA (0.58 mL, 1.33 x 10^{-3} mol), BA (0.127 mL, 8.85 x 10^{-4} mol), CTA (22.3 mg, 8.85 x 10^{-5} mol) and AIBN (2.90 mg, 1.77 x 10^{-5} mol) were dissolved in 12 mL of dioxane in a dry Schlenk flask equipped with a magnetic stirrer bar. The mixture was deoxygenated by purging with Argon for 40 min and then heated to 60 ^{o}C for 24 h under Argon atmosphere. The reaction was stopped by cooling to 0 ^{o}C in an ice bath and exposed to air. The solution was precipitated in diethyl ether (500 mL) and filtered. The polymer was re-dissolved in acetone and precipitated in diethyl ether. The re-dissolving and precipitating process were repeated twice. The light yellow powder product was dried under high vacuum at room temperature for 48 h (yield = 70%).

5.2.2.3 Synthesis of random copolymers. P($NIPAM_{196}$-co-$DMAEA_9$-co-BA_8-co-$PEGMEA_{13}$) *(B).* NIPAM (2.00 g, 1.77 x 10^{-2} mol), DMAEA (0.137 mL, 8.85 x 10^{-4} mol), PEGMEA (0.58 mL, 1.33 x 10^{-3} mol), BA (0.127 mL, 8.85 x 10^{-4} mol), CTA (22.3 mg, 8.85 x 10^{-5} mol) and AIBN (2.90 mg, 1.77 x 10^{-5} mol) were dissolved in 12 mL of dioxane in a dry Schlenk flask equipped with a magnetic stirrer bar. The mixture was deoxygenated by purging with Argon for 40 min and then heated to 60 ^{o}C for 24 h under Argon atmosphere. The reaction was stopped by cooling to 0 ^{o}C in an ice bath and exposed to air. The solution was precipitated in diethyl ether (500 mL) and filtered. The polymer was re-dissolved in acetone and precipitated in diethyl ether. The re-dissolving and precipitating process were repeated twice. The light yellow powder product was dried under high vacuum at room temperature for 48 h (yield = 78%).

5.2.2.4 Synthesis of random copolymers. P($NIPAM_{196}$-co-$DMAEA_4$-co-BA_8-co-$PEGMEA_{14}$) *(C).* NIPAM (2.00 g, 1.77 x 10^{-2} mol), DMAEA (0.068 mL, 4.42 x 10^{-4} mol), PEGMEA (0.58 mL, 1.33 x 10^{-3} mol), BA (0.127 mL, 8.85 x 10^{-4} mol), CTA (22.3 mg, 8.85 x 10^{-5} mol) and AIBN (2.90 mg, 1.77 x 10^{-5} mol) were dissolved in 12 mL of dioxane in a dry Schlenk flask equipped with a

magnetic stirrer bar. The mixture was deoxygenated by purging with Argon for 40 min and then heated to 60 ^{o}C for 24 h under Argon atmosphere. The reaction was stopped by cooling to 0 ^{o}C in an ice bath and exposed to air. The solution was precipitated in diethyl ether (500 mL) and filtered. The polymer was re-dissolved in acetone and precipitated in diethyl ether. The re-dissolving and precipitating process were repeated twice. The light yellow powder product was dried under high vacuum at room temperature for 48 h (yield = 81%).

*5.2.2.5 Synthesis of 10 nm gold nanoparticles (AuNPs).*100 mL of Milli-Q water and 6 mL of 1% sodium citrate solution were added in a 250 mL Erlenmeyer flask, and the solution was heated to boil for 5 min on a hot plate with vigorous stirring. 1 mL of 1% $HAuCl_4$ solution was then added rapidly, and the solution boiled for another 15 min while stirring. The colour of solution turned to a wine red. The AuNPs synthesized from this method give a size in the range of 10-13 nm as confirmed by both DLS and TEM. The solution mixture contained 5 mg of AuNP in 100 mL.

5.2.2.6 Synthesis of RAFT functionalized poly (N, N-diethylacrylamide) (PDMA). RAFT (0.64 g, 2.52 x 10^{-3} mol), AIBN (33.1 mg, 2.02 x 10^{-4} mol), DMA (25.0 g, 2.52 x 10^{-1} mol) were dissolved in DMSO in a 50 mL dry Schlenk flask equipped with a magnetic stirrer bar. The mixture was deoxygenated by purging with Argon for 30 min and then heated to 60 ^{o}C for 1.5 h. The reaction was stopped by cooling to 0 ^{o}C in an ice bath and exposed to the air. The solution was then diluted with dichloromethane (500 mL) and washed with brine (3x100 mL). The dichloromethane (DCM) was then dried over anhydrous $MgSO_4$, filtered and reduced in volume by rotary evaporation. The polymer was recovered by precipitation into large excess of diethyl ether (1 L), and isolated by filtration. The polymer was re-dissolved in acetone and precipitated in diethyl ether. The re-dissolving and precipitation process was repeated twice. The polymer was filtered and then dried under high vacuum for 24 h at room temperature to give a yellow powder product (yield = 71%). M_n = 7300, PDI = 1.14 (SEC-RI calibrated using PSTY Standards in DMAc solution containing 0.03 wt% of LiCl), M_n = 7900 (SEC-Triple Detection, d*n*/d*c* = 0.081); M_n = 7900 (^{1}H NMR). ^{1}H NMR (500 MHz, $CDCl_3$): δ 0.87 (C*H*$_3$CH$_2$CH$_2$-), 1.09 (C*H*$_3$-(CH-COO)-), 2.84-3.05 ((C*H*$_3$)$_2$-N-), 3.29 (-C*H*$_2$-S-(C=S)-S-), 3.60 (C*H*$_3$O-(C=O)-), 5.14 (-(C=S)-S-C*H*-).

5.2.2.7 Coating of RAFT functionalized PDMA on the gold nanoparticles. Poly (N, N-diethylacrylamide**)** (PDMA) (15.88 mg, 1.99 x 10^{-6} mol) was dissolved in 3 mL of cold Milli-Q water and added dropwise to 100 mL of gold solution under vigorous stir. The final red-wine solution was then kept stirring for 16 hours. The polymer grafted AuNPs were purified by three cycles of centrifugation (40000g) /washing/redispersing to remove unbound polymers to remove

excessive amount of polymers. The PDMA coated AuNPs (PDMA-AuNPs) size was determined by both DLS and TEM. The resulting solution was then freeze dried to get the powder-like PDMA coated AuNPs (PDMA-AuNPs).

5.2.2.8 Hydrogel preparation. Polymers were added in cold Milli-Q water and placed in an ice bath to form 30 wt% solutions in a glass vial. These polymer solutions were then gradually heated at 1 ^{o}C interval in a temperature controlled water bath to temperature that the polymer solution transitioned to non-transparent gel (T_{gel}) without flowing when inverting the vial. The gels still maintain upon heating to 37^{o} C.

5.2.2.9 Water content. Polymers were added in cold Milli-Q water and placed in an ice bath to form 30 wt% solutions. These polymer solutions (30 wt%) were placed in a 37^{o} C water bath for gelation. The formed gels were maintained at 37^{o} C for 2 h. Water expelled (supernatant) during the gelation and incubation was not observed, otherwise removed by cotton to give wet mass (w_1), and the gel was then freeze-dried for 5 days to give dry mass (w_2). Water content was defined as the difference between the wet mass (w_1) and dry mass (w_2) of the hydrogel.

$$\textbf{\textit{Water content} = } (w_1-w_2)/w_1 \times 100\%$$

The water content of each hydrogel was averaged from three repetitive experiments.

5.2.2.10 Gelation temperature (^{o}C) of polymer solution (30 wt%) determined by DSC. Polymers were added in cold Milli-Q water and placed in an ice bath to form 30 wt% solutions. These polymer solutions were loaded onto a DSC aluminium crucible cell (40 μL, Mettler Toledo International Inc.) and heated under nitrogen at a constant heating rate of 2 °C /min from 10° C up to 60° C. The transition temperature is the mid-point of inflection of the obtained DSC curves.

5.2.2.11 Hydrogel degradation. Measurement the degradation of hydrogel was designed according to the method developed by Guan and co-workers.[27] Polymers were added in cold Milli-Q water and placed in an ice bath to form 30 wt% solutions. 1.0 g of polymer solutions was transferred into glass vial. The vial was then placed in 37^{o} C water bath for gelation. The formed gels were maintained at 37^{o} C for 5 h, and 2.5 mL of 37 ^{o}C water was then loaded to the top of the hydrogels. The degradation time is the time that the hydrogels transitioned from non-transparent gel to transparent solutions. The degradation time of each hydrogel was averaged from three repetitive experiments.

5.2.2.12 Lower critical solution temperature (LCST) of the polymer solution (5 wt%) determined by observing cloud point over time. Polymers were added in cold Milli-Q water and placed in an ice bath to form 5 wt% solutions. These polymer solutions (5 wt%) were gradually heated in a temperature controlled water bath until the polymer solution became turbid (i.e., cloud point). This temperature was determined as the LCST of polymer. The polymer solutions were then incubated at 37 ^{o}C until they became transparent solutions (i.e., polymers were degraded at 37 ^{o}C). The degraded polymer solutions were gradually heated to higher temperature to determine the LCST of the degraded polymer solutions. A temperature showed a later turbid point was chosen as LCST of the degraded polymer solution. The polymer solutions were further incubated to approximately 240 hours to make sure the polymers were fully degraded demonstrated by a constant LCST over measuring times.

5.2.2.13 Weight loss percentage of PDMA grafted gold nanoparticles (PDMA-AuNPs) determined by TGA. PDMA grafted gold nanoparticles were heated from 30 to 750 °C in TGA at a rate of 10 °C/min. The surface density of polymer (chains/nm^2) can be estimated by TGA according to the following equation.

$$\frac{\left(\frac{W_{polymer}}{100 - W_{polymer}}\right)\rho V_{particle} N_A}{M_{polymer} S_{particle}}$$

where, W_{polymer} is the percent weight loss corresponding to the decomposition of polymer, is the density of gold (19.32 g/cm^3), V_{particle} is the volume of gold nanoparticle calculated from the radius measured by DLS, N_{A} is Avogadro's number, M_{polymer} is the molecular weight of polymer, and S_{particle} is the surface area of gold nanoparticle.

5.2.2.14 Loading and release PDMA grafted AuNPs (PDMA-AuNPs) from thermoresponsive hydrogels. 0.24 mg PDMA-grafted AuNPs was mixed with 0.3 g copolymer and 0.7 g of cold Milli Q water in glass vial and placed in an ice bath to form 30 wt. % polymer solutions. The mixture was then transferred to plastic cuvette, heated up to 37 ^{o}C to form hydrogel and then kept at 37 ^{o}C for 30 min. 2.5 mL of 37 ^{o}C Milli-Q water was then added to the top of the gel and the cuvette was then kept at 37 ^{o}C water bath. Triplicate samples were done for each polymer. The Absorbance (Abs) of PDMA grafted AuNPs diffused up to the aqueous phase on top of the hydrogel was measured by UV-vis at λ_{max}= 527 nm. The Abs values at each time point was the average of three repetitive experiments.

5.2.3 Analytic methodologies

^{1}H Nuclear Magnetic Resonance (NMR). All NMR spectra were recorded on Bruker DRX 500 MHz and 300 MHz using external locks ($CDCl_3$) and referenced to the residual non-deuterated solvent ($CHCl_3$).

Size Exclusion Chromatography (SEC) and Triple Detection_ Size Exclusion Chromatography (TD-SEC). Analysis of the molecular weight distributions of the polymers were determined using a Polymer Laboratories GPC50 Plus equipped with differential refractive index detector. Absolute molecular weights of polymers were determined using a Polymer Laboratories GPC50 Plus equipped with dual angle laser light scattering detector, viscometer, and differential refractive index detector. HPLC grade N,N-dimethylacetamide (DMAc, containing 0.03 wt % LiCl) was used as the eluent at a flow rate of 1.0 mL/min. Separations were achieved using two PLGel Mixed B (7.8 x 300 mm) SEC columns connected in series and held at a constant temperature of 50 ^{o}C. The triple detection system was calibrated using a 2 mg/mL PSTY standard (Polymer Laboratories: M_{wt} = 110K, d*n*/d*c* = 0.16 mL/g and IV = 0.5809). Samples of known concentration were freshly prepared in DMAc + 0.03 wt % LiCl and passed through a 0.45 μm PTFE syringe filter prior to injection. The absolute molecular weights and d*n*/d*c* values were determined using Polymer Laboratories Multi Cirrus software based on the quantitative mass recovery technique.

Dynamic light scattering (DLS). Measurements were performed using a Malvern Zetasizer Nano Series running DTS software and operating a 4 mW He-Ne laser at 633 nm. Analysis was performed at an angle of 173^{o}. The sample refractive index (RI) was set at 1.59 for polystyrene. The dispersant viscosity and RI were set to 0.89 $Ns.m^{-2}$ and 1.33, respectively. The number-average hydrodynamic particle size and polydispersity index are reported. The polydispersity index (PDI_{PDS}) was used to describe the width of the particle size distribution. It was calculated from a Cumulants analysis of the DLS measured intensity autocorrelation function and is related to the standard deviation of the hypothetical Gaussian distribution (i.e., $PDI_{PSD} = \sigma^2/Z_D^2$, where σ is the standard deviation and Z_D is the Z average mean size).

Thermogravimetric Analysis (TGA). TGA was carried out using a Mettler Toledo STARe instrument. Samples were heated from 30 to 750 °C at a rate of 10 °C/min.

Differential scanning calorimetry (DSC). DSC was carried out on a Mettler Toledo DSC1 STARe System calorimeter.

Ultraviolet Visible Absorption (UV-vis). UVvis absorption spectra were recorded using a Cary 500 Scan UV-vis/NIR spectrophotometer at 37 ^{o}C using a 1 cm plastic cuvette.

Fourier Transform Infrared Spectroscopy (FTIR). FTIR spectra were recorded using a Nicolet 6700 FTIR spectrometer

Transmission Electron Microscopy (TEM). The nanostructure appearance of the polymer lattices was analyzed using a JEOL 1010 transmission electron microscope utilizing an accelerating voltage of 100 kV with spot size 6 at ambient temperature. A typical TEM grid preparation was as follows: A formvar precoated copper TEM grid (Proscitech) was dipped into the nanoparticle solution, the excess aliquot was blotted and then allowed to air dry prior imaging on TEM.

5.3 Result and Discussion

Polymer synthesis. The copolymer was synthesized by random copolymerization of four monomers NIPAM, DMAEA, PEGMEA, and BA. PNIPAM provides the thermoresponsive property, PDMAEA acts as self-degradable component, PEGMEA improves water retention, and BA employed to control the LCST of the copolymers. Polymerizations were conducted using the Reversible addition-fragmentation chain transfer (RAFT) technique (Scheme 5.1A) which allows control over molecular weight distributions (MWD) for a wide range of functional polymers.[34-39] The molecular weight of the three polymers at the peak maximum determined by RI-SEC showed number-average molecular weight ranging from 51000 to 55000 (Table 5.1). The slight differences in the molecular weights of the polymers may be due to the difference in the content of PDMAEA which was well consistent with difference in the mol ratios of monomer added to the reactions. In addition, the SEC traces in Figure 5.1 showed unimodal MWD, and the polydispersities (PDI_{SEC-RI}) of the three polymers were below 1.4, demonstrating that polymerization was well controlled even though the copolymer comprised of four monomers. The M_n values determined by triple detection SEC were approximately 34000 to 35000 and the polydispersity index by triple detection SEC (PDI_{SEC-TP}) for all three polymers was less than 1.05, which was found to be a slight underestimation when compared to the PDI_{SEC-RI} (see Table 5.1).

Table 5.1 Molecular weights, polydispersities index (PDI_{SEC}), and ^1H NMR data of RAFT polymerization of thermoresponsive random copolymers at 60 ^oC in dioxane.

	NIPAM]:[DMAEA]:[BA]:[PEGMEA]:[CTA]:[AIBN][a]	SEC[b]				^1H NMR					
		RI		Triple detection[c]		Repeating units				M_n[h]	Percentage of DMAEA (mol %)
		M_n	PDI	M_n	PDI	NIPAM[d]	DMAEA[g]	BA[e]	PEGMEA[f]		
A	200:15:10:15:1:0.2	54700	1.34	35200	1.04	198	12	8	14	32000	5.17
B	200:10:10:15:1:0.2	54100	1.32	34500	1.03	196	9	8	13	31100	3.98
C	200:5:10:15:1:0.2	51000	1.34	34200	1.03	196	4	8	14	30600	1.80

[a] CTA concentration was 8.85 x 10^{-5} mol.

[b] SEC data measured in DMAc solution with 0.03 wt% of LiCl and using PSTY standards for calibration.

[c] Triple detection data measured based on the dn/dc calculated from the polymers' concentration.

[d] Repeating units of NIPAM (N_{NIPAM}) determined by ^1H NMR were calculated based on the conversion of NIPAM. The conversion of NIPAM was calculated based on the ^{1}HNMR spectra in Figure A5.3 with integral area of the peak at 1.08 ppm ($I_{1.08}$) and the peak a 5.57 ppm ($I_{5.57}$) using the following equation: 1- (6 x $I_{5.57}/I_{1.08}$). Repeating units of NIPAM (N_{NIPAM}) = mol feeding ratio of NIPAM x conversion of NIPAM = 200 x [1- (6 x $I_{5.57}/I_{1.08}$)]

[e] Repeating units of BA (N_{BA}) determined by ^1H NMR were calculated based on the repeating unit of NIPAM (N_{NIPAM}) and the integral area of the peak at 1.08 ppm ($I_{1.08}$) and the peak at 0.88 ppm ($I_{0.88}$) using the following equation: $N_{BA} = [2 \times N_{NIPAM} \times (I_{0.88}-3)] / I_{1.08}$

[f] Repeating units of PEGMEA (N_{PEGMEA}) determined by ^1H NMR were calculated based on the repeating unit of NIPAM (N_{NIPAM}) and the integral area of the peak at 1.08 ppm ($I_{1.08}$) and the peak at 3.34 ppm ($I_{3.34}$) using the following equation: $N_{PEGMEA} = [2 \times N_{NIPAM} \times (I_{3.34} - 2)]/I_{1.08}$

[g] Repeating units of DMAEA (N_{DMAEA}) determined by ^1H NMR were calculated based on the N_{NIPAM} , N_{BA}, N_{PEGMEA} and the integral area of the peak at 1.08 ppm ($I_{1.08}$) and the peak in the range 3.95-4.30 ppm ($I_{3.95-4.30}$) using the following equation: $N_{DMAEA} = [3 \times N_{NIPAM} \times (I_{3.95-4.30} - (N_{NIPAM} + 2 \times N_{BA} + 2 \times N_{PEGMEA}))]/I_{1.08}$

[h] Molecular weight determined by ^1H NMR were calculated based on the repeating units of N_{NIPAM}, N_{DMAEA}, N_{BA}, N_{PEGMEA} and the molecular weight of CTA: $Mn = (N_{NIPAM} \times 113) + (N_{DMAEA} \times 143) + (N_{BA} \times 128.2) + (N_{PEGMEA} \times 480) + 252$.

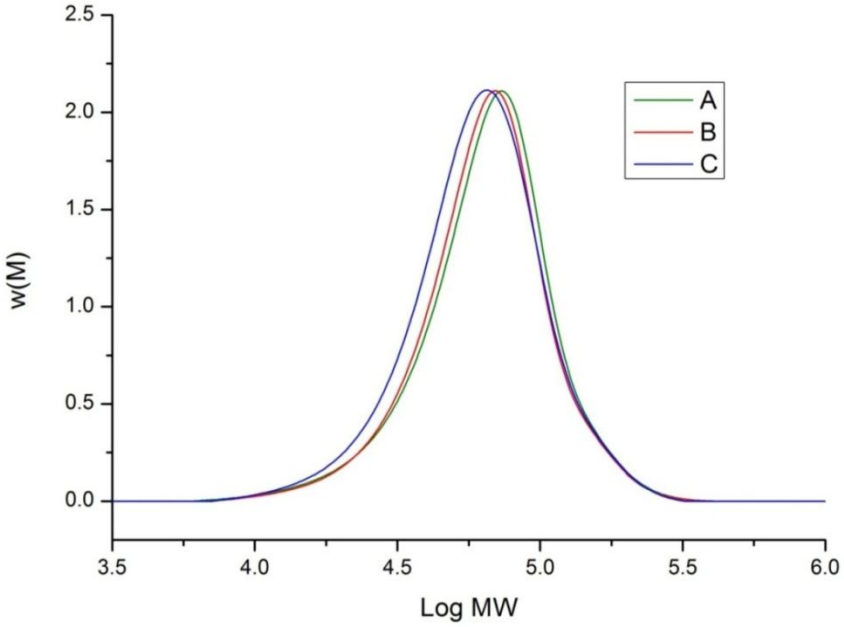

Figure 5.1 Size Exclusion Chromatography (SEC) traces, A: P(NIPAM$_{198}$-co-DMAEA$_{12}$-co-BA$_8$-co-PEGMEA$_{14}$), B: P(NIPAM$_{196}$-co-DMAEA$_9$-co-BA$_8$-co-PEGMEA$_{13}$), C: P(NIPAM$_{196}$-co-DMAEA$_4$-co-BA$_8$-co-PEGMEA$_{14}$). The data were measured by DMAc SEC. The intensity for different distribution curves was normalized.

The three polymers were also characterized by ^{1}H NMR to confirm the structure as well as the composition of the copolymers. Acrylate protons are usually used in the calculation of the polymers conversion. In this work, due to the overlap of most peaks assigned for acrylate protons of the monomers, the conversion of DMAEA, PEGMEA, and BA monomers were not able to be directly determined from ^{1}H NMR of unpurified samples. Only conversion of the NIPAM was able to be calculated by this method. The conversion of PNIPAM, approximately 98.9%, was determined based on the isolated peaks at 5.54 ppm and 1.12 ppm, which were respectively assigned for the acrylamide proton of NIPAM monomer (**b**) and methyl groups (**d, g**) for both the NIPAM monomer and the polymer (Figure A5.1 in Appendix D). ^{1}H NMR spectra of purified and dried polymer samples were then used to calculate the repeating units of the segments in the copolymers. The ^{1}H NMR spectra showed that most of the peaks assigned for the RAFT agent, which are usually used as a calibration value in calculating the repeating units of polymer synthesized by RAFT, were overlapped with the polymers peaks (Figure 5.2). The repeating unit of PNIPAM, obtained from the conversion of NIPAM was thus used as calibration in determination of the repeating units of the other segments in the copolymers (see Table 5.1). The results show that the content of NIPAM, PEGMEA, and BA was similar for the three polymers while the content of DMAEA steadily decreased with 5.17, 3.98, and 1.80 mol % for polymer A, B, and C, respectively. This demonstrates that the composition of the polymers was well controlled. The M_n values for all

polymers determined by ^{1}H NMR were relatively close to those found by triple detection SEC. This data further confirms that the chain lengths of three polymers were almost identical and that small variations in the polymer chain lengths resulted from the differences in the content of PDMAEA among the three polymers.

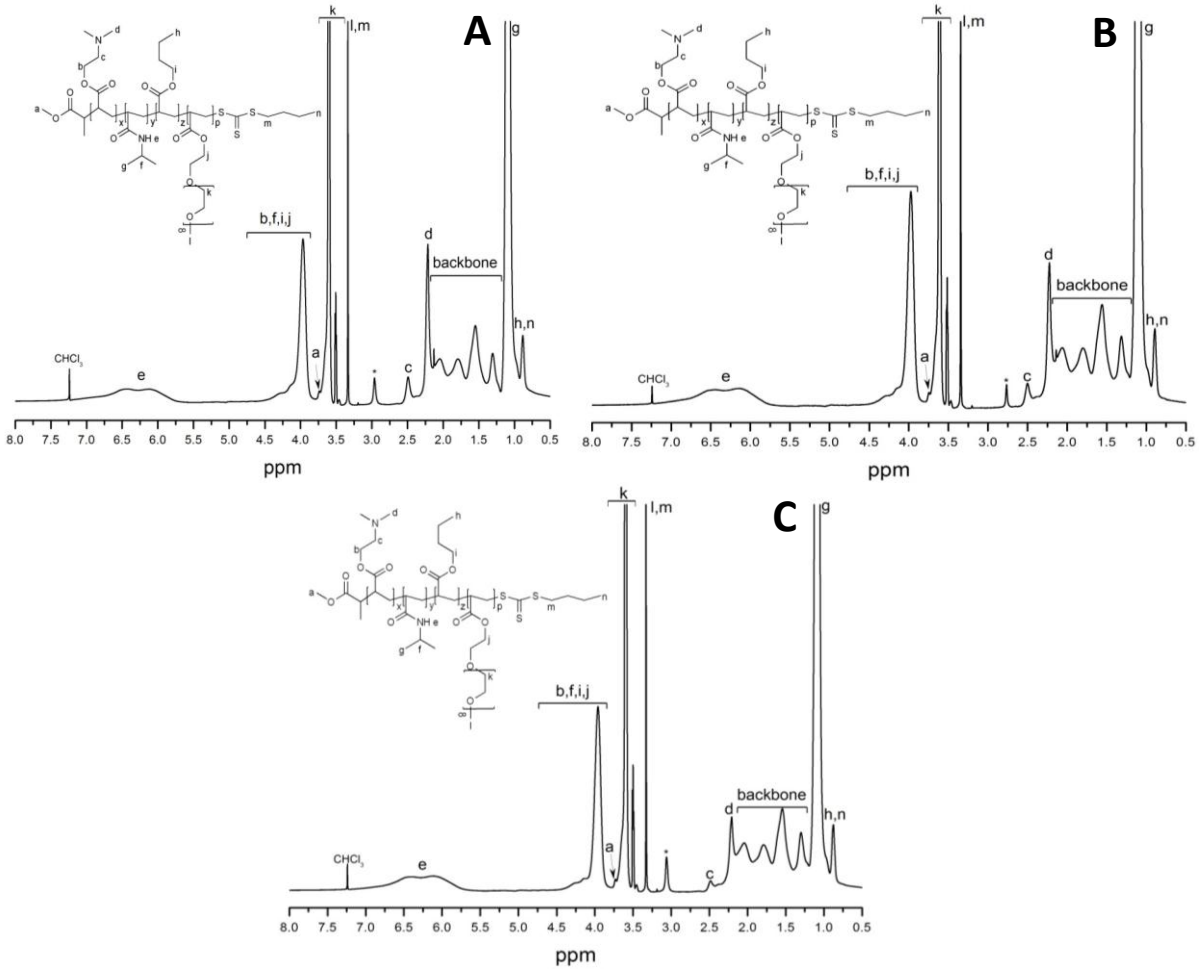

Figure 5.2 ^{1}H NMR spectrum of A: P(NIPAM$_{198}$-co-DMAEA$_{12}$-co-BA$_{8}$-co-PEGMEA$_{14}$), B: P(NIPAM$_{196}$-co-DMAEA$_{9}$-co-BA$_{8}$-co-PEGMEA$_{13}$), and C: P(NIPAM$_{196}$-co-DMAEA$_{4}$-co-BA$_{8}$-co-PEGMEA$_{14}$) in $CDCl_3$.

Hydrogel preparation and thermal properties. Hydrogels were prepared by dissolving copolymers in Milli-Q water in an ice bath to obtain 30 wt% copolymer solutions in glass vials and gradually heated in a temperature controlled water bath to the temperature that the transparent polymer solution transitioned to a non-transparent gel (Scheme 5.1B). The gelation temperature (denoted as T_{gel}) is determined when the vial is inverted and the gel shows no flow for 1 min.[40, 41] The gelation temperatures (T_{gel}) of the three polymers were 34, 33, and 32 ^{o}C for polymer A, B and C, respectively (see Table 5.2).

Table 5.2 Thermo transition temperature of polymer solutions (30 wt%) and water content, and degradation time of hydrogels at 37 ^{o}C.

Polymer code	T_{gel} (^{o}C) determined by vial invert [a]	T_{gel} (^{o}C) determined by DSC	Water content (%) [b]	Degradation time (h) [c]
A	34	33	70.13±0.13	86.0±2.0
B	33	32.5	69.37±0.17	108.6±2.3
C	32	32	68.55±1.35	158.66±3.06

[a]T_{gel} was determined by observing the formation of gel without flowing while inverting the glass vial. [b]The water content of each hydrogel was an average of three repetitive water content experimentscalculated by using the equation showed in the experimental. [c]The degradation time is the time that the all hydrogel completely become solution. The result was averaged from three repetitive experiments.

The gel state of the three polymers still maintained upon heating to 37 ^{o}C. Furthermore, the formed gel can reversely change to the sol state upon cooling below T_{gel} (Scheme 5.1B) showing typical reversible characteristic of thermoresponsive hydrogels. It is reported that the formation of thermoresponsive hydrogels is the result of chain entanglement and hydrophobic interactions, which form as junctions of collapsed copolymer globules at above LCST.[19] A lower polymer concentration 25 wt% was also prepared to test hydrogel formation. However, the solution only became turbid and flowed when inverting the vials at 37 ^{o}C indicating that the concentration of polymer may not sufficient to induce gelation. Therefore, 30 wt% is the minimum concentration required of these copolymers to be able to form stable gels

The sol to gel transition temperature of the polymer solutions was further determined by DSC. The DSC data in Figure 5.3 showed that the gelation temperature of all three polymer solutions were below body temperature, decreased from 33 ^{o}C (for polymer A) to 32.5 ^{o}C (for polymer B), and 32 ^{o}C (for polymer C) corresponding with decrease of hydrophilic DMAEA percentage in the copolymers from 5.17 to 3.98, and 1.8 mol %, respectively. This data matched quite well with the gelation temperature obtained from the vial inverting method that was determined by visible observation (see Table 5.2).

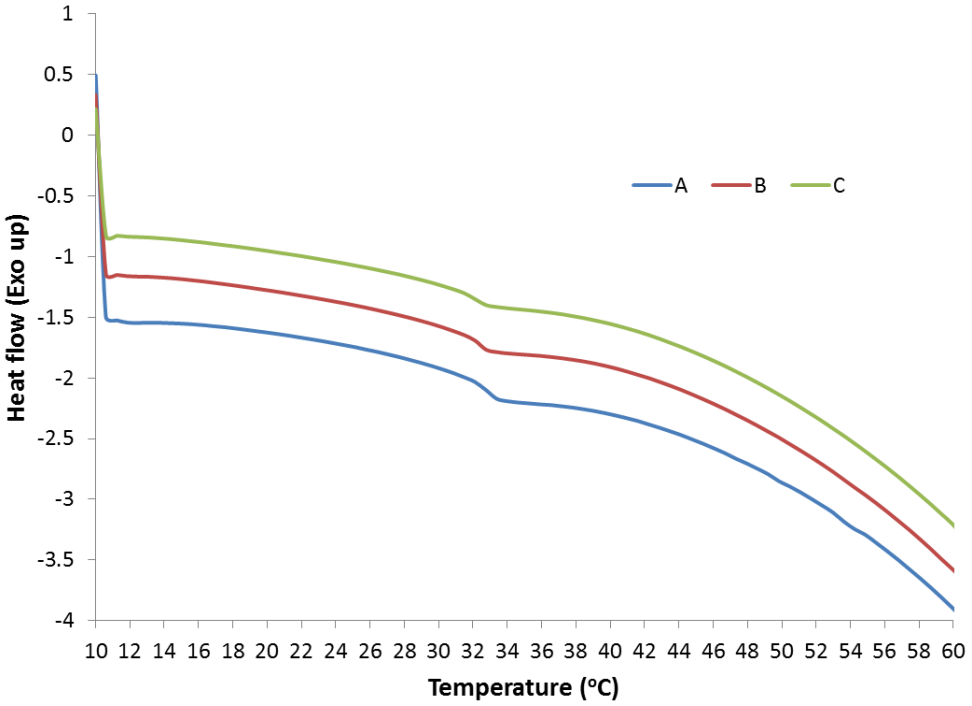

Figure 5.3 Thermo transition temperature (^{o}C) of the hydrogel (polymer weight fraction 30 wt%) measured by DSC (heating rate of 2 ^{o}C min^{-1}). The transition temperature is the middle point of the DSC curve.

Water content. It has been found that the T_{gel} of the polymer was affected by the composition of the hydrogel.[30, 42-44] The more hydrophobic components in the copolymer results in the lower T_{gel} while greater hydrophilicity in the copolymer leads to higher T_{gel}. In our work, because the composition of NIPAM, PEGMEA, and BA were similar for the three polymers, the small change in T_{gel} of the three polymer solutions mainly resulted from the little difference in the amount of hydrophilic PDMAEA in the three polymers. Increasing the DMAEA content resulted in the increase of the T_{gel} due to the higher amount of hydrophilic components.

Hydrogel degradation. The degradation time of the hydrogel was investigated after loading pre-warm Milli-Q water on the top of 1.0 g of freshly formed hydrogels at 37 ^{o}C. The hydrogel periphery layer that was in contact with water gradually degraded until the total gel completely changed to the solution state. This process can be named as a surface-to-core degradation.[27] Basically, the DMAEA units in the copolymers on the gel surface which is in contact with the large amount of free water started to degrade and the gel became solution. The process took place from the gel surface to the core and finally became solution at 37 ^{o}C, which coincides with previous reported gel degradation profiles.[27] It is worth to note that the similar copolymer systems (e.g., diblock or star copolymers of poly(ethylene glycol) (PEG) and PNIPAM) which did not contain DMAEA units can also form hydrogels but are not able to degrade over time.[17] The complete

degradation time of the three hydrogels increased with the decrease of mol% of DMAEA. The degradation time for polymer A (5.17 mol%) was 86 h, polymer B (3.98 mol%)108 h, and polymer C (1.80 mol%) 158 h (Table 5.2). It is expected that the formation of carboxylic acid groups after the self-catalysed hydrolysis of PDMAEA side groups increases the LCST of the copolymers, thus increases the gelation temperature of the polymers. When the amount of carboxylic groups increases sufficiently to shift the gelation temperature above 37 ^{o}C, the polymers become soluble and diffuse into water.[9, 11-13, 20, 27, 30, 43, 45, 46] The evidence of increase in the gelation temperature of the polymers was supported by the change in the LCST (i.e., cloud point) of 5wt% polymer solutions over time (Figure A5.2).

Gold nanoparticles synthesis and functionalization. In order to study the loading and release properties of the novel hydrogels, polymer-coated gold nanoparticles were synthesized. Gold nanoparticles (AuNPs) with a diameter of ~ 10 nm were synthesized by adding $HAuCl_4$ solution to a boiling solution of trisodium citrate (Na_3Ct) under vigorous stirring.[47] Gold nanoparticles obtained were covered by citrate ions which adsorbed onto the naked AuNPs surface during synthesis. The size and the uniformity of the gold nanoparticles were determined by both TEM and DLS. The results from DLS showed that the AuNPs was successfully prepared with a particle size of about 11.27 nm. The polydispersity index (PDI_{DLS}) of the gold nanoparticles was 0.096 suggesting that the particle size distribution was narrow (values <0.1 represents distributions that are narrow) (see Table 5.3). TEM showed that the spherical AuNPs had a diamerter of approximately 12.40 nm supporting for the results obtained from DLS (Figure 5.4A).

Table 5.3 Diameter (D_h) and polydispersities index (PDI_{DLS}), weight loss and surface density of gold nanoparticles (AuNPs) before and after functionalization with PDMA (PDMA-AuNPs).

Material	DLS[a]		TEM (nm)	TGA	
	D_h (nm)	PDI_{DLS}		Weight loss (%) [b]	Surface density of PDMA-AuNPs (chains/nm^2)[c]
Bare AuNPs	11.27 ± 0.53	0.096	12.40	-	-
PDMA-AuNPs	26.55 ± 0.97	0.070	20.00	24.51	0.898

[a]The D_h and PDI_{DLS} were averaged from five measurement on DLS. [b]Weight loss was determined from TGA. [c]Surface density of the polymer on AuNPs was calculated based weight loss, molecular weight of polymer, and diameter of AuNPs.

To increase the compatibility as well as stability of the AuNPs, polymer-functionalized AuNPs was synthesized by "grafting to" approach in which the thiol groups araised from polymer can strongly affinity bind to gold via chemisorption.[47-54] RAFT functionalized PDMA was employed for this purpose because PDMA not only is high soluble to effectively stabilize the AuNPs but also contains trithiocarbonate end- group (from RAFT agent) that can be converted to thiol groups to bind to AuNPs (Scheme 5.2).

Scheme 5.2 PDMA functionalized gold nanoparticles AuNPs (PDMA-AuNPs).

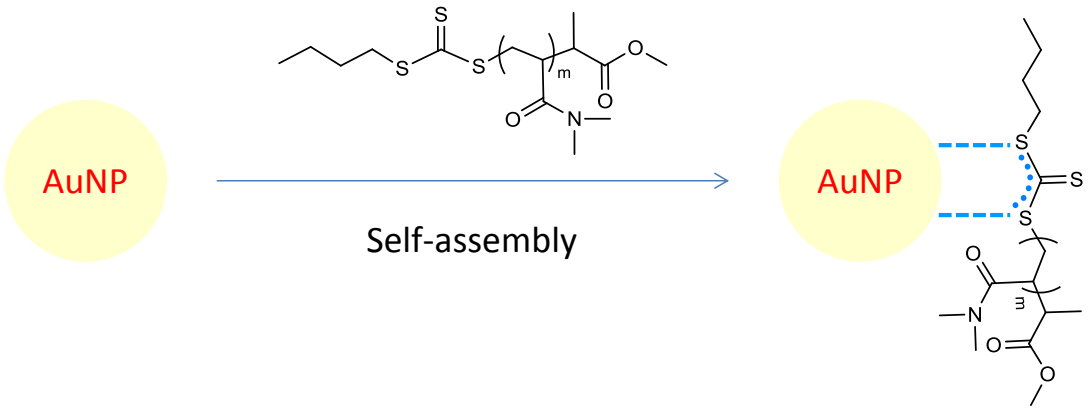

RAFT-PDMA was synthesized with a number-average molecular weight (M_n) of 7900 (RI-SEC) which was close to that measured by ^{1}H NMR (^{1}H NMR, M_n=7900 giving 78 units of DMA by accounting for the molecular weight of the RAFT agent), and polydispersity index ($PDI_{RI\text{-}SEC}$) was 1.14. In ^{1}H NMR spectrum of PDMA, the two protons associated with the RAFT agent's R (**e**) and Z (**a**) groups were observed at 3.60 and 0.87 ppm, respectively, which demonstrated that most of the polymer chains were functionalized by RAFT (Figure A5.3).

To coat the PDMA on the AuNPs surface, the polymer was dissolved in water and added dropwise into the AuNPs solution under stirring for 16 h. The PDMA-AuNPs solution then underwent three cycles of centrifugation/washing/redispersing to remove unbound polymers. The purified PDMA-AuNPs were collected and resuspended in water to measure DLS and TEM. The DLS data showed that the diameter of AuNPs (PDMA-AuNPs) increased to approximately 26.5 nm with a very narrow size distribution (PDI_{DLS} =0.07) suggesting that the PDMA was grafted onto AuNPs and provided steric stabilization to AuNPs (see Table 5.3). TEM images in Figure 5.4B also showed that the spherical shape of AuNPs was preserved with no aggregation after grafting with PDMA.

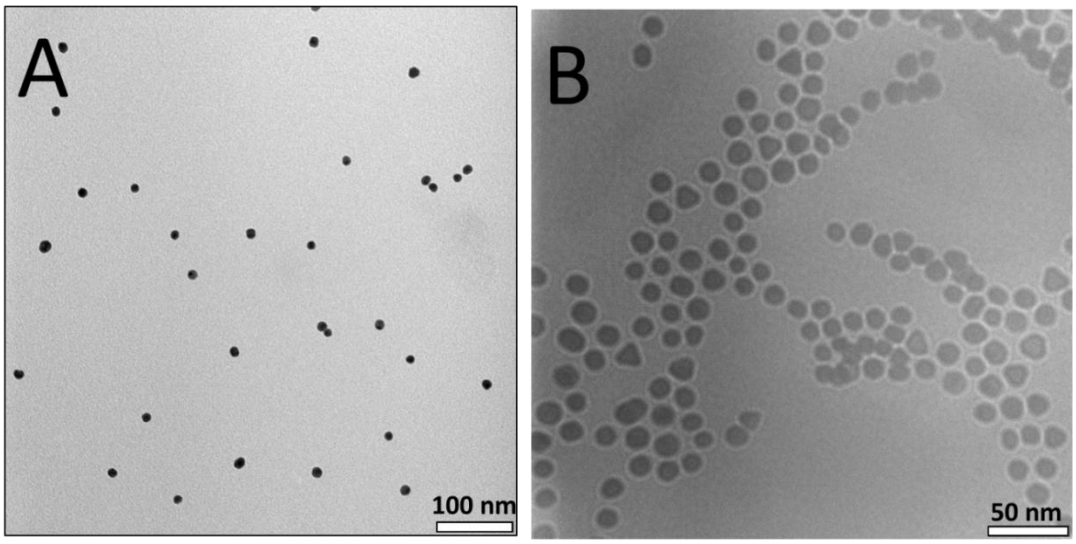

Figure 5.4 TEM of bare gold nanopartciles (AuNPs) (A) and PDMA grafted gold nanopartciles (PDMA-AuNPs) (B).

The purified PDMA-AuNPs solution was also freeze-dried to obtain the powder-like PDMA-AuNPs. The PDMA-AuNPs product was then characterized by ATR-FTIR. The appearance of the C=O stretching vibration at approximately 1700 cm^{-1}, and N-H stretching vibration at about 3400 cm^{-1} on the spectrum of PDMA-grafted AuNP supported that the PDMA was grafted onto the AuNPs. (Figure 5.5).

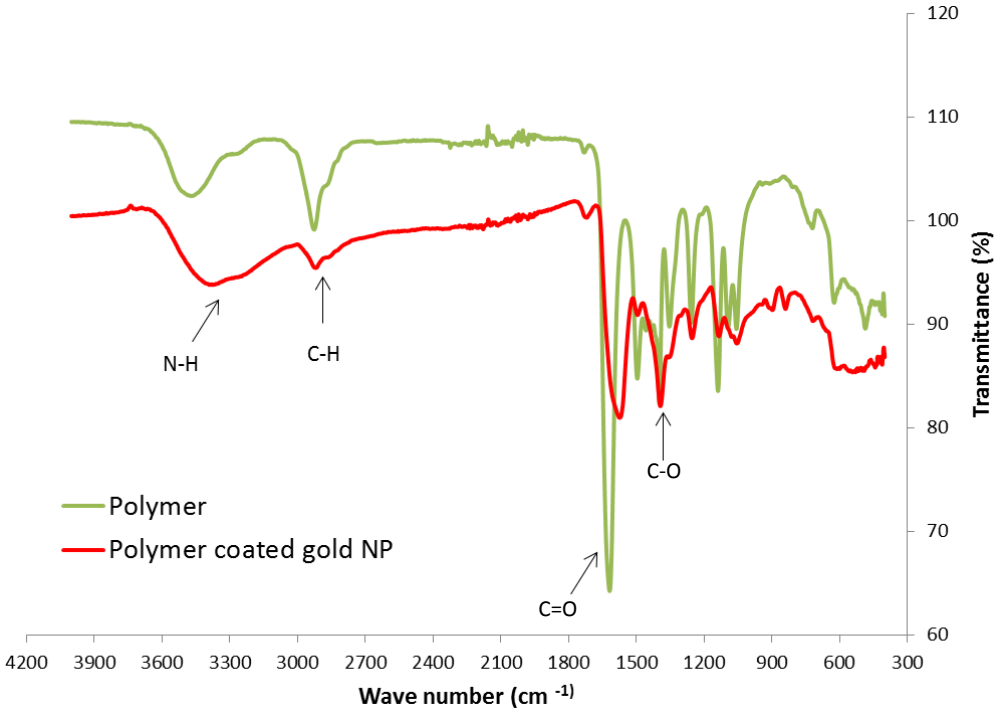

Figure 5.5 ATR-FTIR of pure PDMA and PDMA grafted AuNPs.

TGA was employed to determine the number of polymer chains bound to one AuNP (chains/nm^2) (Figure A5.4). Approximately 24.5 wt% of grafted polymer was decomposed at 380 ^{o}C resulting in a relatively high graft density at 0.898 chains/nm^2 which was calculated based on the following equation: surface density of polymer (chain/nm^2) =

$$\frac{\left(\frac{W_{polymer}}{100 - W_{polymer}}\right)\rho V_{particle} N_A}{M_{polymer} S_{particle}}$$

where, W_{polymer} is the percent weight loss corresponding to the decomposition of polymer, ρ is the density of gold (19.32 g/cm^3), V_{particle} is the volume of gold nanoparticle calculated from the radius measured by TEM, N_{A} is Avogadro's number, M_{polymer} is the molecular weight of polymer, and S_{particle} is the surface area of gold nanoparticle. This high grafting density provided further evidence that the AuNPs were successfully coated with PDMA.

Loading and release of PDMA functionalized gold nanoparticles (PDMA-AuNPs) from hydrogel.
These PDMA-AuNPs were encapsulated in 1.0 g of the hydrogel by mixing PDMA-AuNPs at 2 ^{o}C and then heating up to 37 ^{o}C. Pre-warmed water was loaded onto the top of the gel and incubated at 37 ^{o}C. During the process of the polymer hydrolysing at 37 ^{o}C as well as the hydrogel degrading, the PDMA-AuNPs were able to be released from the hydrogel. The release experiment was carried out in a 4 mL cuvette that allowed the UV-vis beam passing through the middle of the cuvette where the water phase occupied. The percentage of released AuNPs was determined by measuring the absorbance (Abs) of AuNP in water phase at $\lambda_{527\text{nm}}$.

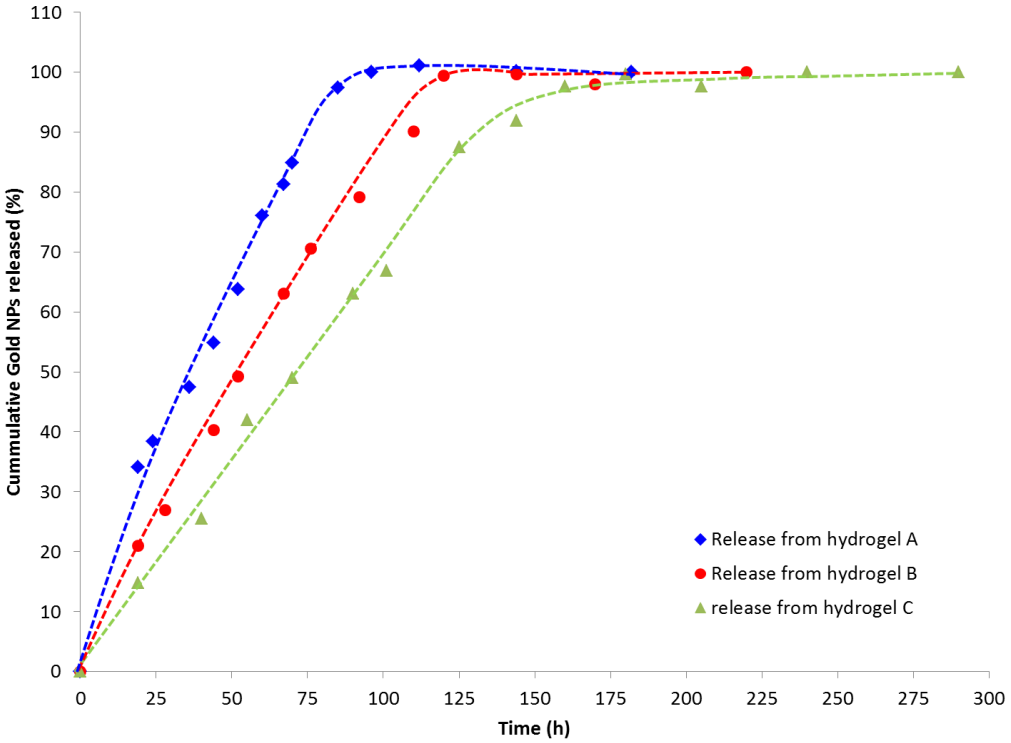

Figure 5.6 Released profile of PDMA-grafted gold nanoparticles (PDMA-AuNPs) from the hydrogels.

Figure 5.6 showed that, under same condition, the release rates of PDMA-AuNPs from gels A, B and C were different. The more DMAEA units resulted in the faster release rates of AuNPs. This result suggests that the release rate of AuNPs can be regulated by the amount of DMAEA component. The time taken to completely release the AuNPs from hydrogels A, B, and C were 72 h, 115 h, and 163 h, respectively (Table 5.4). The release time relatively correlated with the degradation time of hydrogels (without loading PDMA-AuNPs) presented in Table 5.2. This result confirms that the polymer is fully degraded and is completely in solution.

Table 5.4 The release time of PDMA-grafted gold NPs from the hydrogels.

Polymer code	Release time of PDMA-AuNPs (h)[a]
A	72
B	115
C	163

[a]The release of PDMA-AuNPs from hydrogels was determined by UV-vis for three repetitive samples.

The release profiles once again proved that the erosion of the hydrogels initially occurred on the top layer and then gradually invaded to the successive layers. When the polymer layer at the interphase

of hydrogel and water were hydrolysed leading to elevation in the LCST over 37 ^{o}C, the polymer became soluble, allowing the PDMA-AuNPs to diffuse out of the gel. However, the release profiles may be different when thin film hydrogels or microgels are produced from these copolymers.

5.4 Conclusion

We have developed a hydrogel system from injectable thermoresponsive random copolymer P(NIPAM-co-DMAEA-co-PEGMEA-co-BA) with a non-triggerred release characteristic. The copolymer solutions transitioned from sol state at below 37 ^{o}C to opaque gel state at 37 ^{o}C. The hydrogels were formed without syneresis. The hydrogels degraded over time due to self-catalysed hydrolysis of the PDMAEA side chains. Furthermore, the degradation time of the hydrogel can be controlled by varying the number of DMAEA units. The gelation temperature of the copolymers increased with higher DMAEA content resulting in shorter degradation times of the gels. PDMA functionalized gold nanoparticles (PDMA-AuNPs) were employed as a model drug to investigate drug loading and release from the hydrogels. The release of PDMA-AuNPs from the hydrogels was quite effective. Furthermore, the release profile indicates that the hydrogels were able to load and gradually release the gold nanoparticles at different rates through their different degradation times. Further investigation into copolymer compositions and types of gels may provide a better understanding of the mechanisms involved in the gels degradation and control over the release of the encapsulated materials.

5.5 References

1. Li, F.; Griffith, M.; Li, Z.; Tanodekaew, S.; Sheardown, H.; Hakim, M.; Carlsson, D. J., Recruitment of multiple cell lines by collagen-synthetic copolymer matrices in corneal regeneration. *Biomaterials* **2005,** 26, (16), 3093-3104.
2. Liu, S. Q.; Tong, Y. W.; Yang, Y.-Y., Incorporation and in vitro release of doxorubicin in thermally sensitive micelles made from poly(N-isopropylacrylamide-co-N,N-dimethylacrylamide)-b-poly(d,l-lactide-co-glycolide) with varying compositions. *Biomaterials* **2005,** 26, (24), 5064-5074.
3. Park, K.-H.; Yun, K., Immobilization of Arg-Gly-Asp (RGD) sequence in a thermosensitive hydrogel for cell delivery using pheochromocytoma cells (PC12). *Journal of Bioscience and Bioengineering* **2004,** 97, (6), 374-377.
4. Fujishige, S.; Kubota, K.; Ando, I., Phase transition of aqueous solutions of poly(N-isopropylacrylamide) and poly(N-isopropylmethacrylamide). *The Journal of Physical Chemistry* **1989,** 93, (8), 3311-3313.
5. Heskins, M.; Guillet, J. E., Solution Properties of Poly(N-isopropylacrylamide). *Journal of Macromolecular Science: Part A - Chemistry* **1968,** 2, (8), 1441-1455.
6. Lee, B. H.; Vernon, B., Copolymers of N-isopropylacrylamide, HEMA-lactate and acrylic acid with time-dependent lower critical solution temperature as a bioresorbable carrier. *Polymer International* **2005,** 54, (2), 418-422.
7. Stile, R. A.; Burghardt, W. R.; Healy, K. E., Synthesis and Characterization of Injectable Poly(N-isopropylacrylamide)-Based Hydrogels That Support Tissue Formation in Vitro. *Macromolecules* **1999,** 32, (22), 7370-7379.
8. Vernon, B.; Kim, S. W.; Bae, Y. H., Thermoreversible copolymer gels for extracellular matrix4. *Journal of Biomedical Materials Research* **2000,** 51, (1), 69-79.
9. Neradovic, D.; Hinrichs, W. L. J.; Kettenes-van den Bosch, J. J.; Hennink, W. E., Poly(N-isopropylacrylamide) with hydrolyzable lactic acid ester side groups: a new type of thermosensitive polymer. *Macromolecular Rapid Communications* **1999,** 20, (11), 577-581.
10. Neradovic, D.; van Nostrum, C. F.; Hennink, W. E., Thermoresponsive Polymeric Micelles with Controlled Instability Based on Hydrolytically Sensitive N-Isopropylacrylamide Copolymers. *Macromolecules* **2001,** 34, (22), 7589-7591.
11. Neradovic, D.; van Steenbergen, M. J.; Vansteelant, L.; Meijer, Y. J.; van Nostrum, C. F.; Hennink, W. E., Degradation Mechanism and Kinetics of Thermosensitive Polyacrylamides Containing Lactic Acid Side Chains. *Macromolecules* **2003,** 36, (20), 7491-7498.
12. Tran, N. T. D.; Truong, N. P.; Gu, W.; Jia, Z.; Cooper, M. A.; Monteiro, M. J., Timed-Release Polymer Nanoparticles. *Biomacromolecules* **2013,** 14, (2), 495-502.
13. Tran, N. T. D.; Jia, Z.; Truong, N. P.; Cooper, M. A.; Monteiro, M. J., Fine Tuning the Disassembly Time of Thermoresponsive Polymer Nanoparticles. *Biomacromolecules* **2013,** 14, (10), 3463-3471.
14. Cho, J. H.; Kim, S.-H.; Park, K. D.; Jung, M. C.; Yang, W. I.; Han, S. W.; Noh, J. Y.; Lee, J. W., Chondrogenic differentiation of human mesenchymal stem cells using a thermosensitive poly(N-isopropylacrylamide) and water-soluble chitosan copolymer. *Biomaterials* **2004,** 25, (26), 5743-5751.
15. Stile, R. A.; Healy, K. E., Thermo-Responsive Peptide-Modified Hydrogels for Tissue Regeneration. *Biomacromolecules* **2001,** 2, (1), 185-194.
16. Stile, R. A.; Healy, K. E., Poly(N-isopropylacrylamide)-Based Semi-interpenetrating Polymer Networks for Tissue Engineering Applications. 1. Effects of Linear Poly(acrylic acid) Chains on Phase Behavior. *Biomacromolecules* **2002,** 3, (3), 591-600.
17. Lin, H.-H.; Cheng, Y.-L., In-Situ Thermoreversible Gelation of Block and Star Copolymers of Poly(ethylene glycol) and Poly(N-isopropylacrylamide) of Varying Architectures. *Macromolecules* **2001,** 34, (11), 3710-3715.

18. Durand, A.; Hourdet, D., Synthesis and thermoassociative properties in aqueous solution of graft copolymers containing poly(N-isopropylacrylamide) side chains. *Polymer* **1999,** 40, (17), 4941-4951.
19. Gong, C.; Qi, T.; Wei, X.; Qu, Y.; Wu, Q.; Luo, F.; Qian, Z., Thermosensitive Polymeric Hydrogels As Drug Delivery Systems. *Current Medicinal Chemistry* **2013,** 20, (1), 79-94.
20. Cui, Z.; Lee, B. H.; Vernon, B. L., New Hydrolysis-Dependent Thermosensitive Polymer for an Injectable Degradable System. *Biomacromolecules* **2007,** 8, (4), 1280-1286.
21. Kim, S.; Chung, E. H.; Gilbert, M.; Healy, K. E., Synthetic MMP-13 degradable ECMs based on poly(N-isopropylacrylamide-co-acrylic acid) semi-interpenetrating polymer networks. I. Degradation and cell migration. *Journal of Biomedical Materials Research Part A* **2005,** 75A, (1), 73-88.
22. Kim, S.; Healy, K. E., Synthesis and Characterization of Injectable Poly(N-isopropylacrylamide-co-acrylic acid) Hydrogels with Proteolytically Degradable Cross-Links. *Biomacromolecules* **2003,** 4, (5), 1214-1223.
23. Sun, L.-F.; Zhuo, R.-X.; Liu, Z.-L., Studies on the Synthesis and Properties of Temperature Responsive and Biodegradable Hydrogels. *Macromol. Biosci.* **2003,** 3, (12), 725-728.
24. Yoshida, T.; Aoyagi, T.; Kokufuta, E.; Okano, T., Newly designed hydrogel with both sensitive thermoresponse and biodegradability. *J Polym Sci Pol Chem* **2003,** 41, (6), 779-787.
25. Jain, R. K.; Stylianopoulos, T., Delivering nanomedicine to solid tumors. *Nat Rev Clin Oncol* **2010,** 7, (11), 653-664.
26. Wong, C.; Stylianopoulos, T.; Cui, J.; Martin, J.; Chauhan, V. P.; Jiang, W.; Popović, Z.; Jain, R. K.; Bawendi, M. G.; Fukumura, D., Multistage nanoparticle delivery system for deep penetration into tumor tissue. *Proceedings of the National Academy of Sciences* **2011,** 108, (6), 2426-2431.
27. Li, Z.; Wang, F.; Roy, S.; Sen, C. K.; Guan, J., Injectable, Highly Flexible, and Thermosensitive Hydrogels Capable of Delivering Superoxide Dismutase. *Biomacromolecules* **2009,** 10, (12), 3306-3316.
28. Henderson, E.; Lee, B. H.; Cui, Z.; McLemore, R.; Brandon, T. A.; Vernon, B. L., In vivo evaluation of injectable thermosensitive polymer with time-dependent LCST. *Journal of Biomedical Materials Research Part A* **2009,** 90A, (4), 1186-1197.
29. Guan, J.; Hong, Y.; Ma, Z.; Wagner, W. R., Protein-Reactive, Thermoresponsive Copolymers with High Flexibility and Biodegradability. *Biomacromolecules* **2008,** 9, (4), 1283-1292.
30. Lee, B. H.; Vernon, B., In Situ-Gelling, Erodible N-Isopropylacrylamide Copolymers. *Macromol. Biosci.* **2005,** 5, (7), 629-635.
31. Truong, N. P.; Jia, Z.; Burges, M.; McMillan, N. A. J.; Monteiro, M. J., Self-Catalyzed Degradation of Linear Cationic Poly(2-dimethylaminoethyl acrylate) in Water. *Biomacromolecules* **2011,** 12, (5), 1876-1882.
32. Truong, N. P.; Jia, Z.; Burgess, M.; Payne, L.; McMillan, N. A. J.; Monteiro, M. J., Self-Catalyzed Degradable Cationic Polymer for Release of DNA. *Biomacromolecules* **2011,** 12, (10), 3540-3548.
33. Urbani, C. N.; Monteiro, M. J., Nanoreactors for Aqueous RAFT-Mediated Polymerizations. *Macromolecules* **2009,** 42, (12), 3884-3886.
34. Monteiro, M. J., Modeling the molecular weight distribution of block copolymer formation in a reversible addition–fragmentation chain transfer mediated living radical polymerization. *Journal of Polymer Science Part A: Polymer Chemistry* **2005,** 43, (22), 5643-5651.
35. Monteiro, M. J., Design strategies for controlling the molecular weight and rate using reversible addition–fragmentation chain transfer mediated living radical polymerization. *Journal of Polymer Science Part A: Polymer Chemistry* **2005,** 43, (15), 3189-3204.
36. York, A. W.; Kirkland, S. E.; McCormick, C. L., Advances in the synthesis of amphiphilic block copolymers via RAFT polymerization: Stimuli-responsive drug and gene delivery. *Advanced Drug Delivery Reviews* **2008,** 60, (9), 1018-1036.

37. Moad, G.; Rizzardo, E.; Thang, S. H., Living Radical Polymerization by the RAFT Process – A Third Update. *Australian Journal of Chemistry* **2012,** 65, (8), 985-1076.
38. Klumperman, B.; van den Dungen, E. T. A.; Heuts, J. P. A.; Monteiro, M. J., RAFT-Mediated Polymerization—A Story of Incompatible Data? *Macromolecular Rapid Communications* **2010,** 31, (21), 1846-1862.
39. Boyer, C.; Bulmus, V.; Davis, T. P.; Ladmiral, V.; Liu, J.; Perrier, S., Bioapplications of RAFT Polymerization. *Chemical Reviews* **2009,** 109, (11), 5402-5436.
40. Fan, R.; Deng, X.; Zhou, L.; Gao, X.; Fan, M.; Wang, Y.; Guo, G., Injectable thermosensitive hydrogel composite with surface-functionalized calcium phosphate as raw materials. *Int. J. Nanomedicine* **2014,** 9, 615-626.
41. Fu, S.; Guo, G.; Gong, C.; Zeng, S.; Liang, H.; Luo, F.; Zhang, X.; Zhao, X.; Wei, Y.; Qian, Z., Injectable Biodegradable Thermosensitive Hydrogel Composite for Orthopedic Tissue Engineering. 1. Preparation and Characterization of Nanohydroxyapatite/Poly(ethylene glycol)−Poly(ε-caprolactone)−Poly(ethylene glycol) Hydrogel Nanocomposites. *The Journal of Physical Chemistry B* **2009,** 113, (52), 16518-16525.
42. Wang, T.; Wu, D.-Q.; Jiang, X.-J.; Zhang, X.-Z.; Li, X.-Y.; Zhang, J.-F.; Zheng, Z.-B.; Zhuo, R.; Jiang, H.; Huang, C., Novel thermosensitive hydrogel injection inhibits post-infarct ventricle remodelling. *Eur. J. Heart Fail.* **2009,** 11, (1), 14-19.
43. Wang, F.; Li, Z.; Khan, M.; Tamama, K.; Kuppusamy, P.; Wagner, W. R.; Sen, C. K.; Guan, J., Injectable, rapid gelling and highly flexible hydrogel composites as growth factor and cell carriers. *Acta Biomaterialia* **2010,** 6, (6), 1978-1991.
44. Lee, B. H.; Song, S.-C., Synthesis and Characterization of Biodegradable Thermosensitive Poly(organophosphazene) Gels. *Macromolecules* **2004,** 37, (12), 4533-4537.
45. Soga, O.; van Nostrum, C. F.; Hennink, W. E., Poly(N-(2-hydroxypropyl) Methacrylamide Mono/Di Lactate): A New Class of Biodegradable Polymers with Tuneable Thermosensitivity. *Biomacromolecules* **2004,** 5, (3), 818-821.
46. Neradovic, D.; Van Nostrum, C.; Hennink, W., Thermoresponsive polymeric micelles with controlled instability based on hydrolytically sensitive N-isopropylacrylamide copolymers. *Macromolecules* **2001,** 34, (22), 7589-7591.
47. Liang, M.; Lin, I. C.; Whittaker, M. R.; Minchin, R. F.; Monteiro, M. J.; Toth, I., Cellular Uptake of Densely Packed Polymer Coatings on Gold Nanoparticles. *ACS Nano* **2009,** 4, (1), 403-413.
48. Lowe, A. B.; Sumerlin, B. S.; Donovan, M. S.; McCormick, C. L., Facile Preparation of Transition Metal Nanoparticles Stabilized by Well-Defined (Co)polymers Synthesized via Aqueous Reversible Addition-Fragmentation Chain Transfer Polymerization†. *J. Am. Chem. Soc.* **2002,** 124, (39), 11562-11563.
49. Yusa, S.-i.; Fukuda, K.; Yamamoto, T.; Iwasaki, Y.; Watanabe, A.; Akiyoshi, K.; Morishima, Y., Salt Effect on the Heat-Induced Association Behavior of Gold Nanoparticles Coated with Poly(N-isopropylacrylamide) Prepared via Reversible Addition−Fragmentation Chain Transfer (RAFT) Radical Polymerization. *Langmuir* **2007,** 23, (26), 12842-12848.
50. Toyoshima, M.; Miura, Y., Preparation of glycopolymer-substituted gold nanoparticles and their molecular recognition. *J Polym Sci Pol Chem* **2009,** 47, (5), 1412-1421.
51. Fustin, C.-A.; Colard, C.; Filali, M.; Guillet, P.; Duwez, A.-S.; Meier, M. A. R.; Schubert, U. S.; Gohy, J.-F., Tuning the Hydrophilicity of Gold Nanoparticles Templated in Star Block Copolymers. *Langmuir* **2006,** 22, (15), 6690-6695.
52. Duwez, A.-S.; Guillet, P.; Colard, C.; Gohy, J.-F.; Fustin, C.-A., Dithioesters and Trithiocarbonates as Anchoring Groups for the "Grafting-To" Approach. *Macromolecules* **2006,** 39, (8), 2729-2731.
53. Hotchkiss, J. W.; Lowe, A. B.; Boyes, S. G., Surface Modification of Gold Nanorods with Polymers Synthesized by Reversible Addition−Fragmentation Chain Transfer Polymerization. *Chem. Mater.* **2006,** 19, (1), 6-13.

54. Merican, Z.; Schiller, T. L.; Hawker, C. J.; Fredericks, P. M.; Blakey, I., Self-Assembly and Encoding of Polymer-Stabilized Gold Nanoparticles with Surface-Enhanced Raman Reporter Molecules. *Langmuir* **2007,** 23, (21), 10539-10545.

Chapter 6

Summary

The main objective of the work described in this thesis was to synthesize and study novel timed-release polymeric micelles and hydrogels based on thermoresponsive PNIPAM and self-degradable PDMAEA. In particular, the efforts was put towards the understanding of the self-assembly and self-disassembly characteristic of thermoresponsive PNIPAM in the presence of self-degradable components and other factors such as hydrophilic and hydrophobic contents as well as surfactants. Such understanding established some general design principles to serve as guidelines for developing the next generation of nanocarriers with controllable timed-release characteristics.

6.1 Novel timed-release polymer nanoparticles with controllable disassembly time.

The first step towards meeting the overall goals of the project, thermoresponsive PNIPAM and self-degradable PDMAEA were combined with hydrophobic polymers to regulate the LCST and disassembly time of thermoresponsive PNIPAM, and thus control the release time of oligo DNA (i.e., a mimic of siRNA) from the polymer complex. Reversible addition-fragmentation chain transfer (RAFT) polymerization was employed to synthesize the diblock thermoresponsive copolymers which consisted of a hydrophilic block (e.g., PDMA) for stabilization and a second thermoresponsive block with three components (e.g., NIPAM, DMAEA, and BA or Styrene) for self-assembly and disassembly. The copolymers were fully water-soluble below LCST and self-assembled into approximately 25-nm nanoparticles with very narrow particle size distribution, measured by Dynamic Light Scattering (DLS), above the LCST (e.g., 37 ^{o}C). The polymer nanoparticles can sharply disassembled to unimers ~5 nm (i.e., the core of the copolymer became water soluble) when the amount of negatively charged poly (acrylic acid) (PAA) that transformed from the self-catalytic degradation of cationic PDMAEA was sufficiently high to increase the LCST of the copolymers above 37 °C. These nanoparticles excellently bound to oligo DNA through ionic interactions without any leakage and released through the ionic repulsion after full degradation of the polymers or sharp disassembly of the nanoparticles. Interestingly, the disassembly time of the nanoparticles and consequently the release time of oligo DNA could be precisely controlled. These particles could be easily modified with folic acid to enhance cellular uptake by osteosarcoma cells.

6.2 The effect of copolymers components and surfactants on timed-release nanoparticles

The next step is to understand the effect of hydrophilic and self-hydrolysis DMAEA components as well as hydrophobic components on the timed-release nanoparticles. The disassembly time (t_{start}) and time from the start of disassembly to full unimer formation ($t_{degrade}$) of the polymer

nanoparticles could be controlled by manipulating the number of self-degradable DMAEA units and hydrophobic BA units in the copolymer. Increasing BA units resulted in longer t_{start} while adding more DMAEA units made the $t_{degrade}$ shorter. The self-catalysed hydrolysis of the PDMAEA side groups to acrylic acid groups increased the LCST of the polymer to over 37 ^{o}C over time and was postulated as the mechanism of degradation of PDMAEA. In addition, the polymer could be designed to self-assemble into nanoparticles over a wide range of pHs and disassemble to unimers below a pH of 7.3. The polymer nanoparticles have potential for application in drug and gene delivery where one or more therapeutic agents can be released at desired times.

The stabilization and self-disassembly of large thermoresponsive particles self-assembled from the random copolymer of thermoresponsive PNIPAM, hydrophobic PBA or PSTY and self-catalytic degradation PDMAEA were further investigated in the presence of surfactant. The random copolymers (P(NIPAM-co-DMAEA-co-BA) and P(NIPAM-co-DMAEA-co-STY)) were synthesized via one-pot RAFT polymerization. The polymers could self-assemble into large nanoparticles with very narrow size distribution demonstrated a well stabilization as provided by SDS. Interestingly, the polymer particle size increased with the increase in SDS concentration, and these nanoparticles were stable upon intensive dilution. Moreover, the LCST of the polymers were controlled by not only the polymers composition (i.e., lower hydrophobic segment in the copolymers resulted in higher LCST) but also the concentration of the SDS. An increase in the amount of SDS resulted in higher number of hydrophobic interactions between the SDS and PNIPAM molecules, and hence the LCST of copolymers were also raised. Additionally, the self-degradation of DMAEA as well as the self-disassembly characteristic of the polymer nanoparticles were not influenced by the SDS. The polymer nanoparticles sharply disassembled to unimers when the LCST of the polymer elevated to above the conducting temperature (e.g., 37 ^{o}C).

6.3 Novel self-degradable hydrogel

In the final step of this thesis, self-degradable polymeric hydrogel from random copolymers of thermoresponsive PNIPAM self-catalytic degradation PDMAEA, hydrophilic PEGMEA, and hydrophobic PBA were designed based on the understanding of controllably timed-release polymer nanoparticles. The three copolymers were also synthesized via RAFT polymerization with varying the initial concentration of monomer DMAEA in the reactions and keeping the concentration of the other reactants (i.e., NIPAM, PEGMEA, and BA) constant. The compositions of obtained copolymers were also controllable in which the units of NIPAM, PEGMEA, and BA were similar for the three copolymers, and the variation in the units of DMAEA for the three polymers was consistent with that in the initial composition added to the three polymerizations. The thermoresponsive copolymers could form stable gel at the temperatures higher than the gelation

point (e.g., 37 ^{o}C) and then self-degraded into sol state after different times without the need of any triggers. Moreover, there was a dependence of gelation temperature as well as degradation time on the number of DMAEA units. Higher DMAEA units in the copolymer resulted in higher gelation temperature and faster degradation time. To test the encapsulation and release ability of the hydrogels, the gold nanoparticles coated with PDMA (PDMA-AuNPs) were chosen as a model. The encapsulated PDMA-AuNPs gradually released at different rates through the degradation of the hydrogels. These results suggest that this novel non-triggered release hydrogel has promising potential in applications where controlled-release is beneficial.

Appendix A

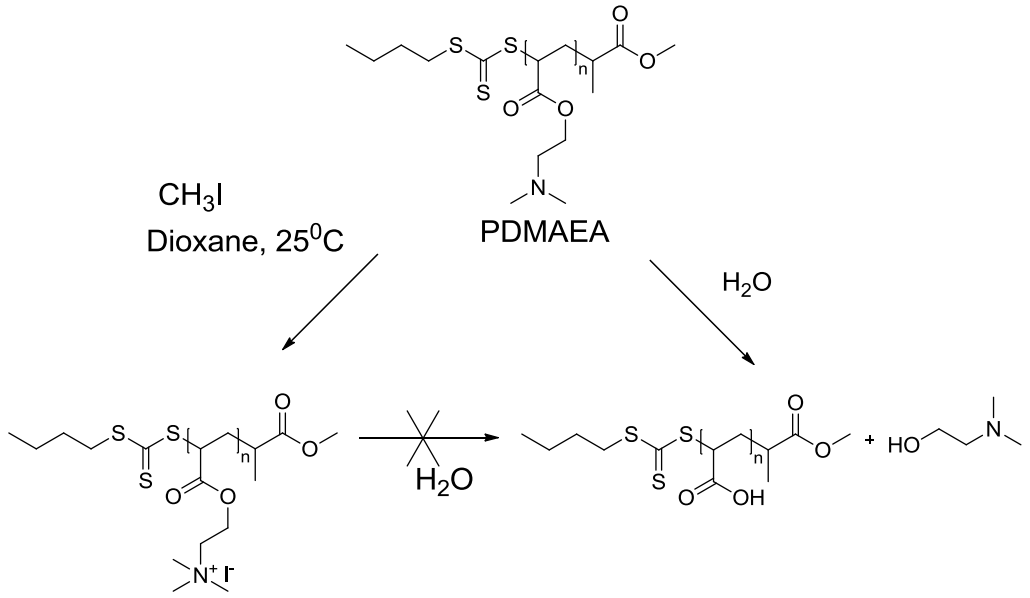

Scheme A2.1. Self-catalyzed hydrolysis of Poly(2-dimethylaminoethyl acrylate).

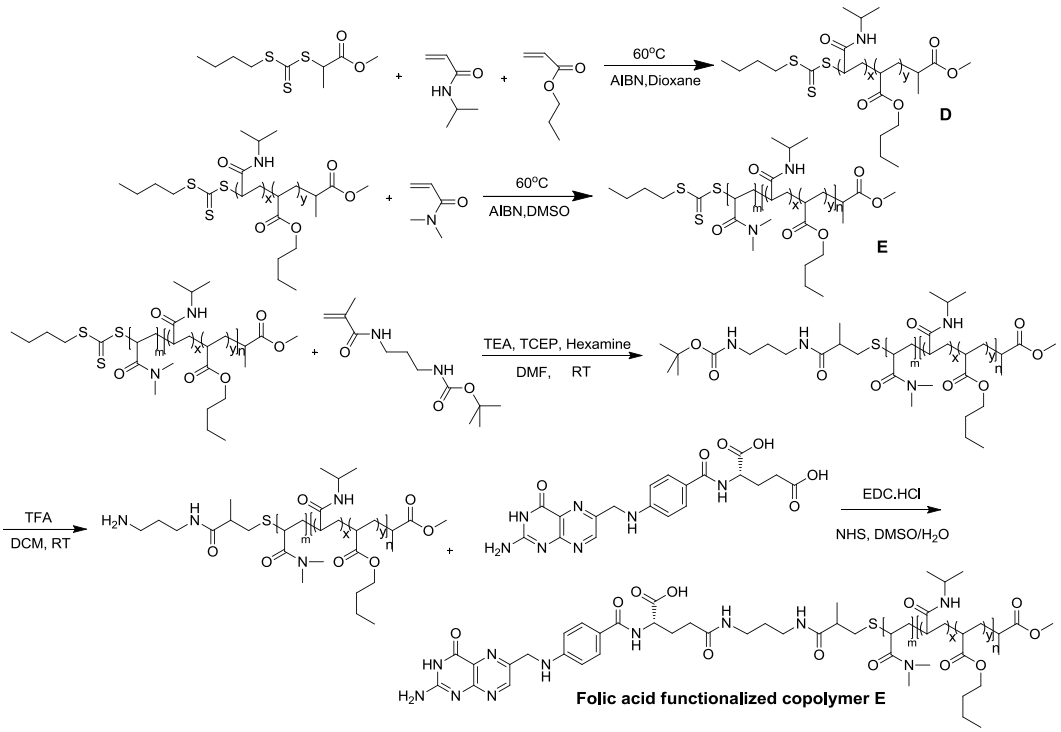

Scheme A2.2 Synthesis of folic acid functional copolymer E

Table A2.1 Molecular weights, polydispersities (PDI), and ^{1}H NMR data of RAFT polymerization of thermo responsive block copolymers at 60 ^{o}C in Dioxane.

Polymer code [a]		SEC[b]				^{1}H NMR					
		RI		Triple detection[c]		Repeating units				M_n[i]	Percentage of BA or STY (%)[k]
		M_n	PDI	M_n	M_w	NIPAM[d]	DMAEA	BA[e]	STY[f]		
A	P(DMA_{96}-b-($NIPAM_{87}$-co-$DMAEA_{25}$))	34500	1.23	23800	24000	87	25[g]	-	-	23175	-
B1	P(DMA_{96}-b-($NIPAM_{88}$-co-$DMAEA_{25}$-co-BA_6))	36200	1.24	28500	28900	88	25[h]	6	-	24057	5.04
B2	P(DMA_{96}-b-($NIPAM_{91}$-co-$DMAEA_{25}$-co-BA_{12}))	36700	1.26	24000	24300	91	25[h]	12	-	25165	9.38
C1	P(DMA_{96}-b-($NIPAM_{84}$-co-$DMAEA_{22}$-co-STY_5))	34300	1.32	24800	25700	84	22[g]	-	5	22927	4.50
C2	P(DMA_{96}-b-($NIPAM_{40}$-co-$DMAEA_{15}$-co-STY_{13}))	24700	1.27	24100	24900	40	15[g]	-	13	17786	19.11

[a] PDMA (Macro-CTA) with repeating unit = 96; Mn = 9769 calculated from ^{1}H NMR. [b] SEC data measured in DMAc solution with 0.03 wt% of LiCl and using PSTY standards for calibration.[c] Triple detection data measured based on the dn/dc calculated from the polymers' concentration.[d] Repeating units of NIPAM (N_{NIPAM}) determined by ^{1}H NMR were calculated based on 96 repeating unit of Macro-CTA by the integral area of a peak at 1.08 ppm ($I_{1.08}$) and a peak in the range 2.85-3.07 ppm ($I_{2.85\text{-}3.07}$) using the following equation: $N_{NIPAM} = 96 \times I_{1.08} / I_{2.85\text{-}3.07}$.[e] Repeating units of BA (N_{BA}) determined by ^{1}H NMR were calculated based on 96 repeating unit of Macro-CTA by the integral area of a peak at 0.88 ppm ($I_{1.08}$) and a peak in the range 2.85-3.07 ppm ($I_{2.85\text{-}3.07}$) using the following equation: $N_{BA} = (96 \times 2 \times I_{0.88} / I_{2.85\text{-}3.07}) - 1$.[f] Repeating units of STY (N_{STY}) determined by ^{1}H NMR were calculated based on 96 repeating unit of Macro-CTA and the N_{NIPAM} by the integral area of the peak in the range 6.20-7.18 ppm ($I_{6.20\text{-}7.18}$) and the peak in the range 2.85-3.07 ppm ($I_{2.85\text{-}3.07}$) using the following equation: $N_{STY} = [(96 \times 6 \times I_{6.20\text{-}7.18})/I_{2.85\text{-}3.07} - N_{NIPAM}]/5$.[g] Repeating units of DMAEA (N_{DMAEA}) determined by ^{1}H NMR were calculated based on 96 repeating unit of Macro-CTA and the N_{NIPAM} by the integral area of the peak in the range 2.85-3.07 ppm ($I_{2.85\text{-}3.07}$) and the peak in the range 3.95-4.30 ppm ($I_{3.95\text{-}4.30}$) using the following equation: $N_{DMAEA} = [(96 \times 6 \times I_{3.95\text{-}4.30} / I_{2.85\text{-}3.07}) - N_{NIPAM}]/2$.[h] Repeating units of DMAEA (N_{DMAEA}) determined by ^{1}H NMR were calculated based on 96 repeating unit of Macro-CTA, and the N_{NIPAM} and N_{BA} by the integral area of the peak in the range 2.85-3.07 ppm ($I_{2.85\text{-}3.07}$) and the peak in the range 3.95 - 4.30 ppm ($I_{3.95\text{-}4.30}$) using the following equation: $N_{DMAEA} = [(96 \times 6 \times I_{3.95\text{-}4.30}/I_{2.85\text{-}3.07}) - (N_{NIPAM} + 2\ N_{BA})]/2$

[i] Molecular weight determined by ^{1}H NMR were calculated based on the repeating units of N_{NIPAM}, N_{BA} or N_{STY} ,N_{DMAEA}, and the molecular weight of macro-CTA: Mn = (N_{NIPAM} x 113) + (N_{BA} x 128.2) or (N_{STY} x 104) + (N_{DMAEA} x 143) + 9769.[k] Percentages of BA or STY were calculated based on N_{DMAEA} ,N_{NIPAM} ,N_{BA} or N_{STY}: Percentage of BA = $N_{BA}/(N_{DMAEA} + N_{NIPAM} + N_{BA})$ and percentage of STY = $N_{STY}/(N_{DMAEA} + N_{NIPAM} + N_{STY})$.

Table A2.2 Hydrodynamic diameter (D_h), Polydispersities (PDIs) of thermoresponsive block copolymers / Oligo DNA 9-27 complexes in Milli-Q water at N/P Ratio 0.5, 1, 2, 5, and 10 with 1 μg DNA. Measurements were carried out on DLS machine.

N/P ratio	Complexed polymers B1/oligo DNA at 37 ^oC		Complexed polymers B2/oligo DNA at 37 ^oC		Complexed polymers C1/oligo DNA at 37 ^oC		Complexed polymers C2/oligo DNA at 37 ^oC	
	D_h (nm)	PDI	D_h (nm)	PDI	D_h (nm)	PDI	D_h (nm)	PDI
0.5	30.33 ± 6.58	0.413	27.16 ± 2.14	0.356	11.10 ± 1.01	0.453	17.20 ± 4.29	0.389
1	29.49 ± 3.44	0.337	27.35 ± 1.23	0.218	24.03 ± 1.07	0.400	24.53 ± 0.86	0.243
2	14.75 ± 4.24	0.450	24.21 ± 0.24	0.240	9.021 ± 2.40	0.430	24.20 ± 1.33	0.361
5	17.72 ± 8.74	0.488	25.56 ± 0.70	0.168	8.872 ± 2.74	0.560	23.75 ± 0.58	0.214
10	27.21 ± 0.20	0.048	29.12 ± 1.02	0.071	29.27 ± 0.69	0.080	20.76 ± 0.54	0.110

B1: P(DMA_{96}-b-($NIPAM_{88}$-co-$DMAEA_{25}$-co-BA_6)), **B2:** P(DMA_{96}-b-($NIPAM_{91}$-co-$DMAEA_{25}$-co-BA_{12})), **C1:** P(DMA_{96}-b-($NIPAM_{84}$-co-$DMAEA_{22}$-co-STY_5)), **C2:** P(DMA_{96}-b-($NIPAM_{40}$-co-$DMAEA_{15}$-co-STY_{13})). Data were reported as soluble polymers in Milli-Q water were incubated with DNA at N/P Ratio 0.5, 1, 2, 5, and 10 at below their LCST for 30 min prior to be measured at 37 ^oC on DLS machines. Data were reported as an average of five measurements. The mean standard of deviation of polymer particle sizes was calculated from five measurements.

Table A2.3 Molecular weights, polydispersities (PDI), and ^{1}H NMR data of RAFT polymerization of thermo responsive random/block copolymers at 60 ^{o}C.

Polymer code		SEC[a]				^{1}H NMR			
		RI		Triple detection[b]		Repeating units			M_n
		M_n	PDI	M_n	M_w	NIPAM[c]	BA[d]	DMA[e]	
D	P(NIPAM$_{97}$-co-BA$_{13}$)	28700	1.16	15900	16100	97	13	-	12880[f]
E	P(DMA$_{99}$-b-(NIPAM$_{97}$-co- BA$_{13}$))	38500	1.19	26900	27200	-	-	99	22694[g]

[a] SEC data measured in DMAc solution with 0.03 wt% of LiCl and using PSTY standards for calibration.

[b] Triple detection data measured based on the dn/dc calculated from the polymers' concentration.

[c] Repeating units of NIPAM (N_{NIPAM}) determined by ^{1}H NMR were calculated by the integral area of a peak at 1.12 ppm ($I_{1.12}$) and a peak at 3.64 ppm ($I_{3.64}$) using the following equation: $N_{NIPAM} = I_{1.12} /(2 \times I_{3.64})$

[d] Repeating units of BA (N_{BA}) determined by ^{1}H NMR were calculated by the integral area of a peak at 0.89 ppm ($I_{0.89}$) and a peak at 3.64 ppm ($I_{3.64}$) using the following equation: $N_{BA} = (I_{0.89} / I_{3.64}) - 1$

[e] Repeating units of DMA (N_{DMA}) determined by ^{1}H NMR were calculated based on N_{BA} by the integral area of the peak in the range 2.86-3.07 ppm ($I_{2.86\text{-}3.07}$) and the peak at 0.89 ppm ($I_{0.89}$) using the following equation: $N_{DMA} =[((N_{BA} + 3) \times I_{2.86\text{-}3.07})/(I_{0.89} \times 6)]$

[f] Molecular weight determined by ^{1}H NMR were calculated based on the repeating units of N_{NIPAM}, N_{BA} and the molecular weight of MCEBTTC: $Mn = (N_{NIPAM} \times 113) + (N_{BA} \times 128.2) + 252.42$

[g] Molecular weight determined by ^{1}H NMR were calculated based on the repeating units of N_{DMA} and the molecular weight of macro-CTA: $Mn = (N_{DMA} \times 99.131) + 12880$.

Table A2.4 Lower critical solution temperature (LCST), hydrodynamic diameter (D_h), Polydispersities (PDI) for thermoresponsive block copolymers (E) and conjugation of (aminopropyl)methacrylamide-click-PDMA-b-P(NIPAM-co-BA) and folic acid (H) determined by dynamic light scattering (DLS).

Polymer code	DLS		
	LCST (^oC)[a]	D_h (nm)[b]	PDI[b]
E	13 – 15	33.83 ± 0.65	0.017
H	15 – 19	31.66 ± 0.98	0.089

[a]LCST determined by DLS (10 mg/mL)

[b]Hydrodynamic diameter (D_h) and Polydispersity (PDI) determined by DLS (10 mg/mL) at 37 ^{o}C.

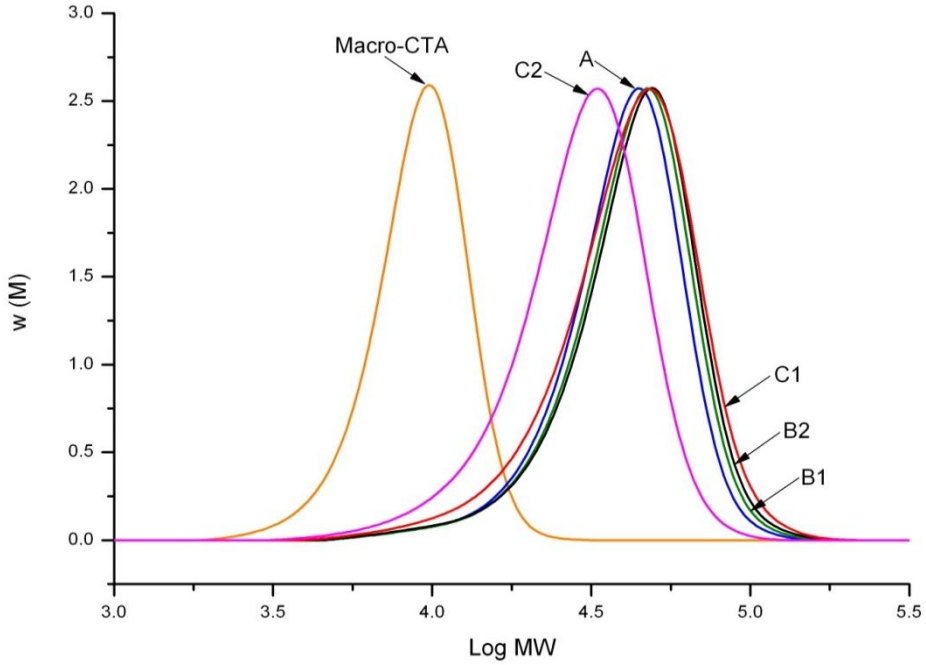

Figure A2.1 Size Exclusion Chromatography (SEC) traces of macro CTA; $PDMA_{96}$, A; P(DMA_{96}-b-($NIPAM_{87}$-co-$DMAEA_{25}$)), B1; P(DMA_{96}-b-($NIPAM_{88}$-co-$DMAEA_{25}$-co-BA_6)), B2; P(DMA_{96}-b-($NIPAM_{91}$-co-$DMAEA_{25}$-co-BA_{12})), C1; P(DMA_{96}-b-($NIPAM_{84}$-co-$DMAEA_{22}$-co-STY_5)), C2; P(DMA_{96}-b-($NIPAM_{40}$-co-$DMAEA_{15}$-co-STY_{13})). The data were measured by DMAc SEC. The intensity for different distribution curves was normalized.

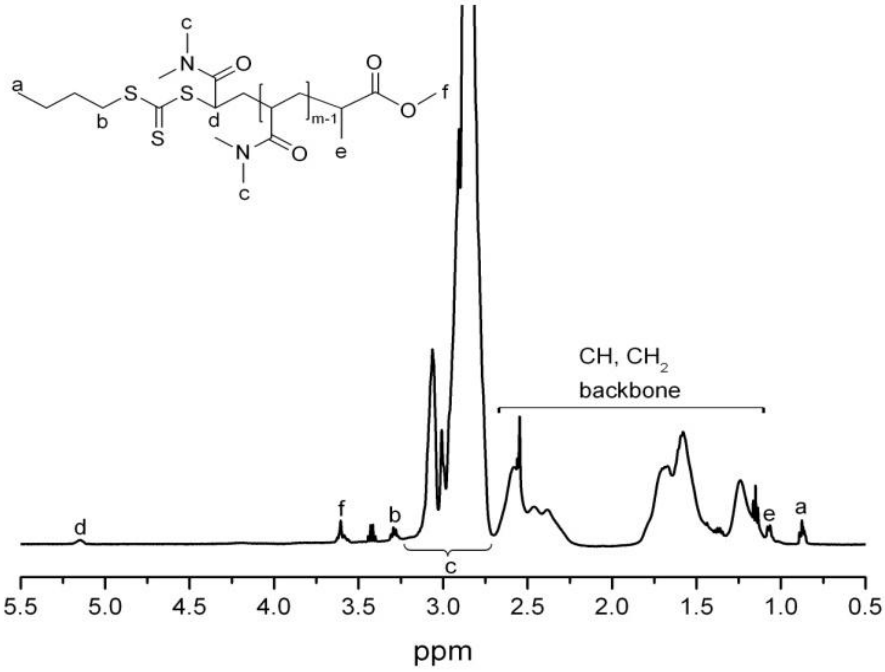

Figure A2.2 ^{1}H NMR spectrum of Macro-CTA: $PDMA_{96}$ in $CDCl_3$.

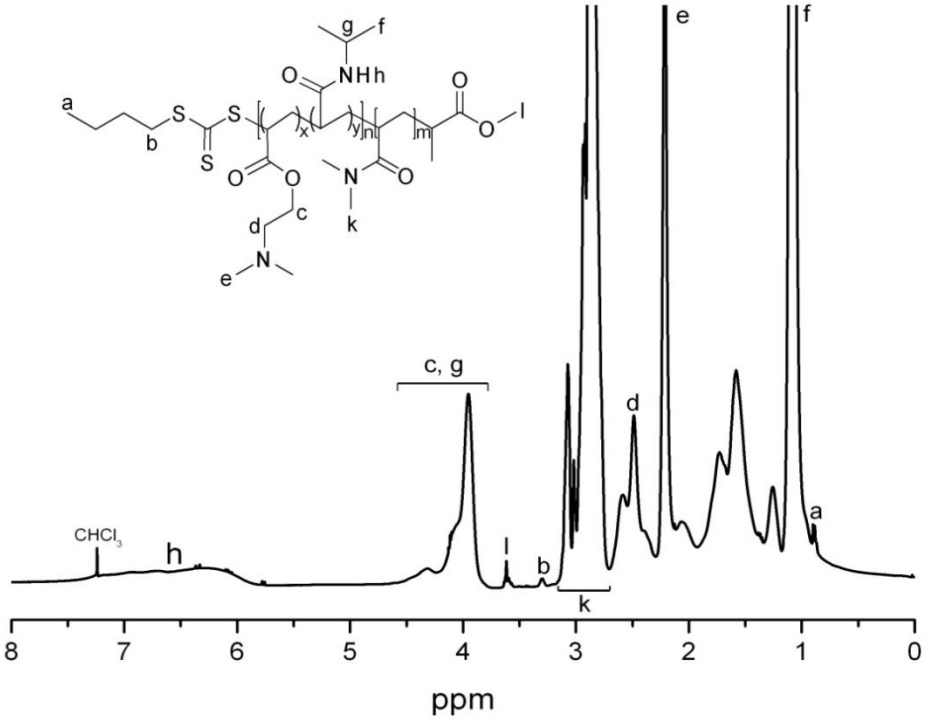

Figure A2.3 ^{1}H NMR spectrum of A: P(DMA_{96}-b-($NIPAM_{87}$-co-$DMAEA_{25}$)) in $CDCl_3$.

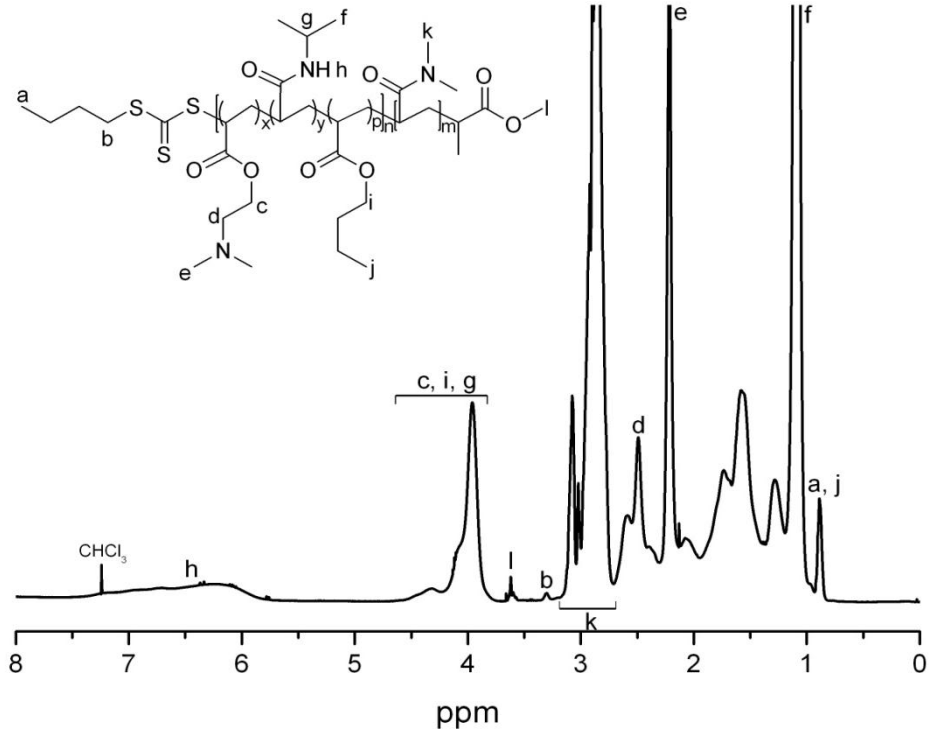

Figure A2.4 ^{1}H NMR spectrum of B1: P(DMA_{96}-b-($NIPAM_{88}$-co-$DMAEA_{25}$-co-BA_6)) in $CDCl_3$.

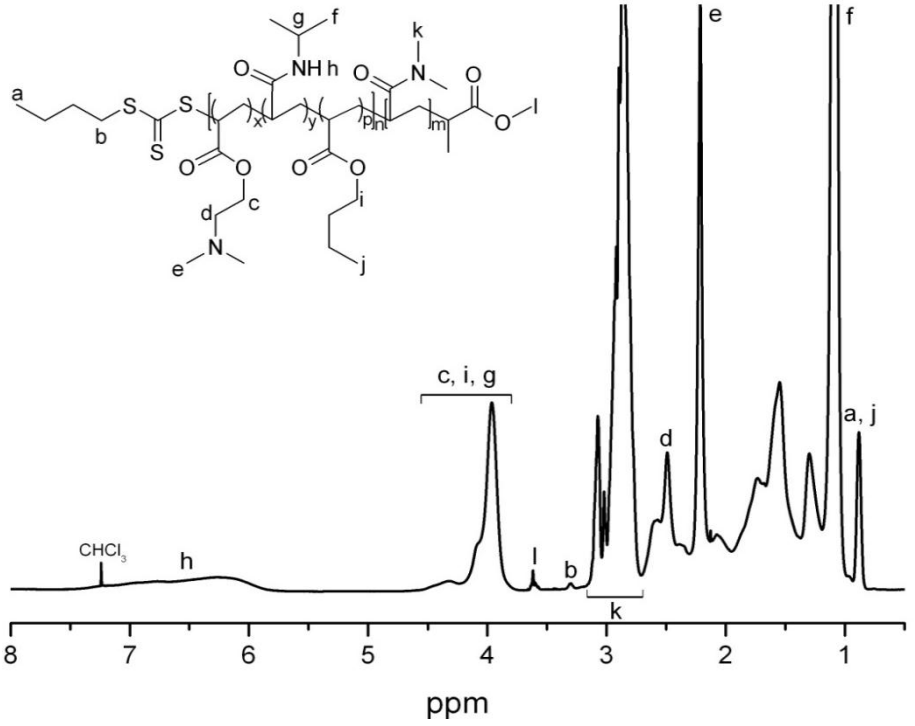

Figure A2.5 ^{1}H NMR spectrum of B2: P(DMA_{96}-b-($NIPAM_{91}$-co-$DMAEA_{25}$-co-BA_{12})) in $CDCl_3$.

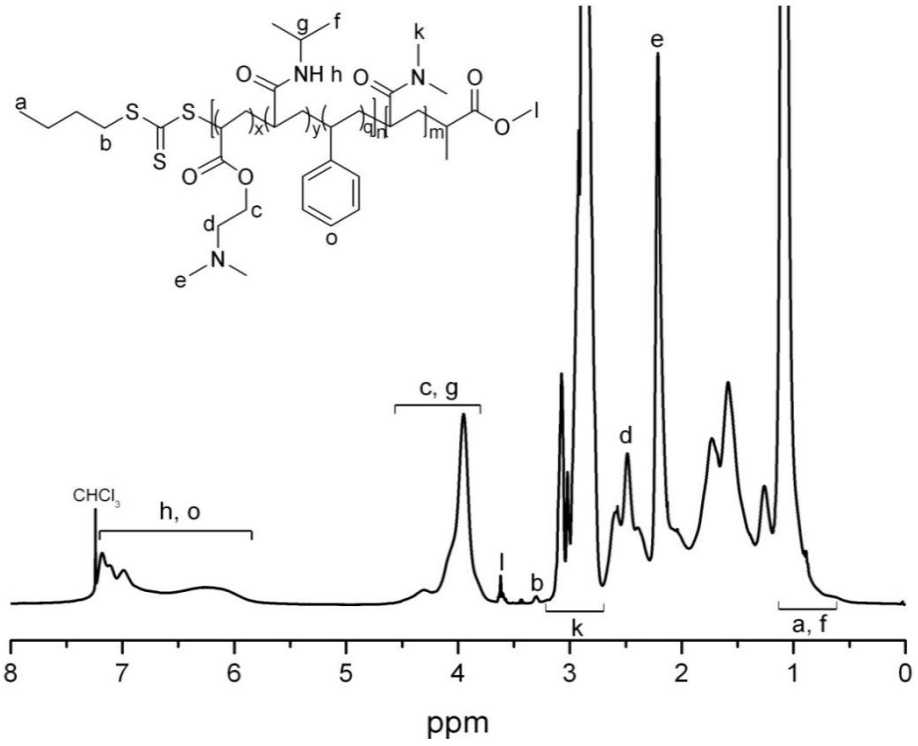

Figure A2.6 ^{1}H NMR spectrum of C1: P(DMA_{96}-b-($NIPAM_{84}$-co-$DMAEA_{22}$-co-STY_5)) in $CDCl_3$.

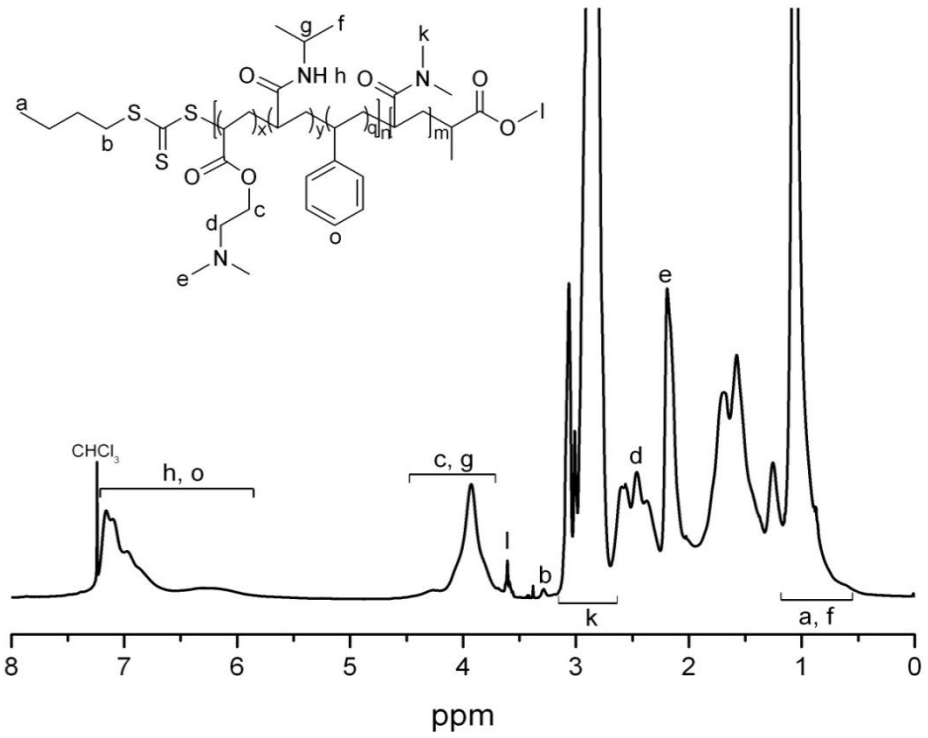

Figure A2.7 ^{1}H NMR spectrum of C2: P(DMA_{96}-b-($NIPAM_{40}$-co-$DMAEA_{15}$-co-STY_{13})) in $CDCl_3$.

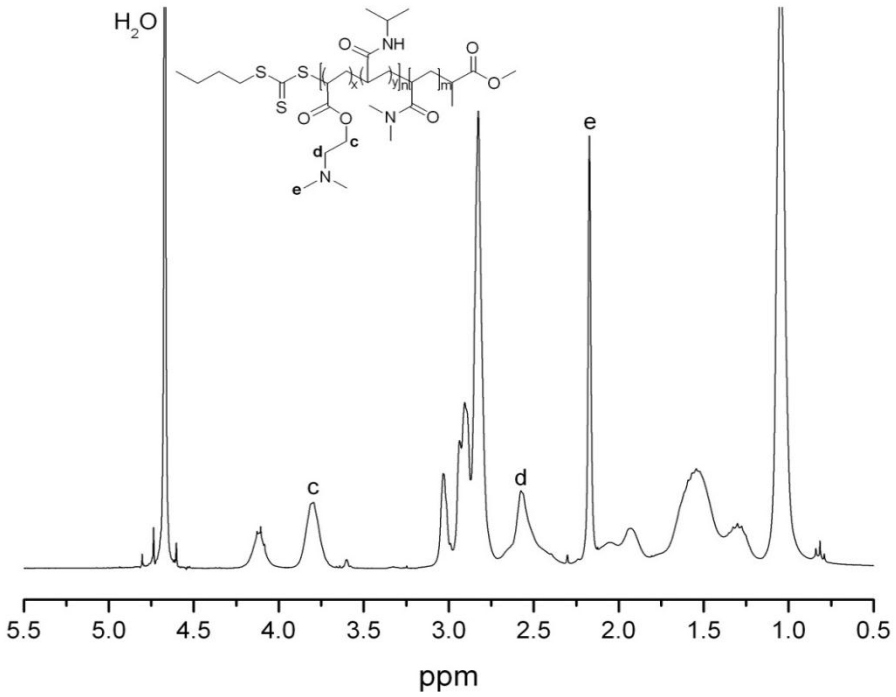

Figure A2.8 ^{1}H NMR spectrum of A: P(DMA_{96}-b-($NIPAM_{87}$-co-$DMAEA_{25}$)) after being dissolved in D_2O and immediately measured at 25 ^{o}C.

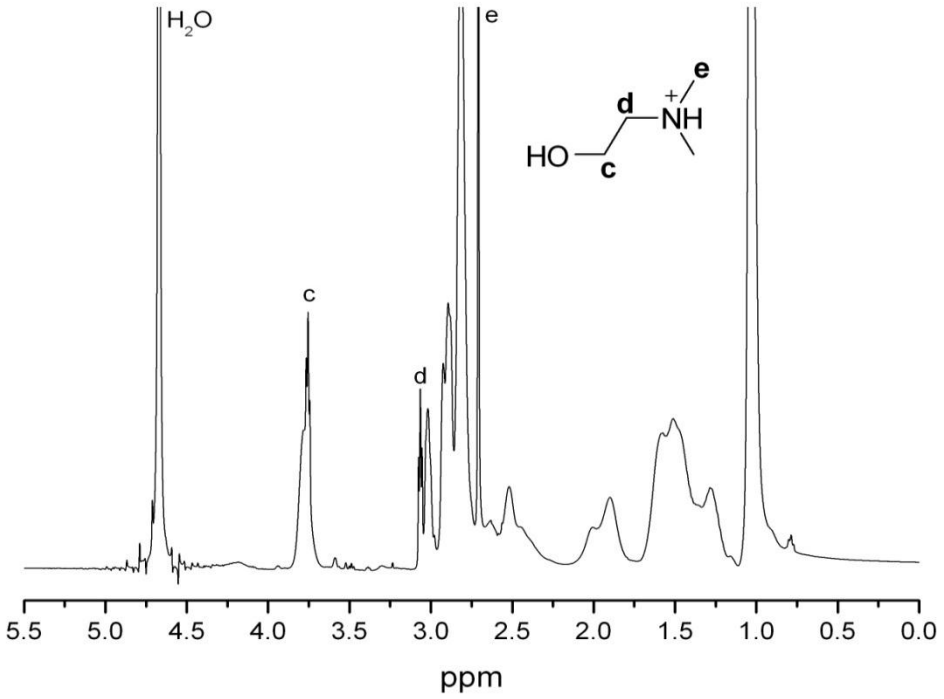

Figure A2.9 ^{1}H NMR spectrum of A; P(DMA$_{96}$-b-(NIPAM$_{87}$-co-DMAEA$_{25}$)) after being dissolved and kept in D_2O for 80 h. The spectrum was measured at 25 ^{o}C.

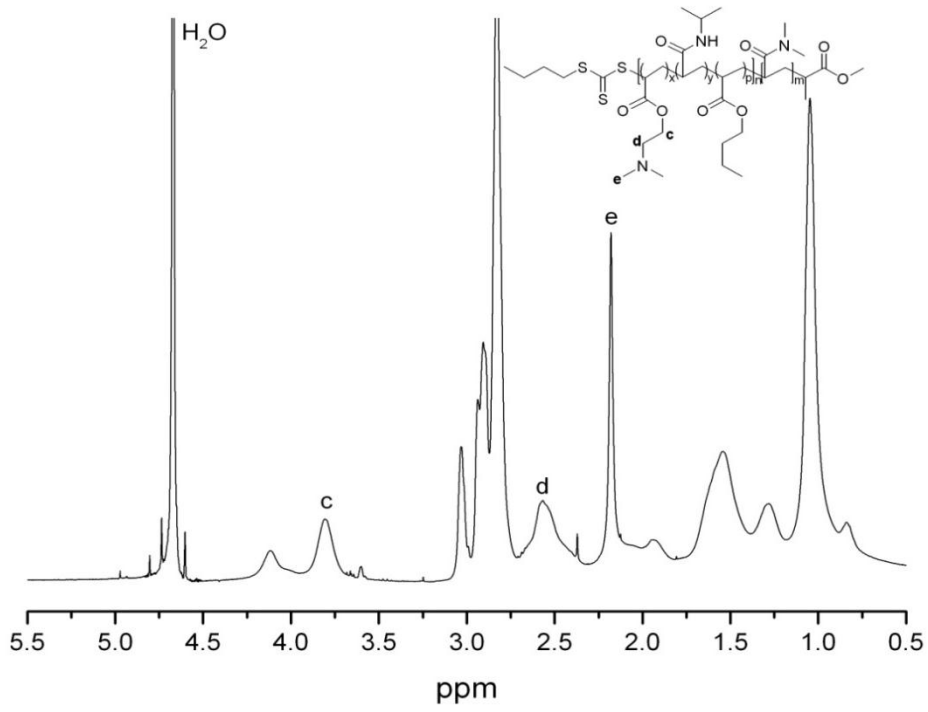

Figure A2.10 ^{1}H NMR spectrum of B1: P(DMA$_{96}$-b-(NIPAM$_{88}$-co-DMAEA$_{25}$-co-BA$_{6}$)) after being dissolved in D_2O and immediately measured at 25 ^{o}C.

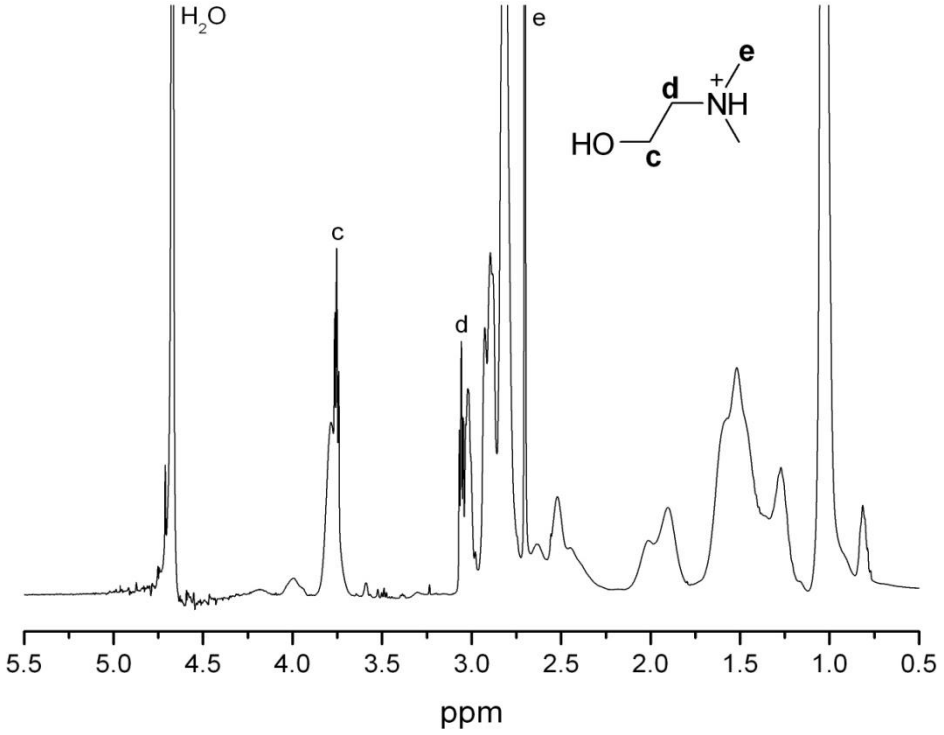

Figure A2.11 ^{1}H NMR spectrum of B1: P(DMA_{96}-b-($NIPAM_{88}$-co-$DMAEA_{25}$-co-BA_6)) after being dissolved and kept in D_2O for 80 h. The spectrum was measured at 25 ^{o}C.

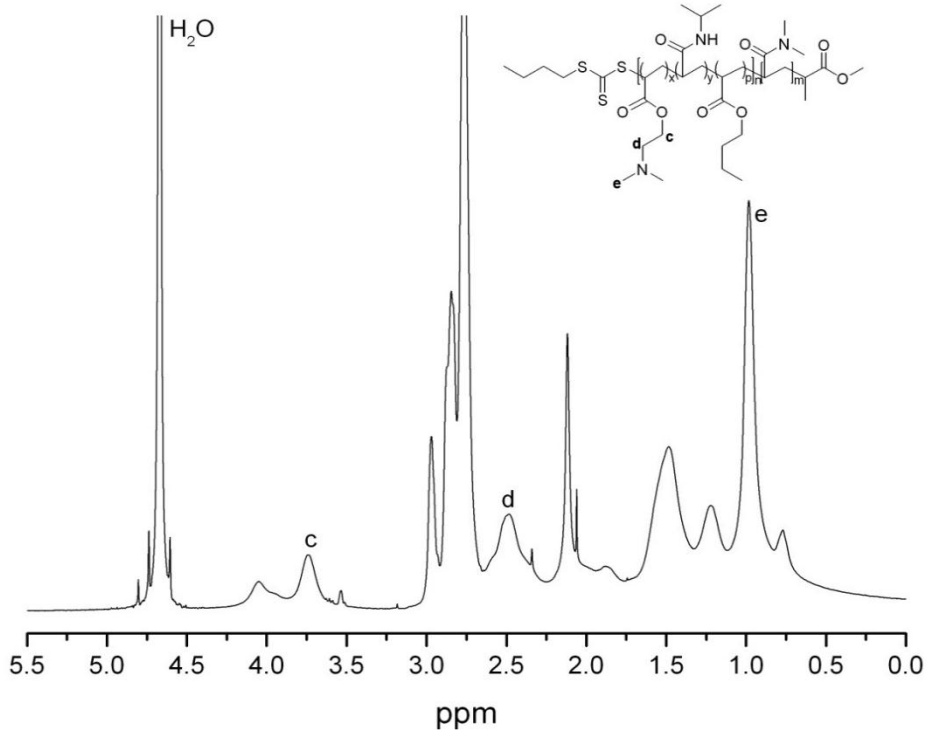

Figure A2.12 ^{1}H NMR spectrum of B2: P(DMA_{96}-b-($NIPAM_{91}$-co-$DMAEA_{25}$-co-BA_{12})) after being dissolved in D_2O and immediately measured at 15 ^{o}C.

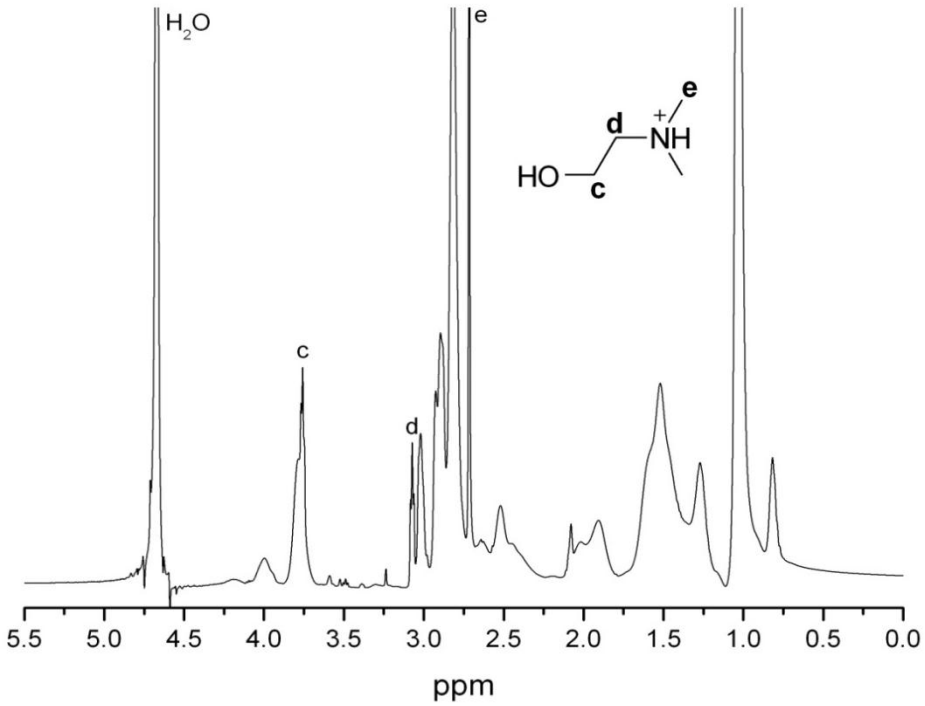

Figure A2.13 ^{1}H NMR spectrum of B2: P(DMA_{96}-b-($NIPAM_{91}$-co-$DMAEA_{25}$-co-BA_{12})) after being dissolved and kept in D_2O for 80 h. The spectrum was measured at 25 ^{o}C.

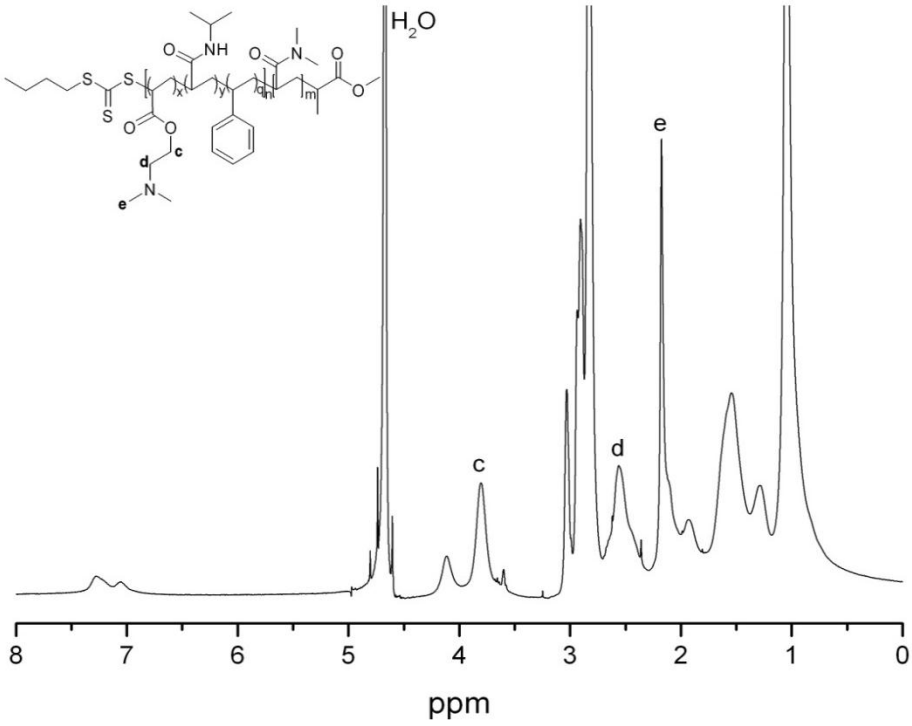

Figure A2.14 ^{1}H NMR spectrum of C1: P(DMA_{96}-b-($NIPAM_{84}$-co-$DMAEA_{22}$-co-STY_{5})) after being dissolved in D_2O and immediately measured at 25 ^{o}C.

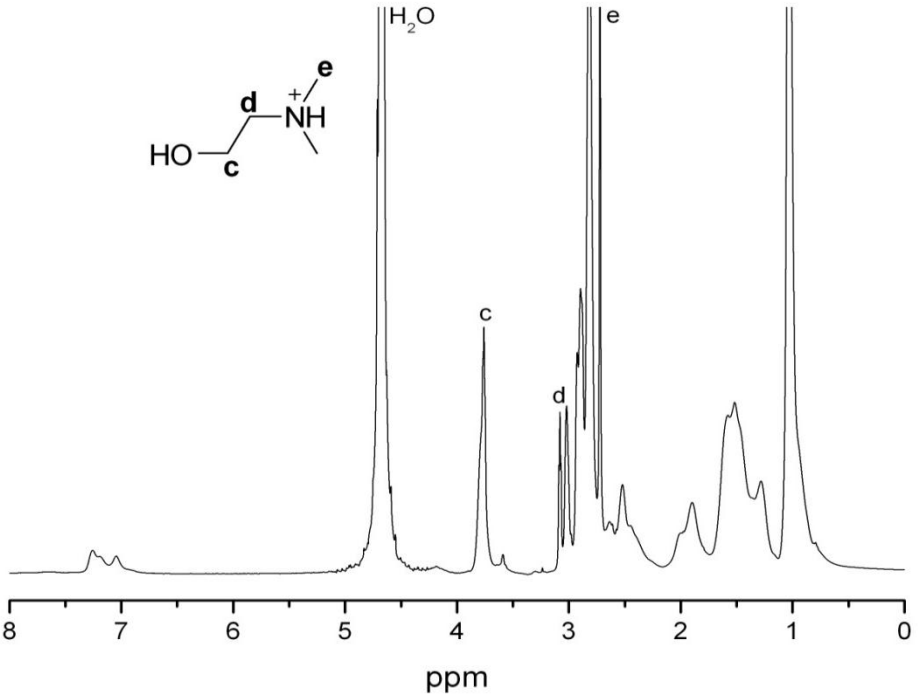

Figure A2.15 ^{1}H NMR spectrum of C1: P(DMA$_{96}$-b-(NIPAM$_{84}$-co-DMAEA$_{22}$-co-STY$_{5}$ after being dissolved and kept in D_2O for 80 h. The spectrum was measured at 25 ^{o}C.

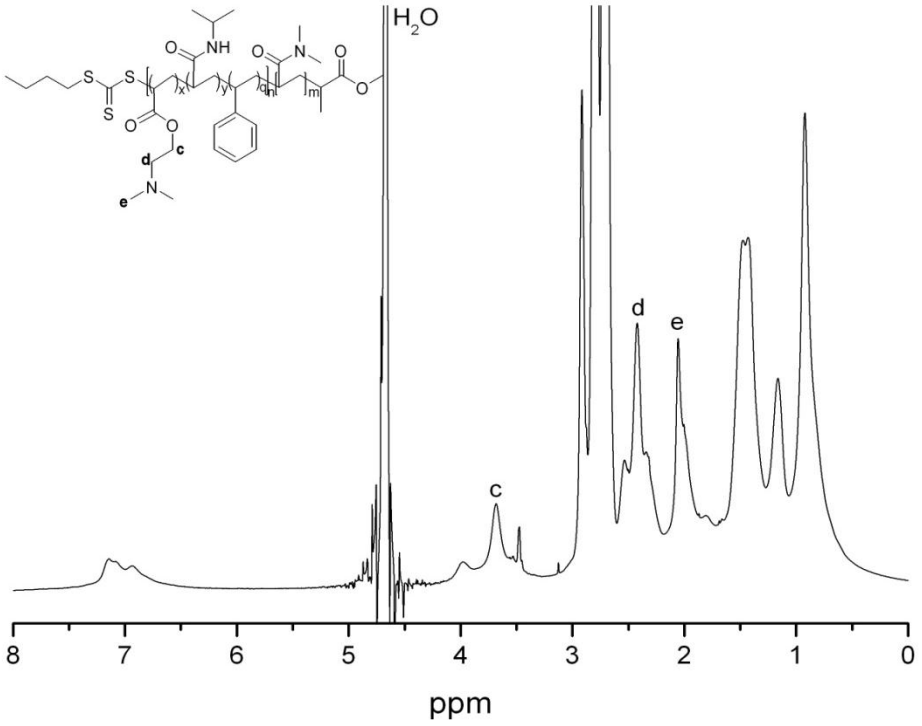

Figure A2.16 ^{1}H NMR spectrum of C2: P(DMA$_{96}$-b-(NIPAM$_{40}$-co-DMAEA$_{15}$-co-STY$_{13}$)) after being dissolved in D_2O and immediately measured at 15 ^{o}C.

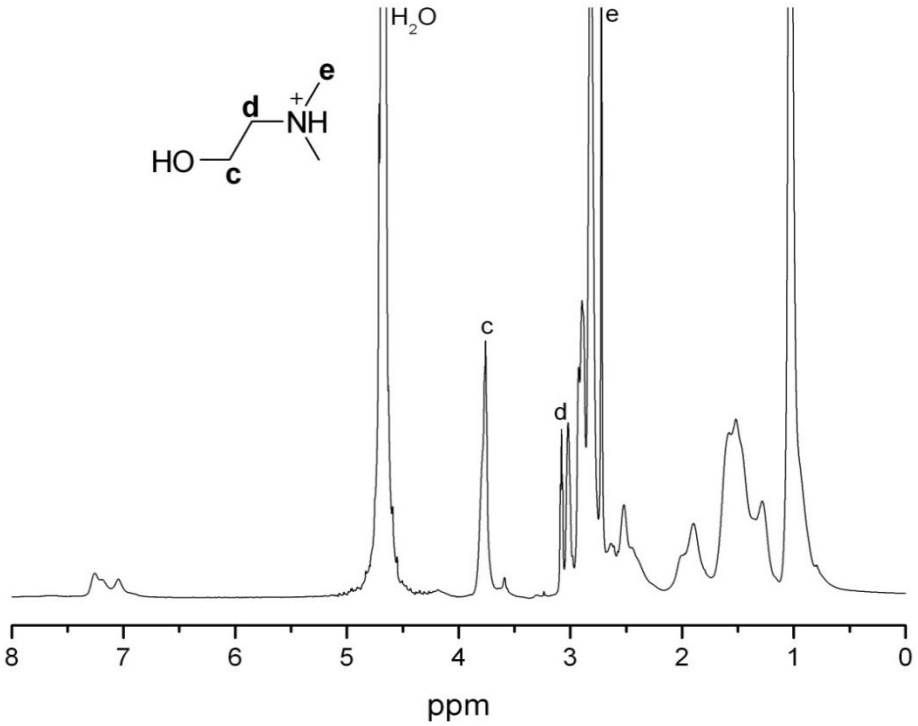

Figure A2.17 ^{1}H NMR spectrum of C2: P(DMA_{96}-b-($NIPAM_{40}$-co-$DMAEA_{15}$-co-STY_{13})) after being dissolved and kept in D_2O for 80 h. The spectrum was measured at 25 ^{o}C.

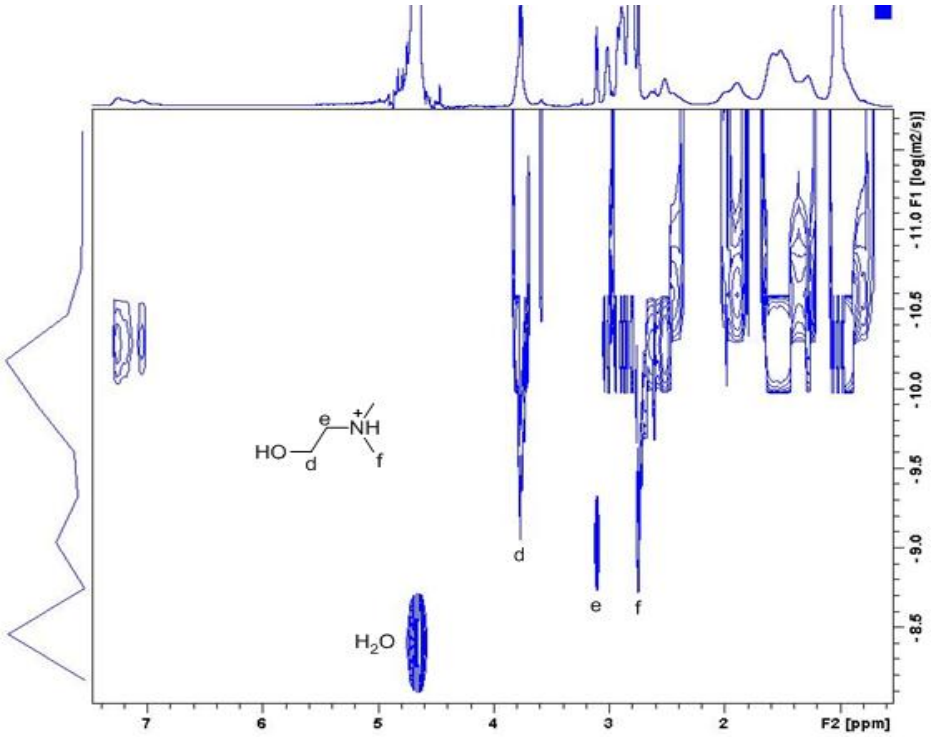

Figure A2.18 DOSY NMR spectrum of C1: P(DMA_{96}-b-($NIPAM_{84}$-co-$DMAEA_{22}$-co-STY_{5})) after being dissolved in D_2O for 80h. The spectrum was measured at 25 ^{o}C.

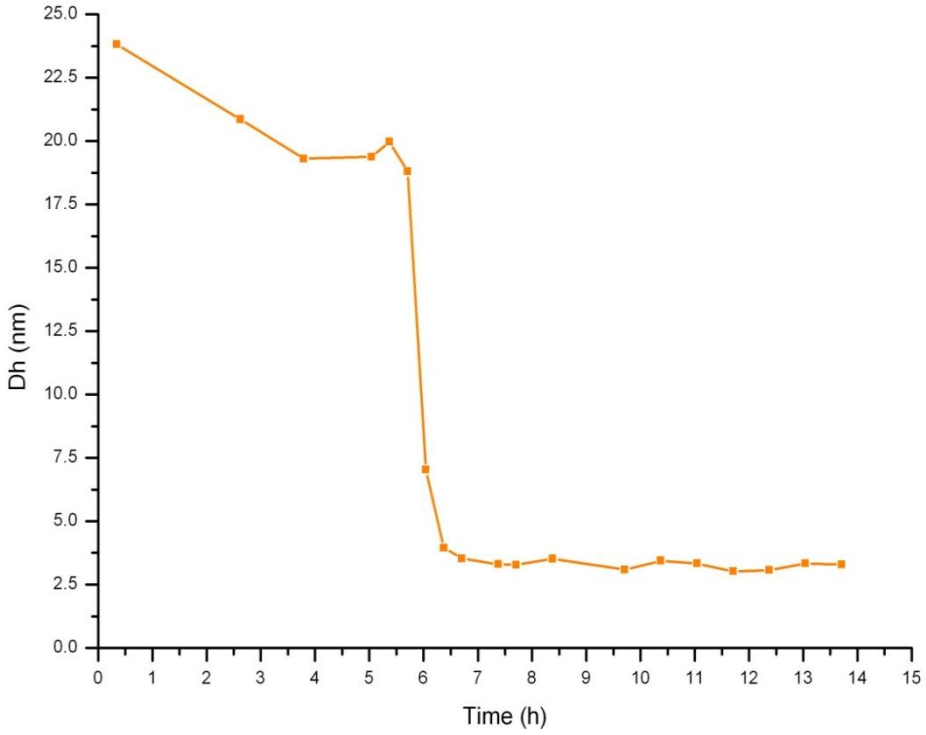

Figure A2.19 Degradation kinetic of A: P(DMA_{96}-b-($NIPAM_{87}$-co-$DMAEA_{25}$)). The data were averaged from five measurements on DLS machine at polymer solution concentration 5 mg/mL at 45 ^{o}C.

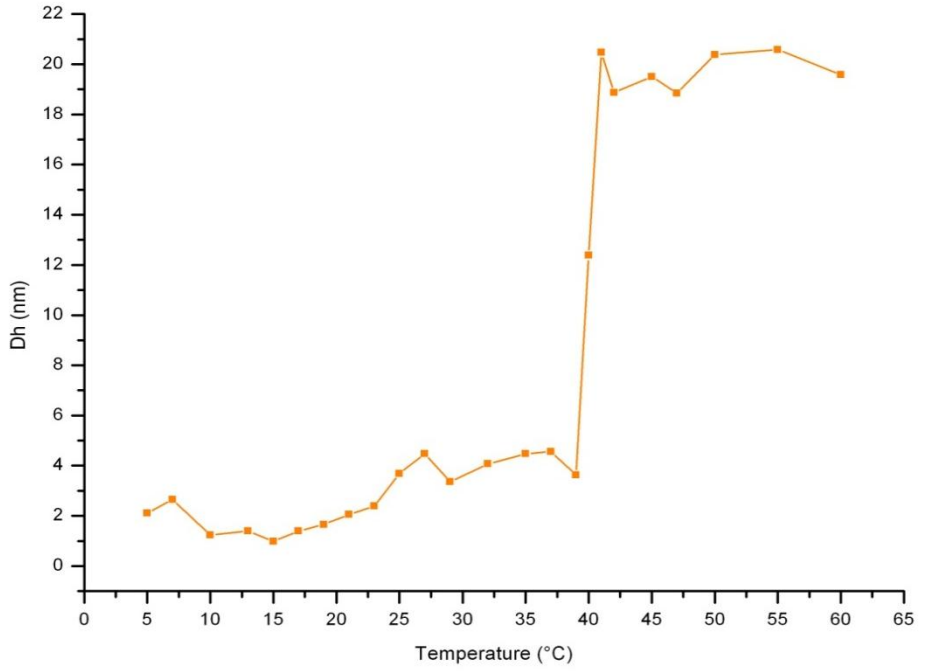

Figure A2.20 LCST of A: P(DMA_{96}-b-($NIPAM_{87}$-co-$DMAEA_{25}$)). The data were reported as average numbers from five measurements on DLS machine at concentration 10 mg/mL.

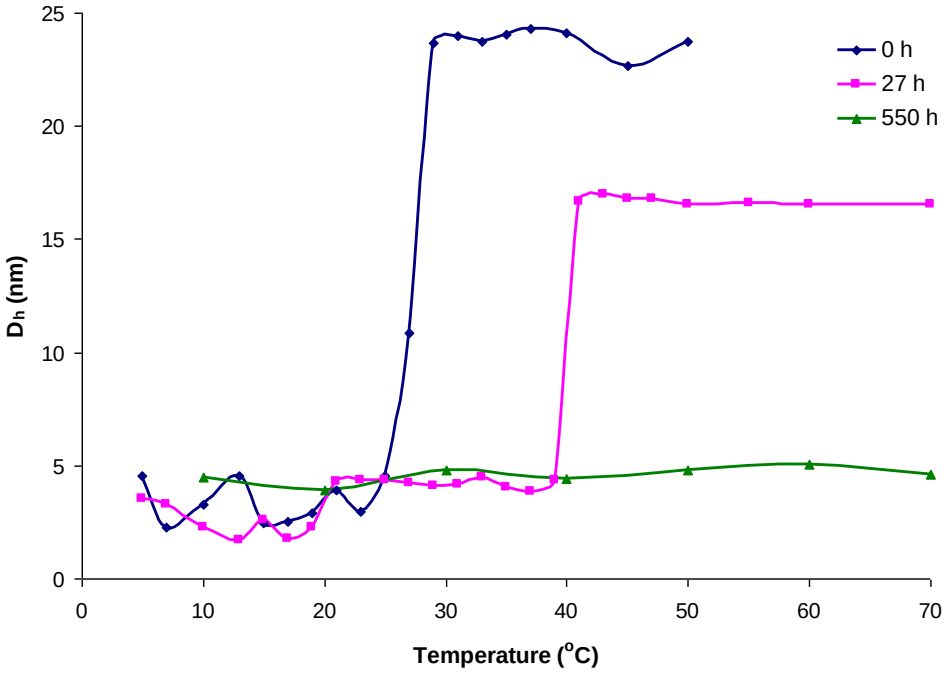

Figure A2.21 LCST of B1: P(DMA_{96}-b-($NIPAM_{88}$-co-$DMAEA_{25}$-co-BA_6)) at different times after the polymer was dissolved in water. The data were reported as average numbers from five measurements on DLS machine at concentration 10 mg/mL.

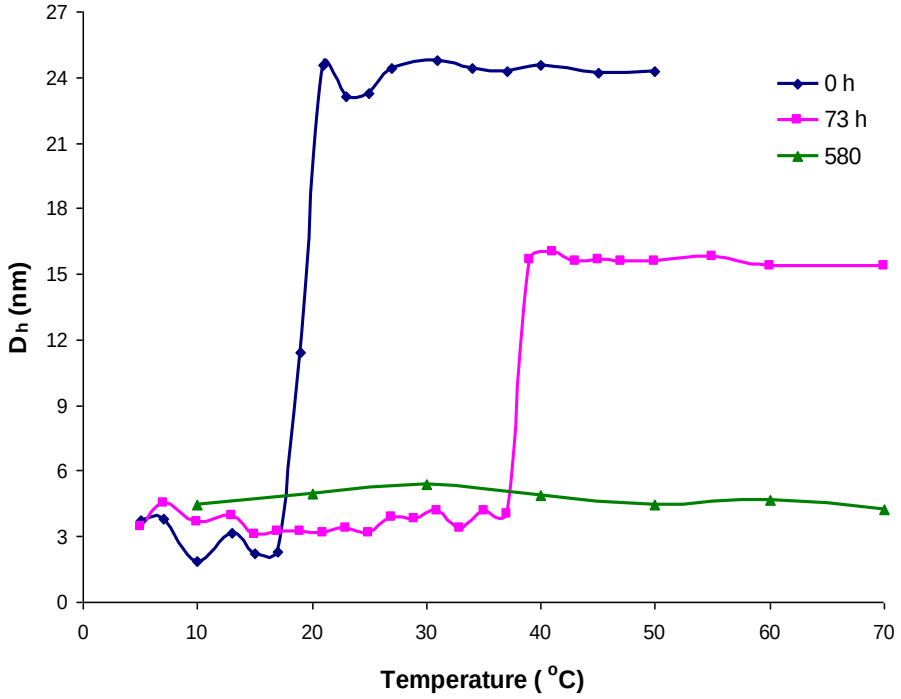

Figure A2.22 LCST of B2: P(DMA_{96}-b-($NIPAM_{91}$-co-$DMAEA_{25}$-co-BA_{12})) at different times after the polymer was dissolved in water. The data were reported as average numbers from five measurements on DLS machine at concentration 10 mg/mL.

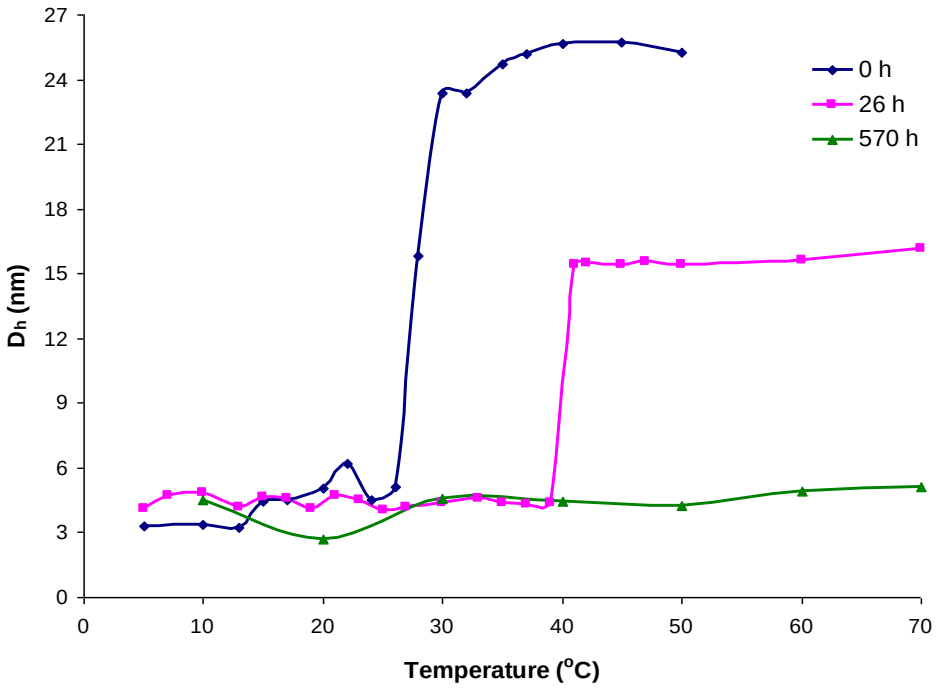

Figure A2.23 LCST of C1: P(DMA_{96}-b-($NIPAM_{84}$-co-$DMAEA_{22}$-co-STY_5 at different times after the polymer was dissolved in water. The data were reported as average numbers from five measurements on DLS machine at concentration 10 mg/mL

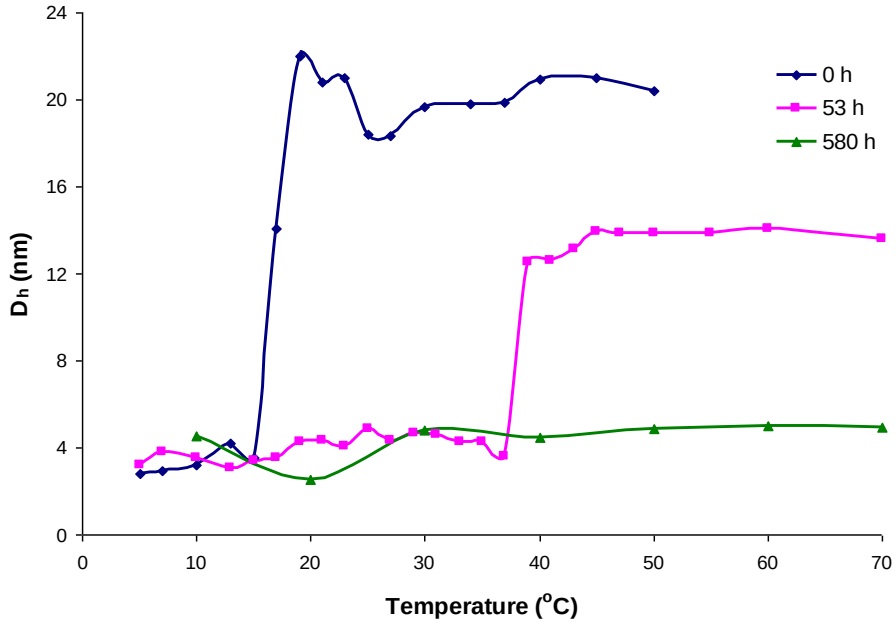

Figure A2.24 LCST of C2: P(DMA_{96}-b-($NIPAM_{40}$-co-$DMAEA_{15}$-co-STY_{13})) at different times after the polymer was dissolved in water. The data were reported as average numbers from five measurements on DLS machine at concentration 10 mg/mL.

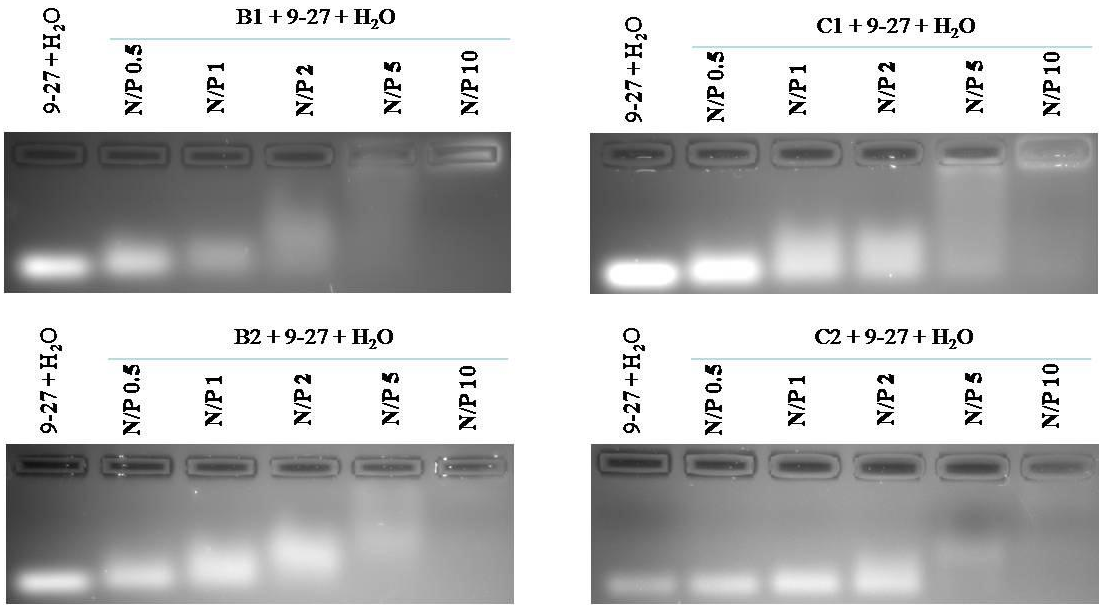

Figure A2.25 Agarose gel assay of Oigo DNA 9-27 / thermoresponsive block copolymers complexes in Milli-Q water at N/P Ratio 0.5, 1, 2, 5, and 10. B1: P(DMA_{96}-b-($NIPAM_{88}$-co-$DMAEA_{25}$-co-BA_6)), B2: P(DMA_{96}-b-($NIPAM_{91}$-co-$DMAEA_{25}$-co-BA_{12})), C1: P(DMA_{96}-b-($NIPAM_{84}$-co-$DMAEA_{22}$-co-STY_5)), C2: P(DMA_{96}-b-($NIPAM_{40}$-co-$DMAEA_{15}$-co-STY_{13})). Soluble copolymers in Milli-Q water were incubated with DNA at different N/P ratios at below their LCST for 30 min and then being heated up to 37 ^oC for 15 min before doing Agarose gel retardation assay.

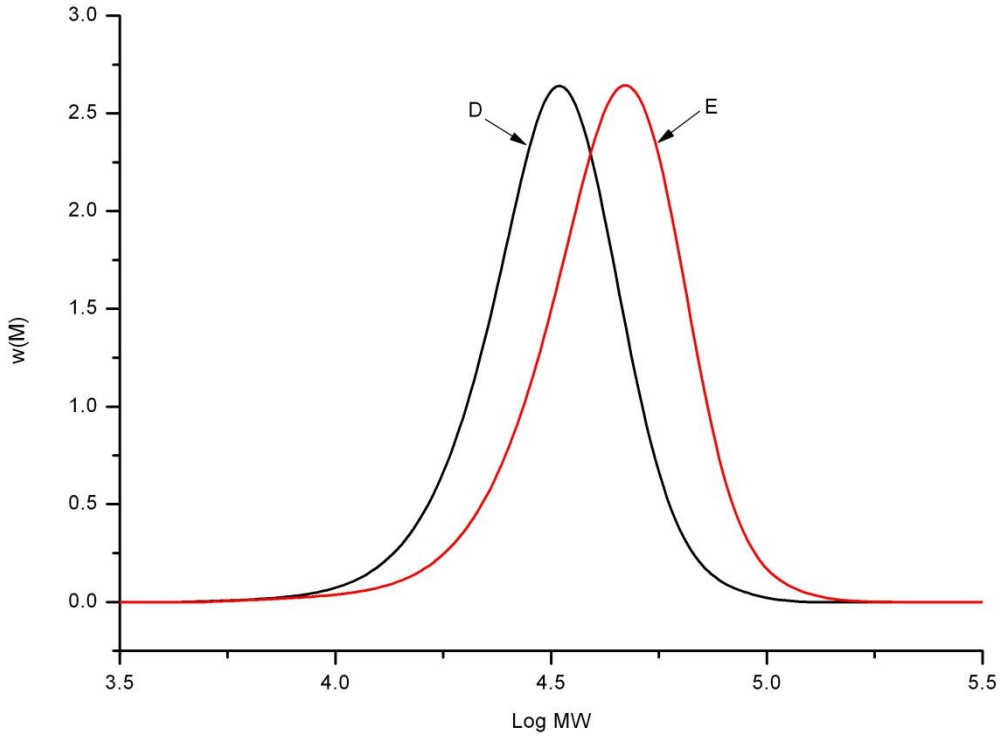

Figure A2.26 Size Exclusion Chromatography (SEC) traces of D: P(NIPAM$_{97}$-co-BA$_{13}$)) and E: P(DMA$_{99}$-b-(NIPAM$_{97}$-co- BA$_{13}$)). The samples were measured by DMAc SEC. The intensity for different distribution curves was normalized.

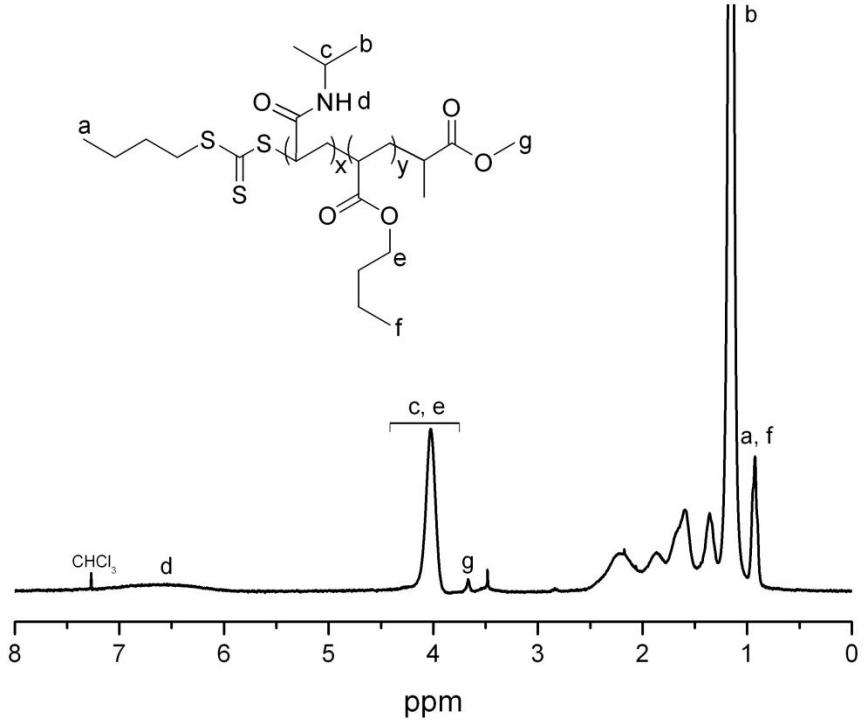

Figure A2.27 ^{1}H NMR spectrum of **D**: P(NIPAM$_{97}$-co-BA$_{13}$)) in $CDCl_3$

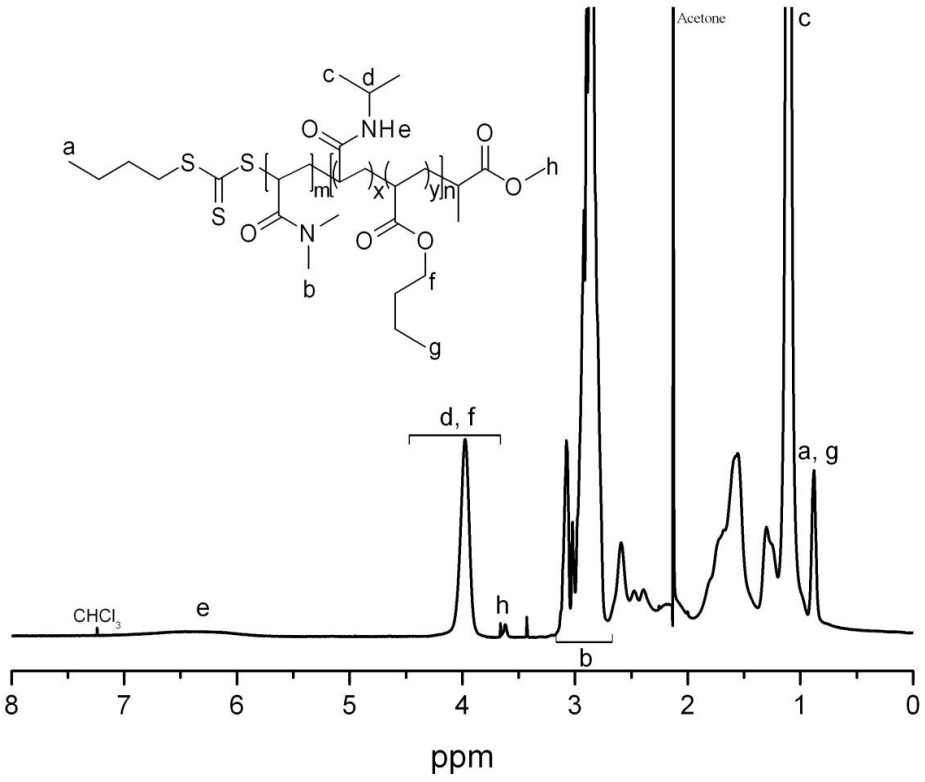

Figure A2.28 ^{1}H NMR spectrum of **E**: P(DMA$_{99}$-b-(NIPAM$_{97}$-co- BA$_{13}$)) in $CDCl_3$

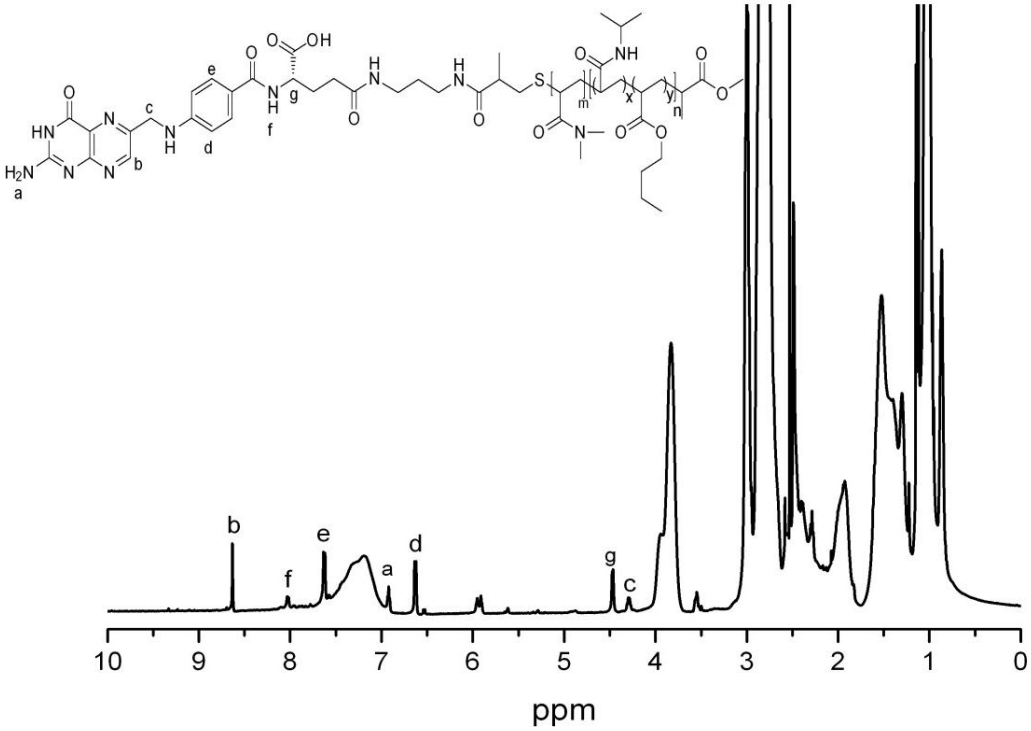

Figure A2.29 ^{1}D DOSY NMR spectrum of folic acid conjugated copolymer E, PDMA-b-P(NIPAM-co-BA) in DMSO-d_6.

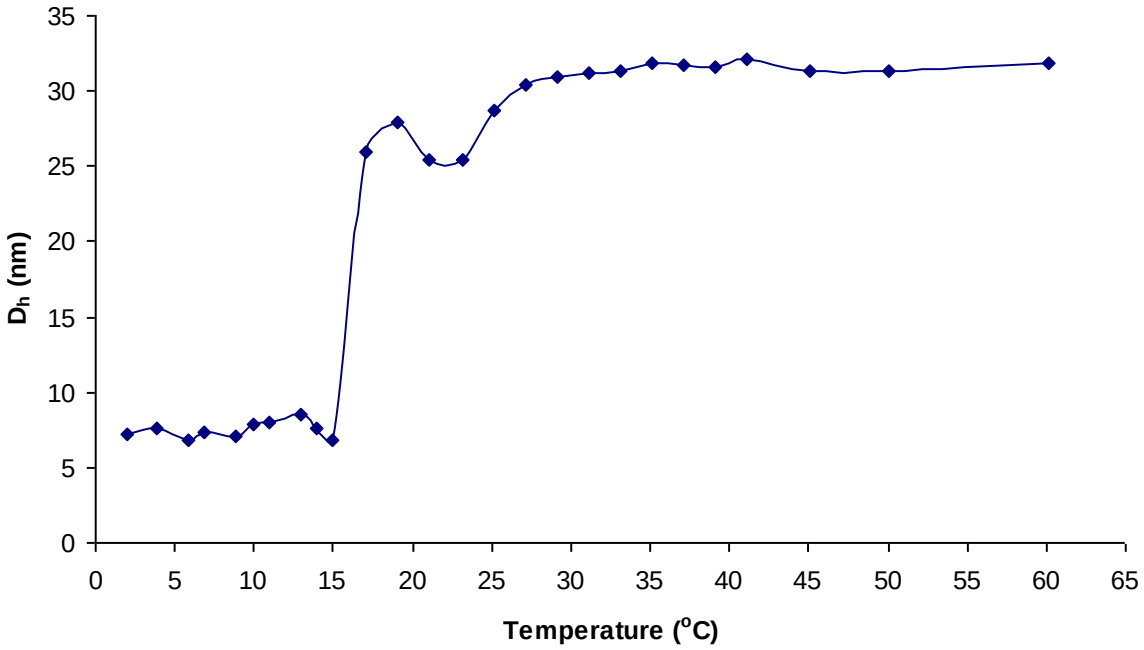

Figure A2.30 LCST of folic acid conjugated copolymer E, PDMA-b-P(NIPAM-co-BA) in DMSO-d_6. The polymer was dissolved in water. The data were reported as average numbers from five measurements on DLS machine at concentration 10 mg/mL. LCST = 15 – 19 ^{o}C.

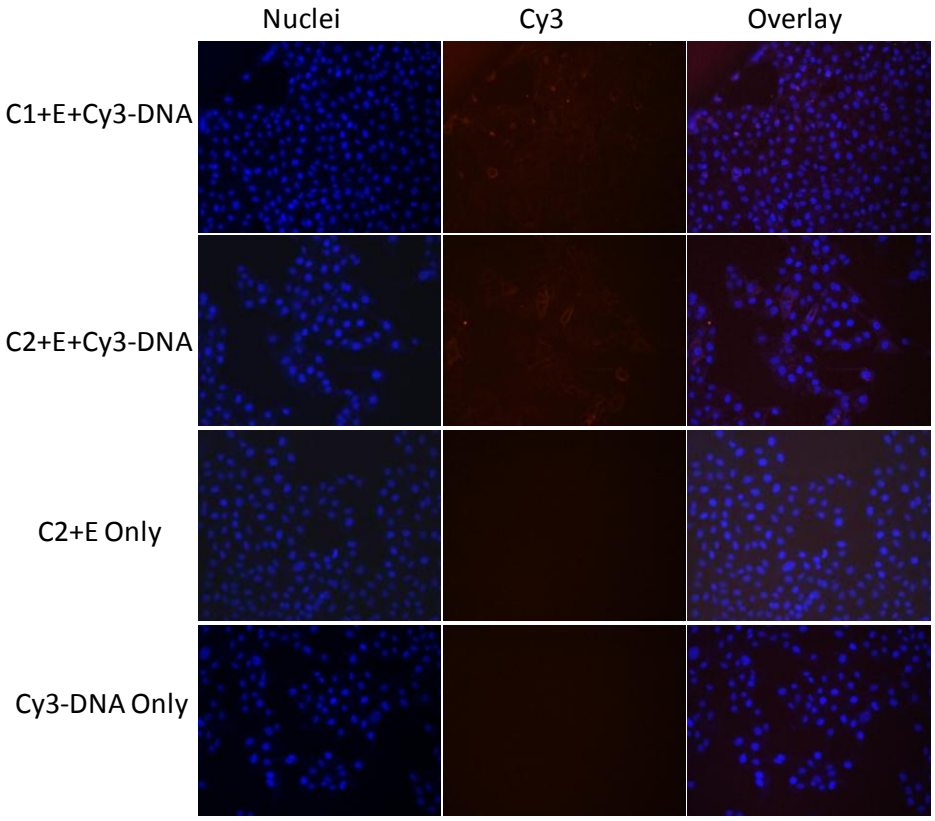

Figure A2.31 Confocal microscopy photos of the osteosarcoma U2OS cells which were dosed with 50 nmol Cy3 oligo DNA and copolymer polyplexes and cultured in 24-well plate ($1x10^5$/well) in completed DMEM medium. The polyplexes were prepared in the ratio to siRNA as 50:1 in water. The mixtures were incubated in ice-bath for 10 minutes and then at 37^oC for 30 minutes. They were then added to the cells and were incubated for 10 hours before washing fixation with 4% paraffinformaldehyde. The cell nuclei were stained with Hoechst 33341 and cell uptake was viewed under fluorescent microscope.

Appendix B

Table A3.1 RAFT polymerization condition, BA amount, SEC-RI, ^{1}H NMR, conversion, and total conversion of thermoresponsive block copolymers (A1 to A8) at 60 ^{o}C in Dioxane.

Polymer	[NIPAM]:[DMAEA]:[BA]:[macro CTA][a]:[AIBN]	BA mol (x 10^{-3}) (Vol (mL))	SEC-Triple detection [b]		^{1}H NMR						
					Repeating units [c]			Conversion (%)[d]			Total conv. (%)[e]
			M_n	PDI	NIPAM	DMAEA	BA	NIPAM	DMAEA	BA	
A1	119:30:8:1:0.12	0.575 (0.083)	23800	1.02	88	76	6	74	82	82	76
A2	119:30:13:1:0.12	0.97 (0.14	27000	1.03	94	78	8	79	84	61	78
A3	119:30:15:1:0.12	1.15 (0.165)	27800	1.03	94	78	10	79	84	67	78
A4	119:30:17:1:0.12	1.24 (0.18)	27400	1.02	91	77	12	76	85	71	77
A5	119:30:21:1:0.12	1.59 (0.23)	28700	1.05	93	78	14	78	82	67	78
A6	119:30:24:1:0.12	1.77 (0.255)	27200	1.03	93	78	16	78	83	68	78
A7	119:30:26:1:0.12	1.95 (0.28)	28400	1.06	93	78	18	78	84	69	78
A8	119:30:29:1:0.12	2.12 (0.31)	30200	1.03	97	80	20	81	85	70	80

[a] PDMA (Macro-CTA) with repeating unit = 96 calculated from ^{1}H NMR; M_n = [(96 x 99.131 + 252.42] = 9770. [b] Triple detection SEC in DMAc containing 0.03 wt % LiCl with PSTY as standards. Calculations were based on the d*n*/d*c* and polymer concentration. The PDI values were underestimated. [c] Repeating units of NIPAM (N_{NIPAM}) determined by ^{1}H NMR were calculated based on 96 repeating unit of Macro-CTA by the integral area of a peak at 1.08 ppm ($I_{1.08}$) and a peak in the range 2.85-3.07 ppm ($I_{2.85\text{-}3.07}$) using the following equation: $N_{NIPAM} = 96 \times I_{1.08} / I_{2.85\text{-}3.07}$; Repeating units of BA (N_{BA}) determined by ^{1}H NMR were calculated based on 96 repeating unit of Macro-CTA by the integral area of a peak at 0.88 ppm ($I_{1.08}$) and a peak in the range 2.85-3.07 ppm ($I_{2.85\text{-}3.07}$) using the following equation: $N_{BA} = (96 \times 2 \times I_{0.88} / I_{2.85\text{-}3.07}) - 1$; Repeating units of DMAEA (N_{DMAEA}) determined by ^{1}H NMR were calculated based on 96 repeating unit of Macro-CTA, and the N_{NIPAM} and N_{BA} by the integral area of the peak in the range 2.85-3.07 ppm ($I_{2.85\text{-}3.07}$) and the peak in the range 3.95 - 4.30 ppm ($I_{3.95\text{-}4.30}$) using the following equation: $N_{DMAEA} = [(96 \times 6 \times I_{3.95\text{-}4.30}/I_{2.85\text{-}3.07}) - (N_{NIPAM} + 2\ N_{BA})]/2$. [d] The conversion of NIPAM was calculated by the concentration ratio [NIPAM] = 119, and its repeating unit determined by ^{1}H NMR (N_{NIPAM}). Conversion of NIPAM = N_{NIPAM} / 119 x 100; The conversion of DMAEA was calculated by the concentration ratio [DMAEA] = 30, and its repeating unit determined by ^{1}H NMR (N_{DMAEA}). Conversion of DMAEA = N_{DMAEA} / 30 x 100; The conversion of BA was calculated by the concentration ratio [BA], and its repeating unit determined by ^{1}H NMR (N_{BA}). Conversion of BA = N_{BA} / [BA] x 100. [e] Total conversion is calculated by the following equation: Total conv. = [(conversion of NIPAM x 119) + (conversion of DMAEA x 30) + (conversion of NIPAM x [BA])] / (119+30+ [BA]).

Table A3.2 RAFT polymerization condition, BA amount, SEC-RI, ^{1}H NMR, conversion, and total conversion of thermoresponsive block copolymers (B1 to B7) at 60 ^{o}C in Dioxane.

Polymer	[NIPAM]:[DMAEA]:[BA]:[macro CTA][a]:[AIBN]	BA mol x 10^{-3} (Vol (mL))	SEC-Triple detection [b]		^{1}H NMR						
					Repeating units [c]			Conversion (%)[d]			Total conv. (%)[e]
			M_n	PDI	NIPAM	DMAEA	BA	NIPAM	DMAEA	BA	
B1	119:54:12:1:0.12	0.89 (0.127)	28400	1.05	87	73	6	73	78	54	73
B2	119:54:14:1:0.12	1.06 (0.153)	29200	1.04	88	74	8	74	77	58	74
B3	119:54:17:1:0.12	1.24 (0.178)	29000	1.05	87	74	10	73	79	63	74
B4	119:54:19:1:0.12	1.42 (0.204)	29400	1.07	85	73	12	72	79	64	73
B5	119:54:21:1:0.12	1.59 (0.229)	29500	1.03	85	73	14	71	78	66	73
B6	119:54:24:1:0.12	1.77(0.255)	29800	1.03	88	74	16	74	78	67	74
B7	119:54:30:1:0.12	2.21(0.319)	30500	1.05	87	74	20	73	80	66	74

[a] PDMA (Macro-CTA) with repeating unit = 96 calculated from ^{1}H NMR; M_n = [(96 x 99.131 + 252.42] = 9770. [b]Triple detection SEC in DMAc containing 0.03 wt % LiCl with PSTY as standards. Calculations were based on the d*n*/d*c* and polymer concentration. The PDI values were underestimated. [c] Repeating units of NIPAM (N_{NIPAM}) determined by ^{1}H NMR were calculated based on 96 repeating unit of Macro-CTA by the integral area of a peak at 1.08 ppm ($I_{1.08}$) and a peak in the range 2.85-3.07 ppm ($I_{2.85\text{-}3.07}$) using the following equation: $N_{NIPAM} = 96 \times I_{1.08} / I_{2.85\text{-}3.07}$; Repeating units of BA (N_{BA}) determined by ^{1}H NMR were calculated based on 96 repeating unit of Macro-CTA by the integral area of a peak at 0.88 ppm ($I_{1.08}$) and a peak in the range 2.85-3.07 ppm ($I_{2.85\text{-}3.07}$) using the following equation: $N_{BA} = (96 \times 2 \times I_{0.88} / I_{2.85\text{-}3.07}) - 1$; Repeating units of DMAEA (N_{DMAEA}) determined by ^{1}H NMR were calculated based on 96 repeating unit of Macro-CTA, and the N_{NIPAM} and N_{BA} by the integral area of the peak in the range 2.85-3.07 ppm ($I_{2.85\text{-}3.07}$) and the peak in the range 3.95 - 4.30 ppm ($I_{3.95\text{-}4.30}$) using the following equation: $N_{DMAEA} = [(96 \times 6 \times I_{3.95\text{-}4.30}/I_{2.85\text{-}3.07}) - (N_{NIPAM} + 2\ N_{BA})]/2$. [d] The conversion of NIPAM was calculated by the concentration ratio [NIPAM] = 119, and its repeating unit determined by ^{1}H NMR (N_{NIPAM}). Conversion of NIPAM = N_{NIPAM} / 119 x 100; The conversion of DMAEA was calculated by the concentration ratio [DMAEA] = 54, and its repeating unit determined by ^{1}H NMR (N_{DMAEA}). Conversion of DMAEA = N_{DMAEA} / 54 x 100; The conversion of BA was calculated by the concentration ratio [BA], and its repeating unit determined by ^{1}H NMR (N_{BA}). Conversion of BA = N_{BA} / [BA] x 100. [e] Total conversion is calculated by the following equation: Total conv. = [(conversion of NIPAM x 119) + (conversion of DMAEA x 54) + (conversion of NIPAM x [BA])] / (119+54+ [BA]).

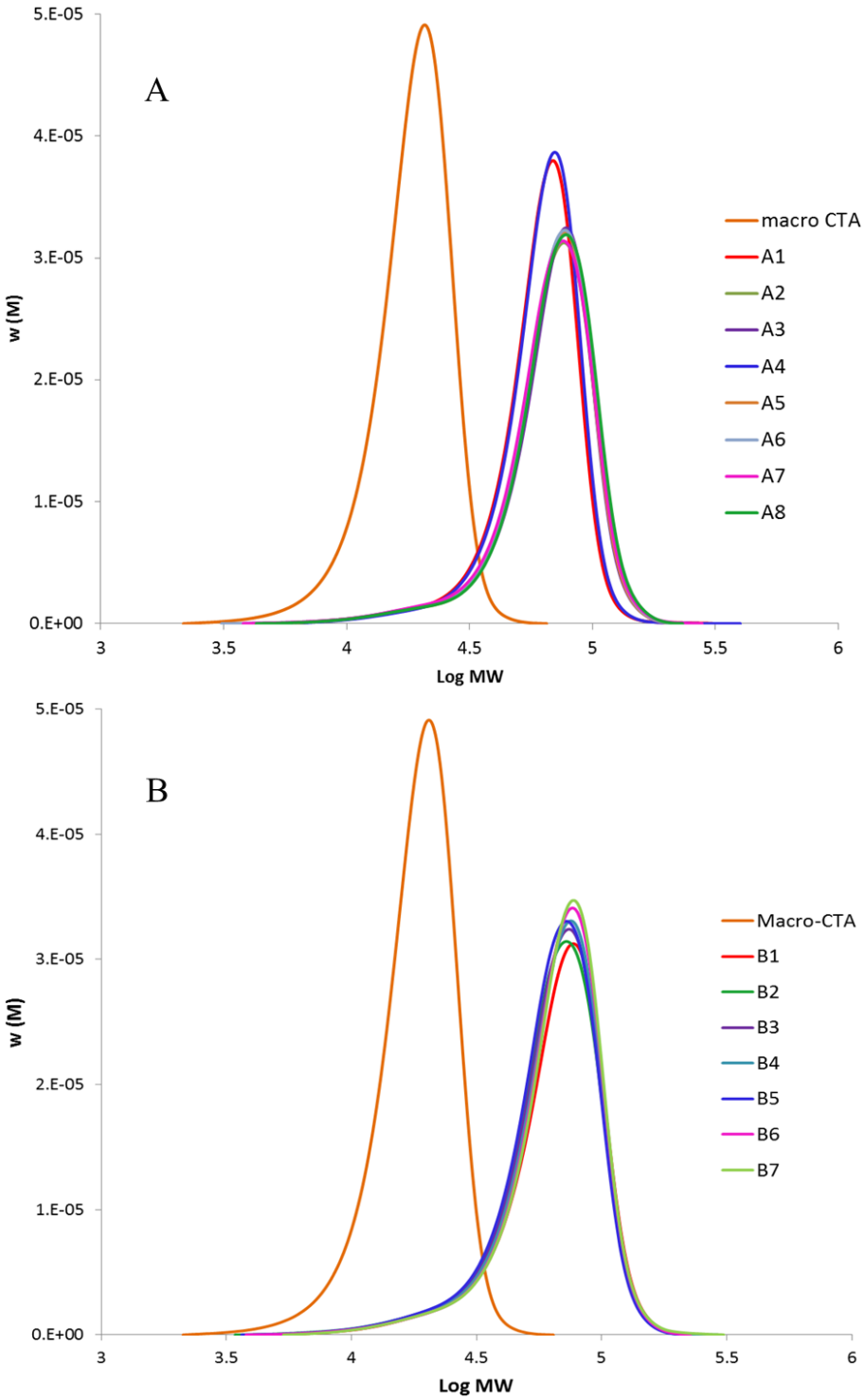

Figure A3.1 SEC traces of PDMA Macro-CTA and block copolymers PDMA-b-P(NIPAM-co-DMAEA-co-BA), A1 to A8 (A) and B1 to B7 (B). The data were measured in eluent DMAc with 0.03 wt% of LiCl and using PSTY standard for calibration and reflective index detector. The areas under these peaks were weight normalized.

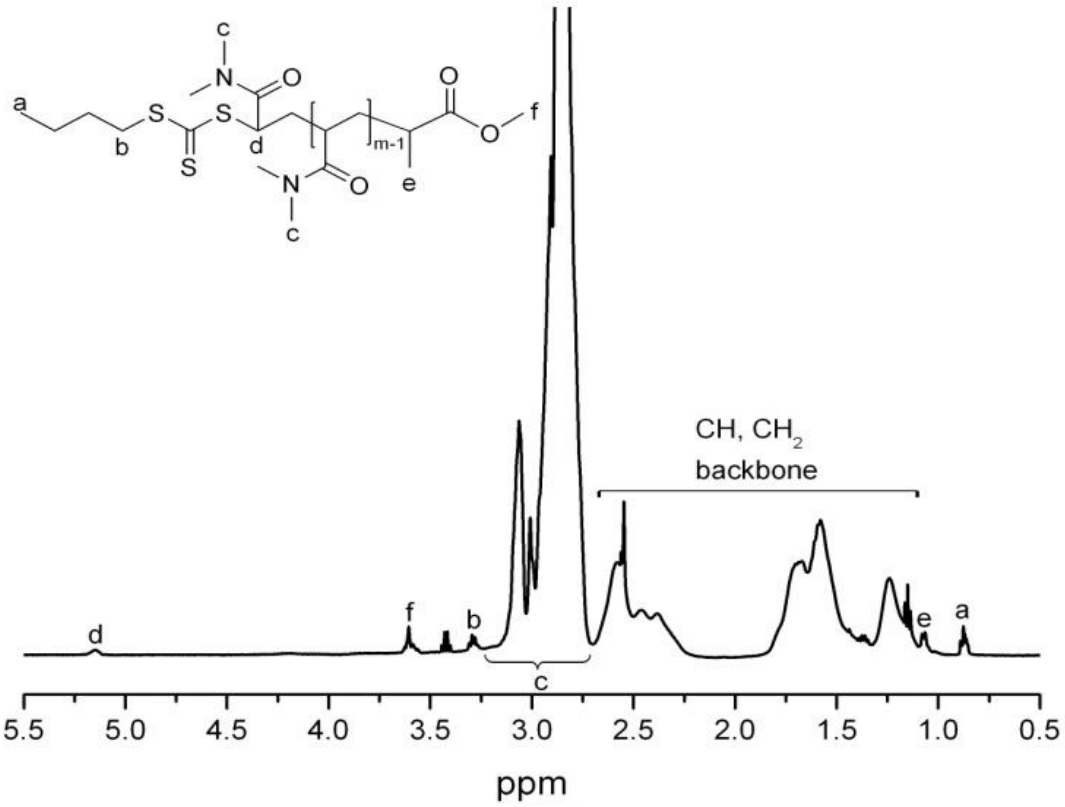

Figure A3.2 ^{1}H NMR spectrum of Macro-CTA: $PDMA_{96}$ in $CDCl_3$.

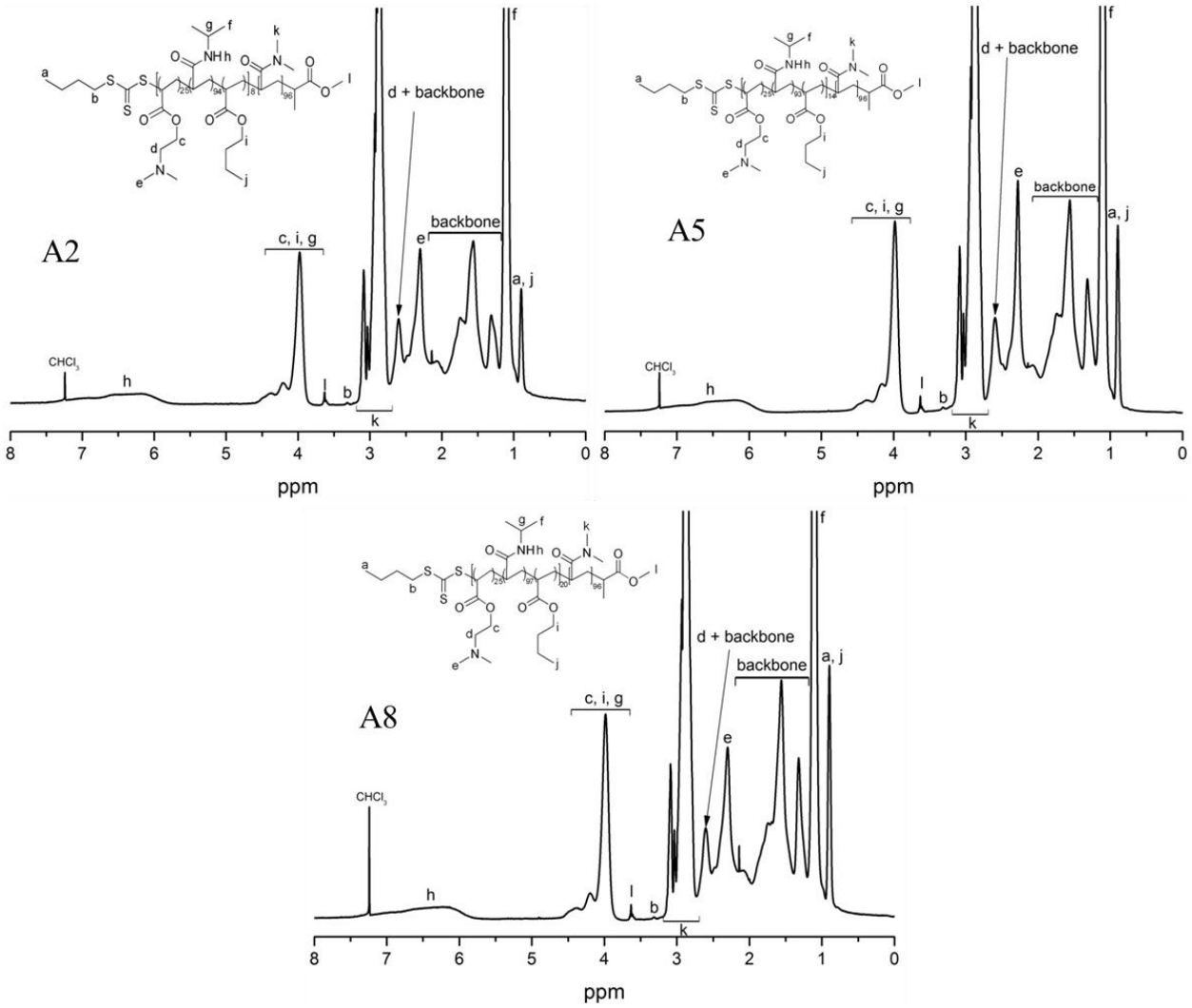

Figure A3.3 ^{1}H NMR spectrum of A2: P(DMA$_{96}$-b-(NIPAM$_{94}$-co-DMAEA$_{25}$-co-BA$_{8}$)), A5: P(DMA$_{96}$-b-(NIPAM$_{93}$-co-DMAEA$_{25}$-co-BA$_{14}$)), and A8: P(DMA$_{96}$-b-(NIPAM$_{97}$-co-DMAEA$_{25}$-co-BA$_{20}$)) in $CDCl_3$.

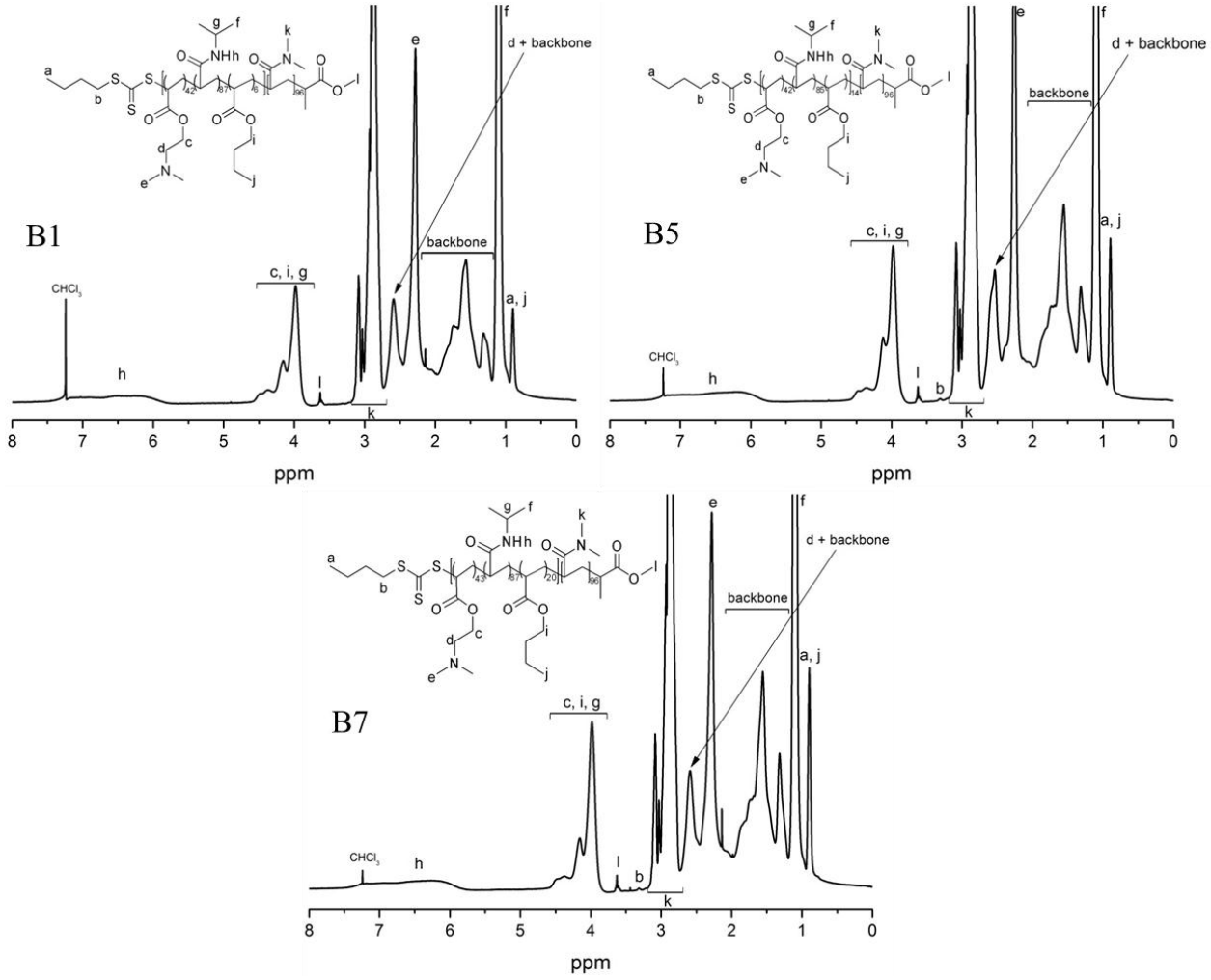

Figure A3.4 ^{1}H NMR spectrum of B1: P(DMA_{96}-b-($NIPAM_{87}$-co-$DMAEA_{42}$-co-BA_{6})), B5: P(DMA_{96}-b-($NIPAM_{85}$-co-$DMAEA_{42}$-co-BA_{14})), and B7: P(DMA_{96}-b-($NIPAM_{87}$-co-$DMAEA_{43}$-co-BA_{20})) in $CDCl_3$.

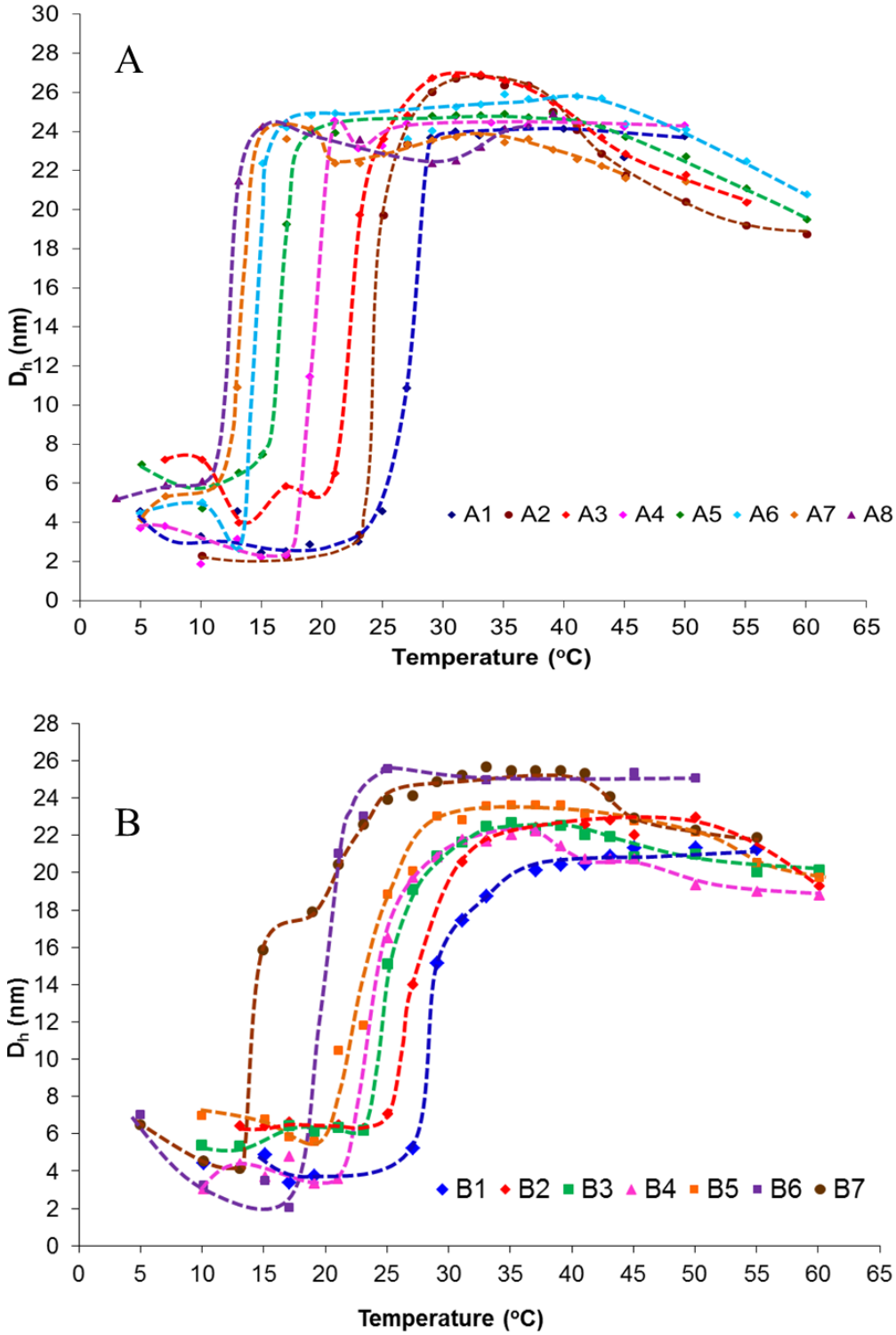

Figure A3.5 LCST of polymers A1 to A8 (A) and polymers B1 to B7 (B) in Milli-Q water. The data were averaged from five measurements by DLS at polymer solution concentration of 10 mg/mL.

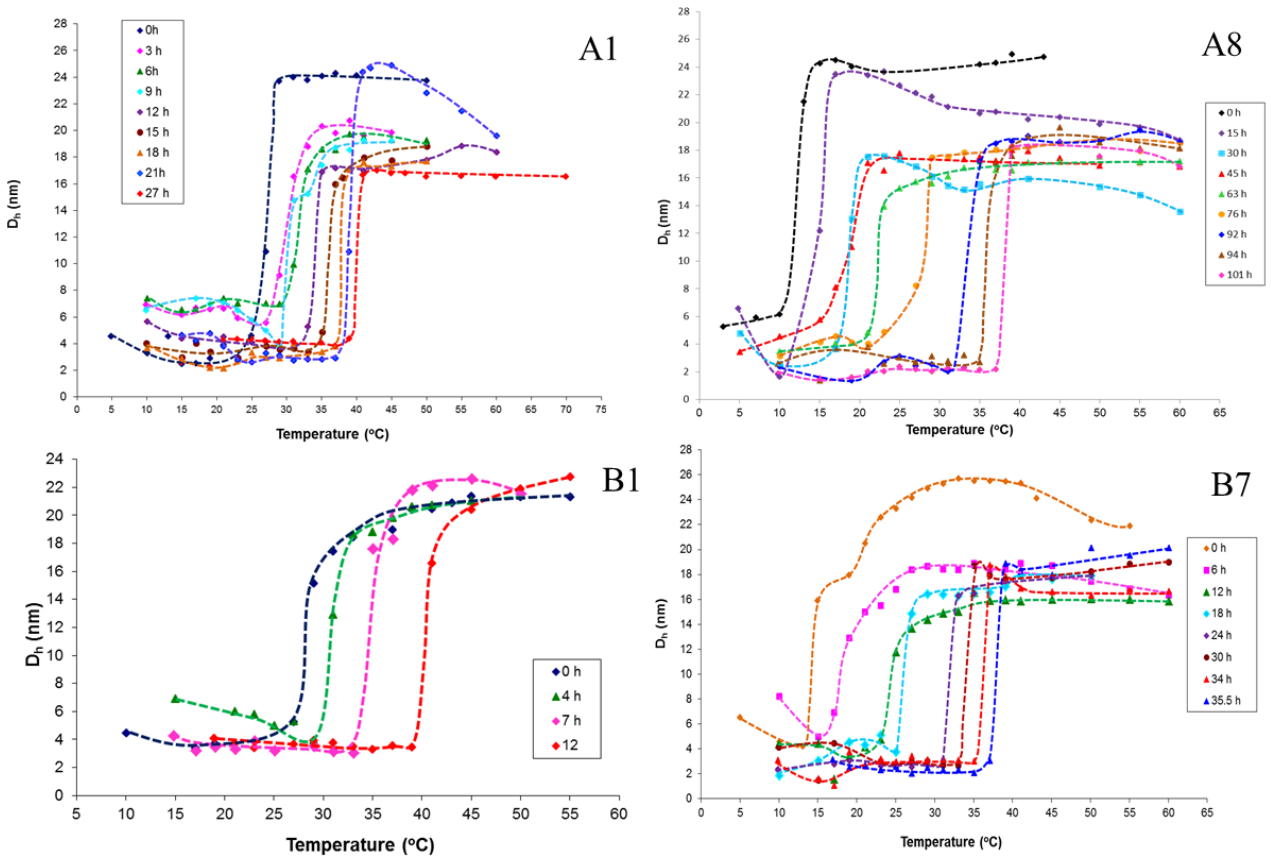

Figure A3.6 LCST of polymer A1: P(DMA$_{96}$-b-(NIPAM$_{88}$-co-DMAEA$_{24}$-co-BA$_6$)), A8: P(DMA$_{96}$-b-(NIPAM$_{97}$-co-DMAEA$_{25}$-co-BA$_{20}$)), B1: P(DMA$_{96}$-b-(NIPAM$_{87}$-co-DMAEA$_{42}$-co-BA$_6$)) and P(DMA$_{96}$-b-(NIPAM$_{87}$-co-DMAEA$_{43}$-co-BA$_{20}$)) in Milli-Q water after incubation in water bath at 37 ^{o}C at different times. The data were averaged from five measurements by DLS at polymer solution concentration 10 mg/mL.

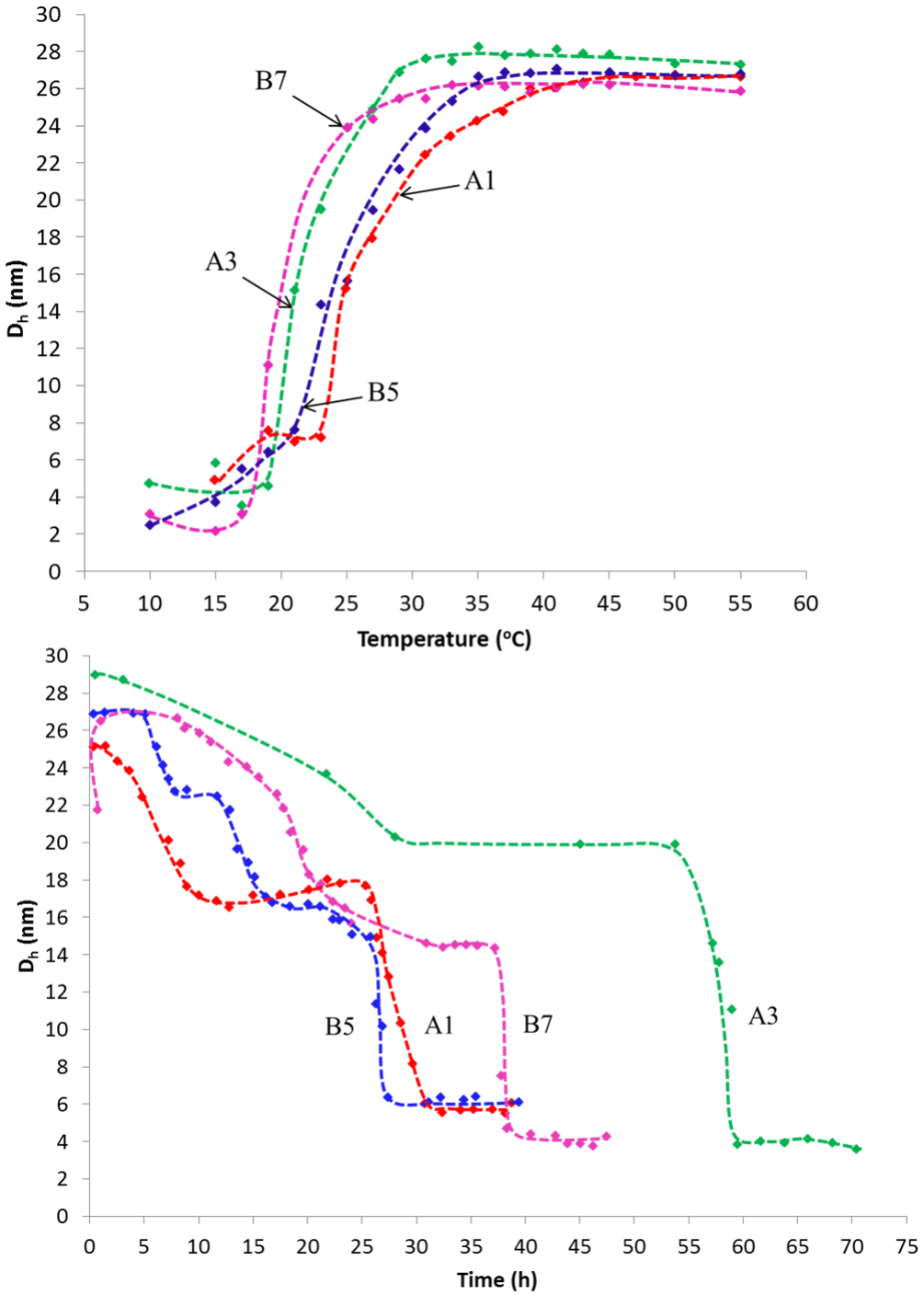

Figure A3.7 (A) The LCST of polymer A1: P(DMA_{96}-b-($NIPAM_{88}$-co-$DMAEA_{24}$-co-BA_6)), A3: P(DMA_{96}-b-($NIPAM_{94}$-co-$DMAEA_{25}$-co-BA_{10})), B5:P(DMA_{96}-b-($NIPAM_{85}$-co-$DMAEA_{42}$-co-BA_{14})) and B7: P(DMA_{96}-b-($NIPAM_{87}$-co-$DMAEA_{43}$-co-BA_{20})) in buffer solution pH 8 at concentration 10 mg/mL. **(B)** The degradation kinetics profiles at 37 ^{o}C for polymer A1, A3, B5, and B7 in buffer solution pH 8 at concentration 5 mg/mL. All data were averaged from five measurements on DLS.

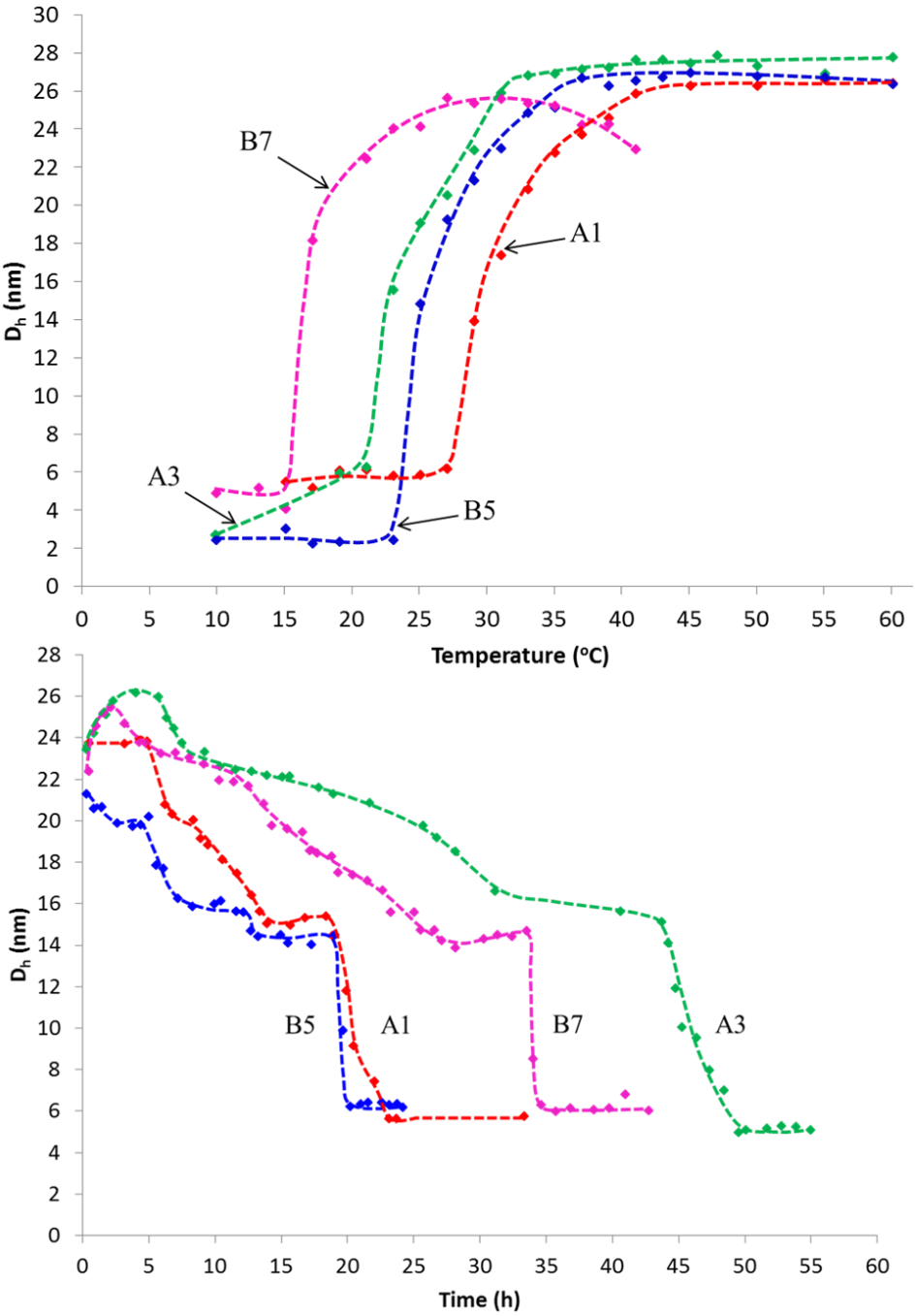

Figure A3.8 (A) The LCST of polymer A1: P(DMA_{96}-b-($NIPAM_{88}$-co-$DMAEA_{24}$-co-BA_6)), A3: P(DMA_{96}-b-($NIPAM_{94}$-co-$DMAEA_{25}$-co-BA_{10})), B5:P(DMA_{96}-b-($NIPAM_{85}$-co-$DMAEA_{42}$-co-BA_{14})) and B7: P(DMA_{96}-b-($NIPAM_{87}$-co-$DMAEA_{43}$-co-BA_{20})) in buffer solution pH 7.4 at concentration 10 mg/mL. **(B)** The degradation kinetics profiles at 37 ^{o}C for polymer A1, A3, B5, and B7 in buffer solution pH 7.4 at concentration 5 mg/mL. All data were averaged from five measurements on DLS.

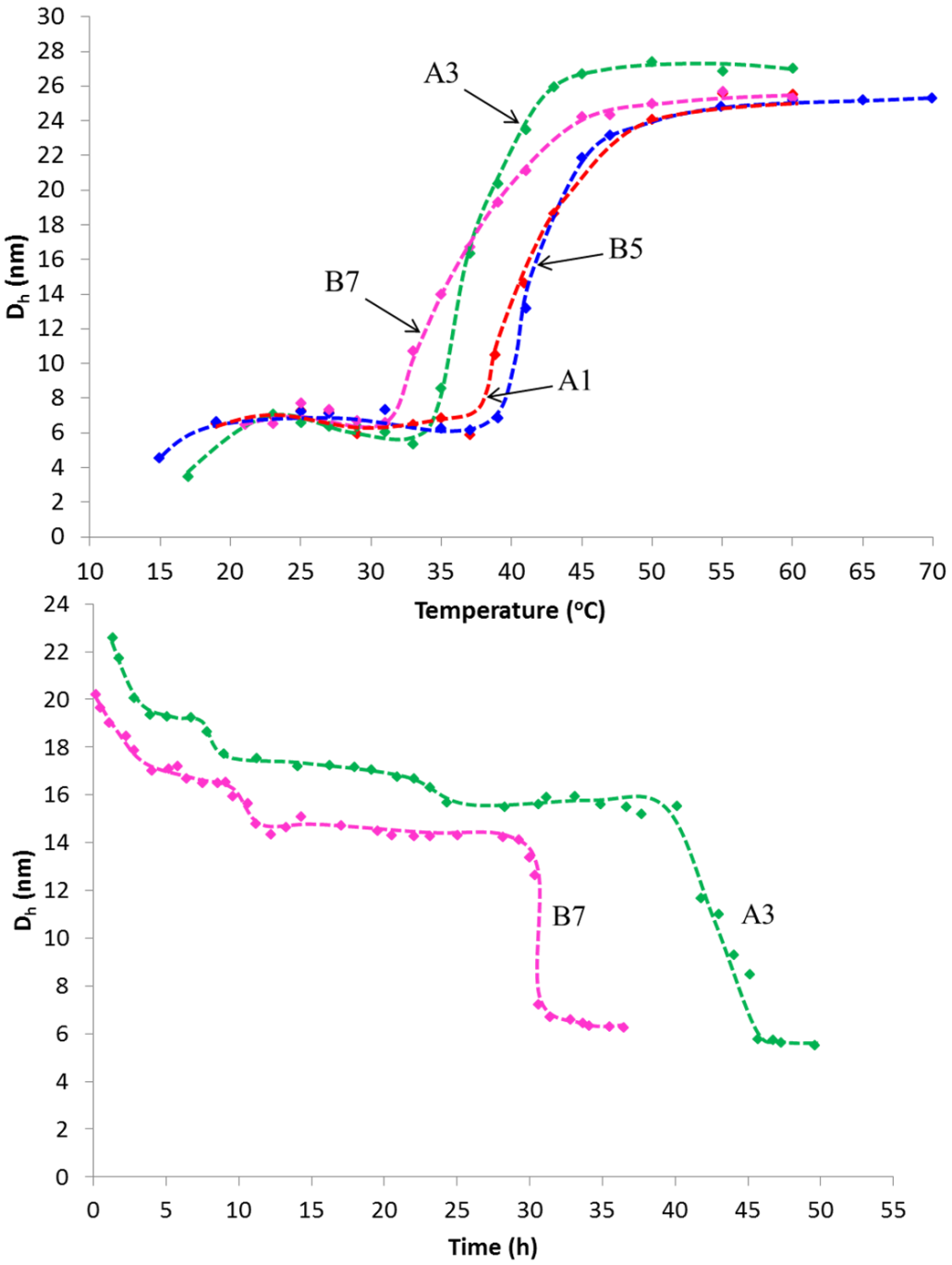

Figure A3.9 (A) The LCST of polymer A1: P(DMA_{96}-b-($NIPAM_{88}$-co-$DMAEA_{24}$-co-BA_6)), A3: P(DMA_{96}-b-($NIPAM_{94}$-co-$DMAEA_{25}$-co-BA_{10})), B5:P(DMA_{96}-b-($NIPAM_{85}$-co-$DMAEA_{42}$-co-BA_{14})) and B7: P(DMA_{96}-b-($NIPAM_{87}$-co-$DMAEA_{43}$-co-BA_{20})) in buffer solution pH 7 at concentration 10 mg/mL. **(B)** The degradation kinetics profiles at 37 ^oC for polymer A3 and B7 in buffer solution pH 7 at concentration 5 mg/mL. All data were averaged from five measurements on DLS.

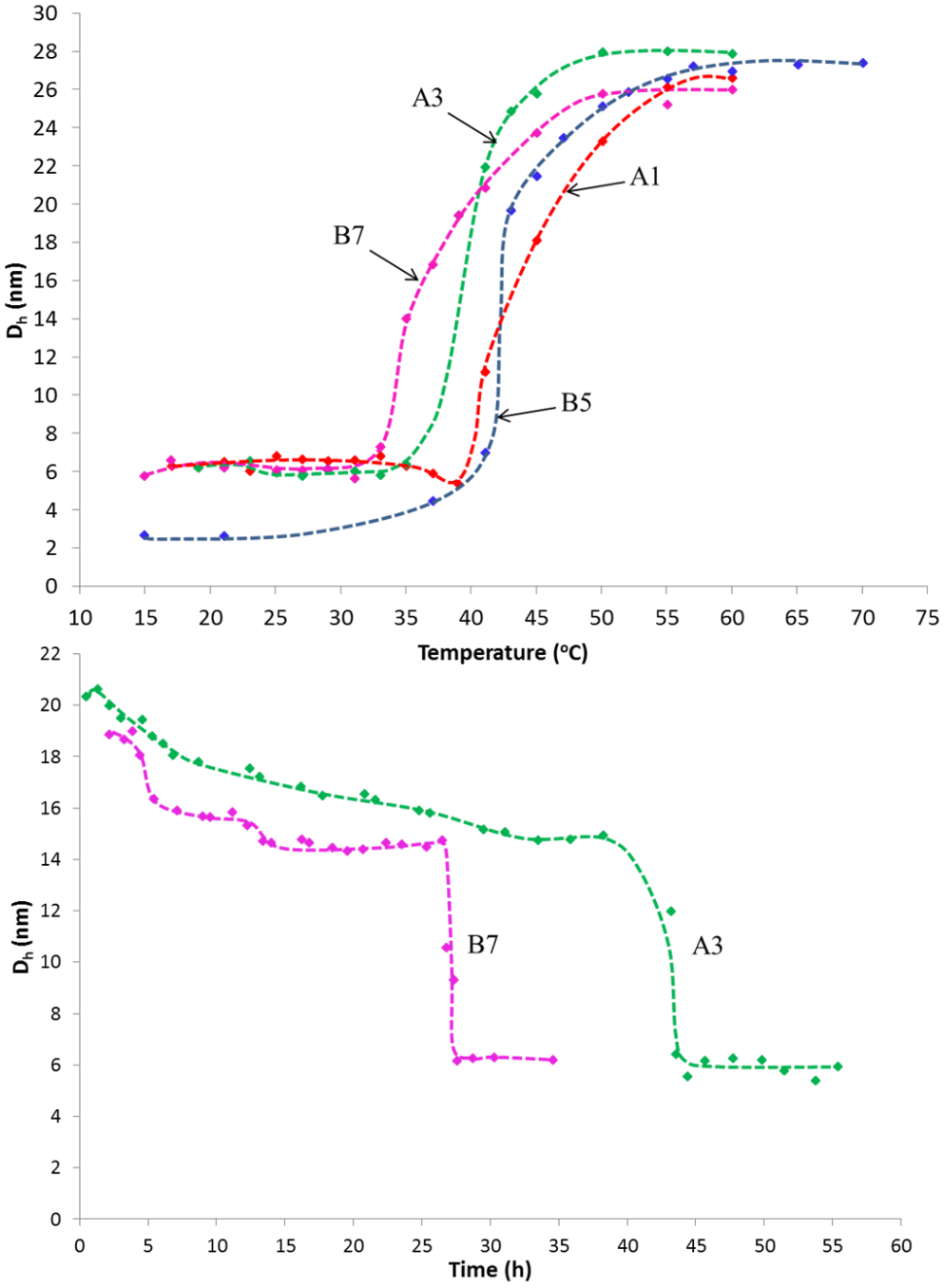

Figure A3.10 (A) The LCST of polymer A1: P(DMA_{96}-b-($NIPAM_{88}$-co-$DMAEA_{24}$-co-BA_6)), A3: P(DMA_{96}-b-($NIPAM_{94}$-co-$DMAEA_{25}$-co-BA_{10})), B5:P(DMA_{96}-b-($NIPAM_{85}$-co-$DMAEA_{42}$-co-BA_{14})) and B7: P(DMA_{96}-b-($NIPAM_{87}$-co-$DMAEA_{43}$-co-BA_{20})) in buffer solution pH 6.5 at concentration 10 mg/mL. **(B)** The degradation kinetics profiles at 37 °C for polymer A3 and B7 in buffer solution pH 6.5 at concentration 5 mg/mL. All data were averaged from five measurements on DLS.

Appendix C

Table A4.1 Reaction time, molecular weights, polydispersities (PDI), and ^{1}H NMR data of RAFT polymerization of thermoresponsive random copolymers at 60 ^{o}C in Dioxane.

Code	[DMAEA]:[BA]:[NIPAM]:[STY]:[CTA]:[AIBN][a]	Time (h)	SEC[b]		^{1}H NMR										
					Repeating unit				M_n[h]	Percentage of BA or STY (%)[i]	Individual conversion (%)				Total conversion (%)[n]
			M_n	PDI	DMAEA[c]	BA[d]	NIPAM	STY[g]			DMAEA[j]	BA[k]	NIPAM[l]	STY[m]	
A	50:0:200:0:1:0.2	15	9600	1.14	17	-	63[e]	-	9800	-	34.0	-	31.5	-	32.0
B1	50:13:200:0:1:0.2	16	12800	1.13	18	7	98[f]	-	14800	5.70	34.0	53.0	49.0	-	46.4
B2	50:28:200:0:1:0.2	16	14900	1.12	22	18	120[f]	-	19270	11.25	44.0	64.0	60.0	-	57.6
C1	50:0:200:13:1:0.2	48	9500	1.14	17	-	76[e]	7	12000	7.00	34.0	-	38.0	54.0	38.0
C2	50:0:200:28:1:0.2	72	10200	1.18	16	-	64[e]	14	11230	14.90	32.0	-	32.0	50.0	33.8

[a] Mol ratio of reactants. CTA concentration was 1.77 x 10^{-4} mol. [b] SEC data measured in THF solution using PSTY standards for calibration.

[c] Repeating units of DMAEA (N_{DMAEA}) determined by ^{1}H NMR were calculated by the integral area of two peaks at 2.50 ppm ($I_{2.50}$) and 3.63 ppm ($I_{3.63}$) using the following equation: $N_{DMAEA} = (3I_{2.50}/2 \times I_{3.63})$.

[d] Repeating units of BA (N_{BA}) determined by ^{1}H NMR were calculated by the integral area of two peaks at 0.88 ppm ($I_{0.88}$)and 3.63 ppm ($I_{3.63}$) using the following equation: $N_{BA} = (I_{0.88} - I_{3.63})/I_{3.63}$

[e] Repeating units of NIPAM (N_{NIPAM}) determined by ^{1}H NMR were calculated based on the N_{DMAEA} by the integral area of a peak at 3.63 ppm ($I_{3.63}$) and the peak in the range 4.00-4.35 ppm ($I_{4.00\text{-}4.35}$) using the following equation: $N_{NIPAM} = (3 \times I_{4.00\text{-}4.35}/ I_{3.63}) - 2 \times N_{DMAEA}$

[f] Repeating units of NIPAM (N_{NIPAM}) determined by ^{1}H NMR were calculated based on the N_{DMAEA} and N_{BA} by the integral area of a peak at 3.63 ppm ($I_{3.63}$) and the peak in the range 4.00-4.35 ppm ($I_{4.00\text{-}4.35}$) using the following equation: $N_{NIPAM} = (3 \times I_{4.00\text{-}4.35}/I_{3.63}) - 2 \times (N_{DMAEA} + N_{BA})$.

[g] Repeating units of STY (N_{STY}) determined by ^{1}H NMR were calculated by the N_{NIPAM} by the integral area of a peak at 3.63 ppm ($I_{3.63}$) and the peak in the range 6.20-7.18 ppm ($I_{6.20\text{-}7.18}$) using the following equation: $N_{STY} = [(3 \times I_{6.20\text{-}7.18}/I_{3.63}) - N_{NIPAM}]/5$

[h] Molecular weight determined by ^{1}H NMR were calculated based on N_{DMAEA}, N_{BA} or N_{STY}, $N_{NIPAM,}$ and the molecular weight of CTA: $Mn = [(N_{DMAEA} \times 143) + (N_{BA} \times 128.2)$ or $(N_{STY} \times 104) + (N_{NIPAM} \times 113)] + 252$

[i] Percentages of BA or STY were calculated based on the N_{DMAEA}, N_{NIPAM}, N_{BA} or N_{STY} : Percentage of BA = $N_{BA} / (N_{DMAEA} + N_{NIPAM} + N_{BA})$ and percentage of STY = $N_{STY} / (N_{DMAEA} + N_{NIPAM} + N_{STY})$

[j] Individual conversion of DMAEA was calculated based on the repeating unit of DMAEA and [DMAEA] using the following equation: Conversion of DMAEA = (Repeating unit DMAEA/[DMAEA]) x 100

[k] Individual conversion of BA was calculated based on the repeating unit of BA and [BA] using the following equation: Conversion of BA = (Repeating unit BA /[BA]) x 100

[l] Individual conversion of NIPAM was calculated based on the repeating unit of NIPAM and [NIPAM] using the following equation: Conversion of NIPAM = (Repeating unit NIPAM/[NIPAM]) x 100.

[m] Individual conversion of STY was calculated based on the repeating unit of STY and [STY] using the following equation: Conversion of STY = (Repeating unit STY /[STY]) x 100

[n] Total conversion was calculated using the following equation: Total conversion = [(Repeating unit of NIPAM + Repeating unit of DMAEA + Repeating unit of BA + Repeating unit of STY) / ([NIPAM] +[DMAEA] + [BA] + [STY])] x 100

Table A4.2 LCST and disassembly time of thermoresponsive random copolymers B1 and C1 determined by dynamic light scattering (DLS). The polymer concentration was 2.5 wt% in different Sodium dodecyl sulfate (SDS) solutions concentrated at 0.0123, 0.0164, 0.0205, and 0.0246 mol/L.

SDS concentration (mol/L)	B1: P(NIPAM$_{98}$-co-DMAEA$_{18}$-co-BA$_7$)		C1: P(NIPAM$_{76}$-co-DMAEA$_{17}$-co-STY$_7$)	
	LCST (^{o}C)	Disassembly time (h)[a]	LCST (^{o}C)	Disassembly time (h)[a]
0.0123	30	17.25	28	23.93
0.0164	33	11.23	32	18.61
0.0205	35	9.9	34	13
0.0246	37	8.17	36	10.12

[a] Disassembly time is when polymer nanoparticles became unimers measured by DLS measured by dynamic light scattering (DLS) at 37^{o}C.

Table A4.3 LCST of the random copolymers (2.5 wt%) in 0.0123 mol/L SDS solution after the polymer was fully degraded at 37 ^{o}C.

Polymer code		Disassembly time (h)	LCST (^{o}C) after disassembly at 37 ^{o}C
B1	P(NIPAM$_{98}$-co-DMAEA$_{18}$-co-BA$_7$)	18	42
B2	P(NIPAM$_{120}$-co-DMAEA$_{22}$-co-BA$_{18}$)	47	39
C1	P(NIPAM$_{76}$-co-DMAEA$_{17}$-co-STY$_7$)	24	39
C2	P(NIPAM$_{64}$-co-DMAEA$_{16}$-co-STY$_{14}$)	102	39

Table A4.4 Disassembly times for thermoresponsive random copolymers determined at 37 ^{o}C by Dynamic Light Scattering (DLS). The polymer concentration was 2.5 wt% in 0.0246 mol/L SDS solution.

Polymer		Disassembly time (h)[a]
B1	P(NIPAM$_{98}$-co-DMAEA$_{18}$-co-BA$_7$)	8.17
B2	P(NIPAM$_{120}$-co-DMAEA$_{22}$-co-BA$_{18}$)	15.82
C1	P(NIPAM$_{76}$-co-DMAEA$_{17}$-co-STY$_7$)	10.12
C2	P(NIPAM$_{64}$-co-DMAEA$_{16}$-co-STY$_{14}$)	37.77

[a] Disassembly time = when polymer particle became unimers measured at 37 ^{o}C by DLS

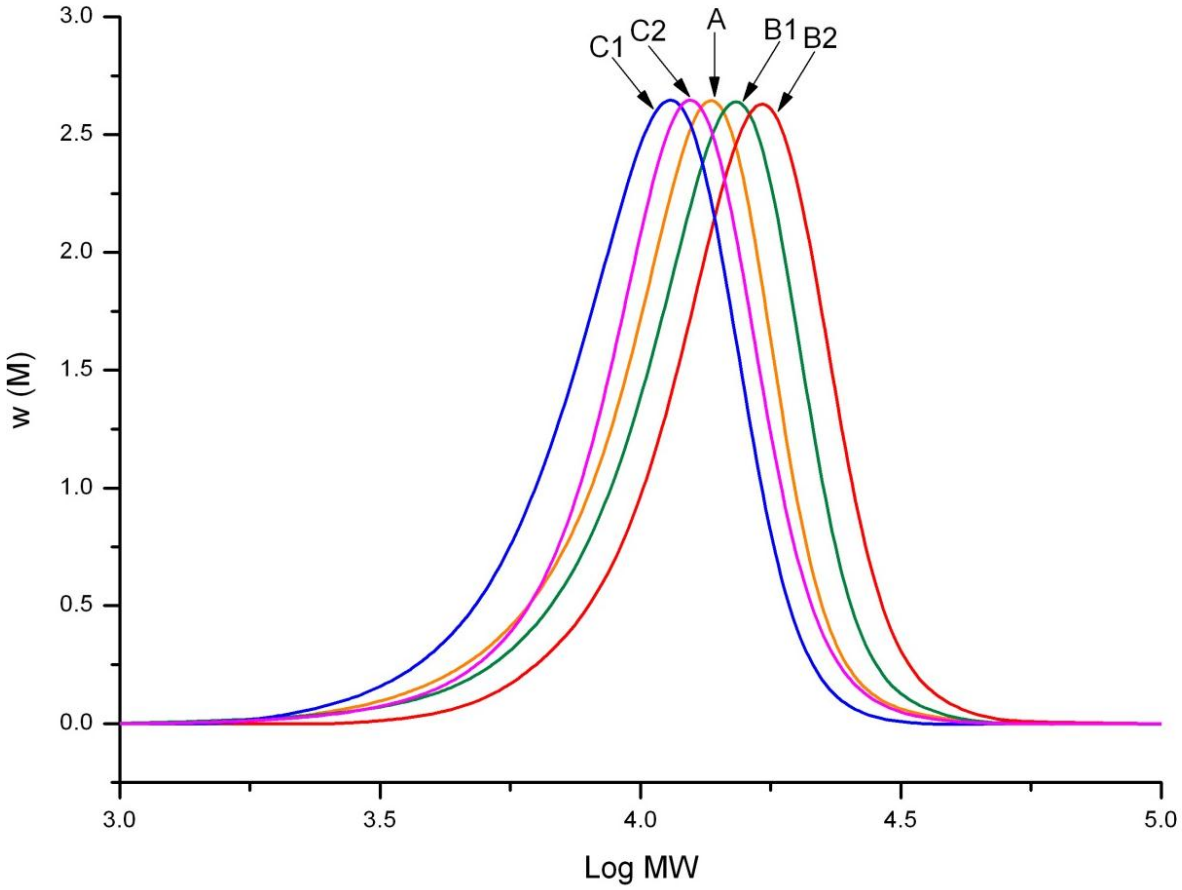

Figure A4.1 SEC traces of A; P(NIPAM$_{63}$-co-DMAEA$_{17}$), B1; P(NIPAM$_{98}$-co-DMAEA$_{18}$-co-BA$_{7}$), B2; P(NIPAM$_{120}$-co-DMAEA$_{22}$-co-BA$_{18}$), C1; P(NIPAM$_{76}$-co-DMAEA$_{17}$-co-STY$_{7}$), and C2; P(NIPAM$_{64}$-co-DMAEA$_{16}$-co-STY$_{14}$). The data were measured by THF GPC. The intensity for different distribution curves was normalized.

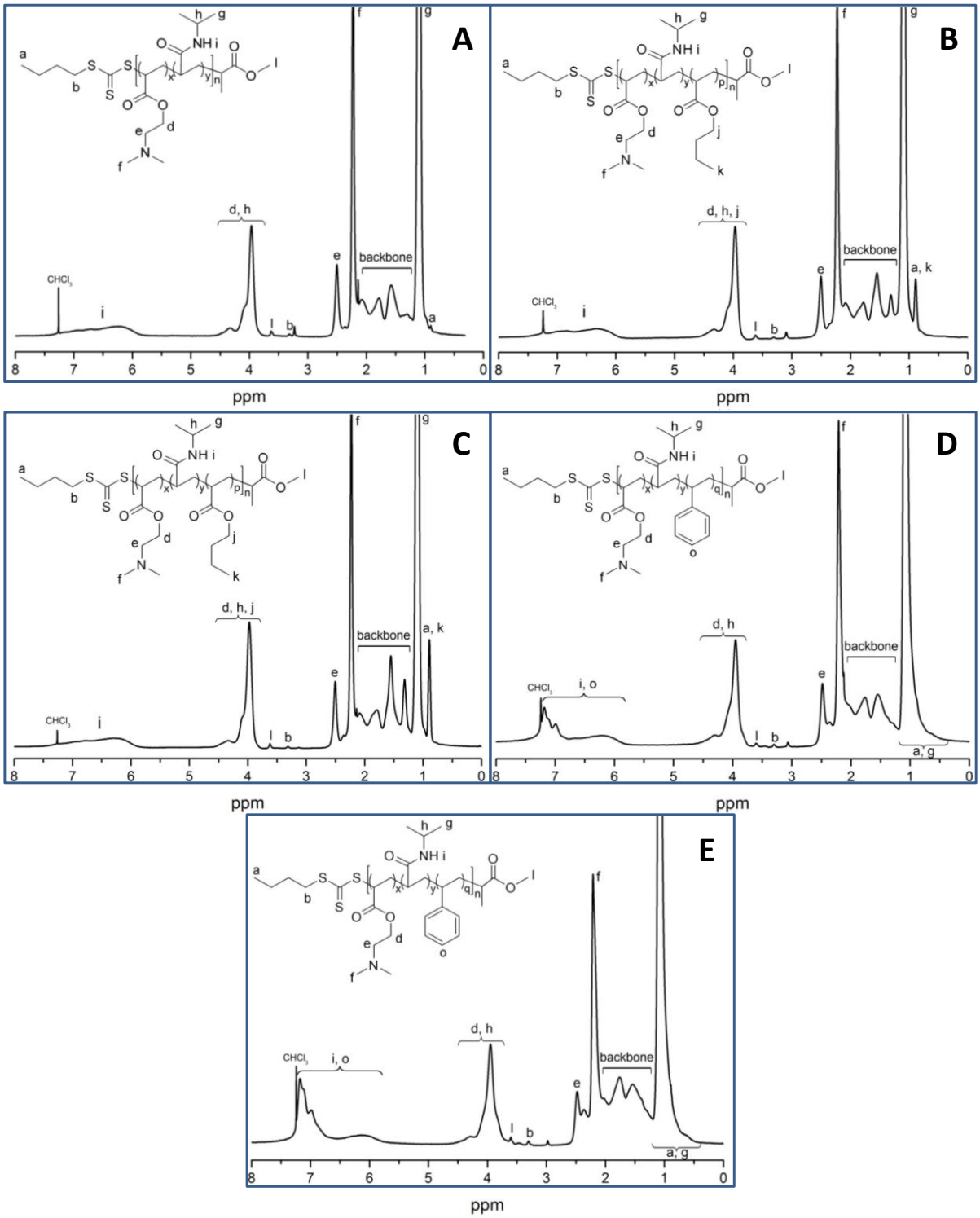

Figure A4.2 ^{1}H NMR spectrum of **A**: (A) P(NIPAM$_{63}$-co-DMAEA$_{17}$), **B**: (B1) P(NIPAM$_{98}$-co-DMAEA$_{18}$-co-BA$_{7}$), **C**: (B2) P(NIPAM$_{120}$-co-DMAEA$_{22}$-co-BA$_{18}$), **D**: (C1) P(NIPAM$_{76}$-co-DMAEA$_{17}$-co-STY$_{7}$), and **E**: (C2) P(NIPAM$_{64}$-co-DMAEA$_{16}$-co-STY$_{14}$) in $CDCl_3$.

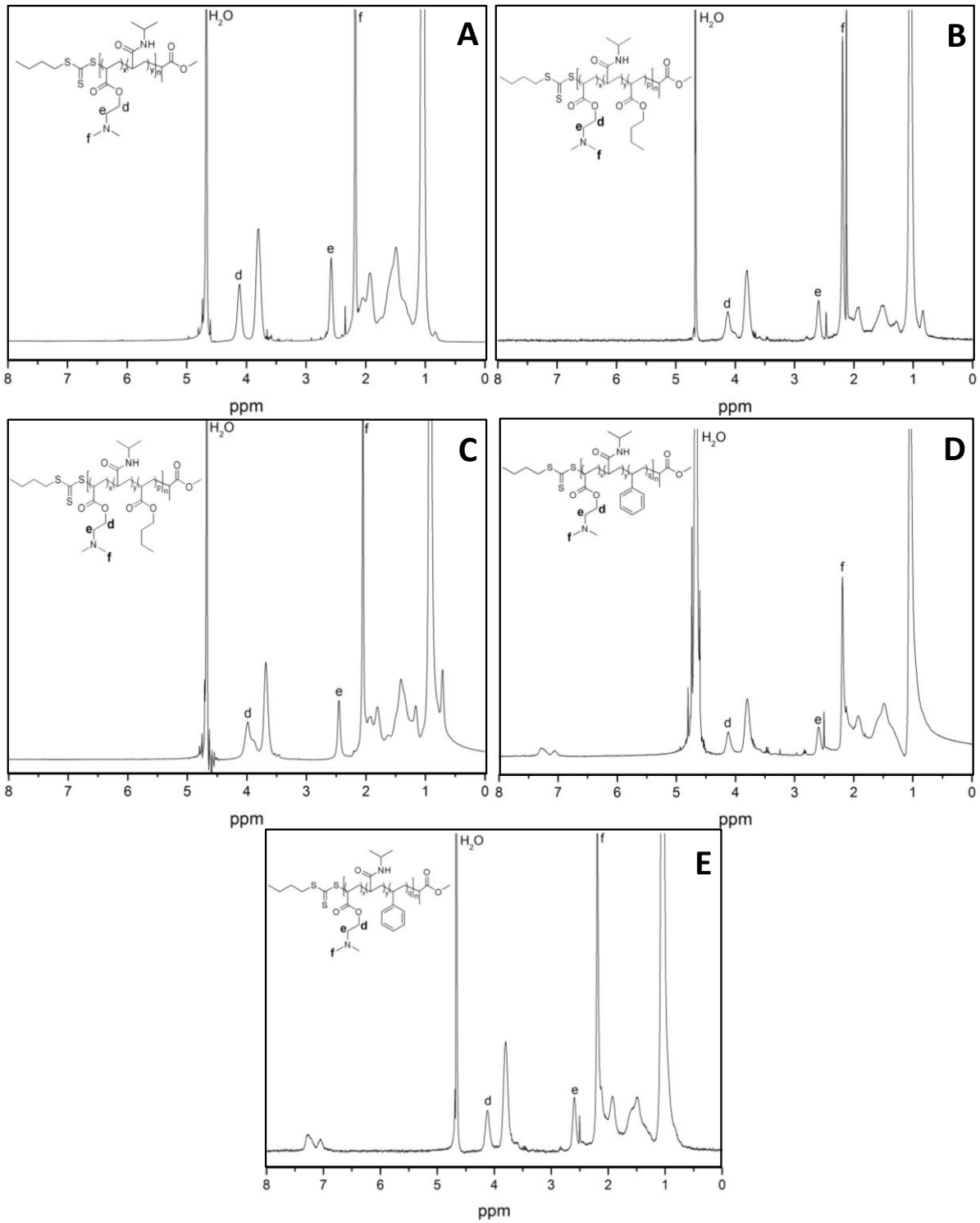

Figure A4.3 ^{1}H NMR spectrum of polymer **A**: (A) P(NIPAM$_{63}$-co-DMAEA$_{17}$) at 25 ^{o}C, **B**: (B1) P(NIPAM$_{98}$-co-DMAEA$_{18}$-co-BA$_{7}$) at 20 ^{o}C, **C**: (B2) P(NIPAM$_{120}$-co-DMAEA$_{22}$-co-BA$_{18}$) at 15 ^{o}C, **D**: (C1) P(NIPAM$_{76}$-co-DMAEA$_{17}$-co-STY$_{7}$) at 20 ^{o}C, and **E**: (C2) P(NIPAM$_{64}$-co-DMAEA$_{16}$-co-STY$_{14}$) at 15 ^{o}C in D_2O. The polymer was measured immediately after being dissolved in D_2O.

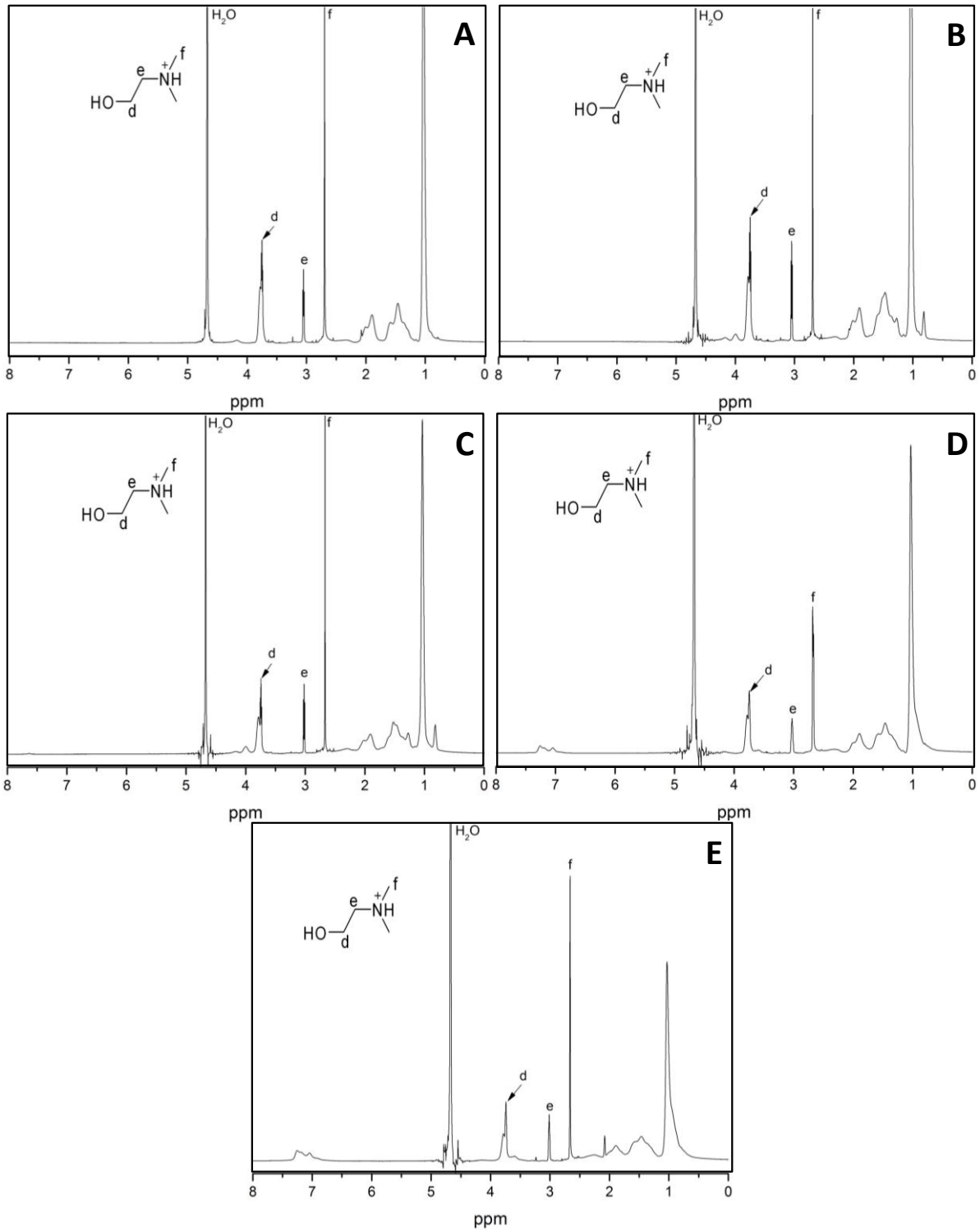

Figure A4.4 ^{1}H NMR spectrum of polymer **A**: (A) P(NIPAM$_{63}$-co-DMAEA$_{17}$), **B**: (B1) P(NIPAM$_{98}$-co-DMAEA$_{18}$-co-BA$_{7}$), **C**: (B2) P(NIPAM$_{120}$-co-DMAEA$_{22}$-co-BA$_{18}$), **D**: (C1) P(NIPAM$_{76}$-co-DMAEA$_{17}$-co-STY$_{7}$), and **E**: (C2) P(NIPAM$_{64}$-co-DMAEA$_{16}$-co-STY$_{14}$). The polymers were measured at 25 ^{o}C in D_2O after being kept in D_2O for 350 h.

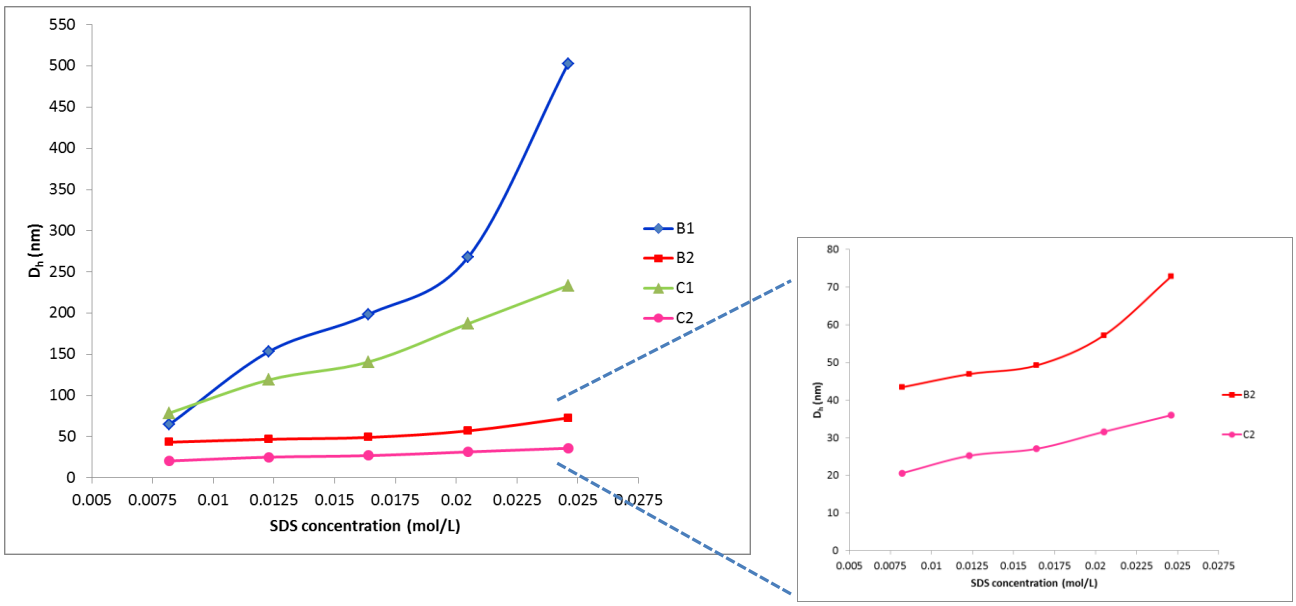

Figure A4.5 Diameter (D_h) of thermoresponsive random copolymers determined at 37 ^{o}C by dynamic light scattering (DLS). The polymers concentration were 2.5 wt% in five different Sodium dodecyl sulfate (SDS) solutions concentrated at 8.2, 12.3, 16.4, 20.5, and 24.6 mM.

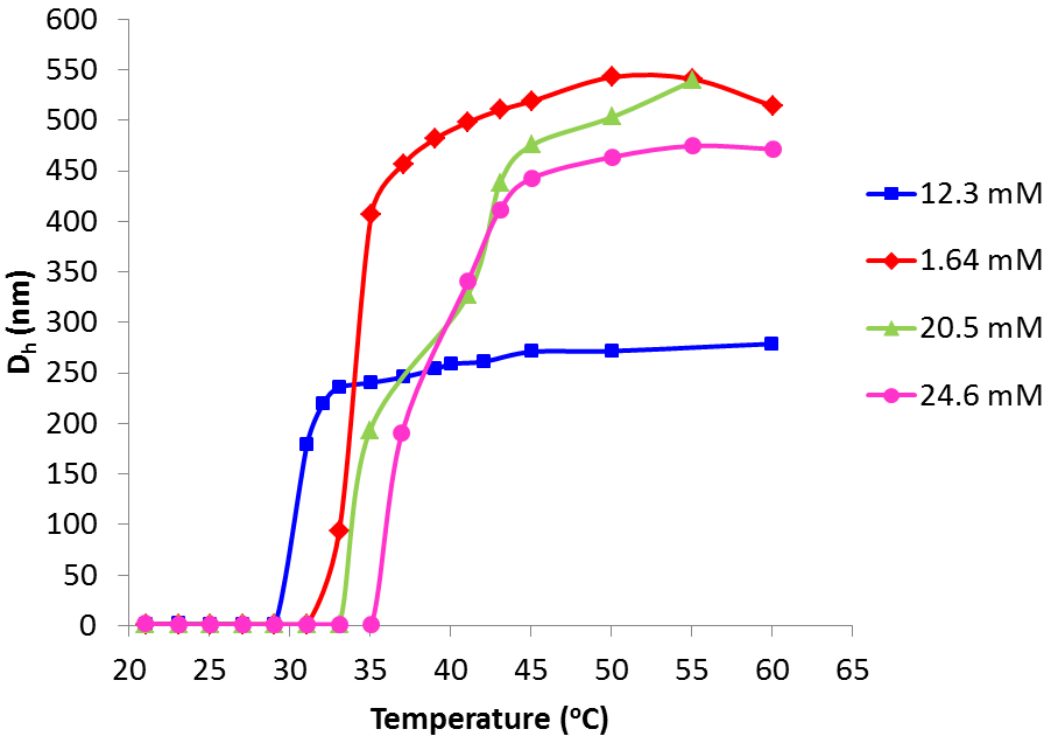

Figure A4.6 D_h vs temperature of polymer B1: P(NIPAM$_{98}$-co-DMAEA$_{18}$-co-BA$_7$ in different SDS solution concentrations: 12.3, 16.4, 20.5, and 24.6 mM. The data were reported as average numbers from five measurements on DLS machine. Polymer concentration was 2.5 wt%

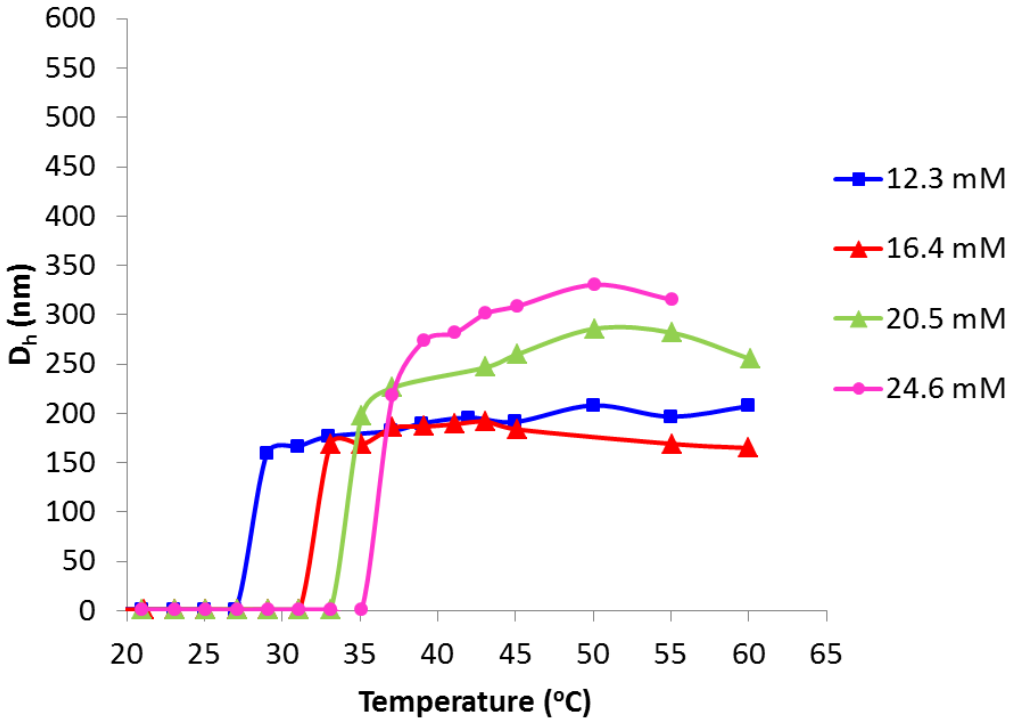

Figure A4.7 D_h vs temperature of polymer C1: P(NIPAM$_{76}$-co-DMAEA$_{17}$-co-STY$_7$) in different SDS solution concentrations: 12.3, 16.4, 20.5, and 24.6 mM. The data were reported as average numbers from five measurements on DLS machine. Polymer concentration was 2.5 wt%.

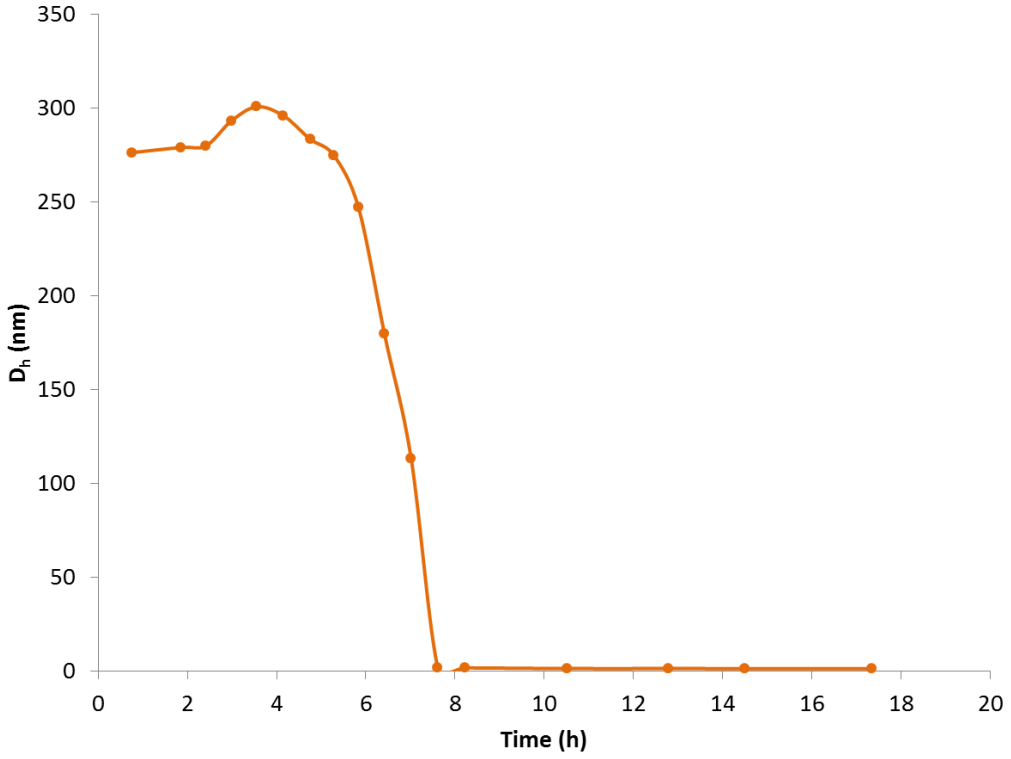

Figure A4.8 Degradation kinetics profile for the random copolymers A: P(NIPAM$_{63}$-co-DMAEA$_{17}$). The polymer concentration was 2.5wt% in 12.3 mM SDS solution. The data were averaged from five measurements by DLS at 45 ^{o}C.

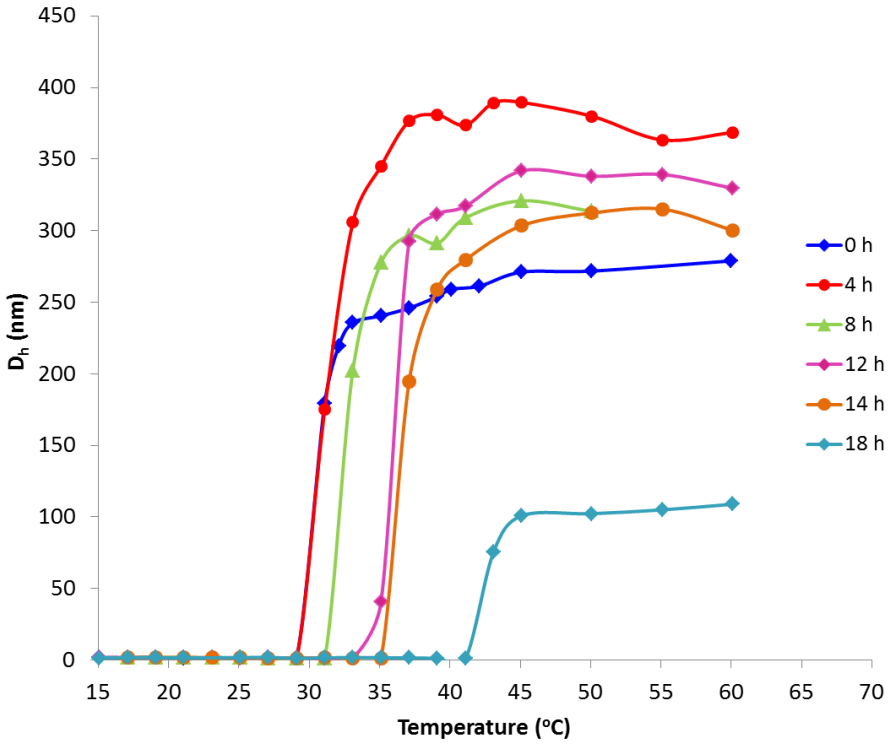

Figure A4.9 LCST of polymer B1: P(NIPAM$_{98}$-co-DMAEA$_{18}$-co-BA$_{7}$), after the incubation in water bath at 37 °C at different time points. The polymer concentration was 2.5 wt% in 12.3 mM SDS solution The data were averaged from five measurements by DLS.

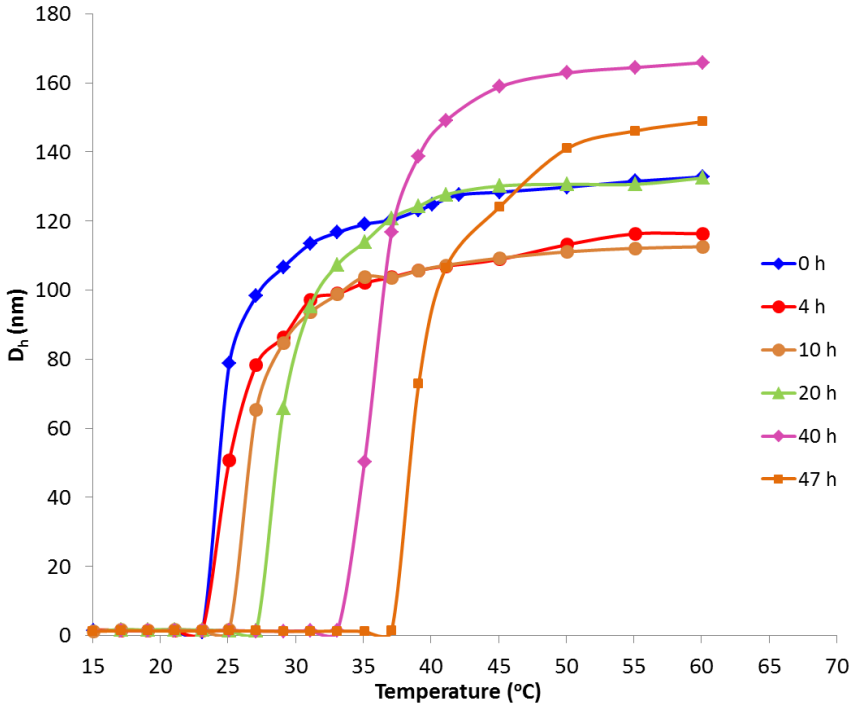

Figure A4.10 LCST of polymer B2: P(NIPAM$_{120}$-co-DMAEA$_{22}$-co-BA$_{18}$), after the incubation in water bath at 37 °C at different time points. The polymer concentration was 2.5 wt% in 12.3 mM SDS solution. The data were averaged from five measurements by DLS.

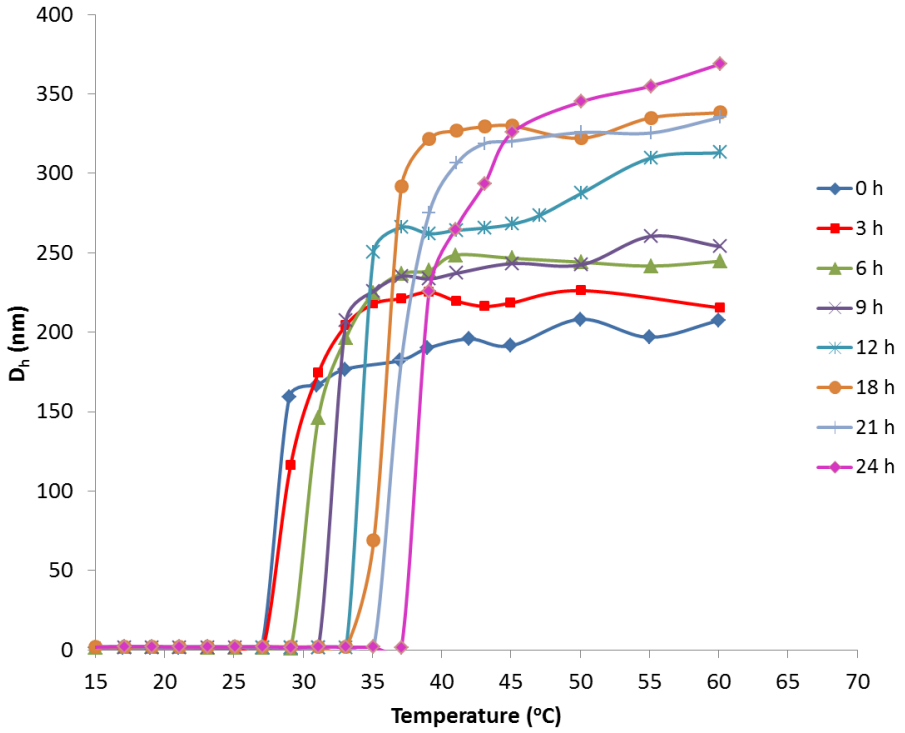

Figure A4.11 LCST of polymer C1: P(NIPAM$_{76}$-co-DMAEA$_{17}$-co-STY$_7$) after the incubation in water bath at 37 °C at different time points. The polymer concentration was 2.5 wt% in 12.3 mM SDS solution.The data were averaged from five measurements by DLS.

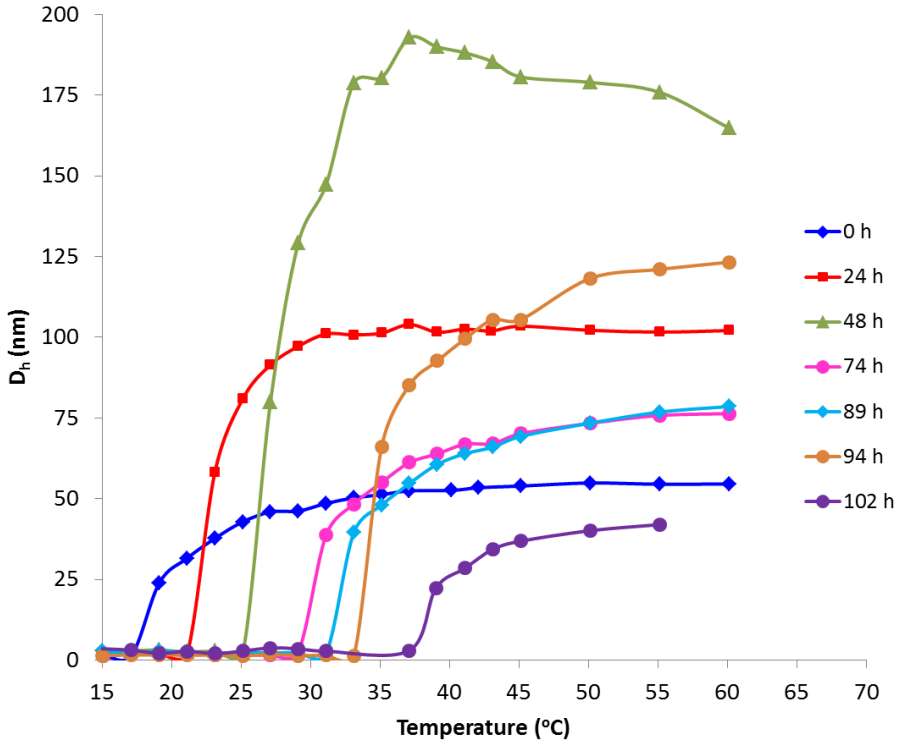

Figure A4.12. LCST of polymer C2: P(NIPAM$_{64}$-co-DMAEA$_{16}$-co-STY$_{14}$), after the incubation in water bath at 37 °C at different time points. The polymer concentration was 2.5 wt% in 12.3 mM SDS solution. The data were averaged from five measurements by DLS.

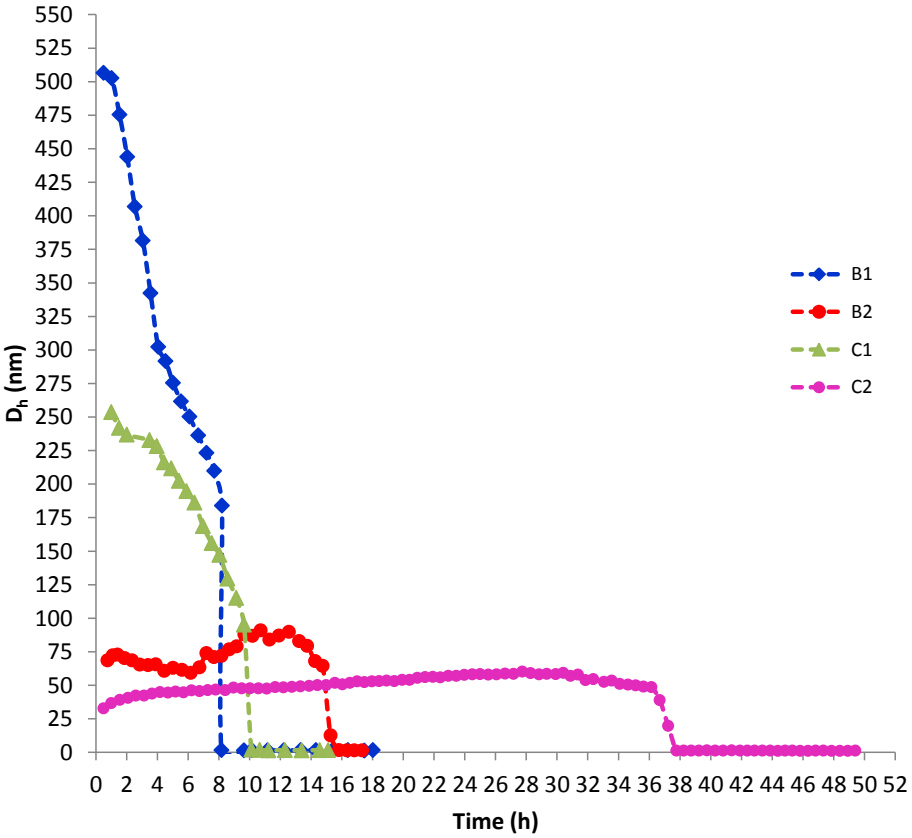

Figure A4.13 Degradation time of thermoresponsive random copolymers B1: P(NIPAM$_{98}$-co-DMAEA$_{18}$-co-BA$_7$), B2: P(NIPAM$_{120}$-co-DMAEA$_{22}$-co-BA$_{18}$), C1: P(NIPAM$_{76}$-co-DMAEA$_{17}$-co-STY$_7$), and C2: P(NIPAM$_{64}$-co-DMAEA$_{16}$-co-STY$_{14}$) at 37 ^{o}C, determined by dynamic light scattering (DLS). The polymer concentration was 2.5wt% in 24.6 mM SDS solution.

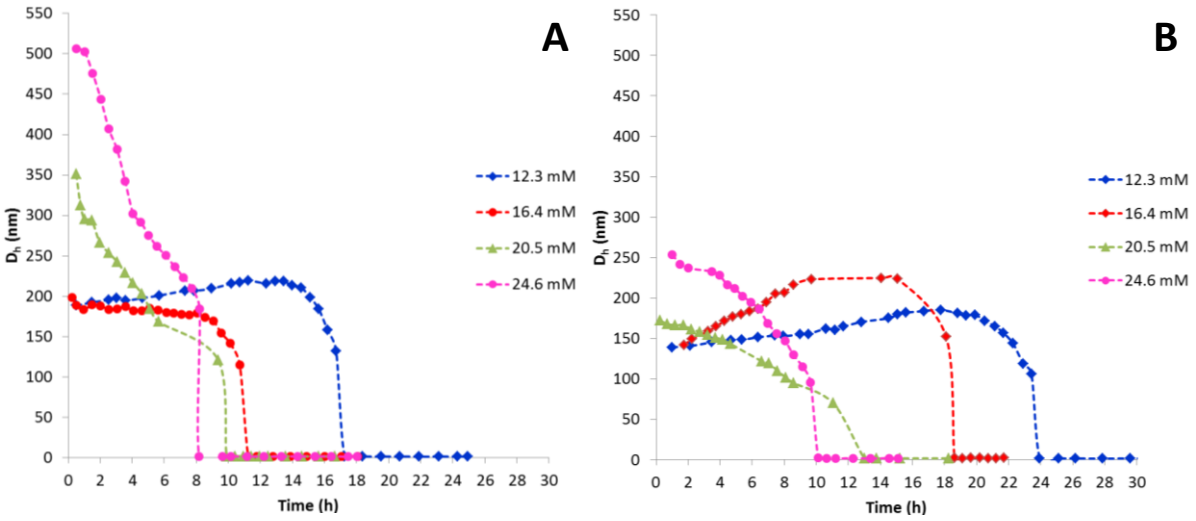

Figure A4.14 Disassembly profile of B1: P(NIPAM$_{98}$-co-DMAEA$_{18}$-co-BA$_7$) (A) and C1: P(NIPAM$_{76}$-co-DMAEA$_{17}$-co-STY$_7$) (B) determined at 37^{o}C by DLS. The polymer concentration was 2.5 wt% in different SDS solution concentrations: 12.3, 16.4, 20.5, and 24.6 mM.

Appendix D

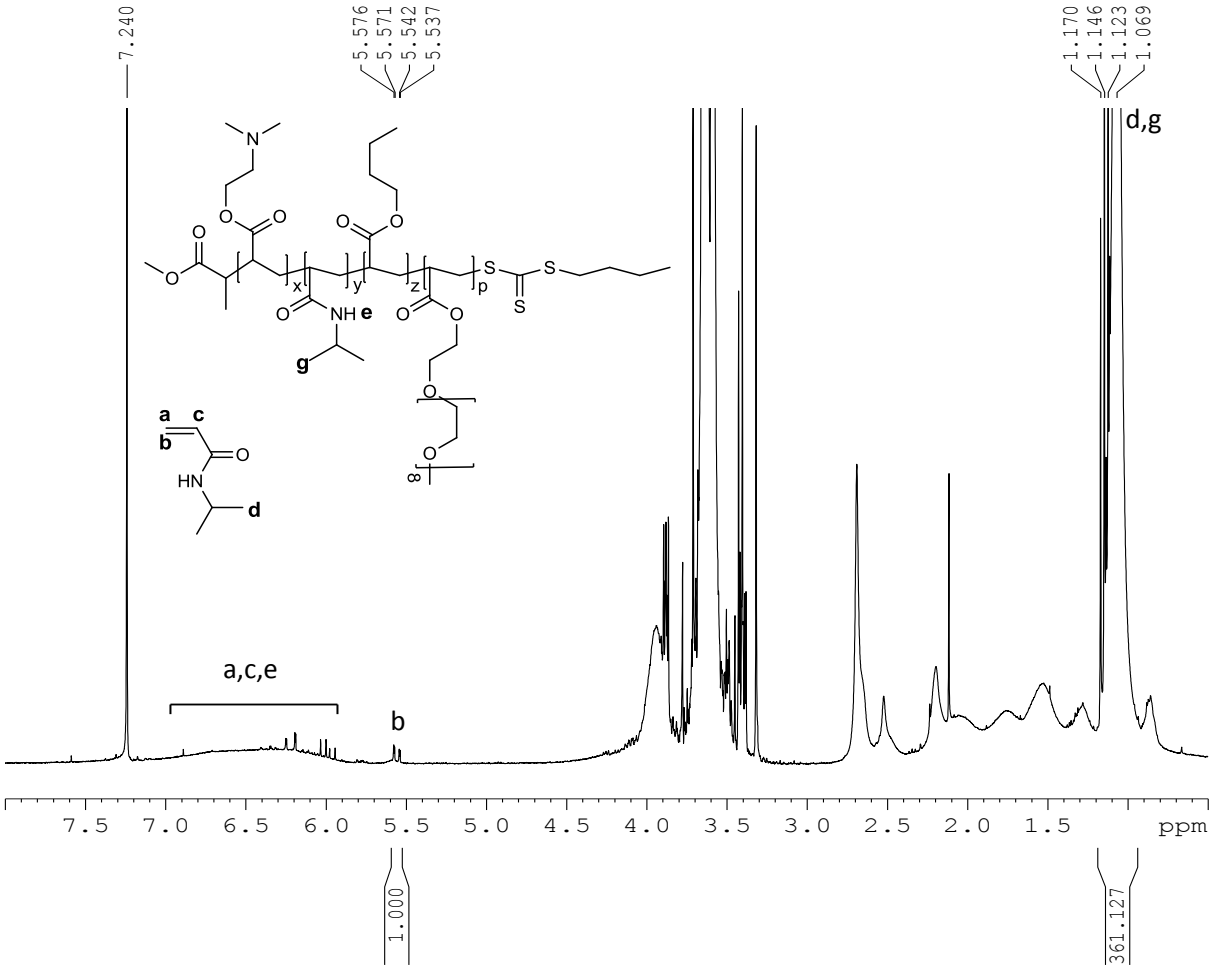

Figure A5.1 ^{1}H NMR spectrum of polymer B in $CDCl_3$ before purification used for calculation of the conversion of NIPAM in polymer B.

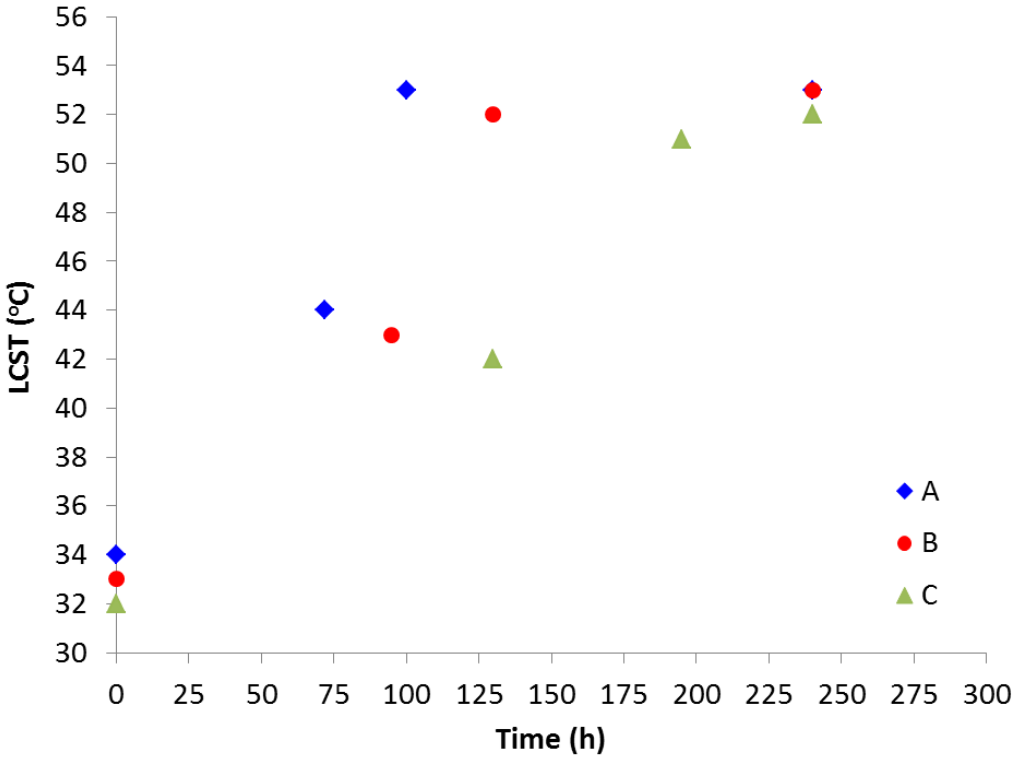

Figure A5.2. The rate of change in the LCST (^{o}C) of the polymers determined by observation the cloud point of polymer solutions 5 wt% over time.

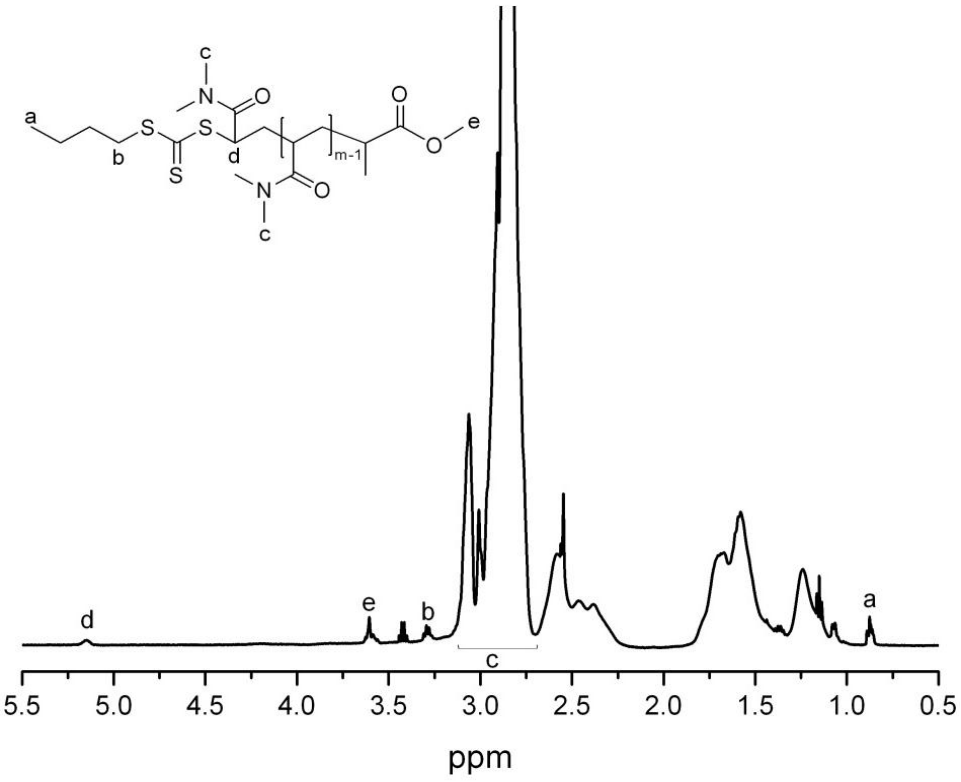

Figure A5.3 ^{1}H NMR spectrum of PDMA in $CDCl_3$.

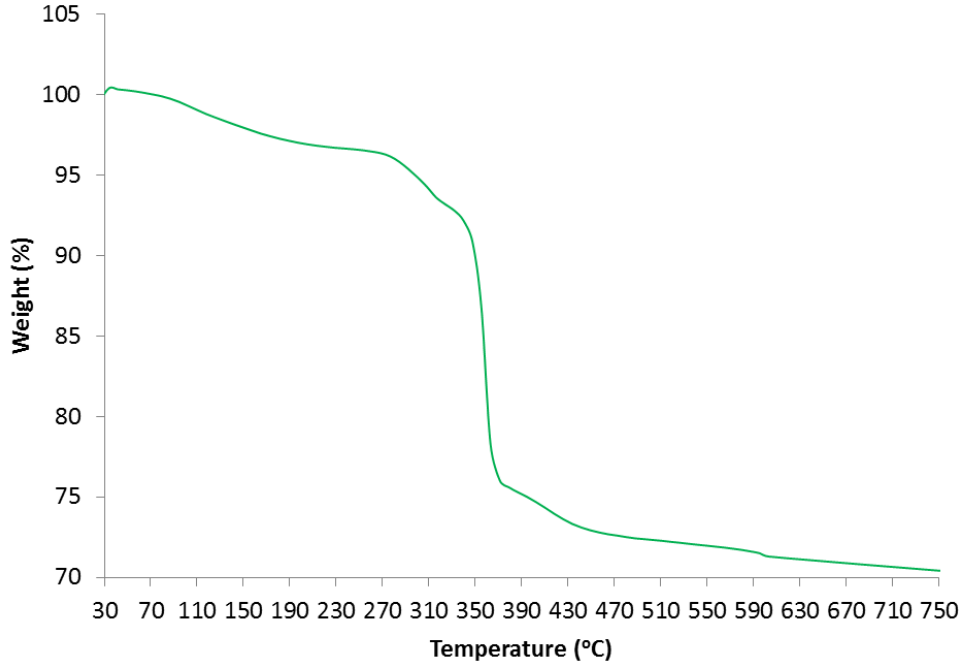

Figure A5.4 TGA of PDMA grafted gold nanoparticles (PDMA-AuNPs).

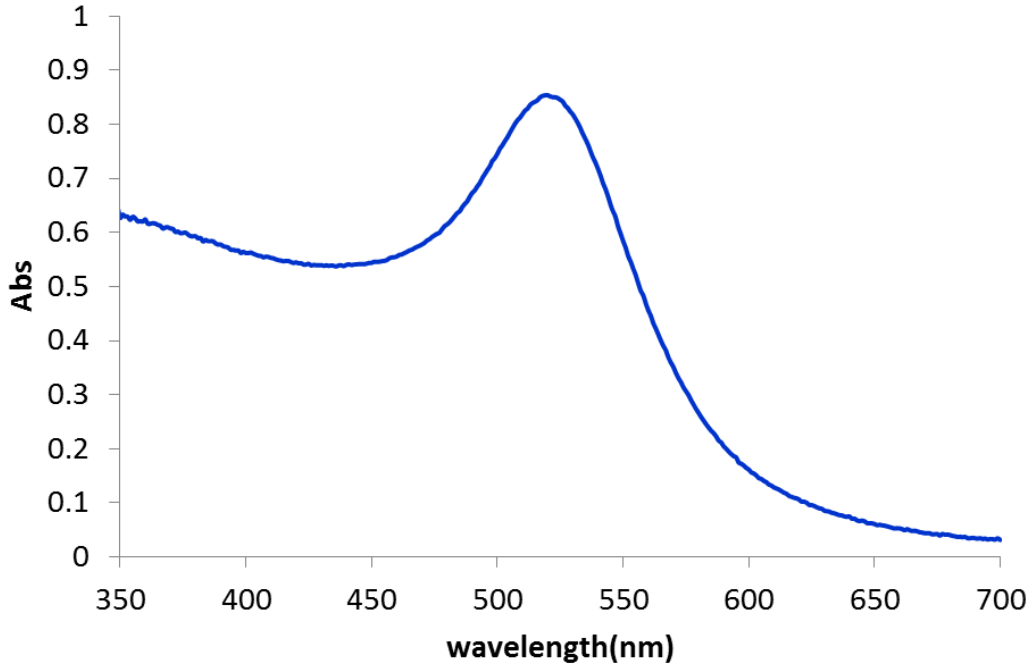

Figure A5.5 Absorbance of PDMA-grafted gold nanoparticles (PDMA-AuNPs) measured on UV-vis machine.